TOPICS IN ORGANOMETALLIC CHEMISTRY 18

Volume Editor M. Beller

Catalytic Carbonylation Reactions

Springer

18
Topics in Organometallic Chemistry

Topics in Organometallic Chemistry

Recently Published and Forthcoming Volumes

Organometallic Oxidations Catalysis
Volume Editors: F. Meyer, C. Limberg
Vol. 22, 2006

N-Heterocyclic Carbenes (NHC) in Transition Metal Catalysis
Volume Editor: F. Glorius
Vol. 21, 2006

Dendrimer Catalysis
Volume Editor: L. H. Gade
Vol. 20, 2006

Metal Catalyzed Cascade Reactions
Volume Editor: T. J. J. Müller
Vol. 19, 2006

Catalytic Carbonylation Reactions
Volume Editor: M. Beller
Vol. 18, 2006

Bioorganometallic Chemistry
Volume Editor: G. Simonneaux
Vol. 17, 2006

Surface and Interfacial Organometallic Chemistry and Catalysis
Volume Editors: C. Copéret, B. Chaudret
Vol. 16, 2005

Chiral Diazaligands for Asymmetric Synthesis
Volume Editors: M. Lemaire, P. Mangeney
Vol. 15, 2005

Palladium in Organic Synthesis
Volume Editor: J. Tsuji
Vol. 14, 2005

Metal Carbenes in Organic Synthesis
Volume Editor: K. H. Dötz
Vol. 13, 2004

Theoretical Aspects of Transition Metal Catalysis
Volume Editor: G. Frenking
Vol. 12, 2005

Ruthenium Catalysts and Fine Chemistry
Volume Editors: C. Bruneau, P. H. Dixneuf
Vol. 11, 2004

New Aspects of Zirconium Containing Organic Compounds
Volume Editor: I. Marek
Vol. 10, 2004

Precursor Chemistry of Advanced Materials
CVD, ALD and Nanoparticles
Volume Editor: R. Fischer
Vol. 9, 2005

Metallocenes in Stereoselective Synthesis
Volume Editor: T. Takahashi
Vol. 8, 2004

Transition Metal Arene π-Complexes in Organic Synthesis and Catalysis
Volume Editor: E. P. Kündig
Vol. 7, 2004

Organometallics in Process Chemistry
Volume Editor: R. D. Larsen
Vol. 6, 2004

Organolithiums in Enantioselective Synthesis
Volume Editor: D. M. Hodgson
Vol. 5, 2003

Organometallic Bonding and Reactivity: Fundamental Studies
Volume Editor: J. M. Brown, P. Hofmann
Vol. 4, 1999

Activation of Unreactive Bonds and Organic Synthesis
Volume Editor: S. Murai
Vol. 3, 1999

Catalytic Carbonylation Reactions

Volume Editor: Matthias Beller

With contributions by

M. Beller · S. Castillón · G. Cavinato · C. Claver · M. Costa
O. Dechy-Cabaret · M. Diéguez · P. Eilbracht · B. Gabriele
A. Haynes · A. Jacobi von Wangelin · P. Kalck · K. Nakano
H. Neumann · K. Nozaki · D. Obst · O. Pàmies · G. Salerno
A. M. Schmidt · D. Strübing · L. Toniolo · M. Urrutigoïty
A. Vavasori · K.-D. Wiese

Springer

The series *Topics in Organometallic Chemistry* presents critical overviews of research results in organometallic chemistry. As our understanding of organometallic structure, properties and mechanisms increases, new ways are opened for the design of organometallic compounds and reactions tailored to the needs of such diverse areas as organic synthesis, medical research, biology and materials science. Thus the scope of coverage includes a broad range of topics of pure and applied organometallic chemistry, where new breakthroughs are being achieved that are of significance to a larger scientific audience.
The individual volumes of *Topics in Organometallic Chemistry* are thematic. Review articles are generally invited by the volume editors.
In references *Topics in Organometallic Chemistry* is abbreviated *Top Organomet Chem* and is cited as a journal.

Springer WWW home page: springer.com
Visit the TOMC content at springerlink.com

Library of Congress Control Number: 2006924679

ISSN 1436-6002
ISBN-10 3-540-33002-X Springer Berlin Heidelberg New York
ISBN-13 978-3-540-33002-8 Springer Berlin Heidelberg New York
DOI 10.1007/b105253

Springer is a part of Springer Science+Business Media

springer.com

Printed in Germany

Cover design: *Design & Production* GmbH, Heidelberg
Typesetting and Production: LE-TEX Jelonek, Schmidt & Vöckler GbR, Leipzig

Printed on acid-free paper 02/3100 YL – 5 4 3 2 1 0

Volume Editor

Matthias Beller

Leibnitz-Institut für Katalyse
Universität Rostock
Albert-Einstein-Str. 29a
18059 Rostock, Germany
matthias.beller@ifok-rostock.de

Editorial Board

Topics in Organometallic Chemistry
Also Available Electronically

For all customers who have a standing order to Topics in Organometallic Chemistry, we offer the electronic version via SpringerLink free of charge. Please contact your librarian who can receive a password or free access to the full articles by registering at:

springerlink.com

If you do not have a subscription, you can still view the tables of contents of the volumes and the abstract of each article by going to the SpringerLink Homepage, clicking on "Browse by Online Libraries", then "Chemical Sciences", and finally choose Topics in Organometallic Chemistry.

You will find information about the

- Editorial Board
- Aims and Scope
- Instructions for Authors
- Sample Contribution

at springer.com using the search function.

Preface

The development of environmentally benign and clean synthetic methodologies is still one of the most important goals of current research in chemistry. In this regard, catalysis and organometallic chemistry are key technologies to achieve these objectives and to contribute to a "greener" chemistry in the future. From its start, *Topics in Organometallic Chemistry* has been devoted to a significant extent to publishing volumes that go in this direction. The present issue also follows this track. More specifically it tries to give an overview of the current status and future trends of catalytic carbonylation reactions.

One could ask, why especially carbonylation reactions? A straightforward answer is provided by the fact that although carbonylation processes constitute industrial core technologies for converting bulk chemicals to a variety of useful products for our daily lives, they are still relatively seldom used in advanced organic chemistry. Up until now, most basic organic textbooks pay hardly any attention to carbonylation chemistry. Thus, this volume tries to bridge the well-established organometallic chemistry of carbon monoxide and synthesis gas (mixture of carbon monoxide and hydrogen) with novel organic applications. Hence, it is not surprising that several chapters in this volume, such as the carbonylation of aldehydes and epoxides, as well as Pauson–Khand carbonylations stress this point. By comparing the different carbonylation reactions it is apparent that especially the transformations allowing for the conversion of olefins—the basic raw materials for the chemical industry—into more valuable products, such as aldehydes, alcohols, and carbonyl compounds, are of general importance (see, for example, the chapters by Gabriele, Kalck, and Toniolo). Thus, a significant part of the book is devoted to recent inventions and gradual improvements in hydroformylation and alkoxycarbonylation reactions. In addition, it is nicely demonstrated in the chapters of Wiese and Haynes how industrial applications in this area are actively pursued.

When the potential content of this issue was initially discussed with the authors from industry and academia it was immediately clear that the various chapters should give a general overview, but should focus on developments of the last decade. After having finished the project we can state that this goal has been achieved. Thus, the reader will find a balanced view of basic knowledge and current progress.

Finally as editor I would like to thank all contributors for their participation in this project and for their patience when it took longer than expected. I also acknowledge the continuous support by Jörn Mohr from Springer, who did not push but challenged. I hope that readers will enjoy this volume and discover aspects that stimulate further discoveries in this timely and exciting area of scientific research.

Rostock, July 2006 Matthias Beller

Contents

Hydroformylation
K.-D. Wiese · D. Obst 1

Asymmetric Hydroformylation
C. Claver · M. Diéguez · O. Pàmies · S. Castillón 35

Synthetic Applications of Tandem Reaction Sequences Involving Hydroformylation
P. Eilbracht · A. M. Schmidt 65

Hydroxy- and Alkoxycarbonylations of Alkenes and Alkynes
P. Kalck · M. Urrutigoïty · O. Dechy-Cabaret 97

Carbonylation of Ethene in Methanol Catalysed by Cationic Phosphine Complexes of Pd(II): from Polyketones to Monocarbonylated Products
G. Cavinato · L. Toniolo · A. Vavasori 125

The Pauson–Khand Reaction
D. Strübing · M. Beller 165

Acetic Acid Synthesis by Catalytic Carbonylation of Methanol
A. Haynes 179

Carbonylations of Aldehydes
A. Jacobi von Wangelin · H. Neumann · M. Beller 207

Carbonylation of Epoxides
K. Nakano · K. Nozaki 223

Oxidative Carbonylations
B. Gabriele · G. Salerno · M. Costa 239

Author Index Volumes 1–18 273

Subject Index 281

Top Organomet Chem (2006) 18: 1–33
DOI 10.1007/3418_015

Published online: 11 August 2006

Hydroformylation

Klaus-Diether Wiese (✉) · Dietmar Obst

OXENO Olefinchemie GmbH, Paul-Baumann-Straße 1, 45772 Marl, Germany
klaus-diether.wiese@degussa.com

1 Introduction 2

2 Catalysts 4
2.1 Active Metals 4
2.2 Reaction Mechanism with an Unmodified Catalyst 5
2.3 Impact of Ligands on the Reaction Cycle 6
2.4 Types of Ligands 8

3 Methods for Mechanistic Investigations 12
3.1 In Situ Infra-red (IR) Spectroscopy 12
3.2 In Situ Nuclear Magnetic Resonance (NMR) 13
3.3 Theoretical Methods 14
3.4 Kinetic Investigations 16

4 Industrial Application of Hydroformylation 20
4.1 Basic Process Principles 20
4.2 Enemies of the Catalyst 21
4.3 Hydroformylation of Lower Alpha-Olefins 23
4.4 The Challenge: Higher Internal and Branched Olefins 28

5 Conclusion 30

References 31

Abstract Discovered in 1938, hydroformylation is the most important example of the industrial application of homogeneous catalysis. Production is now well beyond 10 million metric tons annually. Propene-based products still account for two-thirds of this volume. Highly selective processes using ligand-modified rhodium catalysts have been developed and are state of the art. Technology and markets for the products have matured, so there is little room for improvement. With the industry placing more emphasis on speciality chemicals, researchers are interested in applying this versatile reaction to more sophisticated chemistry and are focusing on modifying rhodium with ligands to tune the properties. Over the last 20 years, a myriad of ligands have been developed. In-situ NMR and IR under reaction conditions and molecular modeling are modern tools for gaining insight into the intricate mechanism, but the reaction is still far from being understood. From the viewpoint of engineers, the crucial problem of homogeneous catalysis, recycling the generally expensive catalysts, has not been satisfactorily solved. As a consequence, old but robust high pressure processes are witnessing a revival. After 60 years, hydroformylation is just beginning to be a general tool for chemists, and new frontiers and challenges have to be met.

Keywords Hydroformylation · Rhodium · Cobalt · Ligands · Processes · Mechanism

1 Introduction

The reaction between alkenes and synthesis gas (syngas), an equimolar mixture of carbon monoxide and hydrogen, to form aldehydes was discovered in 1938 by Otto Roelen [1, 2]. Originally called "oxo-reaction", "hydroformylation" is the term used today. This reflects the formal addition of formaldehyde to the olefinic double bond. Commercially, homogeneous metal complexes based on cobalt and rhodium are used as catalysts. With more than 10 million metric tons of oxo products per year, this reaction represents the most important use of homogeneous catalysis in the chemical industry.

A typical feature of hydroformylation is the fact that both sides of the double bond are in principle reactive, so only ethene yields propanal as a single product. From propene, two isomers are formed: linear or normal butanal and 2-methylpropanal (branched or iso product). With longer chain 1-alkenes, the isomerization of the double bond to the thermodynamically more favored internal positions is possible, yielding the respective branched aldehydes (Fig. 1). Frequently, terminal hydroformylation is targeted because of the better biodegradability of the products. Thus, not only stability, activity, and chemoselectivity of the catalysts are important. A key parameter is also the regioselectivity, expressed by the n/i ratio or the linearity n/(n+i).

Aldehydes themselves are of little commercial interest, but they open a way to alcohols via hydrogenation, to carboxylic acids via oxidation, and to amines via reductive amination. Aldolization is the starting point for branched alcohols, carboxylic acids, and amines with a double carbon number. As an example of co-aldolization, the route to polyols is shown. All

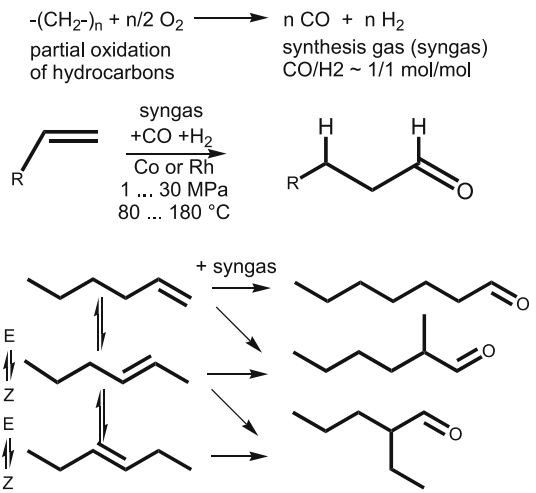

Fig. 1 Basic reactions

reactions shown in Fig. 2 are commercially employed, starting from propene (R = H).

In the beginning, research in hydroformylation was performed mainly by the industry. Remarkably, the number of scientific papers in the past 20 years

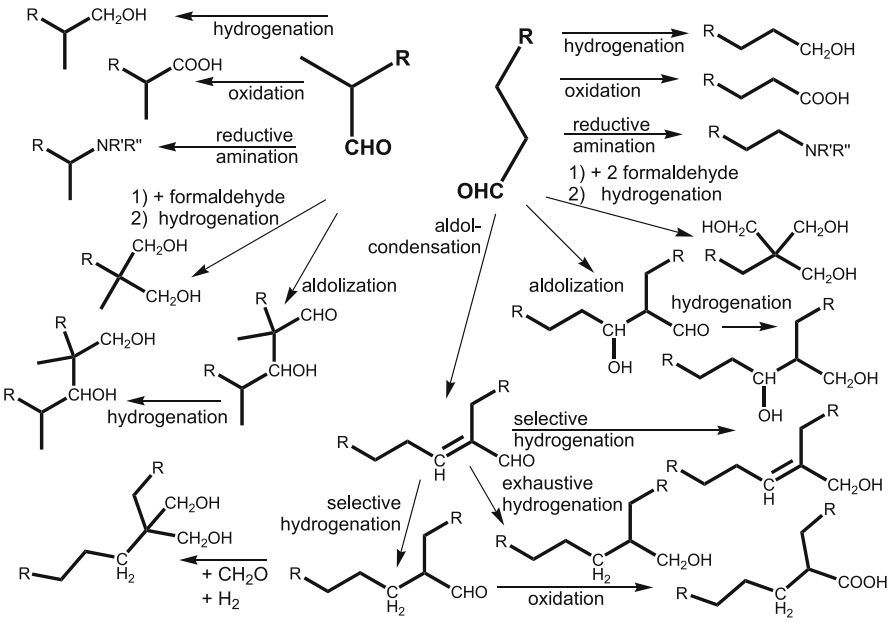

Fig. 2 Overview of uses of aldehydes

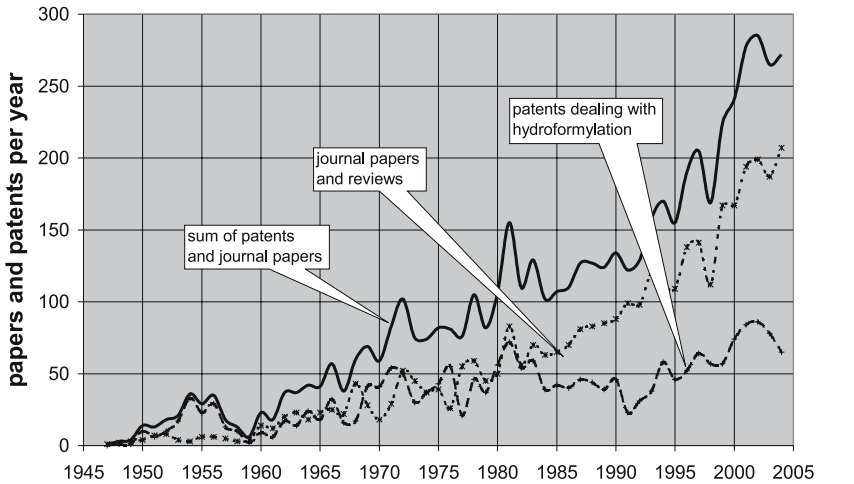

Fig. 3 Literature and patents issued per year

has exploded (Fig. 3) to an output of more than 200 annually, compared to some 80 patents per year.

This brief review can provide only a snapshot of the state of art. The older literature up to 1980 is covered by the still important review by Falbe [3]. A concise overview up to 2002 can be found in Cornils and Herrmann [4]. Hydroformylation with rhodium catalysts is covered by the book of van Leeuwen and Claver [5]. Ungvary reviews new developments in hydroformylation, mainly in scientific papers, every year [6–9].

2 Catalysts

2.1 Active Metals

All metals in the neighborhood of rhodium on the periodic table are known to be active in hydroformylation. Rhodium is by far the most active metal being used in concentrations of 10–100 mg/kg, usually at temperatures below 140 °C. Typical concentrations of cobalt-based catalysts are in the range of 1–10 g/kg at temperatures up to 190 °C to get sufficient space-time yield. Apart from some specialized applications, other metals are only of scientific interest because of their low activity. A proper comparison of metal activity is difficult because of the different requirements on the reaction conditions. A generally accepted rough order of activity is given in Table 1.

The mentioning of exotic hydroformylation catalysts in patents does not reflect their real importance, because it is frequently done for completeness ("metals of Group VIII"). Sometimes cooperative or synergistic effects are claimed when bimetallic catalysts are used. A recent example for manganese/rhodium is found in [10, 11].

Initially, hydroformylation was performed with heterogeneous cobalt catalysts of the Fischer Tropsch type. But very soon it was recognized that the real active species is the homogeneous complex hydridocobaltcarbonyl; H-$Co(CO)_4$, a yellow liquid and strong acid, which above the melting point (– 26 °C) is stable only under CO/H_2 pressure. Decomposition yields $Co_2(CO)_8$, an air-sensitive orange-red solid that in turn decomposes above the melting point (51 °C). Both species are extremely toxic, similar to $Ni(CO)_4$. The higher carbonyl clusters are insoluble solids, representing

Table 1 Activity of metals in hydroformylation

active metal	Rh	Co	Ir	Ru	Os	Tc	Mn	Fe	Re
log(relative activity)	3	0	– 1	– 2	– 3	– 3	– 4	– 6	< – 6

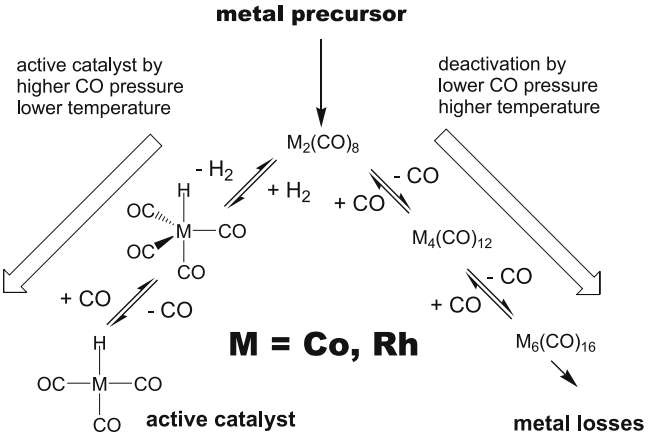

Fig. 4 Formation and deactivation of active species

one pathway of cobalt deposits in hydroformylation plants. The equilibria for the formation and the deactivation of the active species are shown in Fig. 4. Recent reinvestigations have confirmed the picture [12–14].

A similar pattern has always been discussed for rhodium, with hydridotetracarbonylrhodium H-Rh(CO)$_4$ as a real catalyst species. The equilibria between $Rh_4(CO)_{12}$ and the extremely unstable $Rh_2(CO)_8$ were measured by high pressure IR and compared to the respective equilibria of cobalt [15, 16]. But it was only recently that the "missing link" in rhodium-catalyzed hydroformylation, the formation of the mononuclear hydridocomplex under high pressure conditions, has been proven. Even the equilibria with the precursor cluster $Rh_2(CO)_8$ could be determined quantitatively by special techniques [17]. Recent reviews on active cobalt and rhodium complexes, also ligand-modified, and on methods for the necessary spectroscopic in situ methods are given in [18, 19].

2.2
Reaction Mechanism with an Unmodified Catalyst

The first catalyst used in hydroformylation was cobalt. Under hydroformylation conditions at high pressure of carbon monoxide and hydrogen, a hydrido–cobalt–tetracarbonyl complex ($HCo(CO)_4$) is formed from precursors like cobalt acetate (Fig. 4). This complex is commonly accepted as the catalytic active species in the cobalt-catalyzed hydroformylation entering the reaction cycle according to Heck and Breslow (1960) (Fig. 5) [20–23].

The hydrido–cobalt–tetracarbonyl complex **(I)** undergoes a CO-dissociation reaction to form the 16-electron species $HCo(CO)_3$ **(II)**. This structure forms a π-complex **(III)** with the substrate and is a possible explanation for the formation of further (C = C)-double bond isomers of the substrate. In the

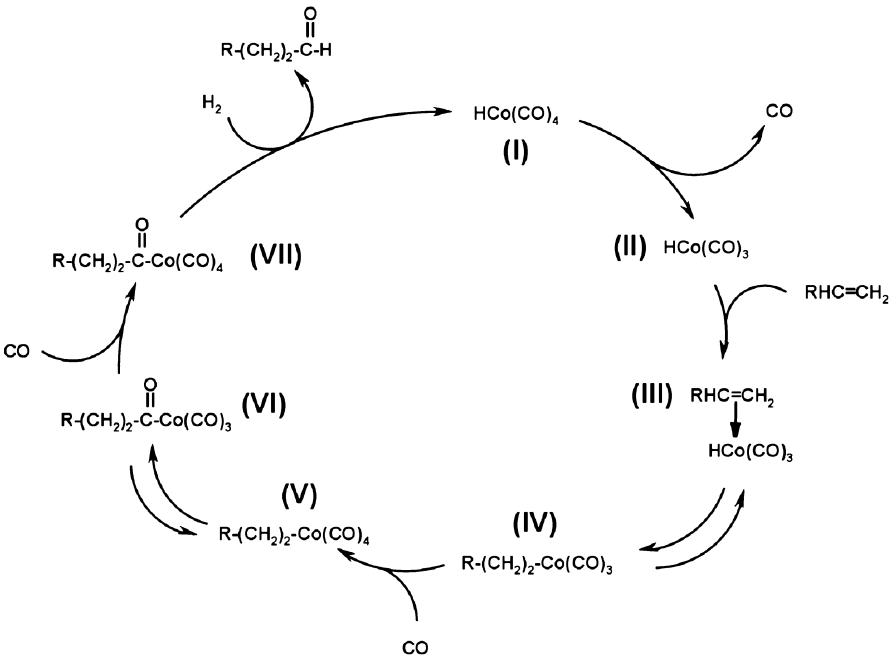

Fig. 5 Cobalt-catalyzed hydroformylation reaction cycle

next equilibrium reaction step, the π-complex is converted into the corresponding σ-complex **(IV),** which has the opportunity to add carbon monoxide to form the 18 electron species **(V)**.

In the next step of the reaction cycle, the carbon monoxide is inserted into the carbon–cobalt bond. At this time, the subsequent aldehyde can be considered as preformed. This step leads to the 16 electron species (**VI**). Once again, carbon monoxide is associated to end up in the 18 electron species (VII). In the last step of the reaction cycle, hydrogen is added to release the catalytically active hydrido–cobalt–tetracarbonyl complex (I). Likewise, the aldehyde is formed by a final reductive elimination step.

The reaction cycle discussed is generally accepted for unmodified cobalt and unmodified rhodium catalysts. But it has to be stressed here that to date no one has been able to prove the single steps conclusively; it is still a subject of research, with modern techniques like in situ spectroscopic methods and molecular modeling in conjunction with kinetic investigations.

2.3 Impact of Ligands on the Reaction Cycle

A fundamental topic in hydroformylation research is the control of regioselectivity and the suppression of side-reactions like the hydrogenation reac-

tion. The possibilities offered by optimization of reaction variables such as temperature and pressure are limited. However, a powerful tool for tuning the catalyst properties is modification with ligands of the type PR_3 (phosphines, phosphites), especially for rhodium.

In the late 1960s, Wilkinson postulated the reaction cycle of the ligand-modified rhodium catalyzed hydroformylation (Fig. 6).

It is also called dissociative because one of the rate-determining steps is the dissociation of carbon monoxide. The cycle is started by the dissociation of a ligand, which results in the release of the planar 16 electron species **(I)**. In analogy to the cobalt mechanism (see Wiese KD and Obst D, 2006, in this volume), the next step is the addition of an olefin molecule to form the π-complex **(II)**. This complex undergoes a rearrangement reaction to the corresponding σ-complex **(III)**. These two reaction steps decide whether a branched or a linear aldehyde is the product of the hydroformylation experiment. The next step is the addition of a carbon monoxide molecule to the 18 electron species **(IV)**. Now, the insertion of carbon monoxide takes place and

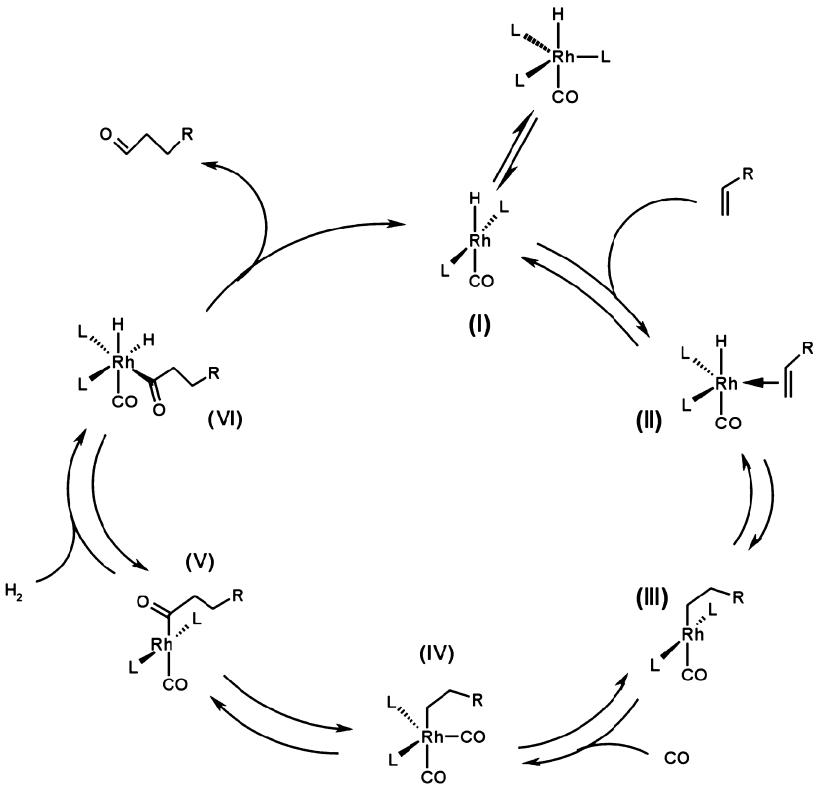

Fig. 6 Ligand-modified rhodium-catalyzed hydroformylation reaction cycle

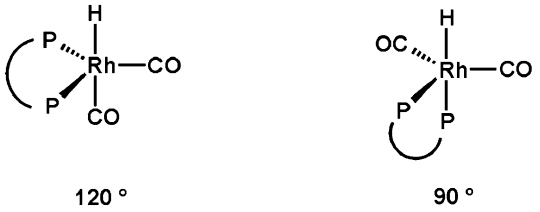

Fig. 7 Two configurations of a bidentate phosphorous ligand with rhodium

the 16 electron species **(V)** is formed. This insertion step determines the final structure of the aldehyde. The hydrogenation to the structure **(VI)** and the reductive elimination of the aldehyde represent the last two steps of the reaction cycle and are analogous to Heck and Breslow's cobalt mechanism.

For monodentate ligands, e.g., triphenylphosphane, Tolman's cone-angle θ and the electronic parameter χ have a significant influence on the activity and the selectivity of the resulting catalyst system [24, 25]. As regards bidentate ligands, which provide two coordination centers for the transition metal, the so-called bite angle β determines the selectivity of the formed aldehydes. β is the angle that is formed by the two coordination centers and the transition metal (Fig. 7).

Van Leeuwen came to the conclusion that the equatorial/equatorial configuration in particular imposes a high linearity on the formed aldehydes [26–29]. Thus, the best selectivities to the linear aldehyde species should be obtained when the bite angle has a value of about 120°. The configuration of the ligand in equatorial/axial positions (bite angle 90°) leads to lower linearity of the formed aldehydes.

2.4 Types of Ligands

The main classes are phosphanes PR_3 and phosphites $P(OR)_3$ (R = alkyl, aryl). Phosphinites and phosphonates are rarely used but represent a transition between the two classes. In principle, a part of the carbon monoxide is replaced by the ligands according to $H\text{-}M(CO)_m(P^*)_n$ (M = Co, Rh; m + n = 3–4). To what an extent a ligand replaces carbon monoxide depends primarily on the equilibrium constant of the ligand and the excess of ligand used. Besides the electronic properties of the substituents, steric properties too, the bulkiness of the ligand, play a decisive role. On the other hand, the carbon monoxide pressure has a strong influence, with higher pressure shifting the equilibrium to the carbon monoxide-rich complexes. Bidentate ligands with appropriate distance of the two P atoms can work like pincers and induce a strong binding effect to the metal. While all these modifications generally apply to classical homogeneous catalysts soluble in the organic phase, the introduction of sulfonic groups gives rise to water-soluble catalysts, which are

applied in "two-phase" systems. The catalyst is then solved in water, whereas the olefin is present in a second organic phase. This short but incomplete overview shows the versatility of ligand-modified catalysis, and an immense number of different ligands were developed. But only a few are of industrial importance.

The hydroformylation of olefins with cobalt, modified by phosphines and phosphites, has been described in a patent from ESSO 1964 [30], but SHELL was the first to apply a ligand-modified cobalt catalyst industrially in 1970. The literature frequently mentions tributylphosphane (Fig. 8, 1a). In fact, a phosphabicyclononane [31] like 1b is presumably used on account of the stability of the complex at high temperatures. In contrast to unmodified cobalt catalysts, the separation of the products by distillation is possible. The main feature is the relatively high regioselectivity of 75–85% linear products, even from internal olefins. The main disadvantage is the extensive build up of high boilers and the low activity in comparison to unmodified cobalt. The catalyst system is still used today by SHELL for the production of surfactant alcohols from internal linear olefins. Recent patents suggest a renewed interest in this type of ligands [32].

The discovery of triphenylphosphane (2a) as ligand by Wilkinson 1965 [33] and the subsequent development of an industrial process in the 1970s represented a break-through for rhodium catalysis. If this ligand is applied in high molar excess to rhodium in the range 100–200, the hydroformylation of terminal olefins becomes highly regioselective. Starting from propene, the formation of the unwanted branched byproduct is suppressed to less than 10%. This ligand has become a standard and is being widely used for hydroformylation, despite new developments. Through sulfonation, complete solubility in water is achieved, and with the ligand, rhodium is transferred to water. This is the basis of the two-phase process developed by Ruhrchemie (today CELANESE), which is discussed later in detail. The ligand has also found widespread interest as regards other homogeneously catalyzed processes (details see [34]).

Phosphite ligands (Fig. 9) are known to be better π-acceptors than phosphane ligands. The stronger electron-withdrawing ligand increases the reaction rate because CO from the metal center is dissociated faster than with phosphane ligands. For different mono-phosphites, the selectivity to the

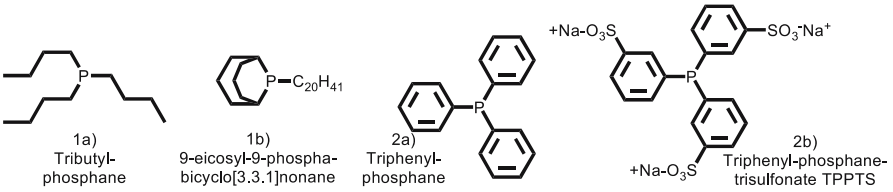

Fig. 8 Commercially used phosphane ligands

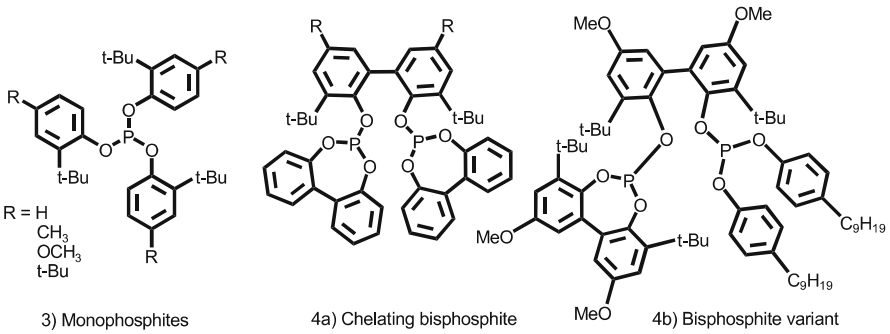

Fig. 9 Commercially used phosphite ligands

linear aldehyde increases with increasing electron-withdrawing properties. Mono-phosphites with a *t*-butyl group in *o*-position (3 in Fig. 9) have received special attention. It has been shown [35] that these ligands are not capable of replacing more than one single carbon monoxide to the complex due to their bulky nature. But with a sufficient molar excess to the metal, they convert at low pressures (e.g., 20–50 bar) inactive rhodium clusters into the highly active complex H–Rh(ligand)$(CO)_3$. The fast isomerization of double bonds is another feature of this type of catalyst. The disadvantage is the low regioselectivity. Starting from terminal olefins, the hydroformylation takes place along the chain at the usual applied temperatures (100–130 °C). On the other hand, internal and branched olefins, which are usually very resistant to hydroformylation, are converted at an acceptable reaction rate. Thus, this type is used industrially in difficult cases if regioselectivity plays no role. Examples are the hydroformylation of branched internal olefin mixtures like "tributene" (trimerized butene-2) [36] and of di- and tricyclopentadiene [37] to dialdehydes as intermediates for diols, dicarboxylic acids, and diamines. Another example is the hydroformylation of methacrylic acid alkyl esters, where only one product is possible, as an intermediate for 3-methylsuccinic acid [38].

Bisphosphites from type 4 (Fig. 9) had been reported in 1956 [39]. In 1987 they were introduced by Bryant [40, 41] as ligands for hydroformylation. Because of their chelating nature, only a low excess of ligand to metal has to be used to obtain highly active chemo- and regioselective catalysts. Selectivities exceeding 95% are obtained starting from α-olefins at lower temperatures and pressures (e.g., 100 °C, 20 bar). This is surprising because they are also strong isomerization catalysts. In 2005 Behr and coworkers published an article on the isomerizing hydroformylation of *trans*-4-octene to linear nonanal in propylene carbonate as a solvent. A linearity of 96% was observed using a catalyst system consisting of $Rh(acac)(CO)_2$ and the BIPHEPHOS ligand (Fig. 9, ligand 4a, R = O – Me) [42]. Rhodium catalysts of type 4 are now the benchmark for hydroformylation of short chain olefins.

Numerous ligands have been developed, and new ones are being reported. Only some arbitrarily selected examples can be given. Chelating bisphosphanes (Fig. 10) give rise to highly regioselective rhodium catalysts. Particularly the sulfonated analogs are a subject of interest for hydroformylation in water. The star is BINAS (6b in Fig. 10), with more than 98% linear aldehyde from propene; the activity is one order of magnitude higher in comparison to the well-known TPPTS (2b in Fig. 8) [43]. With sulfonated XANTPHOS in ionic liquids, a similar regioselectivity is found [44].

Another field of ligand design is the development of isomerizing catalysts for the predominantly terminal hydroformylation of internal olefins (Fig. 11). Introducing electron-withdrawing substituents in NAPHOS (ligand 6a [45, 46]) is an interesting approach. Replacing one biphenol moiety in bisphosphites with salicylic acid and their derivatives yields catalysts with medium regioselectivity but high activity (ligand 9 [47–49]). Structural elements from bisphosphites, with the XANTPHOS backbone, are also a recent development.

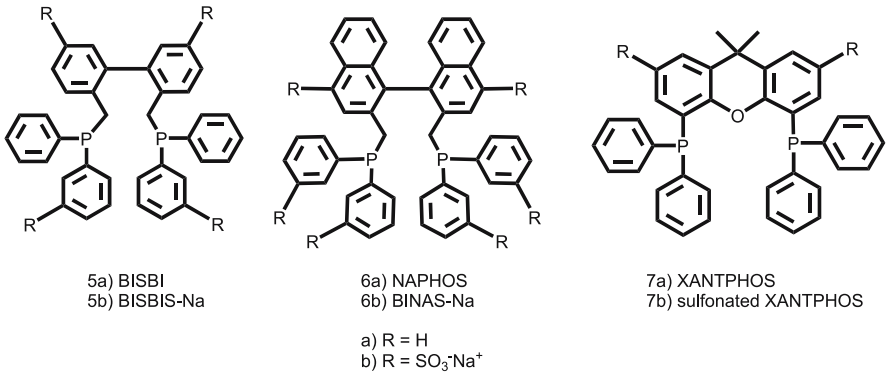

Fig. 10 Some examples of bisphosphines

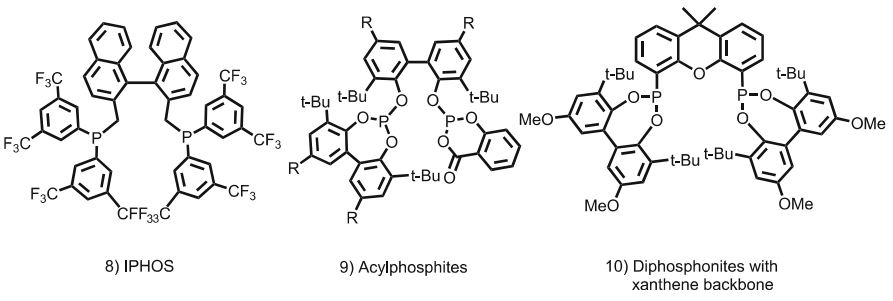

Fig. 11 Some recent developments for isomerizing hydroformylation of internal olefins

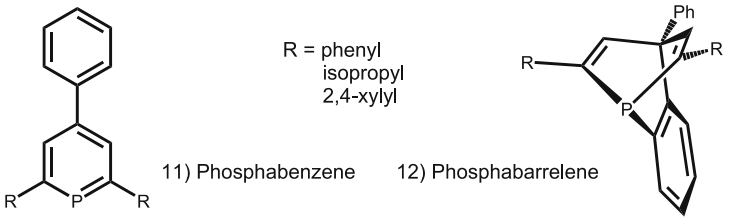

Fig. 12 Heterocyclic P-ligands

A very different line of development (Fig. 12) started from substituted phosphabenzenes as π-acceptor ligands (ligand 11), which yield highly active catalysts for highly resistant branched internal olefins, but with minor regioselectivity [52–55]. Until recently, phosphabarrelenes with very unusual properties were introduced. According to [56, 57] they yield highly active catalysts for the hydroformylation of internal olefins, without isomerizing the double bond.

3
Methods for Mechanistic Investigations

The reaction cycles discussed in Sects. 2.2 and 2.3 are generally accepted, but the validity has not been proven until now; only some intermediates have been characterized. An in-depth understanding of the mechanism is not only important for theoretical considerations, it could be the basis for a more rational design of catalyst systems. A fascinating possibility for gaining an insight is offered by in situ spectroscopic methods (IR, NMR, Raman, XRD, UV). Especially for IR and NMR, methods and techniques have been developed for applying these methods directly in the reaction at realistic pressures and temperatures. Much progress in computational chemistry, supported by the rapidly growing power of computers, offers new possibilities as regards in situ methods. Reaction kinetics are also a tool for gaining an insight into the reaction because it should reflect all the rate-determining steps involved in the reaction.

3.1
In Situ Infra-red (IR) Spectroscopy

A method for observing intermediates directly in the reaction cycle is in situ IR spectroscopy under reaction conditions. As early as 1975, Penninger published a contribution concerning in situ IR spectroscopic studies of cobalt carbonyl modified by tri-*n*-butylphosphine as a hydroformylation catalyst [58] at relatively low catalyst concentrations of 2 mmol l^{-1}. The observed carbonyl

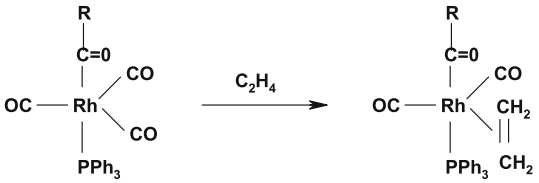

Fig. 13 Interaction of $RC(O)Rh(CO)_4$ with ethene

species were found to be controlled by the following equilibria:

$$H_2 + Co_2(CO)_8 \rightleftharpoons 2\,HCo(CO)_4$$
$$Co_2(CO)_8 + PBu_3 \rightleftharpoons Co_2(CO)_7(PBu_3) + CO$$
$$Co_2(CO)_7(PBu_3) + H_2 \rightleftharpoons HCo(CO)_4 + HCo(CO)_3(PBu_3)$$
$$HCo(CO)_4 + PBu_3 \rightleftharpoons HCo(CO)_3(PBu_3) + CO$$

Twenty-five years later, the observation of the respective olefin rhodium intermediate **(III)** in Fig. 6 was successful using in situ IR-techniques [59]. In 2003, George investigated the hydroformylation of 1-octene, 1-butene, propene, and ethene using in situ IR in combination with a polyethylene matrix [60]. Using $Rh(acac)(CO)_2$ as a metal precursor and triphenylphosphine as the ligand, he observed the acyl intermediates of rhodium tricarbonyl triphenylphosphine. The IR spectra suggested a trigonal bipyramidal structure, with the acyl ligand and the PPh_3 occupying the axial positions (Fig. 13). The investigations showed that one carbon monoxide can easily be replaced by ethene.

In 2004 Caporali investigated the hydroformylation of 1-hexene and cyclohexene using $HRh(CO)(PPh_3)_3$ [61]. The collected data indicated that the rate-determining step in the hydroformylation cycle depends upon the structure of the olefin. With an alpha-olefin like 1-hexene, the slowest step seems to be the hydrogenolysis of the acyl rhodium complex. In the presence of cyclohexene as a model for an internal olefin, the rate-determining step is the reaction of the olefin with the rhodium hydride complex (intermediate **II** in Fig. 6).

3.2 In Situ Nuclear Magnetic Resonance (NMR)

Further information on the reaction intermediates is achieved by in situ NMR experiments. Because the signals in NMR spectra depend upon the concentration of the investigated species, a quantitative treatment is possible. Bianchini and coworkers investigated the hydroformylation of 1-hexene [62], using high-pressure NMR spectroscopy to evaluate the influence of synthesis gas on the equilibria of rhodium triphenylphosphine species. They were able to establish at least four resting states of rhodium (catalyst species that do not participate directly in the reaction). When synthesis gas interacted with

the reaction mixture, several new NMR signals appeared. The group was able to point out that the $[HRh(CO)(PPh_3)_3]$ complex was transformed into the five-coordinated $[HRh(PPh_3)_2(CO)_2]$ complex. A signal corresponding to the $[Rh(acyl)(CO)_2(PPh_3)_2]$ was also present in the reaction mixture. Another interesting contribution was published by Kent as early as 1987 [63]. He was able to show that the $[HRh(PPh_3)_2(CO)_2]$ complex performs a fast change in configuration. The ligands can coordinate in two different ways: equatorial/equatorial (ee) or equatorial/axial (ea).

3.3 Theoretical Methods

Since a detailed characterization of the reaction cycle was not successful until now solely by experimental means, many researchers have turned to computational chemistry as a complementary source of information. The ultimate goal of these theoretical studies is to provide unbiased and easily quantifiable parameters for the description of ligand properties that correlate with the performance of the catalytic system.

Probably the most studied single theoretical parameter in Rh-catalyzed hydroformylation is the so-called "natural bite angle" introduced by Casey and Whiteker in 1990 [64]. Conceptually, this quantity represents the preferred chelation angle determined with reference only to the ligand backbone and not to metal valence angles. It is determined by molecular mechanics calculations in which a "dummy" atom is used for the metal atom and a typical metal–P bond length is chosen from the X-ray structures of similar complexes. The force constant of the P–metal–P angle is set to zero, which means that the structure is determined only by the organic part of the ligand. The results depend on the metal–P distance employed and the force field used. Casey and Whiteker furthermore introduced the quantity "flexibility range", the interval of angles showing energy values differing by less than 3 kcal mol^{-1} from those of the natural bite angle. Dierks and van Leeuwen have shown that the bite angles of a large number of different complexes determined by X-ray structures show values within the calculated flexibility range [65]. However, one must bear in mind that different force fields may produce significantly different values of natural bite angles; in some cases, significant deviations from crystal structure values are therefore to be expected. In the majority of investigations, a wider bite angle correlates with a higher regioselectivity for the linear aldehyde (see e.g., [66]). Catalysts that do not fit in this correlation are reported independently by Casey and Whiteker [67] and Yamamoto et al. [68], who found low selectivities for the 2,5-dppm-nor ligand with a calculated bite angle of 126°. This seems to be related to the inability of this ligand to form stable chelates. For a review of natural bite angle effects, we refer to [69]. Despite the successful application of structure activity relations based on the natural bite angle, a rationaliza-

tion of the quantity has proven difficult. The question of why a wide bite angle favors normal aldehydes has not yet been answered. Further heuristic approaches are reported by Röper et al. [70] and by Franke et al. [71], but are highly specialized.

One of the most useful features of modern quantum chemical calculations is the localization and characterization of stationary points on those parts of a potential energy surface that are associated with a chemical reaction. The first ab initio calculation of the whole catalytic cycle for ethene in the presence of PH_3-ligated Rh was presented by Morukuma et al. [72]. Rocha and Almeida studied the insertion of propene into the Rh – H bond for the $HRh(CO)(PH_3)_2$ catalyst on the MP4(SDQ) level (geometries: DFT-BP86) [73]. The ratio of normal to branched aldehydes was determined (theory: 96 : 4; experiment: 95 : 5) based on the relative energies of the metal-alkyl compounds formed after the insertion step. Decker and Cundari presented a thorough reinvestigation of this model catalyst employing DFT with B3LYP for the geometry optimization and CCSD(T) single-point calculations for the energy profile [74]. The CO insertion step was predicted to be the rate-determining step with the activation barrier calculated to be 20.4 kcal mol^{-1}. Herrmann et al. investigated a variety of catalysts of more practical importance using a loosely coupled QM/MM approach [75]. The calculated relative energies of transition states were in accordance with the different regioselectivities of the BISBI and DiPHOS catalyst.

For the family of XANTPHOS ligands, both detailed experimental studies and theoretical mechanistic investigations have been published. These show that the natural bite angles of diphosphines derived from xanthene and related compounds range from 102 to 121° [76]. Bo et al. reported on QM/MM calculations with the IMOMM method for benzoxantphos and homoxantphos [77]. Eight possible reaction paths were characterized through the respective transition states of the pentacoordinated equatorial–equatorial HRh(CO)(alkene)(diphosphine) intermediate. The predicted regioselectivity corresponds to the experimentally observed trends. By artificially suppressing the steric effects of phenyl substituents, different contributions to the regioselectivity can be calculated, leading to the conclusion that the nonbonding interaction between diphenylphosphino substituents and the substrate is responsible for this selectivity. To date, by far the most extensive and thorough quantum chemical study concerning the Rh-catalyzed hydroformylation of propene is that performed by Landis and Uddin, who investigated the complete catalytic cycle for the XANTPHOS ligand [78]. Using the two-layered ONIUM method (DFT-B3LYP : HF), they located 56 stationary points along the reaction pathway, of which more than 20 represent transition states relevant to the catalyst mechanism. As discovered in experimental studies, they predicted that the resting state of the catalyst is a mixture of diequatorial and axial–equatorial isomers. Their computed ratio of normal- and iso-propyl Rh-alkyl also agrees well with comparable experimental values. However, the

activation free energies, in particular those for insertion of propene into Rh – H bonds, are computed far too high. Consequently, any insights into the kinetics of hydroformylation are precluded. Landis and Uddin speculate that the reasons may lie either in a wrongly computed mechanism or in deficiencies of the DFT method. By comparing the results from the high level ab initio calculations of Decker and Cundari [74], they come to the conclusion that the latter is more likely.

The desired accuracy of the thermodynamic and kinetic activation parameters in systems of commercial interest has not yet been achieved in quantum chemical studies of the hydroformylation. Nevertheless, theoretical investigations have cast considerable light on this still little understood catalytic reaction.

3.4 Kinetic Investigations

The investigation of the kinetic aspects of hydroformylation is still an underdeveloped field. The reason is the complexity of the reaction, especially with ligand-modified catalysts. The reaction rate r will certainly depend on temperature T and on the following concentrations:

$\mathbf{C^o}$ (catalyst metal), $\mathbf{C_S}$ (substrate olefin), $\mathbf{C_{CO}}$ (carbon monoxide),

$\mathbf{C_{H2}}$ (hydrogen), $\mathbf{C_L}$ (ligand)

Because hydroformylation is a gas-liquid two-phase reaction, the active concentrations of CO and H_2 in the liquid reaction medium are dependent on the respective partial pressures in the gas phase. If we assume the validity of the simple Henry equation, and if we further assume that mass transfer from the gas to the liquid phase can be neglected, the gas concentrations can be substituted by the partial pressure p_i

$$C_{CO} = (K_{CO})^* p_{CO} \quad \text{and} \quad C_{H2} = (K_{H2})^* p_{H2}$$

the constants K_i being modified inverse Henry constants. The gas solubilities are dependent on solvent and temperature, so in any case the solvent has a systematic influence apart from other solvent effects. According to the mechanism, the catalytic cycle is initiated by a carbon monoxide-deficient hydridocarbonyl forming a π-complex with the starting olefin. A simplified scheme of the possible equilibria is shown in Fig. 14, with the active catalyst species entering the reaction cycle in row 1. For the simple case of unmodified catalysis, only the equilibria in column A are relevant. The total concentration of the catalyst metal C^o is given by the sum of all species in equilibrium, active or not. If we assume sufficient pressure, the concentration of inactive clusters can be neglected, the metal concentration can be approximated by

$$C^o = (C_{A1} + C_{A2} + 1/2C_{A3} + \ldots)(C_{A1} + C_{A2}) \,. \qquad (1)$$

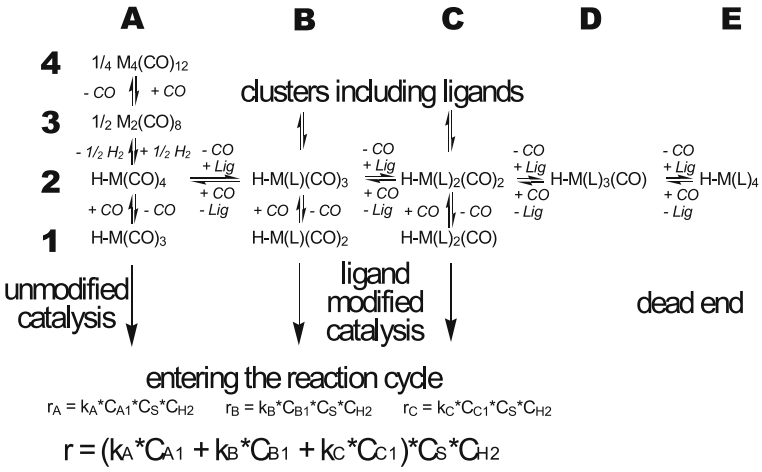

Fig. 14 Preequilibria in hydroformylation

C_{A2} is given by the equilibrium A2/A1, with the equilibrium constant $K_{A2A1} = C_{A2}/(C_{A1}{}^{*}C_{CO})$. Substituting the carbon monoxide concentration by the partial pressure and applying Eq. 1 yields

$$C^{o} = C_{A1} + K_{A2A1}{}^{*}C_{A1}{}^{*}K_{CO}{}^{*}p_{CO} = C_{A1}{}^{*}(1 + K_{A2A1}{}^{*}K_{CO}{}^{*}p_{CO})\,. \tag{2}$$

Solving for the very low concentration of the active species A1 entering the reaction cycle, we get

$$C_{A1} = C^{o}/(1 + K_{A2A1}{}^{*}K_{CO}{}^{*}p_{CO})\,. \tag{3}$$

In almost all kinetic investigations it is found that hydroformylation is first order in substrate and hydrogen concentration. This suggests slow steps in the reaction cycle involving olefin and hydrogen, and the reaction rate r_A becomes

$$r_A = k_A{}^{*}K_{H2}{}^{*}C^{o}{}^{*}C_S{}^{*}p_{H2}/(1 + K_{A2A1}{}^{*}K_{CO}{}^{*}p_{CO})\,. \tag{4}$$

At high pressure, the inhibition term is $K_{A2A1}{}^{*}K_{CO}{}^{*}p_{CO} \gg 1$, and the equation is simplified to the well-known and accepted Natta equation for hydroformylation with unmodified catalysts (all constants combined in k'_A)

$$r = k'_A{}^{*}C^{o}{}^{*}C_S{}^{*}p_{H2}/p_{CO}\,. \tag{5}$$

Lowering the carbon monoxide pressure should result in higher concentrations of the active species A1 and hence higher reaction rate according to Eq. 5. But by destabilization of the intermediate species A2, the equilibria are also shifted to the carbon monoxide-deficient clusters. Higher clusters like A4 and $M_6(CO)_{16}$ cannot be neglected in Eq. 1, and even become the predominant species. This lowers the concentration of A2/A1 and hence the reaction

rate, but is also the starting point for extensive metal losses, because higher clusters are insoluble and are withdrawn from the equilibrium.

The introduction of ligands changes the picture because stable complexes are formed with the metal as depicted in Fig. 14, Row 2. Of course the equilibria can also be defined between, e.g., A1–B2 or A1–B1 and so on, but this yields the same results, all equilibria being interconnected. The first lesson is the fact that even at lower pressures, the pressure independent concentration of the ligand will diminish the cluster concentration, yielding complexes in the range of column B and C.

The exact action on the reaction rate depends on the characteristics of the ligand. If a ligand has a strong tendency for complexation, even a slight molar excess in relation to the metal will drive the equilibrium to the species B2–B1 (Fig. 14). If a big excess is chosen, the equilibria will be forced completely to the right yielding stable complexes. This is well known for the most used ligand triphenylphosphane, tpp. The hydridocomplexes H–Rh(CO)$(tpp)_3$ and H–Rh$(tpp)_4$ are commercially used precatalysts because of their stability. In respect to hydroformylation, they are a "dead end", if the ligand is used in a very high excess to force the equilibrium completely to the right (columns D, E). If a very strong ligand is used, even a small excess can kill the hydroformylation activity. Assuming a ligand excess driving the equilibrium to B2 as the main species in equilibrium with A2 and C2, the reaction rate will be determined mainly by $r_B = k_B * C_{B1} *$[kinetic term]. Using the equilibria between the main species as shown in Eqs. 1–5 yields the following expression for the reaction rate (Henry constants already included in the equilibrium constants):

$$r_B = k_B * C^o * [\text{kinetic term}]/[1 + K_{A2B1} * (p_{CO})^2 / C_L + K_{B2B1} * p_{CO} + K_{C2B1} * C_L] \,. \tag{6}$$

At very low ligand concentrations, $K_{A2B1} * (p_{CO})^2 / C_L \gg 1$ becomes the predominant expression in the inhibition term and Eq. 6 can eventually be simplified to (k'_B modified constant including the equilibrium constants)

$$r_B = k'_B * C^o * [\text{kinetic term}] * C_L / (p_{CO})^2 \,. \tag{6a}$$

Even if the simplification is not applicable, $1/C_L$ in Eq. 6 will have the accelerating effect of raising the ligand concentration in the reaction rate. Care has to be taken, because in this case appreciable amounts of unmodified catalyst can already be present, so the unmodified reaction r_A can also play a role, but usually the predominant effect is driving inactive clusters from column A in Fig. 14 to the active species in column B. On the other hand, at very high concentrations of ligand, $K_{A2B1} * (p_{CO})^2 / C_L$ becomes small, and $K_{C2B2} * C_L$ in Eq. 6 becomes predominant. This means that high ligand concentrations will shift the reaction from B to C and maybe to the dead end: the reaction rate slows down. If we now assume further that complexes with ligand/metal ra-

tios greater than 1 favor the formation of linear products, the model describes the well-known behavior of rhodium modified by triphenylphosphane in the hydroformylation of propene. At low triphenylphosphane concentrations the rate of reaction is accelerated and reaches a maximum at a molar ratio of tpp/Rh approx. 8–10. In the same range the portion of linear butanal rises significantly. Further rise in the tpp/Rh ratio of up to 50/1 slows the reaction rate to about 1/4 of the initial rate, and the maximum regioselectivity is reached.

A special case are bulky monophosphite ligands from the type shown in Fig. 15, which were intensively studied by the group of van Leeuwen [5]. Because of their bulkiness, only one ligand can coordinate to the metal, even if binding is very strong or a high excess is used. This means that at high ligand concentrations, the complete metal is transferred from the cluster region A to B. Because no further ligand can block the reaction, Eq. 6 is simplified to

$$r_B = k_B * C^o * [\text{kinetic term}]/[1 + K_{A2B1} * (p_{CO})^2/C_L + K_{B2B1} * p_{CO}] . \qquad (6b)$$

With the phosphite shown in Fig. 15, the reaction rate is accelerated by a factor of 20 compared to the unmodified rhodium catalyst at the same reaction conditions (e.g., 120 °C, 40 w – ppm Rh, molar ratio ligand/Rh up to 50, 50 bar synthesis gas; own unpublished results). But regioselectivity is low, not much better than with unmodified rhodium.

Another special case are bidentate ligands. With an appropriate distance of the two phosphorus atoms, they bind the metal like pincers (chelate structure), shifting the equilibria in Fig. 14 directly to column C. Those ligand systems are known to be appreciably slower than the corresponding bulky monophosphites, but highly regioselective (e.g., ligand 4 in Fig. 9).

It has already been mentioned that usually a first order kinetics with respect to substrate concentration is found. This would be consistent with the

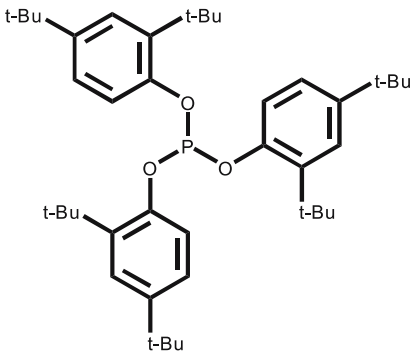

Tris- (2,4-di-*tert*-butyl-phenyl) phosphite

Fig. 15 Bulky phosphite

first step, the insertion of the olefin, as a rate-determining step. The frequently reported first order in hydrogen is also surprising, because according to the accepted reaction mechanism, hydrogen is involved in a very late step. Empirically, it is appropriate in most cases to set [kinetic term] = $C_S * P_{H2}$, but it is an example waiting for clarification, e.g., by in situ methods.

It should be noted that the discussion is valid only for simple reactions like the hydroformylation of cyclohexene and cyclooctene, where only one product can be formed irrespective of the possibility that, in parallel to hydroformylation, isomerization of the olefinic double bond can take place. The extension to propene hydroformylation is still feasible assuming a parallel formation of the two isomers. For higher olefins, a whole set of reactions has to be solved including isomerization reactions. It has also to be stressed that the discussion was very simplified with regard to the main features. To solve such complex networks of reactions, huge data sets of kinetic measurements are needed over a broad range of all relevant parameters. This is one reason a comprehensive investigation of the kinetics of hydroformylation is still lacking.

A review about kinetic investigations in hydroformylation is given in [4]. Detailed information about solving complex reaction networks with many examples on hydroformylation is found in the excellent book by Helferich [80].

4
Industrial Application of Hydroformylation

4.1
Basic Process Principles

In Fig. 16 a general representation of the reaction section of a hydroformylation process is given. The first step A is a thorough mixing of the reaction partners, olefin, synthesis gas and catalyst solution. Spargers for synthesis gas, static mixers, or nozzle mixers are used. The design of the reaction section B depends mainly on the kinetics of the process. If the reaction is relatively slow (space–time yield in the magnitude of 0.1 mt m^{-3} h^{-1}), stirred tanks are normally used. For faster reactions, tube reactors are more suited like bubble columns, often equipped with internals like perforated plates to maintain an efficient mixing of liquid and synthesis gas. Because of the enormous heat of reaction, internal heat exchangers are usually used. Industrially, hydroformylation is always conducted under pressure (dependent on catalyst system 15–300 bar). The pressure has to be released (C) to a gas-separation step. Now the liquid reactor effluent is separated from the catalyst (D) and is further processed. The options for recycling unconverted synthesis gas and unconverted olefins are shown for completeness. All steps are more or less

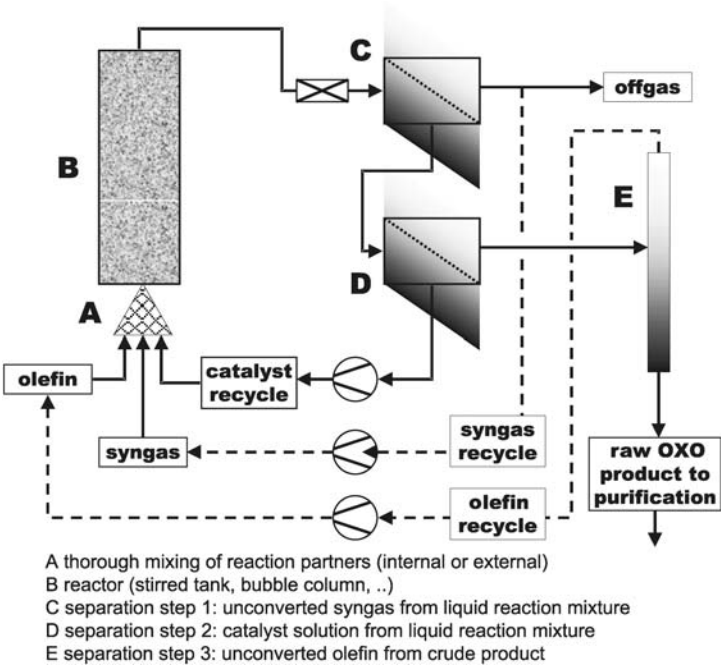

Fig. 16 General scheme of an OXO process

conventional engineering problems, with exception of step D, the separation of the solved catalyst from the liquid products for recycle. The solution of this problem is characteristic for all processes applied in industry and will be discussed in more detail in Sect. 4.3.

4.2 Enemies of the Catalyst

Before discussing the existing technical solutions to the problem of the catalyst recycle, an unscientific topic should be addressed: The problem of catalyst losses. This is obvious, especially in rhodium-catalyzed processes, because of its high price (Fig. 17). Assuming a loss of only 1 ppm (1 mg/kg of product), this would correspond to a loss of 400 kg/Rh, or about € 16 million per year on the current price basis of rhodium for a world scale 400 kt plant. If ligand modified catalysts are used, this has also to be considered. Assuming typical data, e.g., molecular weight of ligand 1000 g/mol, a ratio of ligand/Rh approx. 10/1 mol/mol and a price of about € 500 per kg for exclusive synthesis of a not too sophisticated bidentate ligand, the corresponding loss of ligand would be 40 metric tons a year or € 20 million. This simple beer mat calculation shows the problem: Losses have to be minimized far below the ppm

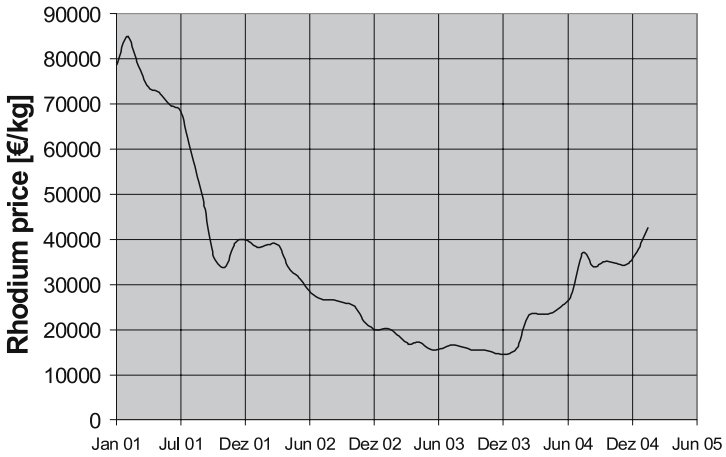

Fig. 17 Rhodium price bulk – monthly average 2001–2005

level. From available data, the average consumption of all rhodium-based oxo processes can be estimated with 50–100 mg/mt of products.

Going around the reaction system in Fig. 16, the first problem are poisons for rhodium such as traces of sulfur compounds in the raw materials. 3 valent P-compounds as ligands are highly prone to oxidation according to $PR_3 + [O] \rightarrow O{=}PR_3$. In a continuous process, even traces of peroxides in the starting olefin and traces of oxygen in the synthesis gas accumulate over the time, so meticulous purification steps are a must if ligand-modified rhodium catalysts are used.

At higher temperatures and lower pressures, deactivation by cluster formation and plating out of metal in the reactor can occur, which can be partly met by applying high concentrations of ligand if possible. On the other hand, reactive deactivation of the ligand itself is an issue in the reaction section. Saponification of the ligand in the case of phosphites by traces of water, generated by aldol condensation of aldehydes, yields free acid. Because saponification is catalyzed by acids, an autocatalytic process is initiated.

After depressurizing and separating the off gas, the stabilizing carbon monoxide is missing, and cluster formation becomes the major way for losses as shown in Figs. 4 and 14. The most dangerous part is the separation step for the *catalyst*, especially if vacuum distillation has to be used in case of higher boiling products. Not only cluster formation of rhodium has to be considered, thermal stress also destroys the ligand.

Before catalyst recycling, a small purge stream is inevitable to avoid an accumulation of high boilers like aldolization products and an accumulation of deactivation products of the ligands. With the purge stream, the catalyst may also be lost.

In principle, with cobalt catalysts similar pathways for deactivation exist. Because of the low price of cobalt compared to rhodium, this is less important in unmodified cobalt catalysis, but the deposition of cobalt clusters and metallic cobalt can cause nozzles and valves to plug up, resulting in the shutdown of the plant. In case of a ligand-modified cobalt catalysis, the same problems of ligand deterioration e.g., by oxygen and peroxides, arise, necessitating a meticulous purification of the starting materials.

4.3 Hydroformylation of Lower Alpha-Olefins

Butanal by hydroformylation of propene is the most important oxo product in terms of volume. Six million metric tons per year of butanals were consumed in 2003, vis-à-vis a capacity of 7.6 million metric tons. Highly chemo- and regioselective processes based on ligand-modified rhodium catalysts have been developed and replaced the original cobalt high pressure technology.

The first application of a rhodium-ligand system was realized in the LPO-process (low pressure oxo Fig. 18). Huge stirred tank reactors are used, equipped with internal heat exchangers to control the heat of reaction. The solution of the catalyst recycle is simple but efficient. The catalyst remains in the reactor, products and unconverted propene are stripped by a huge excess of synthesis gas. Because of strong foaming, only a part of the reaction volume is used. After the gas has left the reactor, the products are removed by condensing, the big part of synthesis gas is separated from the liquid products and recycled via compressors. The liquid effluent of the gas-liquid separator

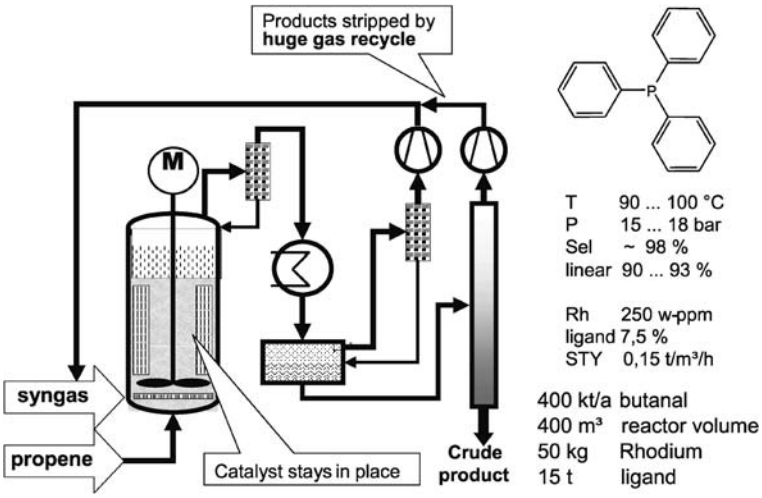

Fig. 18 Low pressure oxo process with gas recycle

still contains propene and some synthesis gas, which are removed in a column for recycle.

As ligand triphenylphosphane tpp is used in large molar excess to rhodium, up to 250/1 to shift the equilibrium of the complexes far away from the clusters to H-Rh(CO)(tpp)$_3$. This is necessary to stabilize the complex and to minimize the side reaction to the unwanted branched 2-methylpropanal (isobutyraldehyde) to less than 10%. But the reaction rate is lowered by the huge excess of ligand. The space–time yield is approximately 0.15 mt m^{-3} h^{-1} (liquid volume), 0.10 mt m^{-3} h^{-1} with regard to the complete reactor volume. This process, developed by UCC, has been licensed all over the world and is still in use today. The very simple and hence elegant process is applicable only to hydroformylation of propene because of the low boiling point of butanal (75.7 °C). For higher aldehydes with higher boiling points, the huge gas recycle required to strip the products is uneconomical.

The latest version of the LPO process is the distillative separation of the products (Fig. 19). The catalyst remains solved in a high boiling solvent, usually the high boiling byproducts of the reaction itself. Because the reaction section is not changed, a *revamp* of older LPO plants with gas recycle is possible. With the small gas recycle left, foaming in the reactor no longer is a problem, and the whole reactor volume can be used pushing up the productivity. The real break through for this process was the introduction of the new class of bisphosphite ligands with unrivaled chemo- and regioselectivities.

This process is also applicable to hydroformylation of 1-butene to produce pentanal with high linearity of approx. 98%, if bisphosphite ligands are used. In contrast to phosphanes monophosphite/rhodium catalysts often

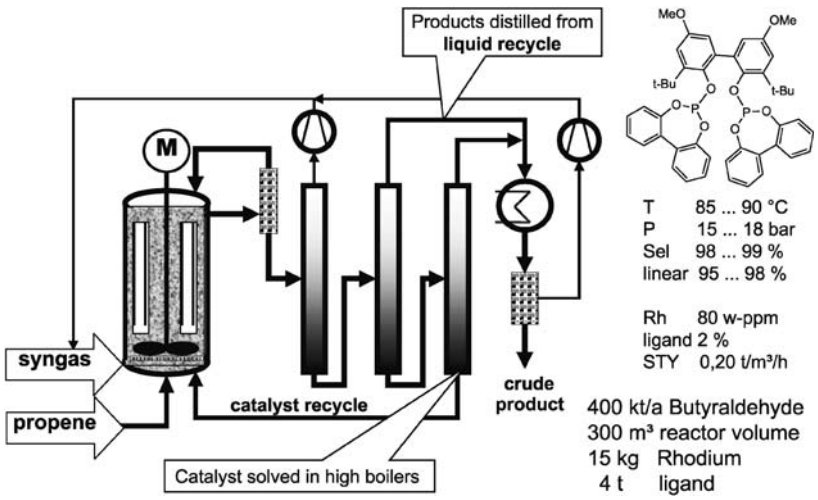

Fig. 19 Low pressure oxo process with liquid recycle

exhibit a strong isomerization tendency for double bonds at temperatures greater than 100 °C. Normally, this is a disadvantage, giving high yields of branched products by hydroformylation of internal double bonds. Bisphosphite/rhodium complexes are also very active in isomerization, but extremely slow in the hydroformylation of internal double bonds. Through this feature, hydroformylation of 2-butene yields high selectivities of greater than 90% for the linear pentanal, though with lower activity. Technical C4-cuts like raffinate II (typically in the range 40% 1-butene, 30% 2-butene, 30% saturated C4) can be used to produce pentanal with approx. 95% regioselectivity. Aldol condensation with subsequent hydrogenation is a way to 2-propylheptanol, a plasticizer alcohol (Sect. 4.4).

A completely new design (Fig. 20) for the catalyst recycle was introduced in the 1980s by Ruhrchemie (now Celanese) on the basis of an older patent of Kuntz from Rhône Poulenc. By careful sulfonation of the original ligand triphenylphosphane at low temperature complete water solubility is achieved, and with the ligand, rhodium is also transferred to the water phase by complexation. The products being sparingly soluble in the aqueous catalyst phase, separation from the products is achieved by simple settlers. The separation step is simplified enormously in comparison to distillation techniques. The reaction section is more sophisticated: Synthesis gas, liquid propene, and liquid aqueous catalyst phase have to be contacted very efficiently, so multistage stirrers are used. Because of the low solubility of propene in the catalyst phase, higher pressure and higher temperature have to be applied and also higher catalyst concentrations. Additionally, an excess of catalyst phase is necessary, the ratio of aqueous product phase being in the range 5–10. The

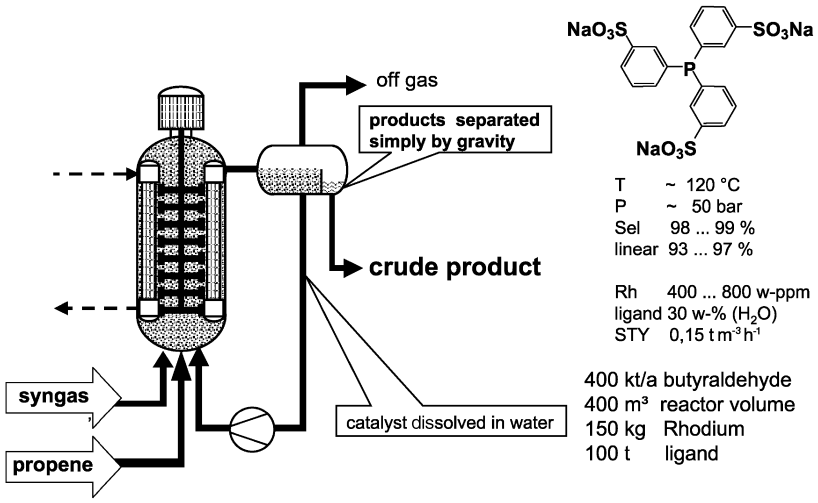

Fig. 20 Two-phase process of Ruhrchemie/Rhône Poulenc

space–time yield is similar to the other processes, again huge reactors of approx. 100 m^3 for 100 kt y^{-1} of butanal are in use. The chemoselectivity is excellent. The somewhat lower regioselectivity of approx. 95% is not a problem, if the byproduct isobutyraldehyde is used, e.g., for production of neopentylglycol, which has a growing market. The process has been reviewed many times, a very recent one is found in [81].

Because the thermal separation of products has been substituted by a liquid–liquid separation, the two phase technology should be best suited for hydroformylation of longer chain olefins. But with rising chain length of the olefins the solubility in the aqueous catalyst phase drops dramatically and as a consequence the reaction rate. Only the hydroformylation of 1-butene proceeds with bearable space–time yield. This is applied on a small scale for production of valeraldehyde starting from raffinate II. Because the sulfonated triphenylphosphane/rhodium catalyst exhibits only slow isomerization and virtually no hydroformylation of internal double bonds, only 1-butene is converted. The remaining raffinate III, with some unconverted 1-butene and the unconverted 2-butene, is used in a subsequent hydroformylation/hydrogenation for production of technical amylalcohol, a mixture of linear and branched C5-alcohols.

Efforts to develop more active water-soluble sulfonated ligand systems have been successful (BISBIS, BINAS; see Fig. 10 and [81]). They were never used industrially, presumably because of too high production costs of the ligands. Another approach is the application of surfactants to produce microemulsions with high mass transfer area. The use of unusual polar nonaqueous solvents is a more recent field of intense research. The application of poly(ethylene glycol) instead of water to achieve higher solubility of the olefins is well known, but catalyst losses and lower regioselectivity are a drawback. Another approach is the use of fluorinated solvents for biphasic catalysis, and special ligands (e.g., fluorinated) are developed. The use of ionic liquids is a top subject. These and other alternative concepts are reviewed in [81]. To date, no major breakthrough to technical realization is visible.

A different engineering approach to the two-phase process (Fig. 20) was the application of a tube reactor, equipped with high surface internals, e.g., static mixers like Sulzer SMV (Fig. 21, see [82–84]). Very high linear velocities of the aqueous catalyst phase are applied up to 0.5 m s^{-1}, corresponding to a residence time (time for reaction) of only 2 s m^{-1}, and the catalyst phase is applied in up to 100-fold excess to the olefin phase. Without changing the other process parameters (temperature, pressure, catalyst concentration), a very high reaction rate results. This cannot be explained solely by the high mass transfer area and the shear stress generated by the internals and the high load. It is assumed that the process has been shifted from the diffusion controlled regime near to the kinetic regime, to a quasi homogeneous reaction. Modeling of the kinetic including mass transfer resulted in a complete description of all data obtained in the pilot plant.

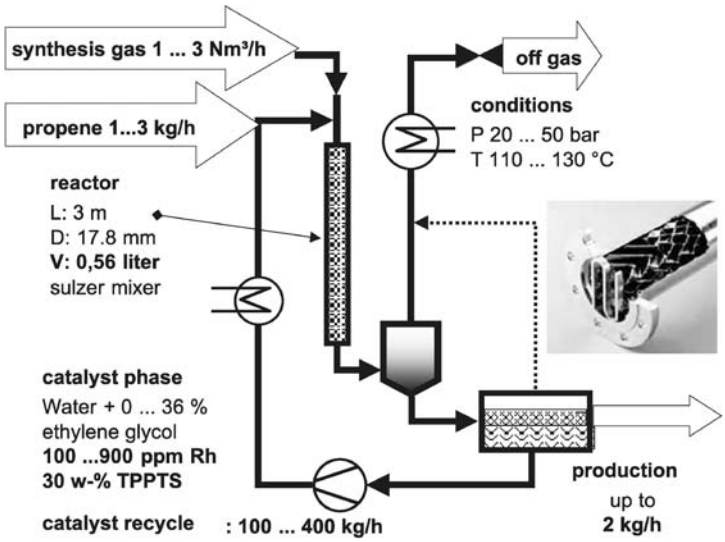

Fig. 21 Two phase hydroformylation with static mixer

By adding up to 36% ethylene glycol to the aqueous catalyst phase, the space–time yield could be boosted up to approx. 3 mt m^{-3} h^{-1} for propene hydroformylation, a factor of 20 in comparison to the conventional two-phase process without changing the reaction conditions. Because of this surprising speed-up, higher alpha-olefins up to 1-octene are converted with high to acceptable space–time yield (Fig. 22). Up to date this process is not commercialized, but has been tested in a continuous pilot plant.

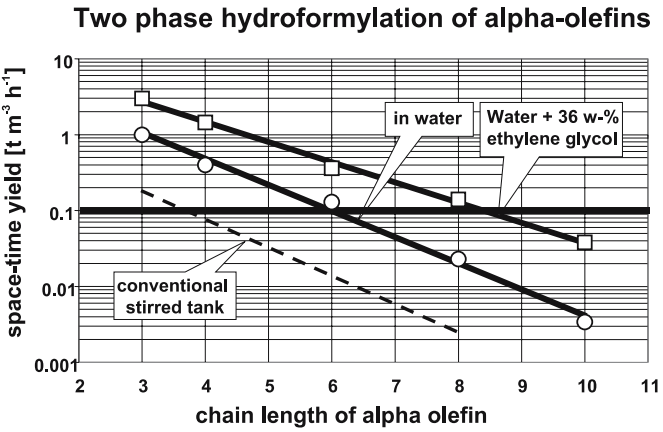

Fig. 22 Static mixer reactor for two-phase process: Comparison with conventional stirred tank

4.4 The Challenge: Higher Internal and Branched Olefins

Plasticizer alcohols in the range C8–C13 are the biggest market for oxo-products accounting for $> 4000\,kt\,y^{-1}$. Within this group 2-ethylhexanol is still the working horse with $3000\,kt\,y^{-1}$ in 2004, but the importance of other higher alcohols is growing. The main routes are depicted in Fig. 23. The traditional raw material is propene. Aldol condensation of butanal from hydroformylation of propene yields 2-ethylhexenal, which is hydrogenated to 2-ethylhexanol. Oligomerization of propene on acid catalysts like zeolites to "tripropene" as the main product, a mixture of branched nonenes with mainly internal double bonds, is also performed on an industrial scale. Branched dodecenes ("tetrapropene") are the major byproduct. Hydroformylation with subsequent hydrogenation yields the corresponding C10- and C13-alcohols isodecanol IDA and isotridecanol ITDA.

A more recent raw material for plasticizer alcohols is crack-C4 as a byproduct of steamcrackers in ethene/propene production. After extraction of butadiene for use and etherification of isobutene with methanol to methyl-tertiary-butylether MTBE as an octane enhancer, a stream is left containing 1-butene, 2-butene, and butanes, so-called raffinate II. Oligomerization of the butenes yields C8 olefin mixtures ("dibutene") as the main product and the corresponding C12 olefins as the main byproduct (tributene). They are the

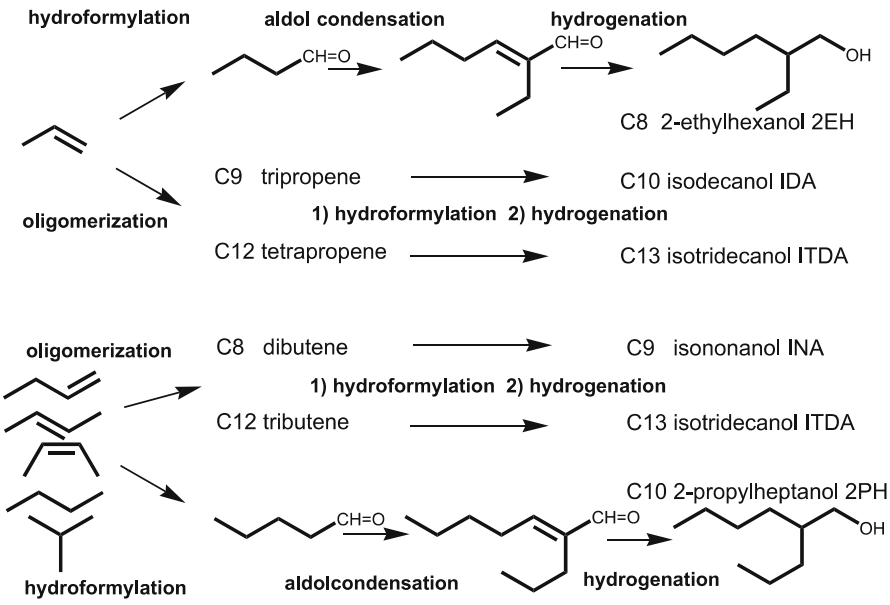

Fig. 23 Plasticizer alcohols starting from propene and C4-cuts

starting materials for the production of the C9- and C13-alcohols isononanol and isotridecanol (Fig. 23).

Propene- and butene-oligomers are complex mixtures. A typical isomer distribution is shown in Fig. 24. According to the thermodynamical stability the double bonds are distributed along the chain, terminal double bonds are present only in traces. To get predominant terminal products, a catalyst must provide extremely fast terminal hydroformylation activity for the traces of terminal olefins, a high isomerization activity to supply the terminal double bonds as fast as they are consumed, and low hydroformylation activity for internal double bonds.

Starting from longer-chain olefins means high boiling points of the products, and hence distillation at higher temperatures and vacuum. These demanding conditions cannot be met by the modern rhodium-catalyzed processes.

The main disadvantage of the old hydridocobaltcarbonyl was the isomerizing activity yielding appreciable amounts of internal products from terminal olefins. This turns out to be an advantage for the problems discussed above: Even from internal double bonds, predominantly terminal aldehydes are formed. For the second problem, the recycling of the catalyst, various solutions are known, the most elegant being oxidative decobalting. After hydroformylation, the poisonous and volatile hydridocobalt-carbonyl is oxidized by air in the presence of aqueous formic or acetic acid to the respective Co^{2+}-salt, which is extracted to the water phase. After recycling to the reaction zone, the active catalyst is regenerated in situ under reaction conditions. The active catalyst is stabilized only by complexing with carbon monoxide, so high pressure is applied at high temperatures (150–180 °C, 200–300 bar, 0.5–1% cobalt, LHSV approx. 1/h). Under these harsh reaction conditions, side reactions occur like aldol condensation to high boilers, hydrogenation of alcohol giving rise to acetals, and olefin loss by hydrogenation to paraffins. The formerly bad chemoselectivities have been improved up to 88% by recent process modifications [85], but 90% seems to be a natural limit. The

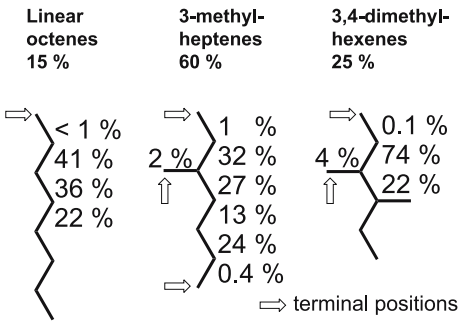

Fig. 24 Dibutene: structure and double bond distribution

regioselectivity for linear internal octenes (Fig. 24) as an example to terminal products is approx. 50%.

Growing demand for higher plasticizer alcohols has initiated a revival of the old cobalt technology. New patents about process modifications [86, 87] and the construction of new plants underline this. Alone the production of isononanol on the basis of dibutene has been a success story, doubling the production to well beyond 1 million mt y^{-1} within a few years.

Modification of cobalt with phosphane ligands yields hydrido-complexes H-Co(CO)$(L)_3$. Often mentioned in the literature is tributylphosphane; in practice phosphabicyclononane derivatives are used because of their high boiling point (ligand 1b in Fig. 9). This catalyst system survives even the harsh conditions of a thermal separation and can be recycled directly solved in the high boilers of the reaction. The main advantage is the high linearity of the products being approx. 80% for linear internal olefins. The main products are alcohols because of the hydrogenation activity of the catalyst, and a hydrogen-rich synthesis gas (H_2/CO approx. 2/1) has to be used. But also starting olefins are partly hydrogenated. Some data from batch experiments at 0.5% Co, Ligand/Co approx. 2 mol/mol, 180–190 °C, 80–100 bar, 1.5 h: chemoselectivity approx. 90%, regioselectivity with linear internal C12–C16 olefins 75–85%, conversion 95%. The process has been used solely by SHELL for more than 50 years; combined name plate capacity (UK, US) is 575 kt/y [88]. Products are plasticizers and surfactant alcohols from technical linear internal olefins.

The highest chemoselectivities greater than 95% for dibutene, tripropene, and the like are possible with unmodified rhodium, and even highly branched olefins up to C20 give satisfactory results and negligible hydrogenation of the starting olefins. Typical conditions are 120 °C, 200–300 bar. But the recycling by thermal separation is accompanied by high rhodium losses because of the extreme instability of hydridorhodiumcarbonyl and precipitation of insoluble rhodium clusters. Another drawback is the low regioselectivity of only 10–20% linear products from internal linear olefins. Nevertheless, the start up of a 115 kt y^{-1} plant in 2002 has been announced for higher branched and internal olefins using the unmodified rhodium high-pressure process [89]. According to a new patent, rhodium in the reactor effluent is adsorbed on a basic ion exchanger, which after exhaustion is incinerated. Rhodium is recovered from the ash by conventional methods [90].

5 Conclusion

Hydroformylation as a very versatile method for functionalization of readily available olefins is to date applied mainly for bulk chemicals. The great potential for speciality and fine chemicals is only sparsely exploited and is still an open field. Research in development of new ligands is not the problem,

organometallic chemists being highly innovative. Solving the problems of catalyst stability and new more general applicable solutions of the recycle will be an important key for further progress.

A better understanding of the theoretical background is another key for progress. A basic requirement for a more rational design of catalyst systems is to get more insight into the complex mechanism. The tools are in situ spectroscopic methods under reaction conditions.

In fact after more than 60 years, hydroformylation is at the beginning of a new epoch leaving bulk chemistry and entering speciality and fine chemistry. Further networking of different professionals such as organometallic chemists, theoretical chemists, and engineers will be a prerequisite for success.

References

1. Roelen O (1938) DE 849548
2. Roelen O (1943) US 2327066
3. Cornils B (1980) In: Falbe J (ed) New Syntheses with Carbon Monoxide 1-225
4. Cornils B, Herrmann WA (eds) (2002) Applied Homogeneous Catalysis with Organometallic Compounds, 2nd edn. Wiley, Weinheim
5. Van Leeuwen PWNM, Claver C (eds) (2000) Rhodium Catalyzed Hydroformylation, 2nd edn. Kluwer CMC, Dordrecht
6. Ungvary F (2004) Application of transition metals in hydroformylation annual survey. CCHRAM 248(9–10):867–880
7. Ungvary F (2003) Application of transition metals in hydroformylation annual survey. CCHRAM 241(1–2):295–312
8. Ungvary F (2002) Application of transition metals in hydroformylation annual survey. CCHRAM 228(1):61–82
9. Ungvary F (2001) Application of transition metals in hydroformylation annual survey. CCHRAM 218:1–41
10. Garland M et al. (2003) JACSAT 125(18):5540–5548
11. Garland M et al. (2004) Organometallics 23(17):4131–4138
12. Tannenbaum R et al. (2004) JMCADS 215(1–2):33–43
13. Tannenbaum R et al. (1999) JORCAL 586(1):18–22
14. Tannenbaum R et al. (1998) JORCAL 570(1):39–47
15. Oldani F et al. (1985) JORCAL 279:459–460
16. Oldani F et al. (1983) JORCAL 246:309–324
17. Garland M et al. (2002) ACIEAY 41(20):3786–3789
18. Damoense L et al. (2004) Coordination Reviews 248(21–24):2393–2407
19. Kamer PCJ et al. (2004) Coordination Reviews 248(21–24):2409–2424
20. Heck R, Breslow D (1960) CHIKA 3:467
21. Heck R, Breslow D (1961) J Am Chem Soc 83:4023
22. Wilkinson G et al. (1970) JCSIAP (9):1392–1401
23. Wilkinson G et al. (1970) JCSIAP (17):2753–2764
24. Tolman C et al. (1974) J Am Chem Soc 96(1):53–60
25. Tolman C (1977) CHREAY 77(3):313–348
26. Freixa Z, van Leeuwen P (2003) Dalton Trans (10)m:1890–1901

27. van der Veen L, Kamer P, van Leeuwen P (2002) CATTFB 6(3):116–120
28. Dielemann C, Kamer P, Reek J, van Leeuwen P (2001) HCACAV 84:3269–3280
29. van Leeuwen P, Kamer P, van der Veen L, Reek J (2001) CJOCEV 19(1):1–8
30. ESSO (1964) NL 6400701
31. SHELL (1966) NL 6604094
32. SHELL (2004) WO 2004054946
33. Wilkinson G (1968) BSCFAS (12):5055–5058
34. Cornils B, Herrmann WA (2004) Aqueous-Phase Organometallic Catalysis. Wiley, Weinheim
35. Jongsma T, Challa G, van Leeuwen P (1991) JORCAL 42(1):121–128
36. OXENO (2003) WO 2003095402
37. Mitsubishi (2003) JP 2003146931
38. Kuraray (1995) JP 07258149
39. Anschutz L, Marquardt W (1956) CHBEAM 89:1119–1123
40. UCC (1987) EP 214622
41. UCC (1988) US 4769498
42. Behr A, Obst D, Turkowski B (2005) JMCADS 226(2):215–219
43. Herrmann WA et al. (1995) JMCADS 97(2):65–72
44. CELANESE (2004) EP 1400504
45. OXENO (2002) WO 2002076996
46. Klein H, Jackstell R, Wiese KD, Borgmann C, Beller M (2001) ACIEAY 40(18):3408–3411
47. UCC (2003) WO 2003078444
48. OXENO (2002) EP 1201675
49. Selent D, Hess D, Wiese KD, Roettger D, Kunze C, Boerner A (2001) ACIEAY 40(9):1696–1698
50. van der Vlugt JI, Sablong R, Magusin P, Mills A, Spek A, Vogt D (2004) Organometallics 23(13):3177–3183
51. BASF (2002) WO 2002022261
52. Breit B (1999) JMCADS 143(1–3):143–154
53. Breit B, Winde R, Mackewitz T, Paciello R, Harms K (2001) CEUJED 7(14):3106–3121
54. BASF (1997) DE 19621967
55. BASF (2000) WO 2000055164
56. Breit B, Fuchs E (2004) CCOMA8 (6):694–695
57. BASF (2003) DE 10320139
58. van Boven M, Alemdaroglu N, Penninger JML (1975) JORCAL 84(1):65–74
59. Liu G, Garland M (2000) JORCAL 613(1):124–127
60. Zhang J, Poliakoff M, George MW (2003) Organometallics 22(8):1612–1618
61. Caporali M, Frediani P, Salvini A, Laurenczy G (2204) ICHAA3 357(15):4537–4543
62. Bianchini C, Lee HM, Meli A, Vizza F (2000) Organometallics 19(5):849–853
63. Brown JM, Kent AG (1987) JCPKBH (11):1597–1607
64. Casey CP, Whiteker GT (1990) ISJCAT 30(4):299–304
65. Dierkes P, van Leeuwen PW (1999) JCDTBL (10):1519–1530
66. Casey CP, Whiteker GT, Melville MG, Petrovich LM, Gavney JA, Powell DR (1992) JACSAT 114(14):5535–5543
67. Casey CP, Whiteker GT (1990) JOCEAH 55(4):1394–1396
68. Miyazawa M, Momose S, Yamamoto K (1990) SYNLES (11):711–712
69. Kamer PCJ, van Leeuwen PWNM, Reek JNH, Joost NH (2001) ACHRE4 34(11):895–904
70. Paciello R, Siggel L, Kneuper HJ, Walker N, Roeper M (1999) JMCADS 143(1–3):85–97

71. Franke R, Borgmann C, Hess D, Wiese KD (2003) ZAACAB 629(14):2535–2538
72. Matsubara T, Koga N, Ding Y, Musaev DG, Morokuma K (1997) Organometallics 16(5):1065–1078
73. Rocha WR, de Almeida WB (2000) IJQCB2 78(1):42–51
74. Decker SA, Cundari TR (2001) Organometallics 20(13):2827–2841
75. Gleich D, Schmid R, Herrmann WA (1998) Organometallics 17(22):4828–4834
76. van der Veen LA, Keeven PH, Schoemaker GC, Reek JNH, Kamer PCJ, van Leeuwen PWNM, Lutz M, Spek AL (2002) Organometallics 19(5):872–883
77. Carbó JJ, Maseras F, Bo C, van Leeuwen PWNM (2001) JCSIAP 123(31):7630–7637
78. Landis CR, Uddin J (2002) JCPKBH (5):729–742
79. Bergounhou C, Neibecker D, Mathieu R (2004) JMCADS 220(2):167–182
80. Helfferich FG (2003) Kinetics of Homogeneous Multistep Reactions, 2nd ed. Elsevier, Amsterdam
81. Cornils B, Herrmann WA (eds) (2004) Aqueous-Phase Organometallic Catalysis, 2nd ed. Wiley, Weinheim, p 351–428
82. Wiese KD, Moeller O, Protzmann G, Trocha M (2003) CATTEA 79–80:97–103
83. OXENO (2001) DE 19957528
84. OXENO (2000) EP 1057524
85. OXENO (2002) EP 1172349
86. OXENO (2004) DE 10241266
87. EXXONMOBIL (2003) WO 2003082789
88. http://www.shellchemicals.com/
89. http://www.synetix.co.uk/new864s/16864072002-nan.htm
90. ICI (2002) WO 2002020451

Top Organomet Chem (2006) 18: 35–64
DOI 10.1007/3418_016

Published online: 15 July 2006

Asymmetric Hydroformylation

Carmen Claver[1] (✉) · Montserrat Diéguez[1] · Oscar Pàmies[1] · Sergio Castillón[2]

[1]Department of Physical Chemistry and Inorganic Chemistry, Universitat Rovira i Virgili, Campus Sescelades, c/Marcel.li Domingo s/n, 43007 Tarragona, Spain
carmen.claver@urv.net

[2]Department of Analytical Chemistry and Organic Chemistry, Universitat Rovira i Virgili, Campus Sescelades, c/Marcel.li Domingo s/n, 43007 Tarragona, Spain

1 Introduction . . . 36
1.1 Asymmetric Hydroformylation. State of the Art . . . 36
1.2 Rhodium Versus Platinum-Catalyzed Asymmetric Hydroformylation . . . 37
1.3 Catalytic Cycle and Mechanistic Highlights . . . 39
1.4 Focus and Scope . . . 41

2 Rhodium-Catalyzed Asymmetric Hydroformylation of Vinyl Arenes . . . 41
2.1 Diphosphite Ligands . . . 42
2.2 Phosphine-Phosphite Ligands . . . 47
2.3 Characterization of Intermediates: Structures of $[RhH(CO)_2(L-L)]$ in Solution . . . 49

3 Rhodium-Catalyzed Asymmetric Hydroformylation of Vinyl Acetate . . . 52
3.1 Diphosphite and Phosphine-Phosphite Ligands . . . 52
3.2 Diphosphine and Bis(diazaphospholidine) Ligands . . . 54

4 Rhodium-Catalyzed Asymmetric Hydroformylation of Dihydrofurans . . . 55
4.1 Phosphine-Phosphite Ligands . . . 56
4.2 Diphosphite Ligands . . . 57

5 Rhodium-Catalyzed Asymmetric Hydroformylation of Unsaturated Nitriles . . . 57
5.1 Rhodium-Catalyzed Asymmetric Hydroformylation of Allylcyanide . . . 58

6 Catalytic Experiments. IR In Situ and High-Pressure NMR Experiments . 60

7 Conclusions and Remarks . . . 61

References . . . 62

Abstract This chapter presents the latest achievements reported in the asymmetric hydroformylation of olefins. It focuses on rhodium systems containing diphosphites and phosphine-phosphite ligands, because of their significance in the subject. Particular attention is paid to the mechanistic aspects and the characterization of intermediates in the hydroformylation of vinyl arenes because these are the most important breakthroughs in the area. The chapter also presents the application of this catalytic reaction to vinyl acetate, dihydrofurans and unsaturated nitriles because of its industrial relevance.

Keywords Aldehydes · Catalysis · Enantioselectivity · Hydroformylation · Intermediates · Rhodium

Abbreviations

b	Branched
l	Linear
ee	Enantiomeric excess
BINAP	2,2′-bis(diphenylphosphino)-1,-1′-binaphthyl
BINAPHOS	(*R*)-2-(diphenylphosphino)-1,1′-binaphthalene-2′-yl (*S*)-1,1′-binaphthalene-2,2′-diyl phosphite)
BDPP	(2S,4S)-bis(diphenylphosphino)pentane
COD	1,5-cyclooctadiene
ESPHOS	{(1R,1′R,3aS,3′aS)-1,1′-(1,2-phenylene)bis[hexahydro-2-phenyl-1*H*-pyrrolo [1,2-*c*][1,3,2]diazaphosphole]}
HPNMR	High-pressure nuclear magnetic resonance
HPIR	High-pressure infrared
TBP	Trigonal bipyramid

1 Introduction

1.1 Asymmetric Hydroformylation. State of the Art

The hydroformylation reaction that converts olefins into aldehydes is the largest volume homogeneous transition-metal catalyzed reaction used today. This reaction has been extensively studied and nowadays a number of efficient catalysts make it possible to control the regioselectivity of the reaction to give terminal or internal aldehydes (Scheme 1).

Although early catalysts were based on cobalt, nowadays, rhodium catalysts are preferred because they require lower pressure and afford higher chemo- and regioselectivity [1, 2]. In recent years, extensive research into the production of only linear aldehydes has provided impressive results. The application of phosphines with a wide bite angle in the rhodium catalyzed hydroformylation of terminal alkenes enable the regioselectivity to be almost totally controlled [3]. Branched selective hydroformylation, al-

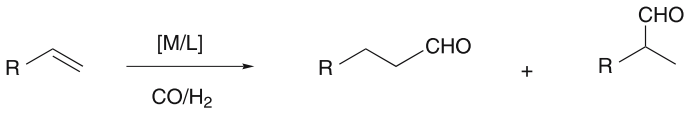

Scheme 1 Asymmetric hydroformylation

though less studied, is a useful tool for organic synthesis [4, 5]. Furthermore, the asymmetric version of the hydroformylation of olefins is one of the most straightforward synthetic strategies for preparing optically active aldehydes, which are versatile intermediates for the synthesis of biologically active compounds as well as for other synthetic transformations [6, 7]. Nonetheless, despite these advantages, hydroformylation has not been used much in fine chemicals synthesis with the exception of the applications in vitamins and in flavors and fragrances [2, 8]. This may be due to the difficulty in simultaneously controlling chemo, regio- and enantioselectivity throughout the reaction. To date, much of the effort in this field has concentrated on the hydroformylation of vinylarenes as a route to obtain enantiomerically enriched 2-aryl propionic acids, the profen class of nonsteroidal drugs. Interestingly, asymmetric hydroformylation has been successfully carried out in the conversion of vinylarenes. The application of asymmetric hydroformylation to other substrates has hardly been studied despite their potential use in the production of fine chemicals [8, 9]. In recent years, however, researchers' interest in asymmetric hydroformylation has increased significantly, mainly in connection with the hydroformylation of vinyl acetate, unsaturated nitriles, or heterocyclic substrates since these processes can be an easy access to enantiopure diols, and other molecules of biological interest.

1.2 Rhodium Versus Platinum-Catalyzed Asymmetric Hydroformylation

Highly enantioselective hydroformylation catalyzed by chiral metal complexes has been obtained with only a few catalytic systems. Many chiral phosphorus ligands have been used in Pt(II) and Rh(I) systems in the asymmetric hydroformylation of styrene. The first highly enantioselective examples of the asymmetric hydroformylation of styrene were reported by Consiglio et al. in 1991 and used Pt – Sn systems. Ligand **1** achieved an ee of 86% (Fig. 1) [10–12].

However, platinum catalysts have several disadvantages: they have low reaction rates, they hydrogenate the substrate and their regioselectivity to the branched aldehyde is low. The selectivity of Pt-diphosphite/$SnCl_2$ systems is also low. When the appropriate diphosphite is used, ee's can be as high as 90% [13]. In the early 90s, several reports were published which described the state of the art in hydroformylation with both rhodium and platinum systems [14–16].

After the discovery of the high ee provided by rhodium/diphosphite and rhodium/phosphine-phosphite complexes, with total conversion in aldehydes and high regioselectivities, rhodium systems became the catalysts of choice for asymmetric hydroformylation. Important breakthroughs in this area have been the use of rhodium systems with chiral diphosphites derived from

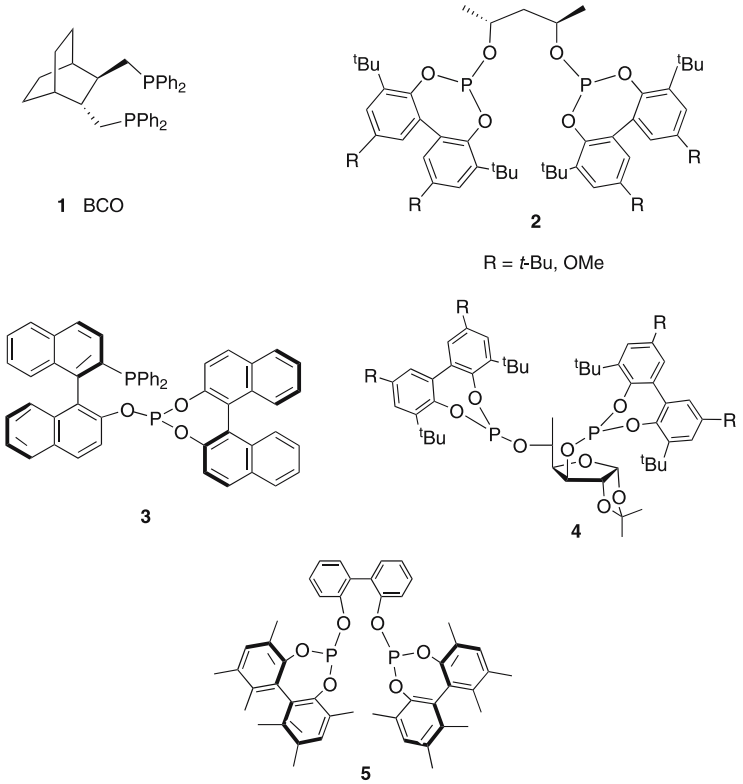

Fig. 1 Phosphorus ligands **1**–**5** providing high enantioselectivity in asymmetric hydroformylation. Ligand **1** for Pt systems. Ligands **2**–**5** for rhodium catalytic systems

homochiral (2R,4R)-pentane-2,4-diol **2** [17, 18], and the efficient phosphine-phosphite ligand BINAPHOS (**3**) [19, 20] (Fig. 1).

Many other rhodium systems have been explored using differently modified ligands, although high ee have been reported only in a few cases. Carbohydrate derived diphosphites **4** have proven to be very efficient at achieving ee up to 93% with high regioselectivity in the asymmetric hydroformylation of vinylarenes (Fig. 1) [21–23]. Recent studies show that the chiral phosphite Kelliphite (**5**) provide high enantioselectivity and excellent branched selectivity in vinyl acetate and allyl cyanide hydroformylation [24, 25]. In asymmetric hydroformylation rhodium systems containing chiral diphosphines do not achieve ee's as high as the rhodium systems with diphosphites or BINAPHOS (**3**). For example, in the rhodium-catalyzed hydroformylation of styrene, the rhodium system containing ferrocenylethyldiphosphine derivatives **6** (Fig. 2) showed the highest values of ee (60–76%) ever found for the hydroformylation of styrene with rhodium/diphosphine catalysts, although the conversions were very low [26].

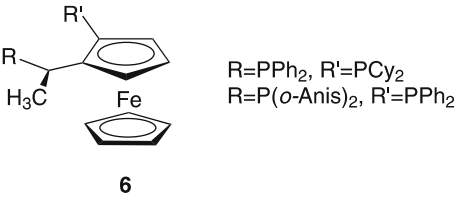

Fig. 2 Ferrocenylethyldiphosphine derivatives **6** providing high ee in rhodium catalyzed asymmetric hydroformylation

1.3 Catalytic Cycle and Mechanistic Highlights

The catalytic cycle for the rhodium catalyzed hydroformylation has been extensively studied mainly for $RhH(CO)(PPh_3)_3$. A general proposal [2, 27] that includes the steps of the reaction is shown in Scheme 2.

For PPh_3 as the ligand a common starting complex is $RhH(CO)(PPh_3)_3$, complex **9**, which under 1 bar of carbon monoxide forms complexes **8a** and **8b**, which contain two phosphine ligands in equatorial positions or one in an apical position and the other in an equatorial position. Dissociating either equatorial L or equatorial CO from **9** or **8** leads to the square-planar in-

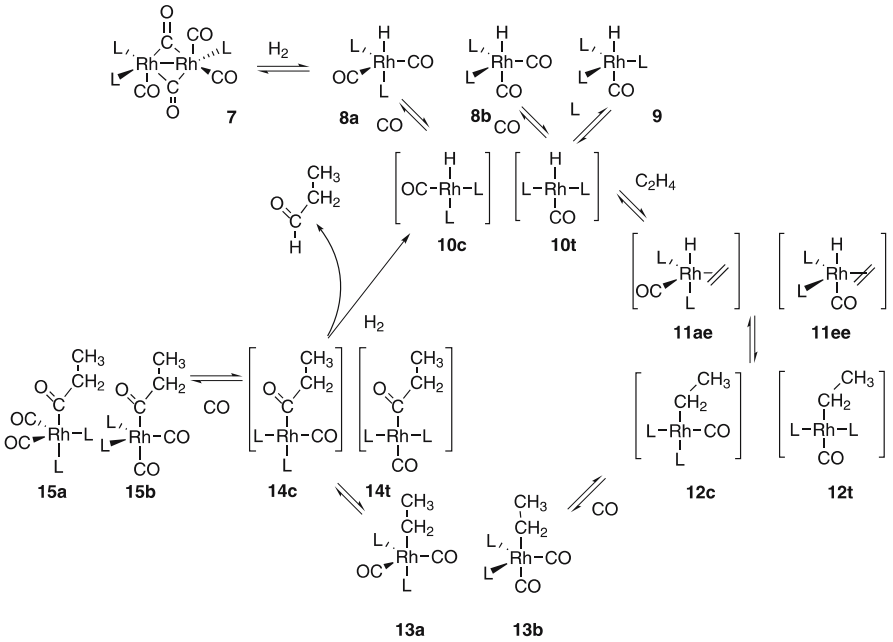

Scheme 2 General mechanism for rhodium-catalyzed hydroformylation of ethene

termediates **10c** and **10t**, (which have never been observed) with phosphines in the *cis* or *trans* configurations, respectively. Complex **10** associate with ethene to give complexes **11**, again in two isomeric forms axial-equatorial and equatorial-equatorial with a hydride in an apical position and ethene coordinating in the equatorial plane. Complex **11** undergoes a migratory insertion to give square-planar alkyl complexes **12c** and **12t**, which are respectively *cis* or *trans*. Complex **12** can undergo β-hydride elimination, thus leading to isomerization when higher alkenes are used, or it can react with CO to form trigonal bipyramidal complexes **13**. Thus, under low pressure of CO more isomerization may be expected. At low temperatures ($< 70\,^{\circ}C$) and a sufficiently high pressure of CO (> 10 bar) the insertion reaction is usually irreversible. Therefore at this point the regioselectivity of hydroformylation of 1-alkenes is also determined. Complexes **13** undergo the second migratory insertion in this scheme to form acyl complexes **14**. Complexes **14** can react either with CO to give the saturated rhodium-acyl intermediates **15**, which have been observed spectroscopically, or with H_2 to give the aldehyde product and the unsaturated intermediates **10**. At low hydrogen pressure and high rhodium concentrations, formation of dirhodium species such as **7** becomes significant [16]. The nature of the phosphorus ligand as well as the conditions of the reaction have a profound effect on each of the individual steps of the catalytic cycle: they determine the activity and selectivity of the reaction. Careful choice of the ligand enables the desired aldehyde to form with high regioselectivity. It has also been reported that the kinetics of the hydroformylation reaction depend on the nature of the catalyst [2]. Kinetic studies on the unmodified system show that hydrogenolysis is the rate-determining step in that system for styrene hydroformylation. In situ IR spectroscopy has revealed that an acyl rhodium complex was the resting state of the catalyst [28, 29]. On the other hand it has been reported that the hydroformylation of styrene catalyzed by rhodium/1,2,5-triphenyl-1-*H*-phosphole is first order in both the styrene concentration and and hydrogen pressure [30]. When the rhodium complex of a monodentate bulky phosphite is used, the rate- determining step depends on the substrate: hydrogenolysis for 1-octene and olefin coordination for cyclohexene [31]. The styrene coordination step is the rate-determining step when the hydroformylation is carried out at high pressure with the bidentate ligand BDPP, although several steps may contribute to the reaction rate at lower pressures [32] as it has also been proposed for the reaction rate in the 1-octene hydroformylation catalyzed by a rhodium monodentate phosphorus diamide system [33]. Thus even with the same catalytic system, the rate-determining step can vary depending on the substrate or the reaction conditions [31, 32]. The HPNMR and in situ HPIR characterization of intermediates in asymmetric hydroformylation catalyzed by rhodium phosphine-phosphite [23, 34–36], diphosphites [21, 37] and diphosphines [38, 39] made it possible to elucidate mechanistic aspects of the reaction, and in particular the steps determining the reaction rate and

the formation of the intermediates of the reaction. Theoretical approaches to rhodium catalyzed hydroformylation have also been reported in recent years [40, 41].

1.4
Focus and Scope

This chapter mainly focuses on the latest achievements and recent developments in asymmetric hydroformylation. Since several reviews have been made in the last decade [9, 14–16], the chapter discusses the contributions reported between 2000–2005 in particular, although the main diphoshites and phosphine-phosphite rhodium catalytic systems discovered since 1995 are also considered because of their significance in the subject. Particular attention is paid to mechanistic aspects and characterization of intermediates in the case of the hydroformylation of vinyl arenes because this is one of the most important breakthroughs in the area. The application of this catalytic reaction to different type of substrates, in particular dihydrofurans and unsaturated nitriles is the other main subject of this chapter because of their interest in organic synthesis and their industrial relevance.

2
Rhodium-Catalyzed Asymmetric Hydroformylation of Vinyl Arenes

Since the early 1970s, rhodium-diphosphine complexes have been used as catalysts in the asymmetric hydroformylation of vinyl arenes (Scheme 3). However, the enantiomeric excesses obtained using these catalysts have generally been moderate (below 60%) [9, 42]. As has been above shown, only when the rhodium catalyst contained (S)-1-[(1S)-2-(Dicyclohexylphosphino)ferrocenyl]ethyldi-phenylphosphine, was the enantioselectivity as high as 76% although the conversion rate was very low [26]. Over the last decades, two new types of ligands, diphosphite [17, 18, 21–23, 43, 44] and phosphine-phosphite [19, 20, 34, 45] have emerged as suitable ligands for the rhodium asymmetric hydroformylation of vinyl arenes. Their activity and selectivity are better than those of the phosphine-based catalytic systems. In this section we will discuss the results obtained using diphosphite and phosphine-phosphite ligands in the most emerging period in which this area

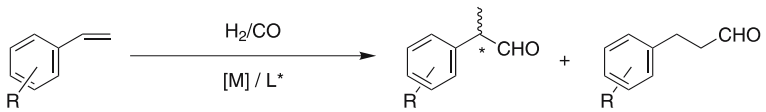

Scheme 3 Model rhodium-catalyzed asymmetric hydroformylation asymmetric of vinyl arenes

of research was emerging (1996 to 2004). We also discuss any reported mechanistic aspects concerning the hydroformylation results.

2.1 Diphosphite Ligands

The first report to use diphosphite ligands in the asymmetric hydroformylation of vinyl arenes revealed no asymmetric induction [46]. An important breakthrough came in 1992 when Babin and Whiteker at Union Carbide patented the asymmetric hydroformylation of various alkenes with ee's up to 90%, using bulky diphosphites **2a–c** derived from homochiral (2*R*, 4*R*)-pentane-2,4-diol (Scheme 4) [17]. Their early results showed that (a) bulky substituents are required at the ortho positions of the biphenyl moieties for good regio- and enantio-selectivity and (b) methoxy substituents in the para positions of the biphenyl moieties always produced better enantioselectivities than those observed for the corresponding *tert*-butyl-substituted analogues.

Inspired by the excellent early results obtained with the Union Carbide-type ligands **2a–c**, other research groups have recently studied several modifications in these types of ligand (Fig. 3, ligands **2**, **16–18**) [18, 37, 47]. In particular, they have studied the influence of the bridge length, the phosphite moieties and the possibility of a cooperative effect between chiral centers on the performance of the catalysts. The influence of the bridge length was studied by comparing ligands **2**, **16–17**. In general, ligands **2**, which have three carbon atoms in the bridge, provided higher enantioselectivities than ligands **16** and **17**, which have two and four carbon atoms in the bridge [18].

The effect of different phosphite moieties was studied with ligands **2d–o**. In general, sterically hindered phosphite moieties are necessary if enantio-

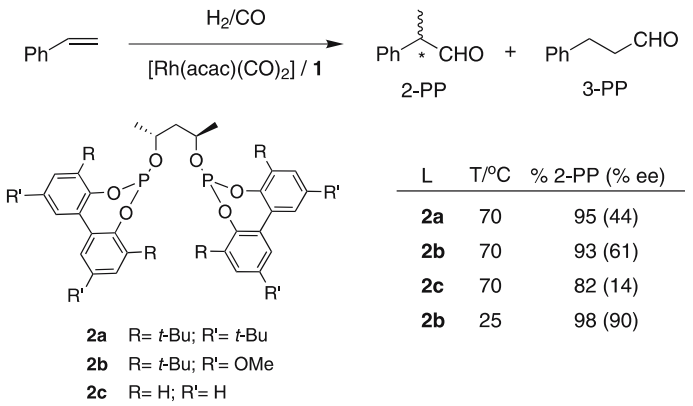

L	T/°C	% 2-PP (% ee)
2a	70	95 (44)
2b	70	93 (61)
2c	70	82 (14)
2b	25	98 (90)

Scheme 4 Rh-catalyzed asymmetric hydroformylation of styrene using ligands **2a–c**

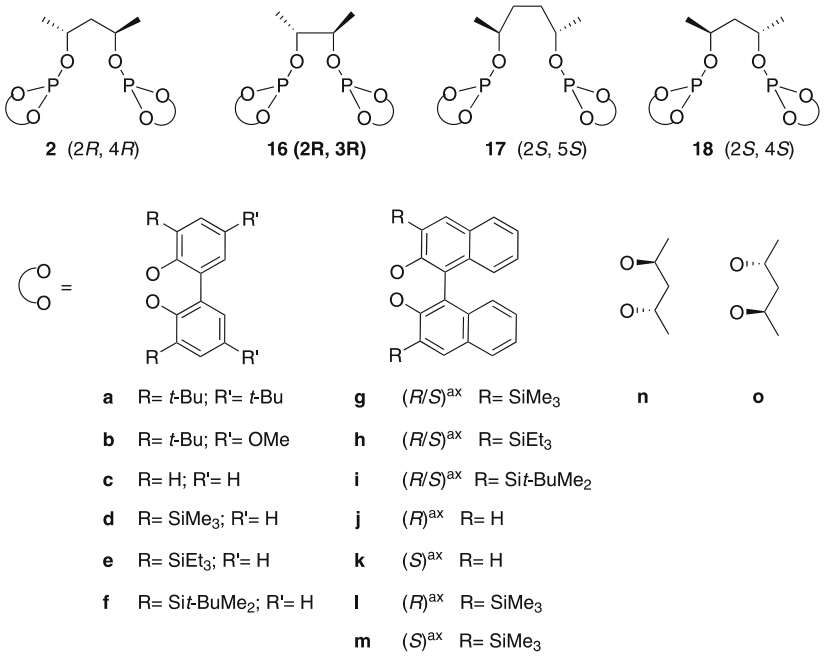

Fig. 3 Diphosphite ligands **2** and **16–18**

selectivities are to be high [37, 47]. Also, the results of using ligands **2d–i** indicated that varying the ortho substituents on the biphenyl and binaphthyl phosphite moieties has a considerable effect on asymmetric induction. The optimal steric bulk in the ortho positions therefore seems to be obtained with trimethylsilyl substituents (i.e., ligand **2d** provided ee's up to 87% at 20 bar of syn gas and 25 °C). This result is similar to the previously reported best result obtained with **2b**.

A possible cooperative effect between the chiral ligand bridge and the axially chiral binaphthyl phosphite moieties was studied by van Leuween and coworkers with ligands **2l**, **2m**, **18l** and **18m**. The hydroformylation results clearly indicate a cooperative effect that leads to a matched combination for ligand **1m** with (Sax, 2R, 4R, Sax) configurations (ee's up to 86%) (Table 1) [40, 41]. Later, Bakos and coworkers found a similar cooperative effect with ligands **2n**, **2o**, **18n** and **18o** between the chiral ligand bridge and the chiral phosphite moiety [47].

Interestingly, the hydroformylation results obtained with ligands **2b** and **2d**, which have conformationally flexible axially chiral biphenyl moieties, are similar to those obtained with ligand **2m**, which have conformationally rigid binaphthyl moieties. This indicates that diphosphite ligands that contain the conformationally flexible axially chiral biphenyl moieties predominantly exist as single atropoisomer in the [$RhH(CO)_2$(diphosphite)] complexes

Table 1 Rh-catalyzed asymmetric hydroformylation of styrene using diphosphites **2l**, **2m**, **18l** and **18m**[a]

Entry	Ligand	TOF[b]	% 2-PP[c]	% ee[d]
1	**2l**	28	95	38 (*S*)
2	**2m**	17	88	69 (*S*)
3	**18l**	4	91	23 (*S*)
4	**18m**	45	94	40 (5)
5[e]	**2m**	11	92	86 (*S*)

[a] $[Rh(acac)(CO)_2] = 0.02$ mmol; ligand/Rh = 2.2; substrate/Rh = 1000; Toluene = 20 mL; $P_{H_2/CO} = 10$ bar; $T = 25\,^{\circ}C$

[b] TOF in mol styrene × mol $Rh^{-1} \times h^{-1}$ determined after 1-h reaction time

[c] Regioselectivity for 2-phenylpropanal

[d] Enantiomeric excess

[e] $T = 15\,^{\circ}C$

when the right bulky substituents in the *ortho* positions are present (vide infra) [37]. It is therefore not necessary to use expensive conformationally rigid binaphthyl moieties to reduce the degrees of freedom of the system.

To investigate whether a relationship exists between the solution structures of the hydridorhodium diphosphite species $[RhH(CO)_2(diphosphite)]$ [48] and catalytic performance, van Leeuwen and co-workers extensively studied the rhodium-diphosphite complexes formed under hydroformylation conditions by high-pressure NMR (HPNMR) techniques. It is well known that these complexes have a trigonal bipyramidal (TBP) structure. Two isomeric structures of these complexes, one containing the diphosphite coordinated in a bis-equatorial (**ee**) fashion and one containing the diphosphite in an equatorial-axial (**ea**) fashion, are possible (Fig. 4).

Van Leeuwen's studies using diphosphite ligands **2** and **18** indicated that the stability and catalytic performance of the $[RhH(CO)_2(diphosphite)]$ species depends strongly on the configuration of the 2,4-pentanediol ligand backbone and the chiral biaryl phosphite moieties. Thus, for example, ligands **2b**, **2d** and **2m**, which form well defined stable bis-equatorial (**ee**)

Fig. 4 Bis-equatorial (ee) and equatorial-axial (ea) coordination modes of diphosphite ligands in the $[RhH(CO)_2(diphosphite)]$ complexes

complexes, lead to high enantiomeric excess, whereas ligands **2l** and **18m**, which form unidentified mixtures of complexes and ligand decomposition lead to low enantioselectivity [37, 49].

Another successful family of ligands is the sugar-based furanoside ligands **4**, **19–23** (Fig. 5) [21–23, 43, 50]. The modular construction of these ligands allows to fine tune (a) the different configurations of the carbohydrate backbone and (b) the steric and electronic properties of the diphosphite substituents. They show excellent enantioselectivity on both the *S* and *R* enantiomer of the product (up to 93%) and excellent regioselectivity (up to 98.8%) under mild conditions (Table 2).

The results of using the biphenyl-based ligands **4a–d**, **19a–d**, **23a–d** (Table 2, entries 1–12) showed that:

(a) a methyl substituent must be in C-5 if enantioselectivities are to be high and it has a positive effect on rate (entries 3–12 vs. 1 and 2);

(b) the level of enantioselectivity is influenced by a cooperative effect between stereocenters C-3 and C-5. Accordingly, ligands **24** and **22** provide better enantioselectivities than ligands **21** and **23** (Table 2, entries 6 and 8 vs 4 and 10);

(c) the absolute configuration of the product is governed by the configuration at the stereogenic center C-3. Accordingly, ligands **19**, **4** and **23**, with *S* configuration at C-3, gave (*S*)-2-phenylpropanal (Table 2, entries 1, 5, 6, 9, 10, 12) while ligands **20**, **21** and **22**, with *R* configuration at C-3, gave (*R*)-2-phenylpropanal (Table 2, entries 2–4, 7, 8, 11);

(d) as observed with the previously mentioned ligands **19a–d**, there is an influence on the substituents in the biaryl phosphite moieties. Thus, ligands **4b,d** and **22b,d**, with either methoxy substituents or trimethylsilyl groups, always produced the best enantioselectivity.

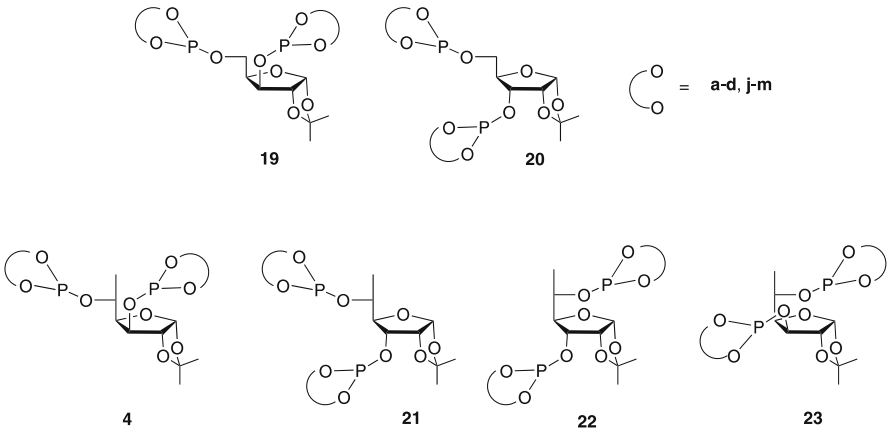

Fig. 5 Furanoside diphosphite ligands **4** and **19–23**

Table 2 Rh-catalyzed asymmetric hydroformylation of styrene using diphosphites **4**, **19**–**23** [a]

Entry	Ligand	TOF [b]	% 2-PP [c]	% ee
1	**19b**	5	97	60 (*S*)
2	**20b**	5	97	61 (*R*)
3	**21a**	14	97.1	46 (*R*)
4	**21b**	13	97.2	58 (*R*)
5	**4a**	19	98.4	74 (*S*)
6	**4b**	18	98.6	90 (*S*)
7	**22a**	16	98.7	76 (*R*)
8	**22b**	17	98.3	89 (*R*)
9	**23a**	15	97.4	52 (*S*)
10	**23b**	12	97.6	64 (*S*)
11	**21d**	10	98.1	62 (*R*)
12	**4d**	11	98.8	93 (*S*)
13	**19j**	126	80	44 (*R*)
14	**19k**	85	83	37 (*S*)
15	**20j**	178	86	20 (*R*)
16	**20k**	158	84	5 (*S*)
17	**21j**	165	85	60 (*R*)
18	**21k**	153	85	25 (*S*)
19	**21m**	149	84	68 (*S*)

[a] $[Rh(acac)(CO)_2] = 0.0135$ mmol; ligand/Rh = 1.1; substrate/Rh = 1000; Toluene = 15 mL; $P_{H_2/CO} = 10$ bar; $T = 20$ °C; $P_{CO}/P_{H_2} = 0.5$

[b] TOF in mol styrene × mol $Rh^{-1} \times h^{-1}$ determined after 1-h reaction time

[c] Regioselectivity for 2-phenylpropanal

Furthermore, the results of using the binaphthyl-based ligands **4**, **19**–**23j**–**m** (Table 2, entries 13–19) suggested that the absolute configuration of the product outcome is controlled by the configuration of the biaryl moieties. This suggests that the configuration of fluxional biphenyl moieties in ligands **4**, **19**–**23a**–**d** is controlled by the configuration of the stereogenic center C-3. The results also indicate a cooperative effect between the chiral sugar backbone stereocenters (C-3 and C-5) and the axial chiral binaphthyl phosphite moieties. This cooperative effect, together with the previously observed cooperative effect between the backbone stereocenters C-3 and C-5, controls enantioselectivity.

The characterization of the rhodium complexes formed under hydroformylation conditions by NMR techniques and in situ IR spectroscopy showed that there is a relationship between the structure of the $[RhH(CO)_2(P-P)]$ (P – P = **4**, **19**–**23**) species and their enantiodiscriminating performance. In general, enantioselectivity was highest with ligands that have a strong bis-equatorial (**ee**) coordination preference, while an equilibrium of

species with bis-equatorial (**ee**) and equatorial-axial (**ea**) coordination modes considerably reduced the ee's [21–23].

Over the years, several authors have developed new diphosphite ligands with binaphthyl, spiro, pyranoside, and macrocyclic backbones for asymmetric hydroformylation of vinyl arenes with low-to moderate success (ee's from 36% to 76%) [48–58].

2.2 Phosphine-Phosphite Ligands

Takaya and co-workers in 1993 were the first to report on asymmetric hydroformylation using phosphite-phosphine ligands [59]. In an attempt to combine the effectiveness of the BINOL chemistry for asymmetric catalysis and the effectiveness of the phosphite moiety for asymmetric hydroformylation, they developed the (*R*,*S*)-BINAPHOS ligand **3**, which turned out to be very efficient (Fig. 6).

In the last few years, a wide range of structural variations has been reported. In this context, in 1997, Nozaki and coworkers used ligands **30**, **24**–**26**

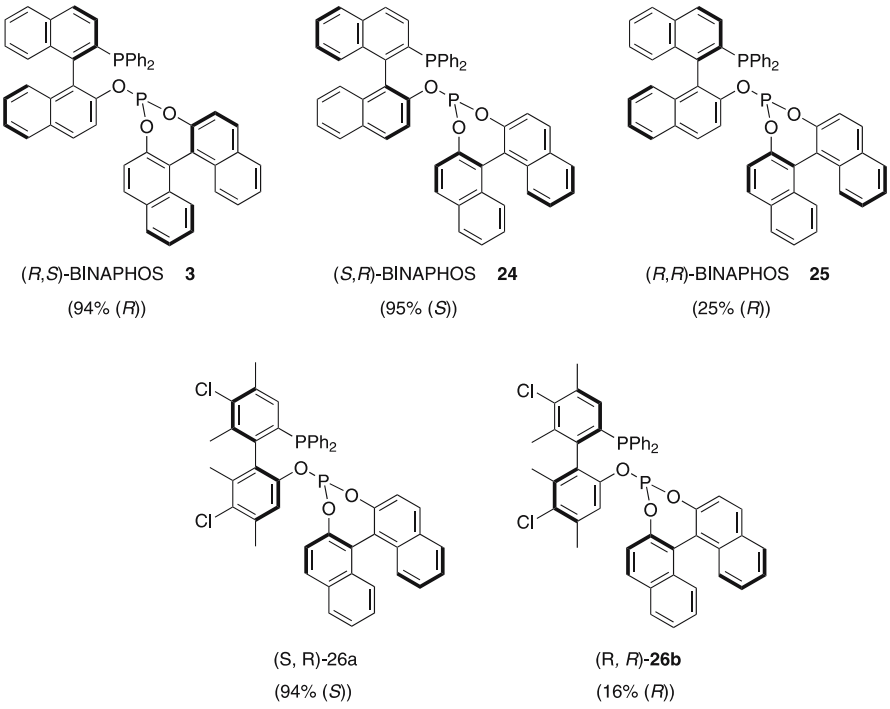

Fig. 6 Rhodium-catalyzed asymmetric hydroformylation of styrene using ligands **3** and **23**–**26**. Enantioselectivities obtained at 100 bars of syngas and 60 °C are shown in *brackets*

and found that the sense of enantioselectivity is governed by the configuration of the binaphthyl bridge, whereas the enantiomeric excess depends strongly on the configuration of both binaphthyl moieties (Fig. 6) [20]. Enantioselectivity is therefore higher when the configurations of the two binaphthyl moieties are opposite (i.e., diastereoisomers *R*,*S* or *S*,*R*). Similar trends were observed with ligands **26a** and **26b**, which have a chiral biphenyl bridge.

To further understand how the chirality at the bridge and the axial chirality at the phosphite moiety affect the transfer of the chiral information to the product outcome, ligands **27** and **28** were studied (Fig. 7) [20]. Ligand **27**, which has an (*R*)-binaphthyl in the bridge, provides an ee of 83% (*R*). This value is close to the (*R*,*S*)-BINAPHOS value (94% (*R*) ee) which suggests that, in the formation of the Rh-complex, the binaphthyl bridge controls the conformation of the biphenyl phosphite moiety. Likewise, ligand **28** provides an ee of 69% (*S*), which suggests that the binaphthyl phosphite moiety also controls the conformation of the biphenyl bridge when it coordinates to rhodium. However, the control by the binaphthyl bridge is more efficient than that of the binaphthyl phosphite moiety.

The effect of several substituents on the phosphine moiety has been extensively studied by Nozaki's group (Fig. 8). Their results indicate that both regio- and enantio-selectivity can be increased by suitable choice of the aryl

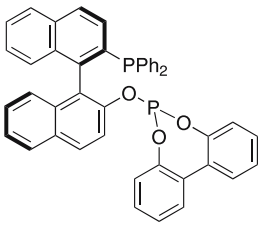

27 (*R*)

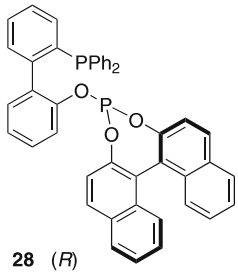

28 (*R*)

Fig. 7 Rh-catalyzed asymmetric hydroformylation of styrene using ligands **27** and **28**

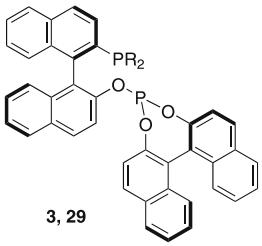

3, 29

Ligand	R	%2-PP	%ee
3	C_6H_5	90.6	95.2 (*R*)
29a	3-MeO-C_6H_4	95.0	97.5 (*R*)
29b	3-^{i}PrO-C_6H_4	94.0	98.3 (*R*)
29c	3-$C_6F_{13}CH_2CH_2$-C_6H_4	92.7	90.6 (*R*)
29d	3-Me-C_6H_4	93.4	94.1 (*R*)
29e	3,5-(MeO)2-C_6H_3	87.5	92.2 (*R*)
29f	4-MeO-C_6H_4	88.8	91.7 (*R*)

Fig. 8 Rh-catalyzed asymmetric hydroformylation of styrene using ligands **3** and **29**

phosphine group. The best combinations of regio- and enantio-selectivity were therefore obtained with ligands **29a** and **29b** [60].

The characterization of the rhodium complexes formed under hydroformylation conditions by NMR techniques and in situ IR spectroscopy showed that there is a relationship between the structure of the [$HRh(CO)_2$(BINAPHOS)] species and their enantiodiscriminating performance. Thus, (*R*,*S*)- and (*S*,*R*)-BINAPHOS ligands show high equatorial-axial (**ea**) coordination preference with the phosphite moiety in the axial position. Meanwhile, the characterization of the (*R*,*R*)- and (*S*,*S*)-BINAPHOS ligands suggests that there is either a structural deviation of the monohydride complexes from an ideal TBP structure or an equilibrium between isomers [20, 34].

Highly crosslinked polymer-supported-BINAPHOS ligands were effective for the hydroformylation of styrene and other functionalized olefins (ee's up to 89%). The catalyst could be recovered and reused at low stirring conditions [61, 62].

Perfluoroalkyl-substituted BINAPHOS ligand **29c** was also developed for the asymmetric hydroformylation of vinyl arenes in $scCO_2$. With this ligand regio-and enantio-selectivity (ee's up to 93.6%) were high without the need for hazardous organic solvents [63, 64].

Inspired by the excellent results using the BINAPHOS ligands, new phosphine-phosphite ligands with different backbones have been developed in recent years. Unfortunately, their Rh-catalyzed hydroformylation provided low-to-moderate enantioselectivity (ee's from 20 to 62%) [35, 36, 65].

2.3 Characterization of Intermediates: Structures of $[RhH(CO)_2(L-L)]$ in Solution

As has been shown in the previous part of this chapter on the asymmetric hydroformylation of vinylarenes, in situ IR and high-pressure NMR studies in hydroformylation reaction conditions of pressure and temperature have been carried out for several rhodium systems with different phosphorous ligands. These studies have made it possible to characterize the pentaccordinate TBP hydrido carbonyl rhodium species determined as the resting state [9]. Figure 4 shows both modes of coordination: bis-equatorial (**ee**) and equatorial-axial (**ea**). The values of the NMR coupling constants $^2J(P-P)$ and $^2J(H,P)$ indicate the coordination mode in the TBP. In the case of diphoshites, as described above, short-bridged diphosphites forming seven-membered rings coordinate in an equatorial-apical fashion, while larger bidentate ligands forming eight- or nine-membered chelate rings show preferentially bis-equatorial coordination. Variable temperature NMR experiments provided evidence for a rapid exchange process between both phosphorus atoms. The fluxional behavior of these pentacoordinate $[RhH(CO)_2(P-P)]$ species on the NMR time scale has also been studied [9].

An interesting relationship between the structure of the $[RhH(CO)_2(P-P)]$ species and their enantio-discriminating performance has been found for several series of diphosphite ligands. In general, enantioselectivities were highest for ligands with a strong bis-equatorial (**ee**) coordination preference, and they were considerable reduced by equilibrium of species with bis-equatorial (**ee**) and equatorial-axial (**ea**) coordination modes (Scheme 5a) [22, 37, 49].

For the systems containing phosphine-phosphite ligands, the intermediates depend on the nature of the ligand. In the particular case of the (*R*,*S*) BINAPHOS, a single species hydrido carbonyl intermediate has been observed to contain the phosphine-phosphite ligand coordinated in an apical-equatorial position, with the phosphite *trans* to the hydride ligand. No apical-equatorial interchange was observed at any temperature. The unique dissymmetric environment in a single species created by the phosphine-phosphite seems to be an important factor for the high enantioselectivity obtained [20]. When other phosphine-phosphite ligands **30–32** (Fig. 9) were used the obtained ee was 40% and the characterization of the solution structures for the intermediate hydride rhodium dicarbonyl phosphine-phosphite species show two diastereoisomers in fast exchange (Scheme 5b) [35, 36].

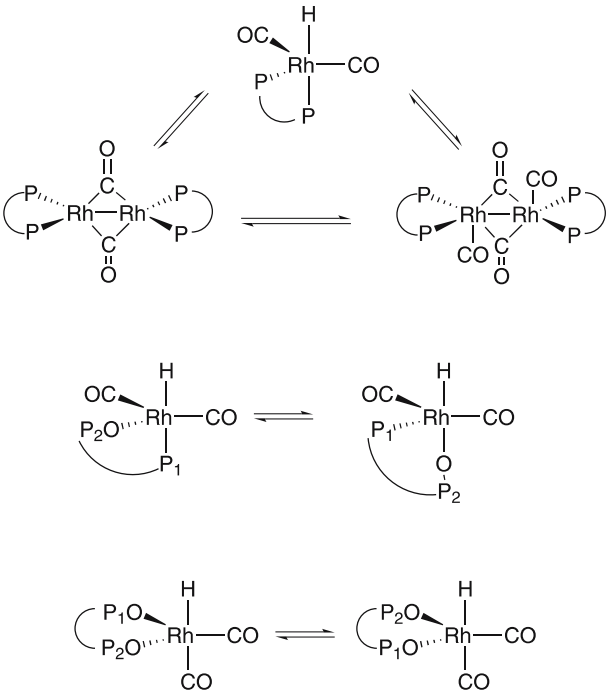

Scheme 5 Equilibrium between intermediate species characterized for: **a** diphosphites **b** phosphine–phosphite and **c** diphosphines

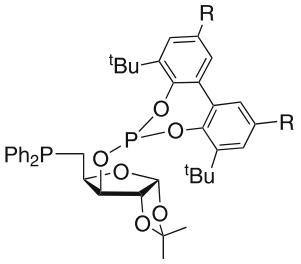

30

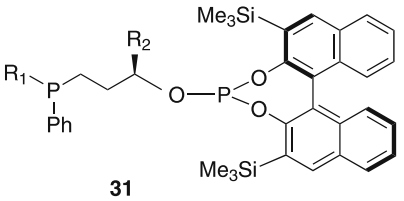

31

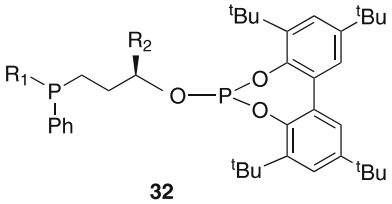

32

Fig. 9 Phosphine-phosphite ligands **30–32**

This equatorial axial phosphorus exchange shows that in the most stable diastereoisomer, the phosphine is in the axial position while the phosphite, the best π-acceptor is located in the equatorial position. This behavior contrasts with the coordination mode found for the BINAPHOS in which the phosphine occupies the equatorial position and the phosphite the axial position.

For diphosphines such as BDPP (**33**) or furanoside diphosphines derived from D-(+)-xylose (**34**) and D-(+)-glucose (**35**) (Fig. 10) the highest ee are of 60% [38, 42, 66].

In the case of BDPP with a bite angle of 90°, the high-pressure NMR and high-pressure IR studies showed the structures of the hydrido dicarbonyl diphosphine resting state as an axial-equatorial BPT. Similar behavior was observed for the furanoside diphosphines. Dinuclear rhodium species in equilibrium with the mononuclear pentacoordinate rhodium hydride carbonyl diphosphines have been found for these ligands. The position of this equilibrium depends on the hydrogen concentration and the ligands. The rate

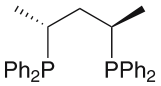

33 BDPP

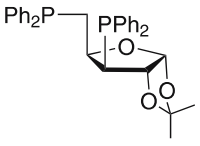

34

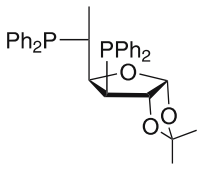

35

Fig. 10 Diphosphine ligands BDPP (**33**) and furanoside diphosphines (**34**, **35**)

of this monomer-dimer equilibrium may be in the same order of magnitude as the hydroformylation reaction. Hence, both the position of the equilibrium and the rate of the process should be considered in hydroformylation studies using diphosphines [38, 66].

When high-pressure NMR studies were carried out to characterize the intermediates for systems with P – S and P – N ligands, (phosphite–thiother ligands for instance) it was clearly observed that in these conditions the ligand acted as a monodentate, coordinated only through the phosphorous atom. This would account for the low or practically null ee obtained in these and other thioether systems [67, 68].

3
Rhodium-Catalyzed Asymmetric Hydroformylation of Vinyl Acetate

The asymmetric hydroformylation of functionalized aliphatic alkenes is generally more difficult than the hydroformylation of vinyl arenes. The rhodium-catalyzed hydroformylation of vinyl acetate (**36**) yields 2- and 3-acetoxypropanals, **37** and **38**, with high chemoselectivity. Ethyl acetate and acetic acid can also be found as by-products. One of the potential applications of vinyl acetate hydroformylation is the production of enantiopure propane 1,2-diol (Scheme 6).

For the vinyl acetate hydroformylation, it has been proposed that the insertion of the alkene into the Rh – H at the branched carbon atom is stabilized by a five-membered ring intermediate, which has been observed by NMR spectroscopy [69].

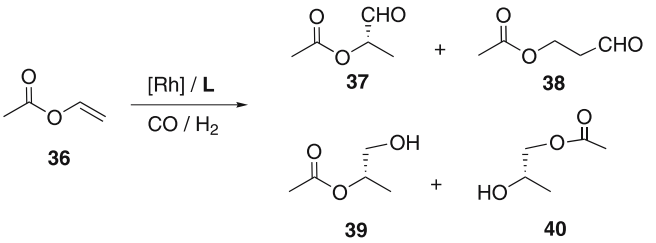

Scheme 6 Hydroformylation of vinyl acetate

3.1
Diphosphite and Phosphine-Phosphite Ligands

In 1992, Takaya et al. published the results of the asymmetric hydroformylation of vinyl acetate with chiral diphosphites, in which they have achieved an ee up to 52% [70]. At that time this result was the highest value reported for the asymmetric hydroformylation of vinyl acetate.

Later, in 1994, the (*R*,*S*-BINAPHOS) ligand **3** (Fig. 1) was found to deliver high regioselectivity in branched aldehyde, excellent yields and up to 92% ee [71]. Until to date this is the highest ee reported for a rhodium-phosphorus ligand catalyst in vinyl acetate asymmetric hydroformylation. Polymer-immobilized chiral phosphine-phosphite-Rh(I) complexes were prepared from vinyl-BINAPHOS, which was copolymerized with divinylbenzene (55% content) in toluene initiated by 2,2′-azobis(2,4-dimethylpentanenitrile). These polymer-supported ligands were treated with $[Rh(acac)(CO)_2]$ to give polymer-supported [Rh(acac)BINAPHOS]. An alternative route for preparing polymer-supported BINAPHOS-rhodium catalytic systems was to treat previously the monomers of vinyl-BINAPHOS with $[Rh(acac)(CO)_2]$ and then copolymerize them with divinylbenzene to give polymer-supported [Rh(acac)BINAPHOS] complexes. The polymer-supported catalysts were successfully applied in the asymmetric hydroformylation of vinyl acetate (i/n-ratio = 85/15–90/10; ee = 89–93 with *S* configuration) [61, 62]. The C_2-symmetry aryl diphosphite derived from chiral binaphthol **41** has also been prepared to be used as a catalyst for the asymmetric hydroformylation of olefins (Fig. 11). Enantioselectivity of up to 38% ee was achieved for the hydroformylation of vinyl acetate and catalytic activity and regioselectivity were good [72].

The influences of the ligand-to-metal ratio, reaction temperature and syngas pressure on the enantioselectivity and regioselectivity were also studied. A multi-substrate screening approach has recently been used by Dow Chemical Company to identify the best catalyst for the hydroformylation of vinyl acetate. Here, the chiral phosphite Kelliphite, **5** (Fig. 1) gave enantioselectivity up 88% ee and excellent regioselectivity for the branched isomer [24, 25].

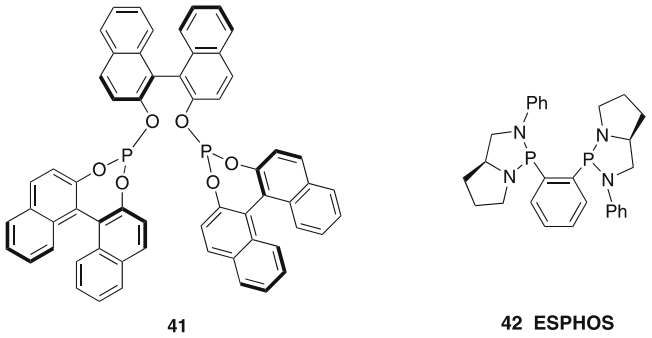

41 42 ESPHOS

Fig. 11 Ligands 41 and 42 for Rh-catalyzed hydroformylation of vinyl acetate

3.2 Diphosphine and Bis(diazaphospholidine) Ligands

The atropoisomeric ligand BINAP has proved to be outstandingly efficient for asymmetric isomerization and hydrogenation reactions. It was previously used for the rhodium-catalyzed hydroformylation of vinyl acetate with moderate results. Enantiomeric excesses did not exceed 47% and the yields were very low (6%) [70]. Later, the same Rh/BINAP system but with different rhodium precursors was optimized and the reaction conditions were modified. This improved the results and lead to enantiomeric excess of 60%. Regioselectivity was high (95–99%) although the yields were still moderate (20–40%) for the $[Rh(acac)(CO)_2]$ precursor. Using the $[Rh(\mu\text{-}OMe)(cod)]_2$ precursor, however, yields to 2-acetoxylpropanal were significantly higher [73]. In addition, in situ-generated rhodium complexes of mono- and bisphosphorylated BINAP ligands **43–45** have been used for the asymmetric hydroformylation of vinyl acetate (Fig. 12).

In comparison to BINAP, the enantioselectivity increased by 6–9%. This enhanced selectivity may be due to the interaction between the polar phosphonate group and the polar substrate vinyl acetate which can favor one of the diasteromeric transition states. When the same catalytic systems were used in the aqueous biphasic system $H_2O/EtOH = 2/1$, the enantioselectivity decreased (25–39%), and the enantioselectivity of the catalytic systems based on the precursor $[Rh(\mu\text{-}OMe)(cod)]_2$ were best [74]. Like the asymmetric hydroformylation of styrene diphosphines generally provide lower ee than the related phosphite containing ligands. In the case of the rhodium-catalyzed asymmetric hydroformylation of vinyl acetate, however, an interesting ligand is bis-(diazaphospholidine) ESPHOS (**42**) which provided ee up to 89% and high regioselectivity in branched aldehyde (92–97%) (Fig. 11) [75, 76]. Furthermore, when the conditions of the reaction are modified increasing the pressure and the reaction time, hydrogenation of the aldehydes takes place providing 59% of alcohols with an enantioselectivity of 84%. The hydro-

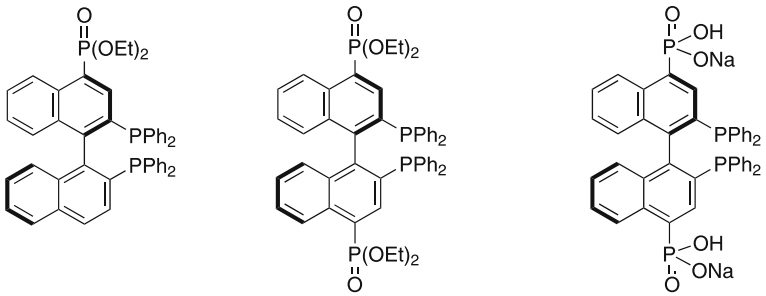

Fig. 12 Mono- and bisphosphorylated enantiopure BINAP ligands **43–45**

genation activity of this catalyst has been attributed to the electron donating nature of the phosphino-amino ligands [75]. Two related ligands based on ferrocene and biphenylether backbones gave worse results in hydroformylation in comparison with ESPHOS by itself [76]. The vinyl acetate hydroformylation results obtained with these ligands have been attributed to monodentate coordination.

4
Rhodium-Catalyzed Asymmetric Hydroformylation of Dihydrofurans

Although aldehydes obtained through the hydroformylation of dihydrofurans are interesting building blocks for organic synthesis, few studies have been reported on the subject. In 1998, previous work on the control of the regioselectivity in the hydroformylation of dihydrofurans has been reported with rhodium systems modified with different ligands [77, 78]. In the hydroformylation of 2,5-dihydrofuran **46** the expected product is the tetrahydrofuran 3-carbaldehyde **49** (Scheme 7).

However, considerable amounts of 2,3-dihydrofuran **50** and tetrahydrofuran-2-carbaldehyde **53** were present because of an isomerization process. The isomerization takes place simultaneously with the hydroformylation reaction. When the 2,5-dihydrofuran **46** reacts with the rhodium hydride complex, the 3-alkyl intermediate **48** is formed. This can evolve to the 2,3-dihydrofuran **50** via β-hydride elimination reaction. This new substrate can also give both 2- and 3-alkyl intermediates **52** and **48**, respectively. Although the formation of the 3-alkyl intermediate **48** is thermodynamically favored, the acylation occurs faster in the 2-alkyl intermediates **52**. Regioselectivity is therefore dominated by the rate of formation of the acyl complexes. The modification of the phosphorus ligand and the conditions of the reaction make it possible to control the regioselectivity and prepare the 2- or 3-substituted aldehyde as the major product [78]. As far as we know, only two

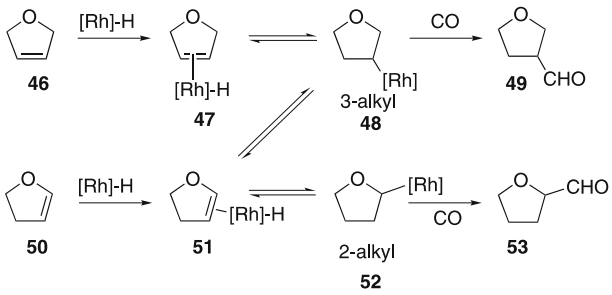

Scheme 7 Mechanism for the hydroformylation-isomerization process of dihydrofurans **46** and **50**

reports have been published on the asymmetric hydroformylation of dihydrofurans using phosphine-phosphite [79] and diphosphite ligands [80].

4.1 Phosphine-Phosphite Ligands

The phosphine-phosphite BINAPHOS ligand was first used in the Rh-catalyzed asymmetric hydroformylation of heterocyclic olefins such as 2,5-dihydrofuran, 3-pyrroline derivatives, and 4,7-dihydro-1,3-dioxepin derivatives. It provided the optically active aldehydes as single products with enantioselectivity between 64–76% ee. In the hydroformylation of 2,5-di-

Table 3 Rh-catalyzed asymmetric hydroformylation of 2,5-dihydrofuran **46** with ligands **30**, **4**, **16**–**19**[a]

Entry	Ligand	% Aldeh (**49**/**53**)	% **50**	% ee of **49**
1	**19**[a]	88 (100/0)	12	53 (*S*)
2	**19**[a,b]	98 (95/5)	2	37 (*S*)
3	**4**[a]	99 (99/1)	1	74 (*S*)
4	**16**[a]	100 (72/28)	0	< 5
5	**17**[a]	99 (95/5)	1	23 (*R*)
6	**18**[a]	100 (64/36)	0	< 5
7	**3**[c]	100 (100/0)	0	64 (*R*)

[a] Pressure 18 bar; $[Rh(acac)(CO)_2]$ = 0.012 mmol; Ligand/Rh = 2/1; Molar ratio **46**/Rh = 400/1; Solvent = toluene; Temperature = 45 °C; Time = 24 h; Conversion 100%
[b] Time = 48 h
[c] Pressure 20 bar; Ligand/Rh = 4/1; Solvent = benzene; Molar ratio **46**/Rh = 400/1; Temperature = 40 °C; Time = 24 h; Conversion 100%

Table 4 Rh-catalyzed asymmetric hydroformylation of 2,5-dihydrofuran **50** with ligands **3**, **4**, **17** and **19**[a]

Entry	Ligand	% Aldeh (**49**/**53**)	% ee of **49**
1	**19**[a,b]	88 (78/22)	48 (*R*)
2	**4**[a]	100 (76/24)	75 (*R*)
3	**17**[a]	100 (68/32)	43 (*S*)
4	**3**[c]	100 (50/50)	38 (*S*)

[a] Pressure 18 bar; $[Rh(acac)(CO)_2]$ = 0.012 mmol; Ligand/Rh = 2/1; Molar ratio **50**/Rh = 400/1; Solvent = toluene; Temperature = 45 °C; Time = 24 h; Conversion 100%
[b] Conversion 88%
[c] Pressure 20 bar; Ligand/Rh = 4/1; Solvent = benzene; Molar ratio **50**/Rh = 400/1; Temperature = 40 °C; Time = 24 h; Conversion 100%

hydrofuran, the rhodium-BINAPHOS system gave ee up to 64% with total regioselectivity in tetrahydrofuran-3-carbaldehyde (Table 3, entry 7). Interestingly, the hydroformylation of 2,3-dihydrofuran led to a mixture of **49** and **53** (50/50), with an ee of 38% in **49** (Table 4, entry 4). The configuration of aldehyde **49** obtained from the hydroformylation of 2,5-dihydrofuran is opposite to that which is obtained from the hydroformylation of 2,3-dihydrofuran with the same catalyst [79].

4.2
Diphosphite Ligands

Recently, diphosphite ligands **2**, **16**, **17**, **4** and **19** (Figs. 1, 3, 5) representative of the most successfully applied families in the hydroformylation of vinylarenes were used for the first time in the rhodium-catalyzed hydroformylation of 2,3- and 2,5-dihydrofurans [80]. The results are presented in Table 3. For ligand **19**, long reaction times increased conversions into aldehydes (entry 2 versus entry 1); however the regio- and enantioselectivity in the desired product **49** decreased. The hydroformylation of the 2,3-dihydrofuran **50** formed should account for this loss of selectivity, as shown by the results obtained in the hydroformylation of 2,3-dihydrofuran (Table 4). After 48 h the hydroformylation of **50** afforded a 78 : 22 mixture of (*R*)-**49** (48%) and **53** in 88% conversion (Table 4, entry 1). Therefore the loss in regioselectivity at the longer reaction time is due to the hydroformylation of the 2,3-dihydrofuran **50** formed under reaction conditions, as it had been previously found [78]. The enantioselectivity decreased because the absolute configuration of the predominant enantiomer of **49**, obtained from 2,3-dihydrofuran **50** is *R*, which is opposite to that obtained from 2,5-dihydrofuran, as was previously demonstrated in the rhodium BINAPHOS catalyzed hydroformylation of these substrates. The use of ligand **4** (Table 3, entry 3), which differs from ligand **19** in the methyl substituent at C-5, showed conversion into aldehydes of 99% with no isomerization, practically total regioselectivity in **49** with an ee of 74% (*S*). It is noteworthy that this ligand also provided high ee in the asymmetric hydroformylation of vinylarenes (up to 93%) [21–23].

5
Rhodium-Catalyzed Asymmetric Hydroformylation of Unsaturated Nitriles

The hydroformylation of unsaturated nitriles such as crotonitrile and allyl cyanide is a potential route towards chiral amino alcohols, which are building blocks in the synthesis of pharmaceuticals. The hydroformylation of acrylonitrile was studied in the early years [5], but lately the hydroformylation of allyl cyanide and crotonitrile have also been investigated [25, 81].

5.1 Rhodium-Catalyzed Asymmetric Hydroformylation of Allylcyanide

The asymmetric hydroformylation of allyl cyanide has recently focused the interest of researchers because the iso-aldehyde derivative can be easily transformed into 2-methyl-4-aminobutanol, a useful building block, for instance for the asymmetric synthesis of tachikinin (**58**), a novel NK1 receptor agonist developed by Takeda [82]. It should be noticed that this aldehyde is not accessible via the hydroformylation of crotononitrile.

J.G. de Vries et al. [81] found that in the rhodium-catalyzed hydroformylation of allyl cyanide the use of phosphites and phosphoramidites as ligands afforded preferentially the iso-aldehyde, while phosphines such as xantphos mainly gave the n-aldehyde. The regioselectivity of the process was favored by the use of bulky phosphite ligands and low temperatures. They also found that the use of BINAPHOS as ligand provided a 66% ee, with an *iso/n*-ratio of 2.57 when the reaction was conducted at a pressure of 30 bar, temperature of 50 °C, 0.2 mol % of Rh pre-catalyst and metal/ligand ratio of 1 : 4 (Table 5, entry 1). Later, Cobley et al. [24] carried out a high-throughput screening of a wide variety of mono- and diphosphites ligands, which were prepared following parallel techniques (Fig. 13).

These ligands were prepared from the commercially available (*S*)-5,5′-6,6′-tetramethyl-3,3′-di-tert-butyl-1,1′-biphenyl-1,1′-diol [(*S*)-BIPHEN-H2] and

Table 5 Rh-catalyzed asymmetric hydroformylation of allyl cyanide with ligands **2**, **5**, **59–62**

Entry	Ligand	Conv. (%)	*iso/n* ratio	% ee
1	**2** [a]	73 [d]	2.57	66 (*S*)
2	**2** [b,c]	47.8	2.7	75.6 (*S*)
3	**3** [b]	21.9	7.3	15.3 (R)
4	**5** [b]	84.8	15.5	78.1 (*S*)
5	**59** [b]	100	12.4	12.1 (*S*)
6	**60** [b]	8.7	7.1	9.2 (*R*)
7	**61** [b]	73.3	8.5	0.7 (*S*)
8	**62a** [b]	11.3	6.3	43.7 (*R*)
9	**62b** [b]	65	5.2	39.7 (*R*)
10	**62c** [b]	30.5	5.0	14.1 (*R*)

[a] Pressure 390 Psi; Ligand/Rh = 4/1; Solvent = toluene; Molar ratio allyl cyanide/Rh = 200/1; Temperature = 50 °C; Time = 3 h

[b] Pressure 150 Psi; Ligand/Rh = 1.2/1 for bidentate and 2.2/1 for monodentate phosphites; Solvent = toluene; Molar ratio allyl cyanide/Rh = 300/1; Temperature = 35 °C; Time = 3 h

[c] Run performed in acetone

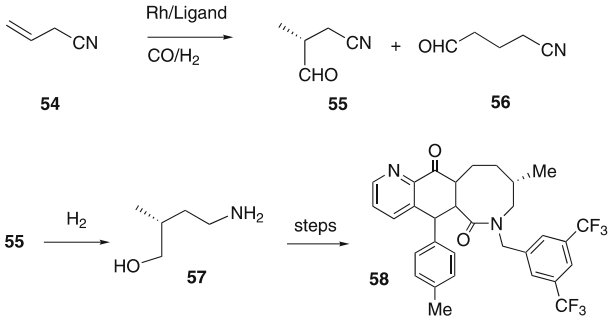

Scheme 8 Hydroformylation of allyl cyanide **54** and preparation of **58**

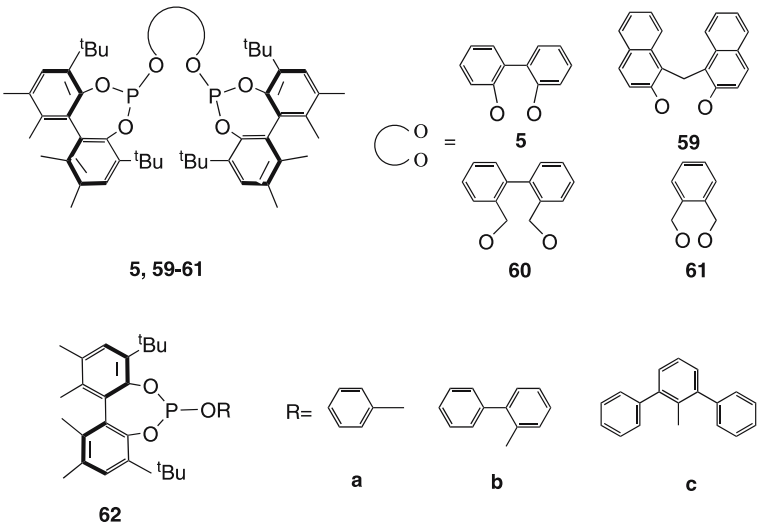

Fig. 13 Monophosphites **62** and diphosphites ligands **5**, **59–61**

phenols. The biphosphite **5** (Kelliphite) was found to be the best ligand for the asymmetric hydroformylation of allyl cyanide giving an ee higher than 78% and *iso/n* ratios > 15 when the reaction was driven at 10 bar of pressure, at 35 °C, and the substrate to catalyst molar ratio was 300 : 1 (Table 5, entry 4) [24]. These authors also found that the enantioselectivity obtained with BINAPHOS could be increased to 75.6% when the reaction was conducted in acetone, although the regioselectivity still had a low *iso/n*-ratio of 2.7 (Table 5, entry 2). The diphosphite **3** gave very low ee in similar conditions (Table 5, entry 3).

Other bisphosphite ligands **59–61**, related to Kelliphite (**5**) were prepared by replacing the 2,2′-biphenol unit with other biphenol moieties. The Rh/**59** catalytic system was the most active, and also afforded a high regioselectivity. The ee, however was very low (entry 5, Table 5). The Rh/**60,61** cata-

lytic systems also provided very low ee (entries 6, 7, Table 5). Curiously, the monophosphite ligands **62a–c** afforded ee's of 43.7, 39.7, and 14.1, respectively, in the rhodium catalyzed hydroformylation allyl cyanide (entries 8–10, Table 5).

6
Catalytic Experiments. IR In Situ and High-Pressure NMR Experiments

Rhodium catalysts for asymmetric hydroformylation are generally prepared in situ by adding the P – P chiral ligand to a solution of $[Rh(acac)(CO)_2]$ or similar starting materials such as $[Rh(\mu\text{-OMe})(COD)]_2$. It is recommended that there be no chloride ligand in the rhodium precursor. When isolated complexes were tested for comparison, the results were generally the same as for the Rh/ligand systems prepared in situ. In some catalytic systems, however, an incubation period is required for the formation of the catalytic species $[RhH(CO)_2(P-P)]$ [9]. These species can be prepared in situ under hydroformylation reaction conditions by adding one equivalent of P – P ligand to the catalyst precursor $[Rh(acac)(CO)_2]$. Initially, displacement of two carbon monoxide molecules by the ligand caused the formation of the $[Rh(acac)(P-P)]$ complexes, which after a short time under hydroformylation conditions evolved to the intermediate species $[Rh(acac)(CO)P-P]$. Reaction times depend on the type of ligand and may take several hours to complete the formation of the desired species (Scheme 9).

In a typical experiment the autoclave was purged three times with CO, then filled with a solution of $[Rh(acac)(CO)_2]$ in toluene or other appropriate solvent. The chiral ligand was added to the solution, and the P – P/Rh ratio depends on the nature of the ligand. After pressurizing to the desired pressure (20–100 bar depending on the nature of the catalyst and substrate) with *syn*-gas and heating the autoclave to the reaction temperature (40–100 °C), the reaction mixture was stirred. After the desired reaction time, the autoclave is cooled to room temperature and depressurized. The reaction mixture was analyzed by gas chromatography or NMR depending on the substrates. HP NMR and in situ IR are experimental techniques for characterizing catalysts. NMR spectroscopy of ^{1}H, ^{31}P, ^{13}C is useful for the characterization of

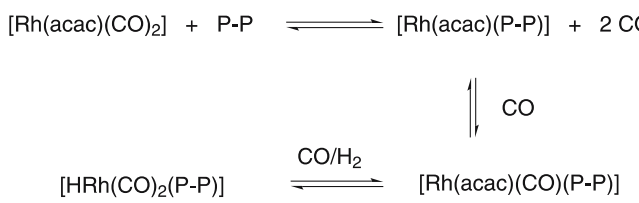

Scheme 9 In situ preparation of the active catalyst species

organometallic species. IR spectroscopy is useful mainly for identifying carbonylated species. Both IR and NMR spectroscopy are used at high pressure in appropriate tubes or cells. The advantages and disadvantages are: (a) For NMR, concentration must be high, and the species observed might not be relevant to the catalytic process. One of the disadvantages of high-pressure NMR tubes is that reactive systems involving gas consumption cannot be studied truly in situ. Its advantages, however, are that high pressure is allowed and the technique provide an accurate analysis of the structures. (b) IR spectroscopy on the other hand allows low concentrations, high pressure and in situ measurements although it provides less structural information.

The HP NMR are recorded in a sapphire tube ($d = 10$ mm) with a titanium head and pressure valve. The tube is filled under argon with a solution of $[Rh(acac)(CO)_2]$ and ligand (the appropriate P/Rh molar ratio) in toluene-d8 or other solvents. The HP NMR tube is purged twice with CO and pressurized to the appropriate pressure of CO/H_2. After the sample has been shaken and the desired temperature reached, the solution is analyzed through NMR. The in situ IR experiments require a special autoclave that contains the IR windows directly in the cell. Although different autoclaves have been used, a cell using transmission IR spectroscopy with a very short time delay in the transport of liquid from the autoclave to the cell by a centrifugal pump and efficient mixing has proved to give efficient results [83, 84].

7 Conclusions and Remarks

Although hydroformylation is the largest volume industrial process that uses homogeneous catalysis, its application in the production of fine chemicals is still limited. In recent years however new ligands have appeared which in combination with rhodium precursors make it possible to control of the chemo-, regio- and enantio-selectivity for the production of aldehydes. The ligands **2–5** depicted in Fig. 1 have proved to be efficient enough to obtain the branched aldehyde with high enantioselectivity. The vinyl arenes, which are the most commonly studied substrates because of their interest as intermediates in the synthesis of arylpropionic acids can be hydroformylated with ee between 90–95%. Apart from the structurally unique BINAPHOS which hydroformylates a wide range of chiral olefins, diphosphites constitute the most efficient ligands for catalytic asymmetric hydroformylation. Although in some cases the rhodium catalyst formed with the diphosphite ligands are not very active, the mild conditions required and the control of the regioselectivity in combination with a high enantioselectivity can provide excellent results. Interestingly, the diphospite ligands related to **2**, **4** and **5** are easy to prepare and particularly modular. All this, together with the high-throughput screening generated to identify new ligands makes it possible to optimize

the process and identify new efficient ligands. The characterization of the structures of the intermediate species in solution for several systems, by HP NMR in the reaction conditions and in situ HP IR, has provided better understanding of the catalytic reaction and is a useful tool for determining the best modifications to obtain efficient ligands. Finally, the hydroformylation of substrates such as vinyl acetate, heteroatom functionalized olefins and unsaturated nitriles open up new routes to synthesize building blocks for the synthesis of a wide variety of products of biological interest. Nowadays if the asymmetric hydroformylation reaction is not used to synthesize enantiopure aldehydes it may be because of technical difficulties. If the ligand is appropriate, rhodium-catalyzed hydroformylation should provide results that justify its application.

References

1. van Leeuwen PWNM, Claver C (eds) (2000) Rhodium-Catalyzed Hydroformylation. Kluwer Academic Press, Dordrecht
2. Frohning CD, Kohlpaintner CW (1996) In: Cornils B, Herrmann W (eds) Applied Homogeneous Catalysis with Organometallic Compounds, vol 1. Wiley-VCH, Weinheim, p 1–15
3. van Leeuwen PWNM, Casey CP, Whiteker GT (2000) Phosphines as Ligands. In: van Leeuwen PWNM, Claver C (eds) Rhodium-Catalyzed Hydroformylation. Kluwer Academic Press, Dordrecht, p 63
4. Breit B, Seiche W (2001) Synthesis, p 1
5. Castillón S, Férnandez E (2000) Hydroformylation in Organic Synthesis. In: van Leeuwen PWNM, Claver C (eds) Rhodium-Catalyzed Hydroformylation. Kluwer Academic Press, Dordrecht, p 145
6. Botteghi C, Marchetti M, Paganelli S (1998) In: Beller M, Bolm C (eds) Transition Metals for Organic Synthesis. Building Blocks and Fine Chemicals. Wiley-VCH, Weinheim, p 25
7. Nozaki K, Ojima I (2000) In: Ojima I (ed) Catalytic Asymmetric Synthesis, 2nd edn. Wiley, New York
8. Chapuis C, Jacoby D (2001) Appl Catal 221:93
9. Claver C, van Leeuwen PWNM (2000) Asymmetric Hydroformylation. In: van Leeuwen PWNM, Claver C (eds) Rhodium-Catalyzed Hydroformylation. Kluwer Academic Press, Dordrecht, p 107
10. Stille JK, Su H, Brechot P, Parrinello G, Hegedus LS (1991) Organometallics 10:1183
11. Consiglio G, Nefkens SCA (1990) Tetrahedron: Asymmetry 1:417
12. Consiglio G, Nefkens SCA, Borer A (1991) Organometallics 10:2046
13. Cserépi-Szücs S, Bakos J (1997) J Chem Commun, p 635
14. Agbossou FF, Carpentier JF, Mortreux A (1995) Chem Rev 95:2485
15. Gladiali S, Bayón JC, Claver C (1995) Tetrahedron: Asymmetry 7:1453
16. Beller M, Cornils B, Frohming CD, Kohlpaintner CW (1995) J Mol Catal 104:17
17. Babin JE, Whiteker GT (1992) (Union Carbide Chem Plastics Techn Co) WO 93/03839, 1993 [Chem Abs 1993, 119, P159872h]
18. Buisman JGH, Vos E J, Kamer PCJ, van Leeuwen PWNM (1995) J Chem Soc Dalton Trans, p 409

19. Sakai N, Mano S, Nozaki K, Takaya H (1993) J Am Chem Soc 115:773
20. Nozaki K, Sakai N, Nanno T, Higashijima T, Mano S, Horiuchi T, Takaya H (1997) J Am Chem Soc 119:4413
21. Diéguez M, Pàmies O, Ruiz A, Castillón S, Claver C(2000) Chem Commun 2000, p 1617
22. Diéguez M, Pàmies O, Ruiz A, Castillón S, Claver C (2001) Chem Eur J 7:3086
23. Diéguez M, Pàmies O, Ruiz A, Claver C (2002) New J Chem 26:826
24. Cobley CJ, Gardner K, Klosin J, Praquin C, Hill C, Whiteker GT, Zanotti-Gerosa A, Petersen JL, Abboud KA (2004) J Org Chem 69:4031
25. Cobley CJ, Closing J, Qin C, Whiteker GT (2004) Org Lett 6:3277
26. Rampf FA, Herrmann WA (2000) J Organomet Chem 601:138
27. For a complete discussion including the detailed aspects of the different steps in this catalytic cycle see: Van Leeuwen PWNM (2004) Homogeneous Catalysis: Understanding the Art. Kluwer Academic Publishers, Dordrecht, p 141
28. Feng J, Garland M (1999) Organometallics 18:417
29. Liu G, Volken R, Garland M (1999) Organometallics 18:3429
30. Bergounhou C, Neibecker D, Réau R (1995) Bull Soc Chim Fr 132:815
31. van Rooy A, Orij EN, Kamer PCJ, van Leeuwen PWNM (1995) Organometallics 14:34
32. del Río I, Pàmies O, van Leeuwen PWNM, Claver C (2000) J Organomet Chem 608:115
33. van der Slot SC, Kamer PJC, Van Leeuwen PWNM (2001) Organometallics 20:1079
34. Nozaki K, Matsuo T, Shibahara F, Hiyama T (2003) Organometallics 22:5994
35. Deerenberg S, Kamer PJC, Van Leeuwen PWNM (2000) Organometallics 19:2065
36. Pàmies O, Net G, Ruiz A, Claver C (2001) Tetrahedron: Asymmetry 12:3441
37. Buisman GJH, van der Veen LA, Klootwijk A, de Lange WGJ, Kamer, Paul CJ, van Leeuwen PWNM, Vogt D (1997) Organometallics 16:2929
38. Castellanos-Paéz A, Castillón S, Claver C, van Leeuwen PWNM, de Lange WGJ (1998) Organometallics 17:2543
39. del Rio I, de Lange W G J, van Leeuwen PW NM, Claver C (2001) J Chem Soc Dalton Trans 8:1293
40. Gleich D, Herrmann WA (1999) Organometallics 18:4354
41. Gleich D, Schmid R, Herrmann WA (1998) Organometallics 17:2141
42. Diéguez M, Pereira MM, Masdeu-Bultó AM, Claver C, Bayón JC (1999) J Mol Catal A: Chemical 143:111
43. Diéguez M, Ruiz A, Claver C (2003) Dalton Trans, p 2957
44. For successful applications with diphosphite ligands see the review: Diéguez M, Pàmies O, Claver C (2004) Tetrahedron: Asymmetry 15:2113
45. Nozaki K, Takaya H, Hiyama T (1997) Top Catal 4:157
46. Wink JD, Kwok TJ, Yee A (1990) Inorg Chem 29:5007
47. Cserépi-Szûcs S, Tóth I, Párkányi L, Bakos J (1998) J Tetrahedron: Asymmetry 9:3135
48. $[HRh(CO)_2(diphosphite)]$ species are known to be the resting state in the hydroformylation reaction. See for instance: van Leeuwen PWNM, Claver C (eds) (2000) Rhodium-Catalyzed Hydroformylation. Kluwer Academic Press, Dordrecht
49. Buisman GJH, van der Veen LA, Kamer PCJ, van Leeuwen PWNM (1997) Organometallics 16:5681
50. Pàmies O, Net G, Ruiz A, Claver C (2000) Tetrahedron: Asymmetry 11:1097
51. Buisman GJH, Martin ME, Vos EJ, Klootwijk A, Kamer PCJ, van Leeuwen PWNM (1995) Tetrahedron: Asymmetry 8:719
52. Cserépi-Szûcs S, Huttner G, Zsolnai L, Bakos JJ (1999) Organomet Chem 586:70

53. Cserépi-Szûcs S, Huttner G, Zsolnai L, Szölösy A, Hegebüs C, Bakos J (1999) Inorg Chim Acta 296:222
54. Vegehetto V, Scrivanti A, Matteoli U (2001) Catal Commun 2:139
55. Jiang YX, Xue S, Li Z, Deng J, Mi A, Chan ASC (1998) Tetrahedron: Asymmetry 9:3185
56. Jiang YX, Yu K, Li Z, Deng J, Mi A, Chan ASC (1999) J Organomet Chem 586:159
57. Kadyrov R, Heller D, Selke R (1999) Tetrahedron: Asymmetry 9:329
58. Freixa Z, Bayón JC (2001) J Chem Soc Dalton Trans 2067
59. Sakai N, Mano S, Nozaki K, Takaya K (1993) J Am Chem Soc 115:7033
60. Nozaki K, Matsuo T, Shibahara F, Hiyama T (2001) Adv Synth Catal 343:61
61. Nozaki K, Itoi Y, Shibayara F, Shirakawa E, Ohta T, Takaya H, Hiyama T (1998) J Am Chem Soc 120:4051
62. Nozaki K, Shibahara F, Itoi Y, Shirakawa E, Ohta T, Takaya H, Hiyama (1999) T Bull Chem Soc Jpn 72:1911
63. Franciò G, Leitner W (1999) Chem Commun, p 1663
64. Franciò G, Wittmann K, Leitner WJ (2001) Organomet Chem 621:130
65. Arena CG, Faraone F, Graiff C, Tiripicchio A (2002) Eur J Inorg Chem, p 711
66. Diéguez M, Pàmies O, Net G, Ruiz A, Claver C (2001) Tetrahedron: Asymmetry 12:651
67. Pàmies O, Diéguez M, Net G, Ruiz A, Claver C (2000) Organometallics 19:1488
68. Aghmiz A, Masdeu AM, Claver C, Sinou D (2002) J Mol Catal 184:111
69. Matsumoto M, Tamura M (1982) J Mol Catal 16:195
70. Sakai N, Nozaki K, Mashima K, Takaya H (1992) Tetrahedron: Asymmetry 3:583
71. Higashizima T, Sakai N, Nozaki K, Takaya H (1994) Tetrahedron Lett 35:2023
72. Yan ML, Xing S, Chan ASC (2004) Chin J Chem 22:203
73. Hoegaerts D, Jacobs PA (1999) Tetrahedron: Asymmetry 10:3039
74. Kockritz A, Bischoff S, Kant M, Siefken R (2001) J Mol Catal 174:119
75. Breeden S, Cole-Hamilton DJ, Foster DF, Schwarz GJ, Wills M (2000) Angew Chem Inter Ed 39:4106
76. Clarkson GJ, Ansell JR, Cole-Hamilton DJ, Pogorzelec PJ, Whittell J, Wills M (2004) Tetrahedron: Asymmetry 15:1787
77. Polo A, Real J, Claver C, Castillón S, Bayón JC (1990) J Chem Soc Chem Commun, p 600
78. Polo A, Claver C, Ruiz A, Castillón S, Bayón JC, Real J, Mealli C, Massi D (1992) Organometallics 11:3525
79. Horiuchi T, Tetsuo O, Shirakawa E, Nozaki K, Hidemasa TJ (1997) J Org Chem 62:4285
80. Diéguez M, Pàmies O, Claver C (2005) Chem Commun, p 2
81. Lambers-Verstappen MMH, de Vries JG (2003) Adv Synth Catal 345:478
82. Natsugari H, Ikeura Y, Kamo I, Ishimaru T, Ischichi Y, Fujishima A, Tanaka T, Kasahara F, Kawada M, Doi T (1999) J Med Chem 42:3982
83. Moser WR, Papite CJ, Brannon DA, Duwell Ra, Weininger SJ (1987) J Mol Catal 41:271
84. For more details see: van Leeuwen PWNM (2004) Homogeneous Catalysis: Understanding the Art. Kluwer Academic Publishers, Dordrecht, p 8

Top Organomet Chem (2006) 18: 65–95
DOI 10.1007/3418_017

Published online: 20 May 2006

Synthetic Applications of Tandem Reaction Sequences Involving Hydroformylation

Peter Eilbracht (✉) · Axel M. Schmidt

Fachbereich Chemie, Organische Chemie I, Universität Dortmund, Otto-Hahn-Str. 6, 44227 Dortmund, Germany
peter.eilbracht@udo.edu

1 Introduction 66

2 Heterofunctionalization of Aldehydes Obtained via Hydroformylation . . 67
2.1 Hydroformylation/Acetal Formation 68
2.1.1 *O*,*O*-Acetal Formation 68
2.1.2 *N*,*O*-Acetal Formation 69
2.1.3 *N*,*N*-Acetal (Aminal-)Formation 72
2.2 Hydroformylation/Imine/Enamine Formation 72
2.3 Hydroformylation/Reductive Amination 75

3 Additional *C*,*C*-Bond Formation of Aldehydes Obtained via Hydroformylation 79
3.1 Using Carbonyl Reactivity 79
3.1.1 Hydroformylation/Allylation 79
3.1.2 Hydroformylation/Aromatic Substitution 83
3.2 Using α-CH-Acidity 84
3.2.1 Hydroformylation/Aldol Reaction 84
3.3 Involving Sigmatropic Rearrangements 89
3.3.1 Hydroformylation/Carbonyl Ene Reaction 89
3.3.2 Hydroformylation/Fischer Indole Synthesis 90

4 Conclusions 93

References 93

Abstract Aldehydes obtained from olefins under hydroformylation conditions can be converted to more complex reaction products in one-pot reaction sequences. These involve heterofunctionalization of aldehydes to form acetals, aminals, imines and enamines, including reduction products of the latter in an overall hydroaminomethylation. Furthermore, numerous conversions of oxo aldehydes with additional *C*,*C*-bond formation are conceivable such as aldol reactions, allylations, carbonyl olefinations, ene reactions and electrophilic aromatic substitutions, including Fischer indole syntheses.

Keywords Aldol reactions · Fischer indole synthesis · Homogeneously catalyzed tandem reactions · Hydroaminomethylation · Hydroformylation

1 Introduction

The hydroformylation reaction ("oxo reaction") of alkenes with hydrogen and carbon monoxide is established as an important industrial tool for the production of aldehydes ("oxo aldehydes") and products derived there from [1–6]. This method also leads to synthetically useful aldehydes and more recently is widely applied in the synthesis of more complex target molecules [7–15, 17], including stereoselective and asymmetric syntheses [18–22].

Due to the versatile chemistry of the aldehyde group [23, 24], the products of hydroformylation are easily converted via reduction, oxidation, nucleophilic attack at the carbonyl group or electrophilic attack in the acidic α-position to give alcohols, amines, carboxylic acid derivatives, aldol condensation products and many others. Therefore, following the growing interest in the development of new and efficient non-catalyzed or homogeneously catalyzed one-pot reaction sequences [25], defined as "domino reactions", "reaction cascades" or "tandem reactions" [26], hydroformylation is a powerful synthetic method to be integrated in multi-step reaction sequences [27–29]. Tandem reactions, combining two or more different transformations in one synthetical procedure without change of reaction conditions and without addition of further reagents or catalysts require only one single setup of starting materials, reagents, and solvents and no isolation of intermediates is necessary. Therefore they save time and materials and furthermore they avoid waste of chemicals and solvents. At present, considerable effort is concentrated on the development of new procedures, even in total synthesis of more complex target molecules [30, 31].

Tandem procedures under hydroformylation conditions cannot only make use of the intrinsic reactivity of the aldehyde carbonyl group and its acidic α-position but they also include conversions of the metal alkyl and metal acyl systems which are intermediates in the catalytic cycle of hydroformylation. Metal alkyls can undergo β-elimination leading to olefin isomerization, or couplings, respectively, insertion of unsaturated units enlarging the carbon skeleton. Similarly, metal acyls can be trapped by addition of nucleophiles or undergo insertion of unsaturated units to form synthetically useful ketones (Scheme 1).

In this survey, selected synthetic applications of tandem hydroformylation sequences are described and complementing the more comprehensive reviews covering the literature up to 1998/99 [27], and up to 2003 [28, 29]. The material is ordered according to the type of the additional transformation involving heterofunctionalization of the aldehyde group to form acetals, aminals, imines and enamines, as well as reduction of the latter in an overall hydroaminomethylation. Furthermore, numerous conversions of oxo aldehydes with additional *C*,*C*-bond formation at the carbonyl group or at the acidic

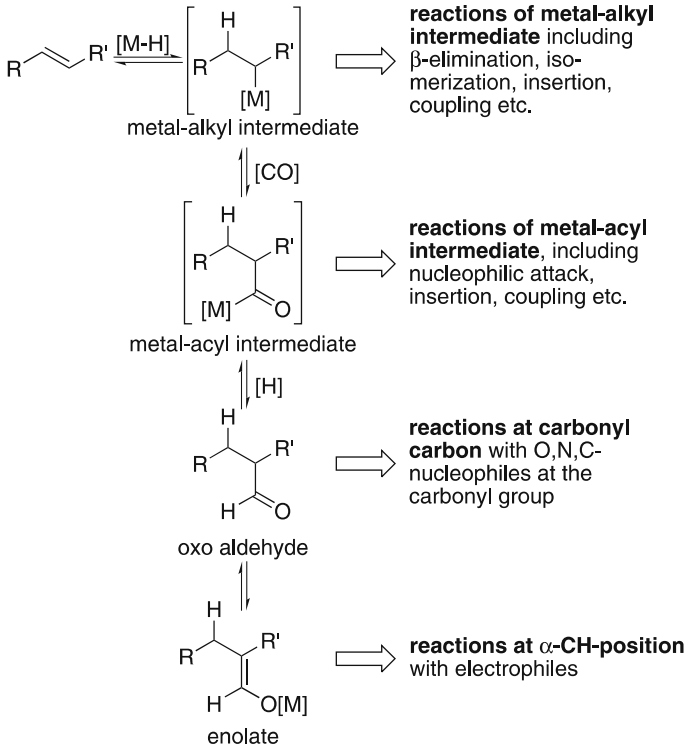

Scheme 1 Different stages of the hydroformylation and options for consecutive reactions

α-position are presented, such as aldol reactions, allylations, carbonyl olefinations, ene reactions and electrophilic aromatic substitutions, including Fischer indole syntheses. Not included here are the comprehensively described tandem reactions with isomerization of the double bond or reduction of aldehydes to alcohols and their further transformations as well as reactions involving conversions of the metals alkyl and metal acyl intermediates mentioned above.

2
Heterofunctionalization of Aldehydes Obtained via Hydroformylation

Hydroformylation in the presence of nucleophiles such as alcohols or amines leads to *O*,*O*- or *N*,*O*-acetals, aminals, imines or enamines (Scheme 2).

Imines and enamines under hydroformylation conditions can also be reduced to give saturated amines. With or without additional reduction, these conversions can be used in synthesis of various types of heterocycles.

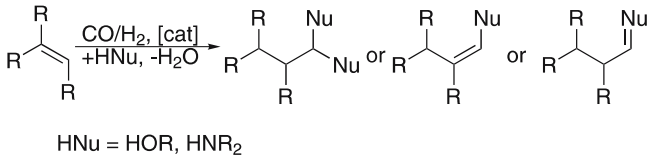

Scheme 2 Principle of hydroformylation in the presence of nucleophiles

2.1 Hydroformylation/Acetal Formation

2.1.1 *O,O*-Acetal Formation

Acetalization of oxo aldehydes is used to protect sensitive aldehyde products, especially in asymmetric hydroformylation preventing racemization of an α-chiral aldehyde product [18–22, 27]. Acetal formation can also be applied to the synthesis of monocyclic or spirocyclic pyranes as potential precursors and building blocks for natural products such as pheromones or antibiotics. A representative example is the synthesis of the pyranone subunit of the Prelog–Djerassi lactone. For this purpose, various 1,2-disubstituted homoallylic alcohols were used (Scheme 3) [32].

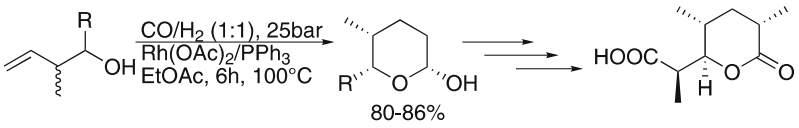

Scheme 3 Formation of *O,O*-acetals under hydroformylation conditions

Di- or tetrahydropyrans with vinyl side chains obtainable by diastereoselective ring closing metathesis or by addition of vinylmagnesium chloride to appropriately functionalized tetrahydropyranones are converted to spirocyclic hemiacetals under hydroformylation conditions (Scheme 4) [33]. Oxidation yields the corresponding lactones.

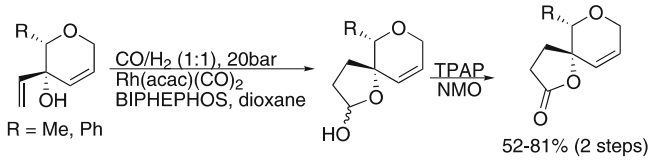

Scheme 4 Synthesis of spirocyclic γ-lactones

Similarly, δ-lactols and δ-lactones are obtainable from the corresponding homo allylic alcohols. With dehydration, the corresponding dihydropyrans are prepared. Spirocyclic γ-butyrolactones of this type and the corresponding δ-lactones are widespread in nature and play a key role as synthetic intermediates.

General Procedure for the Hydroformylation/*O,O*-acetal Formation. Synthesis of Spiro-*δ*-Lactones. A solution of the allylic alcohol (1 eq), $Rh(acac)(CO)_2$ (1.0 mol %), and BIPHEPHOS (4.0 mol %) in anhydrous dioxane was heated at 60 °C for 20 h under an atmosphere of carbon monoxide (10 bar) and hydrogen (10 bar) in an autoclave. The reaction mixture was filtered through basic alumina, and all organics were eluted with MTBE and then ethanol. The solvent was evaporated, and the crude hemiacetals were dissolved in DCM. Powdered molecular sieve (4 Å) and *N*-methyl morpholine-*N*-oxide (1.5 eq) were added, followed by TPAP (5 mol %). The mixture was stirred at ambient temperature until the starting material was completely converted as indicated by TLC (3 : 1 (v/v) hexane/EtOAc). The solvent was evaporated to one-third of the original volume, and the residue was filtered through a pad of silica. The products were eluted with MTBE and purified by flash chromatography, if necessary.

Similarly, furofuranes and benzofurofuranes known as substructure of aflatoxins are obtainable via hydroformylation of unsaturated diols. A representative example is given in Scheme 5 [34].

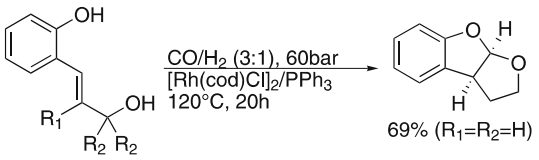

Scheme 5 Synthesis of aflatoxin analogous

2.1.2 *N,O*-Acetal Formation

Hydroformylation of unsaturated amines offer a convenient synthetic access to cyclic *N*,*O*-hemiacetals. If performed in the presence of alcohols or orthoesters *N*,*O*-acetals are formed. With additional *N*-nucleophiles *N*,*N*-acetals are obtained. These compounds are synthetically attractive building blocks and were therefore used as a key step in the synthesis of various natural products [27, 35]. Thus the synthesis of (+)-prosopinine starting from enantiopure (*R*)-serine leads to a cyclic *N*,*O*-acetal functionality with the required functionality for the attachment of the side chain (Scheme 6) [36].

In addition, deoxoprosphylline [36], pipecolic acids, izidines [37], and the bicyclic alkaloids (±)-isoretronecanol, (±)-trachelanthamidine [38] and 6-epi-poranthellidine [39] were synthesized via tandem hydroformyla-

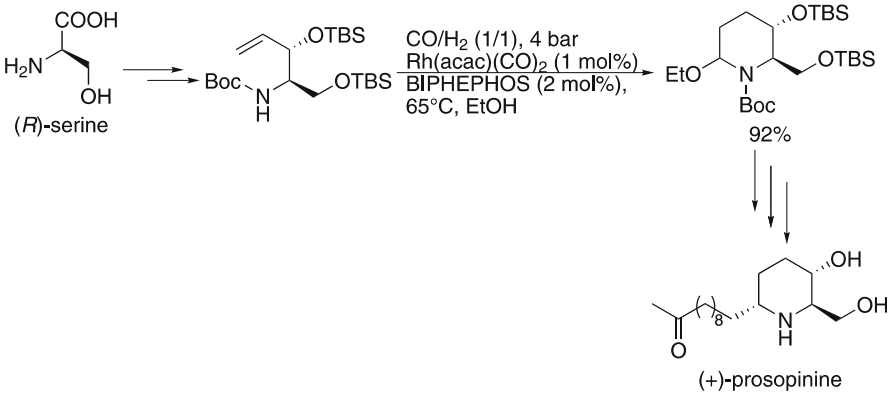

Scheme 6 Synthesis of (+)-prosopinine

tion/cyclization. More recently, highly efficient syntheses of azabi-cyclo[4.4.0] alkane amino acids were achieved by Rh-catalyzed cyclohydrocarbonylation of dipeptides bearing a terminal olefin moiety and a heteroatom nucleophile [40]. Here the amine function as well as a second *O*-, *S*-, or *N*-Boc function are present in the acyclic starting material to form the bicyclic system with *N*,*O*-, *N*,*N*- or *N*,*S*-subunits in one step (Scheme 7).

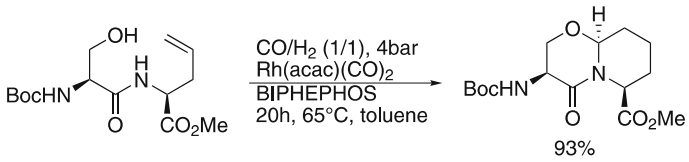

Scheme 7 Formation of *N*,*O*-acetals under hydroformylation conditions

Very recently the tandem hydroformylation/acetalization has been used for the synthesis of new synthetically valuable chiral auxiliary derived from camphor. Stereoselective allylation of camphor and subsequent terminal hydroformylation of the resulting homoallylic alcohol affords the δ-lactol auxiliary (camTHP*OH) in multigram scale (Scheme 8) [41].

If this hydroformylation is conducted in the presence *N*-nucleophile such as glycine dimethylamide the linkage of the substrate can be incorporated in the synthesis of the auxiliary. Subsequent Cbz protection affords a camTHP*-desymmetrized glycinamide building block that undergoes efficient and diastereoselective metal enolate alkylation. Acid mediated deprotection gives the *N*-Cbz protected α-amino amide products which may be converted directly to α-amino ketones on treatment with Grignard or organolithium reagents without loss of stereochemical integrity (Scheme 9) [41]

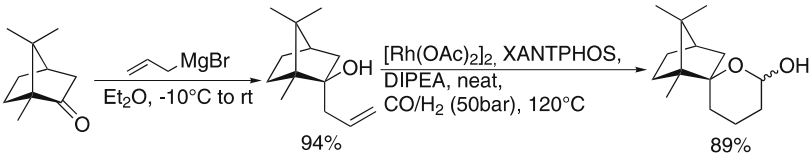

Scheme 8 Synthesis of camTHP*OH – a new chiral auxiliary

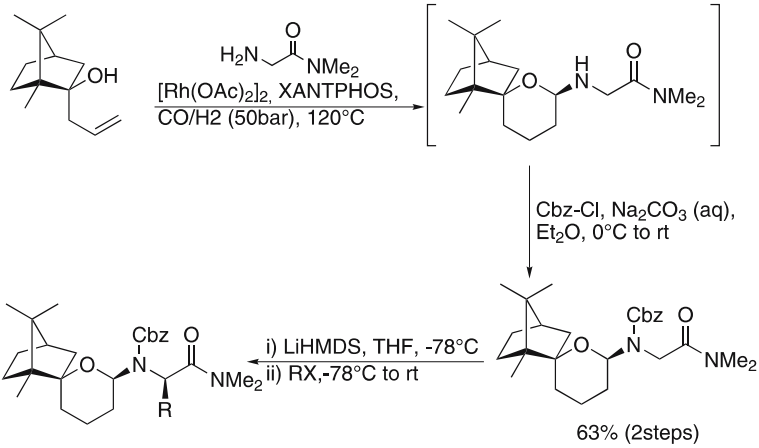

Scheme 9 Synthesis of desymmetrized glycinamide

General Procedure for the Hydroformylation/*N*,*O*-acetal Formation. Synthesis of camTHP*-desymmetrized Glycinamide. A stirred solution of the homoallylic alcohol (1 eq),$[Rh(OAc)_2]_2$ (0.1 mol % Rh), XANTPHOS (1 mol %), and glycinedimethyl amide (1.2 eq) under CO/H_2 (1 : 1, 50 bar) in a stainless-steel pressure vessel was heated to 120 °C for 16 h before being cooled to room temperature and depressurized to yield a yellow oil. The crude reaction mixture was diluted with Et_2O and saturated aqueous Na_2CO_3, cooled to 0 °C and stirred vigorously while benzyl chloroformate (1.5 eq) was added. The reaction was allowed to warm to ambient temperature and stirred under argon for 3 h before the addition of glycine (0.5 eq, to scavenge the excess benzylchloroformate) and the mixture stirred for a further 16 h. The biphasic mixture was diluted with water and extracted with EtOAc (3×). The combined organics were washed with brine, dried over $MgSO_4$, filtered through a pad of silica eluting with EtOAc and concentrated in vacuo to give a pale yellow oil. The crude product was purified by column chromatography (silica, petroleum ether (40–60 °C) : Et_2O, 9 : 1 gradient to neat Et_2O) to yield the title compound as a colorless oil (63%).

2.1.3
N,N-Acetal (Aminal-)Formation

N,*N*-Acetal formation used to prepare diazabicycloalkanes containing medium and large rings from *N*-alkenylpropane-1,3-diamines in excellent yields without the need for high dilution. Selective ring opening of these compounds leads to large heterocyclic rings (Scheme 10) [42–44].

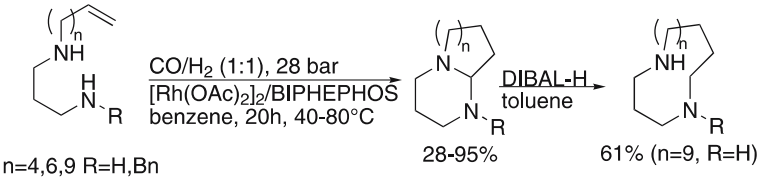

Scheme 10 Formation of *N*,*N*-acetals under hydroformylation conditions

General Procedure for the Hydroformylation/*N*,*N*-acetal Formation. Synthesis of Biazacycloalkanes. The unsaturated diamine (1 eq), $[Rh(OAc)_2]_2$ (0.5 mol % Rh atoms) and BIPHEPHOS (2 mol %) were placed in an autoclave under N_2 followed by deoxygenated benzene The vessel was flushed and evacuated three times with CO/H_2 (1 : 1, 13 bar) and then pressurized to 28 bar. The reaction was kept at 40–80 °C for 20 h. The autoclave was cooled and the gases were released followed by selective extraction of the total product with light petroleum. Concentration of the solvent gave in most cases NMR pure material of the title compounds.

The same methodology can be applied to the synthesis of pharmaceutically relevant quinazolines and quinazolinones containing a fused alicyclic ring [45, 46].

2.2
Hydroformylation/Imine/Enamine Formation

Similar to the formation of *N*,*N*-acetals under hydroformylation conditions attack of the carbonyl carbon by primary or secondary amines can lead to imines and enamines, respectively (Scheme 11).

In this manner, a hydroformylation/condensation sequence of *o*-vinylanilines give indoles directly. The starting *o*-vinylanilines are obtained by Heck reaction of the corresponding *o*-haloanilines. Hydroformylation of these styrene-type olefins proceeds preferably at the benzyl carbon. Intramolecular condensation gives pharmacologically interesting tryptophols and tryptamines in mediocre to good yields (Scheme 12, Table 1) [47].

General Procedure for the Hydroformylation/Enamine Formation. Synthesis of Indole Derivatives. A 300 ml autoclave equipped with a magnetic stirrer was charged with the

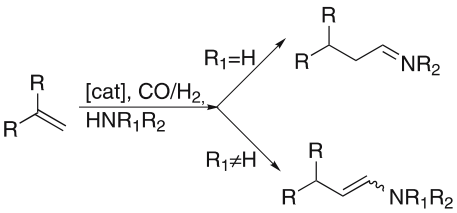

Scheme 11 Basic principle for imine and enamine formation under hydroformylation conditions

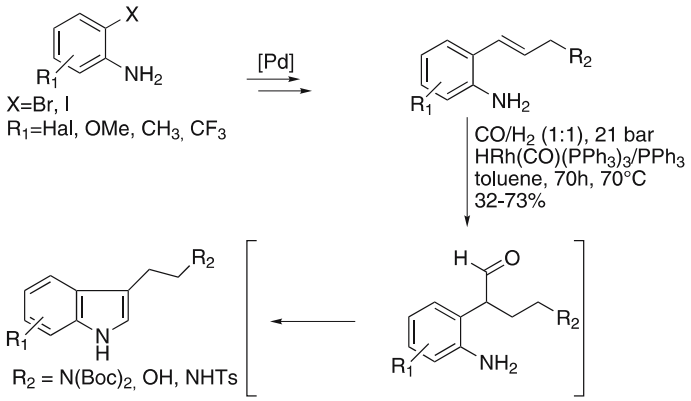

Scheme 12 Synthesis of indole derivatives from styrene-type anilines

Heck adduct (1 eq), $HRh(CO)(PPh_3)_3$ (10 mol %), PPh_3 (50 mol %) and toluene. The autoclave was pressurized to 20 bar with 1 : 1 CO/H_2, and was heated at 70 °C for 72 h while stirring. The autoclave was cooled, cautiously vented, and the volatiles evaporated *in vacuo*. The resulting residue was chromatographed on silica gel eluting with hexane : EtOAc (4 : 1) to furnish the indole derivatives (for examples see Table 1).

A similar formation of indoles has been achieved starting from *o*-nitrostyrenes. Under hydroformylation conditions, the nitro group is reduced to the amino group, which condenses with the in situ generated aldehyde [48].This approach is comparable with the indole syntheses of Reissert [49], Batcho and Leimgruber [50], and Sugasawa [51].

Cyclic α-amino acids with an enamine pattern can be obtained upon enantioselective hydrogenation followed by a hydroformylation/cyclization sequence in a single-pot version Rh(I)-DuPHOS acts as a catalyst for both steps, the enantioselective hydrogenation of prochiral dienamides and the hydroformylation of the resulting homoallylic amines (Scheme 13) [52, 53].

Very recently Jackson reported the use of supercritical carbon dioxide ($scCO_2$) in this tandem reaction, lowering the required total pressures of carbon monoxide and hydrogen [54].

Table 1 Examples for the synthesis of indole derivatives via hydroformylation of styrene-type anilines

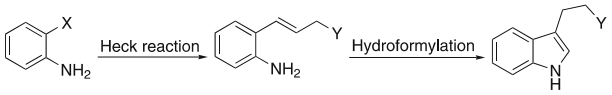

	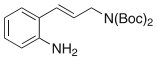	73%	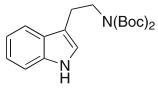 69%
	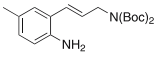	50%	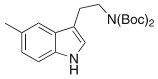 60%
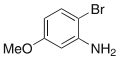	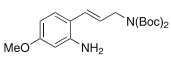	56%	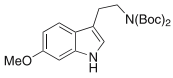 32%
	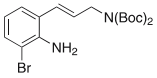	50%	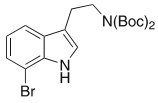 60%
	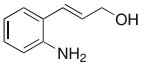	56%	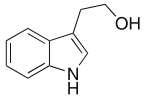 73%

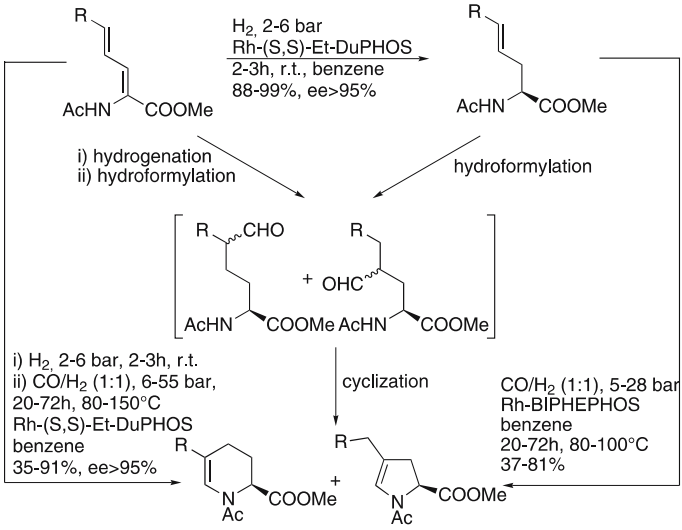

Scheme 13 Enantioselective Hydrogenation/hydroformylation/enamine formation

General Procedure for the Enantioselective Hydrogenation/Hydroformylation/Enamine Formation. Synthesis of Cyclic Enamine Amino Acids. Prochiral dieneamide (1 eq) and [(COD)Rh(I)-(*S*,*S*)-Et-DuPHOS] OTf (5 mol %) were dissolved in benzene and transferred

into an autoclave. The autoclave was charged with hydrogen (5 bar). After 3 h the hydrogen was vented and the autoclave was pressurized with CO/H_2 (1 : 1, 15 bar) and heated to 80 °C for 72 h. The autoclave was then cooled to ambient temperature and the solvent was removed under reduced pressure to give a yellow oil which is purified by column chromatography (silica, EtOAc : petroleum ether; 3 : 1).

2.3 Hydroformylation/Reductive Amination

Secondary and tertiary amines can be obtained if the hydroformylation of olefins is conducted in the presence of primary and secondary amines under elevated hydrogen partial pressures. Here the rhodium catalyst is involved in both steps, the hydroformylation of an olefin as well as the hydrogenation of the imine or enamine resulting from a condensation of the oxo-aldehyde with the amine (Scheme 14). This combination of hydroformylation and reductive amination is also known as hydroaminomethylation and has been applied to the synthesis of various substrates of pharmaceutical interest [55–57] as well as to the synthesis of macrocycles [60–63] and dendrimers [64, 65].

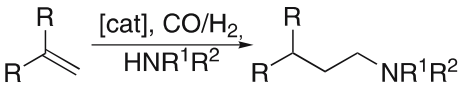

Scheme 14 Basic principle of the hydroformylation/reductive amination

For example, tolterodine, an important urological drug, has been prepared with good yields starting from 1-[2-hydroxy-5-methyl)phenyl]-1-phenylethylene via stepwise hydroformylation and reductive amination [58]. This synthesis can also be performed in a Rh/PBu_3 catalyzed one-pot tandem procedure starting from the diaryl ethene precursor giving 3,3-diarylpropylamine drugs in good yields [59]. If allylated phenothiazines are subjected to the hydroaminomethylation the antihistaminica alimemazine and etymemazine are obtained in good yields. Very recently the hydroaminomethylation has been used in the synthesis of dopamine-4-antagonists.

General Procedure for the Hydroformylation/Reductive Amination. Synthesis of 3,3-Diarylpropylamines. A mixture of the olefin (1 eq, 7.2 mmol), the corresponding primary or secondary amine (1 eq, 7.2 mmol) $[Rh(cod)Cl]_2$ (1 mol % Rh) and a defined amount of PBu_3 in anhydrous dioxane was heated for 3 d at 120 °C in a magnetically stirred autoclave under CO/H_2 atmosphere (9 : 2, 110 bar). The residue was dissolved in Et_2O and filtered through neutral alumina. Product mixtures were separated by column chromatography on neutral alumina using a mixture of MTBE/PE as eluent or by bulb-to-bulb distillation.

Table 2 Hydroaminomethylation in the synthesis of pharmaceuticals

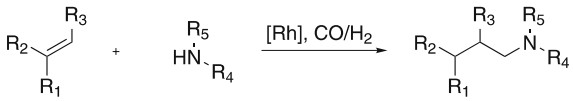

Olefin	Amine	Product	Yield
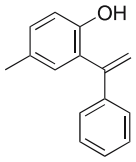		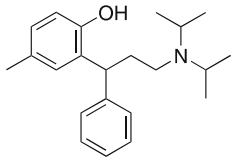	85%
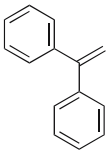		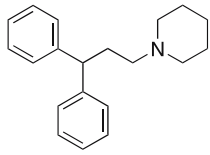	72%
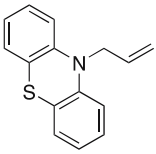		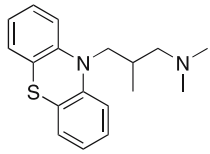	79%
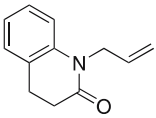	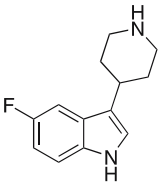	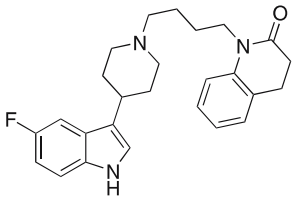	49%

Macrocycles can be synthesized conveniently using rhodium-catalyzed hydroaminomethylation of α,ω-diolefins in the presence of primary amines or secondary α,ω-diamines [60–63]. In comparison to common strategies this methodology is a very efficient synthetic route to substituted macrocyclic polyamines with high variability. 12- to 36-membered macrocycles can be obtained from (hetero)diallylic systems in up to 78% yield. In addition, such macrocyclic systems can be debenzylated and the resulting macrocyclic diamines undergo a second ring-closing bis(hydroamino-methylation) to give cryptand systems (Scheme 15) [60, 61].

More recently macrocycles with rigid and flexible aromatic and chiral binaphthyl systems with interesting fluorescence properties have been synthesized via hydroaminomethylation (Scheme 16) [62, 63].

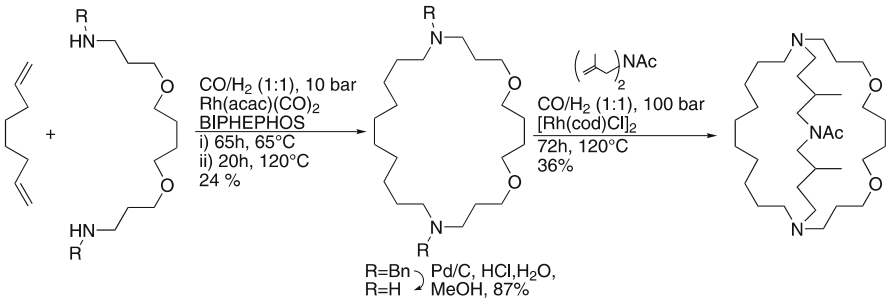

Scheme 15 Hydroaminomethylation in the synthesis of macrocyclic cryptands

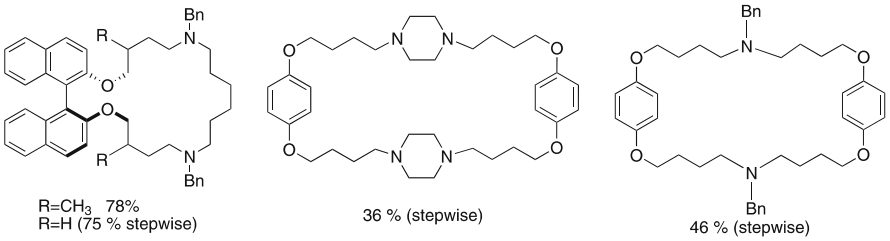

Scheme 16 Hydroaminomethylation in the synthesis of macrocycles

Hydroaminomethylation is also be used for the construction of dendrimers [64]. Here divergent and convergent strategies with wide variabilities can be used. A selected example is shown in Scheme 17.

Sequential hydroformylation/reductive amination of dendritic perallylated polyglycerols with various amines in a one-pot procedure to give dendritic polyamines in high yields (73–99%). Furthermore, the use of protected amines provides reactive core-shell-type architectures after deprotection. These soluble but membrane filterable multifunctional dendritic polyamines are of high interest as reagents in synthesis or as supports in homogeneous catalysis as well as nonviral vectors for DNA-transfection (Scheme 18) [65].

General Procedure for the Stepwise Hydroformylation/Reductive Amination on Allylated Hyperbranched Polyglycerols (PG). Synthesis of Hydroaminomethylated Hyperbranched PG-dendrimers. PG-Allyl, $Rh(acac)(CO)_2$ and XANTPHOS were dissolved in dry toluene and placed in an autoclave. The autoclave was pressurized with CO/H_2 (1 : 1, 30 bar), heated at 70 °C for 5 d. After cooling, the amine was added to the crude PG-aldehyde (1H NMR was used to confirm full conversion) and stirred for 1–2 h. After stirring, $Rh(acac)(CO)_2$ was added and the autoclave was pressurized with CO/H_2 (1 : 6, 70 bar) and heated at 85 °C for 2–5 days. After cooling, the solvent was removed in vacuo and the crude mixture was purified by dialysis (benzoylated cellulose tubing) to give the re-

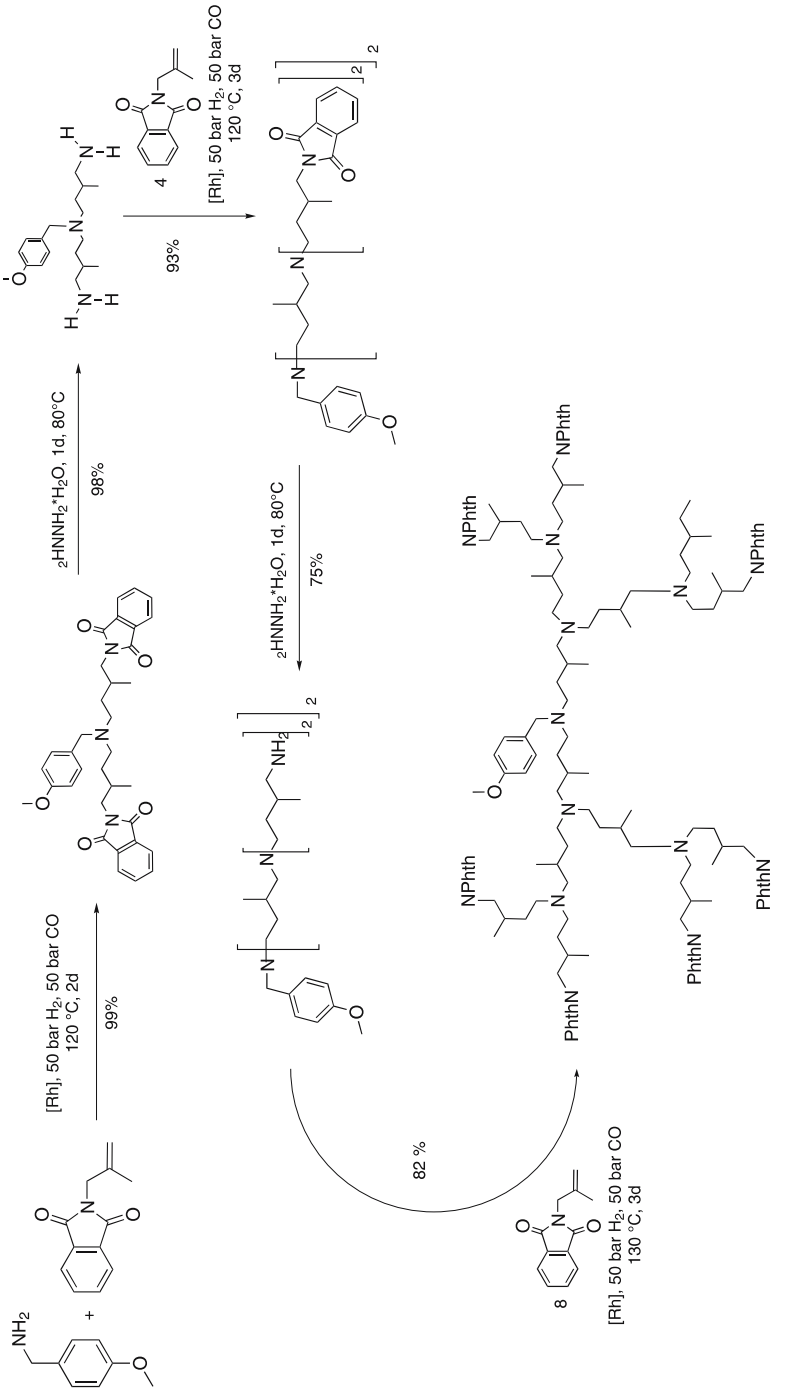

Scheme 17 Hydroaminomethylation in the synthesis of dendrimers

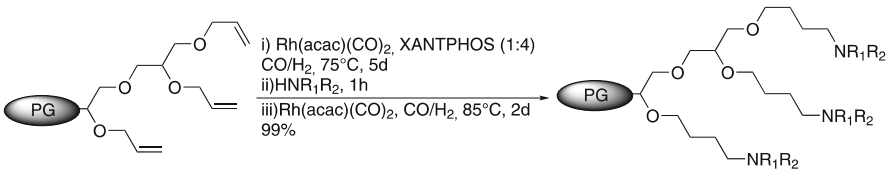

Scheme 18 Amination of allylated hyperbranched polyglycerols via hydroaminomethylation

spective dendritic polyamine. Dialysis performed in 2-L beaker charged with $CHCl_3$ and stored over 24 h, and after this time solvent was exchanged.

In a similar manner, polymers with unsaturated chains or side chains can be converted to polyamines [66–69]. Conjugated diolefins usually undergo hydroformylation with low selectivities [70]. Mostly hydrogenation of at least one double bond occurs and mixtures of various saturated and unsaturated amines and diamines are obtained [71]. Similar to alkenes also alkynes may serve as unsaturated compounds in hydroaminomethylation reaction sequences. Although synthetically attractive, only a few investigations towards hydroformylation and hydroaminomethylation of alkynes in the presence of *N*-nucleophiles are known. Usually a preferred transformation to furanonic derivatives is observed under hydroformylation conditions [27].

3
Additional *C,C*-Bond Formation of Aldehydes Obtained via Hydroformylation

Among all tandem hydroformylation sequences the ones involving additional *C,C*-bond formations are the most synthetically valuable tandem hydroformylation sequences. These *C,C*-bonds can be formed by adding nucleophiles, which attack the carbonyl carbon, or by adding electrophiles, which attack the α-position. Furthermore, tandem reactions in which the aldehyde or an aldehyde derivative is involved in sigmatropic rearrangement are described.

3.1
Using Carbonyl Reactivity

3.1.1
Hydroformylation/Allylation

Allylsilanes and allylboranes are allyl anion equivalents, which are stable enough to be included in subsequent allylation reactions of aldehydes under

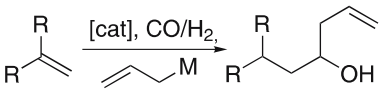

Scheme 19 Basic principle for the hydroformylation/allylation

hydroformylation conditions (Scheme 19). The aldehyde obtained from a hydroformylation of bisallylsilanes for example undergoes intramolecular Sakurai reaction to an intermediate homoallylic alcohol. Double bond migration to an enol results in the final ketone product (Scheme 20) [72] (Bärfacker L, Eilbracht P, personal communication).

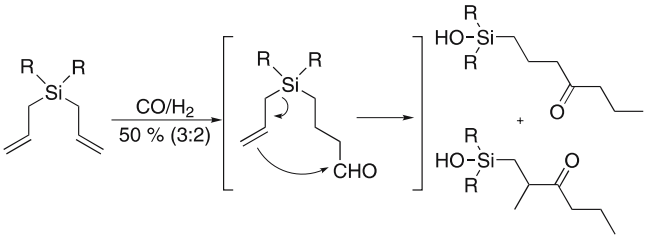

Scheme 20 Hydroformylation/intramolecular Sakurai reaction

In this context, the silylformylation is an interesting alternative to the hydroformylation. Here, hydrogen is replaced with silanes, allowing the formation of an additional carbon-silicon bond and a control of stoichiometry. Silylformylation of a homoallylic bisallylic siloxane gives for example a β-silyl-aldehyde, which undergoes intramolecular Sakurai reaction. The sequence stops at this stage since no further formylation of olefin moieties is possible, due to a lack hydrogen equivalent. Instead, subsequent oxidative work-up and hydrolysis gives valuable polyol fragments for polyketide/macrolide synthesis (Scheme 21) [73, 74].

This tandem intramolecular silylformylation/Sakurai reaction has successfully been applied in a formal total synthesis of mycoticin A [75]. The scope and utility of these reactions was expanded to (*Z*)- and (*E*)-crotyl groups leading to the stereospecific incorporation of both *anti* and *syn* propionate units into the growing polyol chain (Scheme 21) [76].

General Procedure for the Silylformaltion/Sakurai Allylation. Synthesis of Polyol Fragments for Polyketide and Macrolide Synthesis. In a magnetically stirred stainless-steel Parr bomb the substrate (1 eq) is dissolved in benzene. The solution is cooled to – 78 °C until frozen. $Rh(acac)(CO)_2$ (3 mol %) is then added and the Parr bomb is assembled and pressurized with CO (60 bar) and vented. This purge is repeated twice and the Parr bomb is pressurized with CO (60 bar) at – 78 °C. The apparatus is then immersed in an oil bath and heated at 60 °C for 22–24 h. After cooling to 0 °C, the bomb is vented. The solution

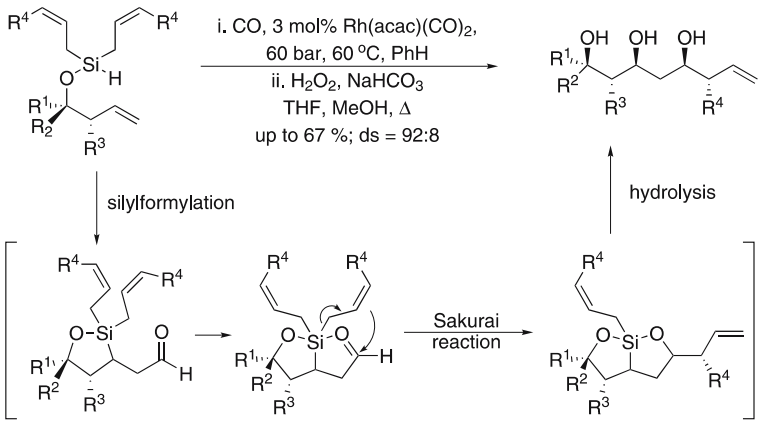

Scheme 21 Synthesis of polyol fragments via silylformylation/Sakurai reaction

is concentrated and the residue is used without further purification in the Tamao oxidation reaction. The product from the silylformylation/allylation is dissolved in THF/MeOH (1 : 1). To this solution is added $NaHCO_3$ (1.5 eq), followed by H_2O_2 (30 wt % in H_2O, 15 eq). The flask is then fitted with a reflux condenser and the solution is heated for reflux for 30–60 min. The solution is cooled to room temperature and NaS_2O_3 (solution in H_2O) is added. The biphasic solution is filtered through a cotton plug in a separatory funnel and extracted with EtOAc five times. The combined organic layers are dried over $MgSO_4$, filtered, and concentrated. The residue is purified by flash chromatography (silica, EtOAc/hexane).

The power of this methodology is demonstrated with the synthesis of polyketide-like structures by repetitive application of the same procedure (Scheme 22) [76].

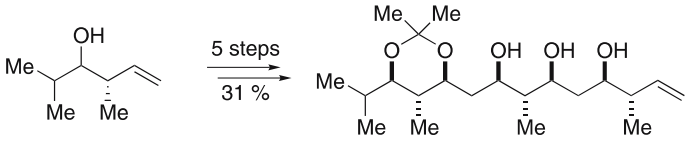

Scheme 22 Application of the silylformylation/Sakurai reaction in the synthesis of polyketides

In a similar fashion, allylboronates can be used as allylation reagents under hydroformylation conditions. Thus condensed 1,5-oxazadecalin systems are achieved via tandem hydroformylation/allylboration/hydroformylation sequences starting from an *N*-allyl-γ-amidoallylboronate (Scheme 23) [77, 78]. The aldehyde obtained from a regioselective hydroformylation undergoes diastereoselective intramolecular allylboration to give an intermediate allylic alcohol derivative. The reaction does not stop at this stage, since this

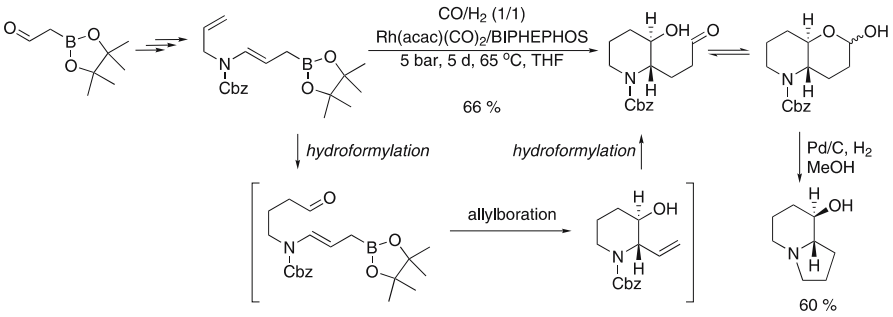

Scheme 23 Hydroformylation/allylboration in the synthesis of hydroindolizines

alkene moiety undergoes a second *n*-selective hydroformylation to give an equilibrium mixture of lactols and an open-chain δ-hydroxy aldehyde. Reductive removal of the Cbz group allows the formation of indolizidine in a further domino-type process consisting of deprotection and reductive amination.

General Procedure for the Hydroformylation/Allylboration/Hydroformylation. Synthesis of γ-hydroxy Aldehydes. BIPHEPHOS (2 mol %) was added to a solution of $Rh(acac)(CO)_2$ (1 mol %) in THF. After stirring for 10 min, a solution of the substrate (1 eq) in THF was added. This mixture was transferred to an autoclave, adding THF in the transfer. The autoclave was heated to 60 °C for 4 days under CO/H_2 (1 : 1, 5 bar). The contents were diluted with MTBE and the mixture was extracted with $NaHCO_3$ (saturated in H_2O). The aqueous phase was extracted with MTBE three times. The combined organic phases were dried over Na_2SO_4 and concentrated. Flash chromatography (silica, cyclohexane/MTBE 3 : 1) furnished a 1 : 1 anomeric mixture of open chain γ-hydroxy aldehyde and the corresponding lactols as a colorless oil.

In almost the same manner *trans*-disubstituted hydrooxepans can be obtained from a tandem hydroformylation/allyl boration of (*E*)-alkoxyallylboronates as a mixture of anomers (Scheme 24) [79].

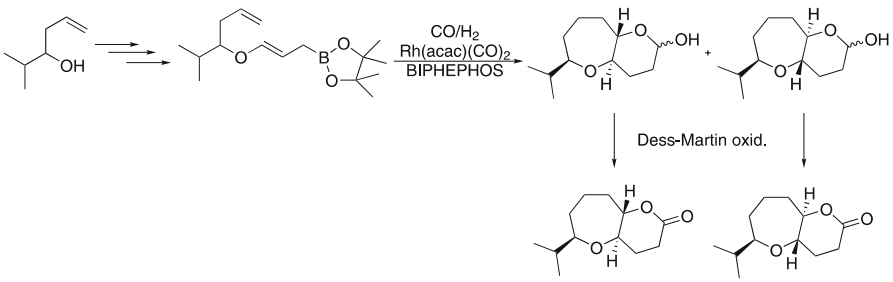

Scheme 24 Hydroformylation/allylboration in the synthesis of oxepans

3.1.2 Hydroformylation/Aromatic Substitution

Aldehydes and imines derived from them can undergo electrophilic attack of activated aromatic systems under harsh hydroformylation conditions (Scheme 25).

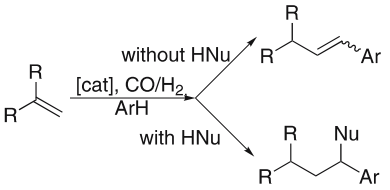

Scheme 25 Basic principle of the hydroformylation/aromatic substitution

Thus β-carbolines can be obtained in a tandem hydroformylation/Pictet–Spengler-type intramolecular electrophilic aromatic substitution of polymer bound olefins (Scheme 26) [80].

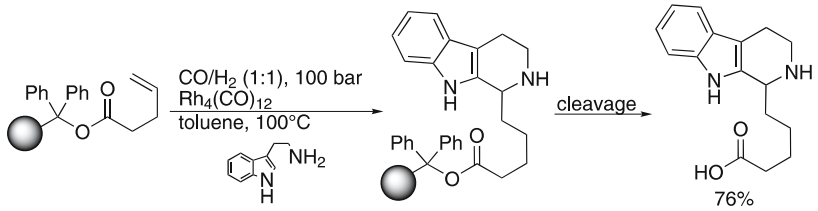

Scheme 26 Hydroformylation/Pictet–Spengler reaction on solid phase – Access to β-carbolins

In a similar fashion, hydroformylation of *N*-allyl-pyrrols leads to 5,6-dihydroindolizines via a one-pot hydroformylation/cyclization/dehydration process (Scheme 27) [81, 82]. The cyclization step represents an intramolecular electrophilic aromatic substitution in α-position of the pyrrole ring. This procedure was expanded to various substrates bearing substituents in the allyl and in the pyrrole unit.

General Procedure for the Hydroformylation/Electrophilic Substitution. Synthesis of 5,6-dihydroindolizines. A solution of 1-allylpyrroles (1 eq) and $Rh_4(CO)_{12}$ (1 mol %) in toluene was introduced by suction into an evacuated stainless-steel reaction vessel. CO (60 bar) was introduced, the autoclave was then rocked, heated to the desired temperature and H_2 (60 bar) was introduced rapidly. When the gas absorption reached the value corresponding to the fixed conversion, the reaction mixture was siphoned out. The degree of conversion and the product distributions were determined by GC and GC-MS, by using acetophenone as an internal standard.

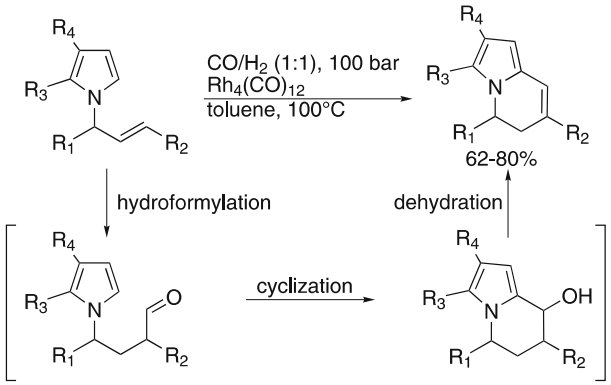

Scheme 27 Synthesis of dihydroindolizines via hydroformylation/aromatic substitution

3.2
Using α-CH-Acidity

3.2.1
Hydroformylation/Aldol Reaction

The aldol reaction is probably one of the most important reactions in organic synthesis. In many industrially important hydroformylation processes self-condensation of aldehydes is observed. Sometimes this consecutive reaction is favored as in the production of 2-ethyl hexanol. But synthetic applications of tandem hydroformylation/aldol reactions seem to be limited due regioselectivity problems of a mixed aldol reaction (Scheme 28). However, various tandem hydroformylation/intramolecular mixed aldol reactions have been described.

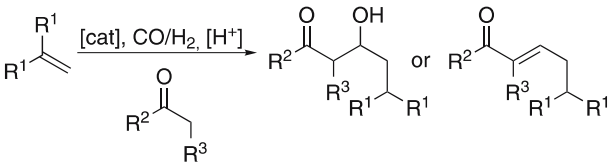

Scheme 28 Basic principle of the hydroformylation/aldol reaction

For example, rhodium catalyzed hydroformylation of 2-formyl-*N*-allyl-pyrrol gives an approx. 1 : 1 mixture of *iso*- and *n*-aldehydes. The latter cyclizes immediately in an aldol reaction followed by dehydration giving 7-formyl-5,6-indolizine in up to 46% (Scheme 29) [83]. Since here only one of the aldehyde groups can act as the enolate nucleophile this cyclization proceed with high regioselectivity (Scheme 29).

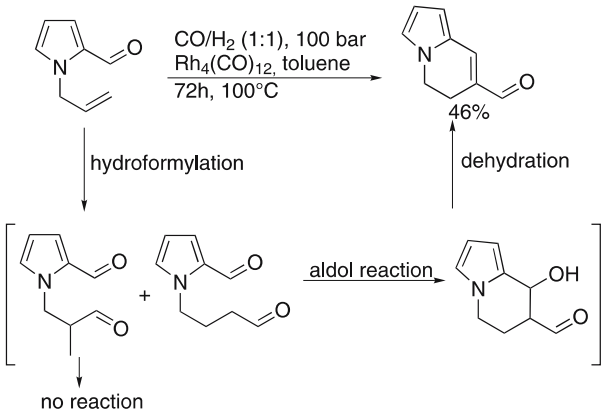

Scheme 29 Synthesis of dihydroindolizines via hydroformylation/aldol reaction

In almost the same manner, tandem hydroformylation/aldol condensation aldol condensation of ketoolefins, such as β,γ-unsaturated ketones, gives a single cyclization product under acid catalysis. Similar to the stepwise reaction, the in situ generated aldehyde preferentially acts as the electrophilic carbonyl component, while the ketone acts as the nucleophilic enol to form the five-membered ring product. Subsequent dehydration and hydrogenation of the resulting enone readily occurs under the reductive reaction conditions used (Scheme 30) [84].

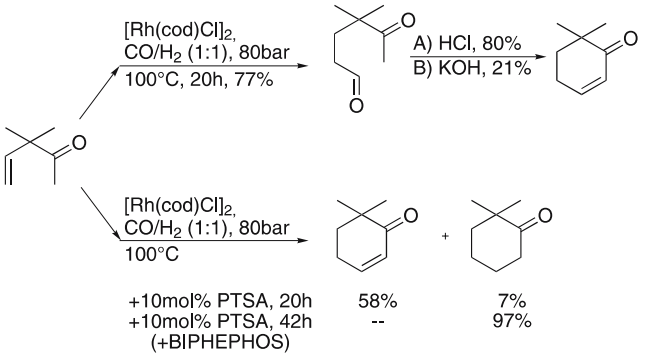

Scheme 30 Hydroformylation/aldol reaction

Although the saturated ketone can be obtained in nearly quantitative yields, the loss of synthetically valuable functionality is unfavorable and can be overcome by a modification of the tandem sequence. The use of the corresponding unsaturated silyl enol ethers in a tandem hydroformylation/Mukaiyama aldol reaction gives the desired aldol adduct with complete

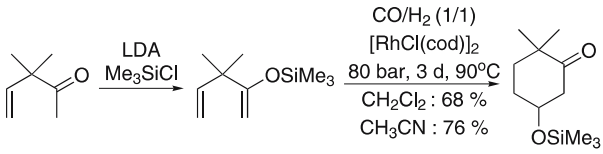

Scheme 31 Hydroformylation/Mukaiyama aldol reaction

transfer of the silyl group to aldol hydroxyl group (Scheme 31) [84, 85]. Obviously the less substituted double bond is hydroformylated selectively resulting in a regioselective tandem reaction.

This method can also be applied to silyl enol ethers of homologous unsaturated ketones as well as of unsaturated aldehydes or esters [85–87]. While unmodified unsaturated esters give only the corresponding aldehydes without cyclization under tandem hydroformylation/aldol reaction conditions, the corresponding silylated ester enolates smoothly cyclize in a tandem hydroformylation/ Mukaiyama aldol reaction (Scheme 32) [85–87].

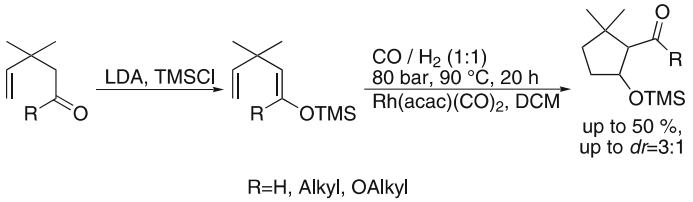

Scheme 32 Unsaturated aldehydes, ketones and esters in the hydroformylation/Mukayama aldol reaction

These examples clearly demonstrate that unsaturated carbonyl compounds can act as precursors for dicarbonyl systems. While the preexisting and less reactive carbonyl or carboxyl unit can conveniently be activated to serve as the enolate unit in aldol reactions the following hydroformylation step generates a second more reactive (aldehyde) carbonyl group in situ. Thus incorporation of the hydroformylation in the aldol reaction can be used to differentiate between carbonyl groups of different reactivity and to activate selectively the less reactive one as enolate allowing to perform an effective chemo-, regio-, and stereocontrol of the aldol cyclization immediately following the hydroformylation step [86, 87].

Similarly, tandem hydroformylation/aldol sequences can be applied to the formation of bicyclic and spirocyclic compounds. Thus silyl enol ethers of 3-vinyl and 3-allyl cycloalkanones give ring anellated products (Scheme 33) [86, 87].

Applying the same methods to 2-allylcycloalkanones can in principle lead to three different aldol products (Scheme 34). While the spiro compound is

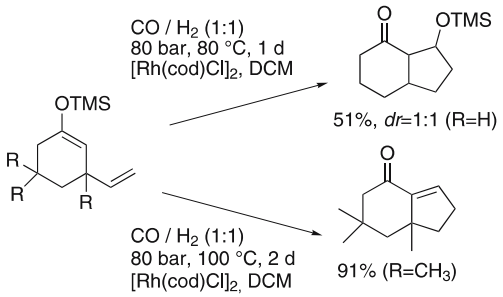

Scheme 33 Bicyclic aldols and enones via hydroformylation/aldol reaction

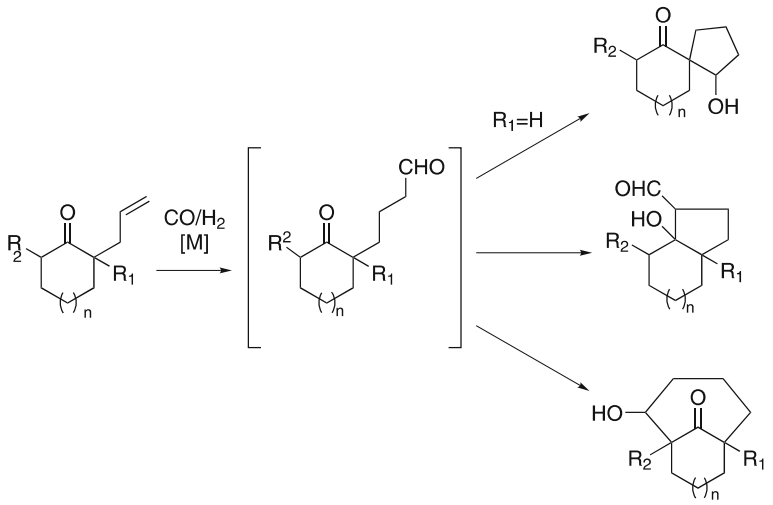

Scheme 34 Hydroformylation/aldol reaction

usually preferred, as already demonstrated [85], the use of various methods, such as regiodirecting and/or reversibly blocking ester groups or the above-described use of enolate equivalents are available to achieve high regioselectivity [86, 87].

Very recently, a tandem sequence consisting of enolboration/hydroformylation/aldol reaction has been described [88]. Here configuration of the enol boronate is transferred to the aldol product, allowing good to excellent diastereoselectivities in the hydroformylation/aldol reaction. With this method, 5–7-membered rings are obtained in excellent yields (Scheme 35).

General Procedure for Sequential Enolboration/Hydroformylation/Aldoladdition. Synthesis of Cyclic Aldol Products. NEt_3 (1.05 eq to carbonyl compound) was precomplexed under an argon atmosphere with $(cy\text{-hex})_2BCl$ (1.05 eq) in dry CH_2Cl_2 at 0 °C for 15 min. The unsaturated carbonyl compound was then added slowly via syringe and the enolbo-

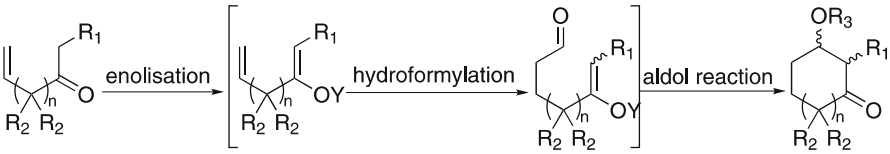

Scheme 35 Enolboration/hydroformylation/aldol reaction – Diastereoselective access to cyclic aldols

Table 3

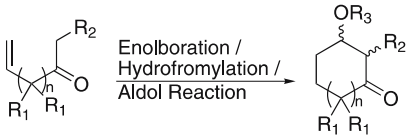

Olefin	Product	Yield	*dr*
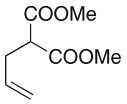	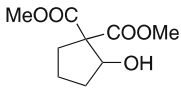	51%	—
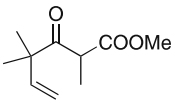	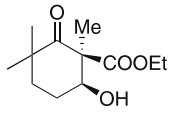	51%	2.5 : 1
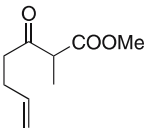	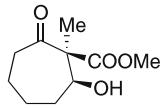	51%	6 : 1
	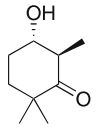	51%	20 : 1

ration was allowed to stir for an additional 30 min. The mixture was simply transferred into the autoclave containing $Rh(acac)(CO)_2$ (0.9 mol %) and solvent. The autoclave was then pressurized with CO/H_2 (1 : 1, 60 bar) and heated overnight to 80 °C. Upon cooling the autoclave to rt, the reaction mixture was removed and concentrated under reduced pressure. Enough MeOH was added to dissolve the solid residue along with a small amount of conc. pH 7 phosphate buffer and H_2O_2 (30 wt % in H_2O), and the reaction was allowed to stir overnight before being extracted with Et_2O, washed with $NaHCO_3$ (saturated in H_2O), dried and concentrated prior to further purification when necessary via flash chromatography or Kugelrohr distillation.

3.3
Involving Sigmatropic Rearrangements

Hydroformylations can also be combined with sigmatropic rearrangements. Here the carbonyls or derivatives derived from them are incorporated in a pseudo aromatic cyclic transition state.

3.3.1
Hydroformylation/Carbonyl Ene Reaction

A tandem hydroformylation/carbonyl ene reaction can be observed in cases, in which substrates with at least two isolated olefinic bonds are hydroformylated at only one double bond selectively. Thus hydroformylation of limonene with $PtCl_2(PPh_3)_2/SnCl_2/PPh_3$ or $PtCl_2$(diphosphine)$/SnCl_2/PPh_3$ gives a mixture of two diastereomeric alcohols upon carbonyl ene reaction of the intermediate aldehyde, (Scheme 36). Best results are achieved with a $PtCl_2$(dppb) complex. The mechanism of the final intramolecular cyclization step resembles an acid catalyzed carbonyl ene reaction [89].

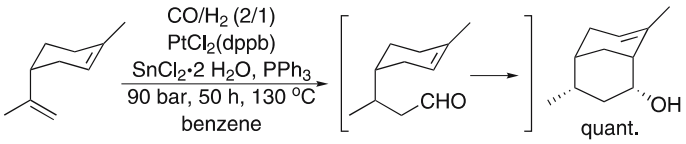

Scheme 36 Hydroformylation/carbonyl ene reaction

In some cases, the resulting olefin is not inert and undergoes consecutive hydroformylation. If aliphatic 1,5-dienes are subjected to a hydro-

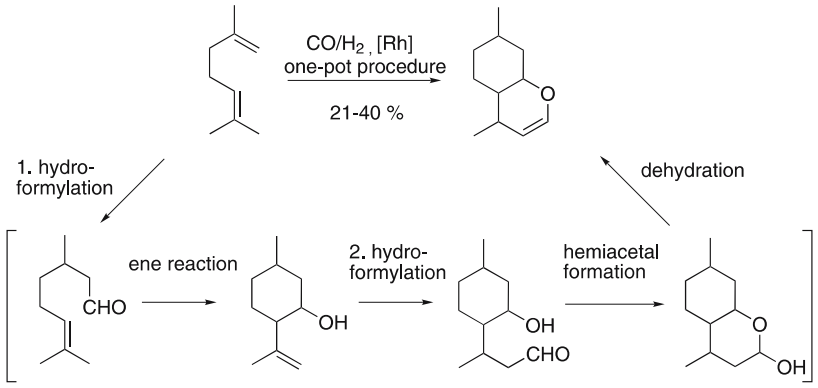

Scheme 37 Synthesis of chromanes via hydroformylation/carbonyl ene reaction

formylation the less substituted double bond is hydroformylated preferably. Subsequent carbonyl ene reaction gives an homoallylic alcohol which is further hydroformylated. Acetalization and dehydration gives the chromane derivative in an overall tandem hydroformylation/carbonyl ene reaction/hydroformylation/acetalization/dehydration, (Scheme 37) [90].

General Procedure for the Hydroformylation/Carbonyl ene Reaction/*O,O*-acetal Formation/Dehydration. Synthesis of Chromane Derivatives. A solution of the substrate (1 eq) $RhCl(PPh_3)_3$ (1 mol %) and PPh_3 (3 mol %) in dry dioxane was heated for 70 h to 120 °C und an atmosphere of CO/H_2 (1 : 1, 100 bar). The crude product was filtered through basic alumina (eluated with MTBE). After evaporation of the solvent further purification by column chromatography (silica, PE/MTBE) furnished the title compounds.

3.3.2 Hydroformylation/Fischer Indole Synthesis

If the hydroformylation of olefins is conducted in the presence of aromatic hydrazines and Brønsted or Lewis acids indoles can be obtained directly in one pot [91–93, 95]. Hydroformylation of the olefin gives an intermediate aldehyde, which is trapped immediately by the present aromatic hydrazine as an aromatic hydrazones similar to the formation of imines under hydroformylation conditions. Under acid mediation these aromatic hydrazones undergo a Fischer indolization, consisting of a [3,3]-sigmatropic rearrangement followed by a cyclization and elimination of ammonia (Scheme 38).

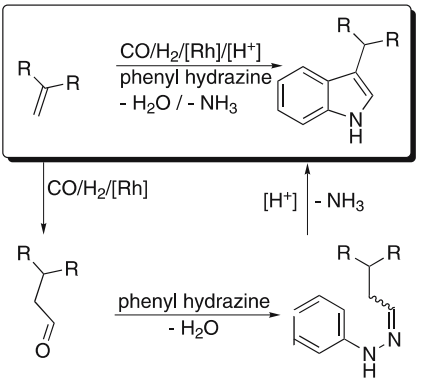

Scheme 38 Hydroformylation/Fischer indole synthesis

With this tandem hydroformylation/hydrazone formation/Fischer indolization 3-substituted indoles such as valuable intermediates for the synthesis of pharmaceuticals as well as pharmaceuticals can be obtained in a very

convenient fashion [94]. In many cases this tandem reaction can be conducted in aqueous sulfuric acid be using water soluble hydroformylation catalysts such as rhodium/TPPTS or rhodium/SulfoXANTPHOS [95]. Chiral information within the starting olefin is conserved and the relative configuration of newly formed stereocenters can be controlled by the use of a catalyst directing auxiliary as Breit has used for diastereoselective tandem hydroformylation [96] (Schmidt AM, Eilbracht P (2005) personal communication).

General Procedure for the Hydroformylation/Fischer Indole Synthesis. Synthesis of Tryptamine Derivatives in Water. Aminoolefin (1 eq), aromatic hydrazine (1 eq), $Rh(acac)(CO)_2$ (0.3 mol %) and TPPTS (1.5 mol %) are dissolved in H_2SO_4 (4 wt % in H_2O, 2.5 wt % olefin), filled in an autoclave and pressurized with 10 bar H_2 and 50 bar CO. After stirring for 3 days at 100 °C ammonia (30 wt % in water) is added and the mixture is extracted with EtOAc. The solvent is evaporated to give the product which purified by column chromatography (silica, CH_2Cl_2, ^iPrOH, NEt_3) if necessary.

Even 2,3-disubstituted indoles can be achieved if internal olefins are used. Regioselective hydroformylation of a styrene-type olefin and subsequent hydrazone formation and Fischer indolization gives an intermediate indole with a quaternary center in 3-position. The regained aromaticity is the driving force for the rearrangement of one substituent into the 2-position of the indole core (Scheme 39).

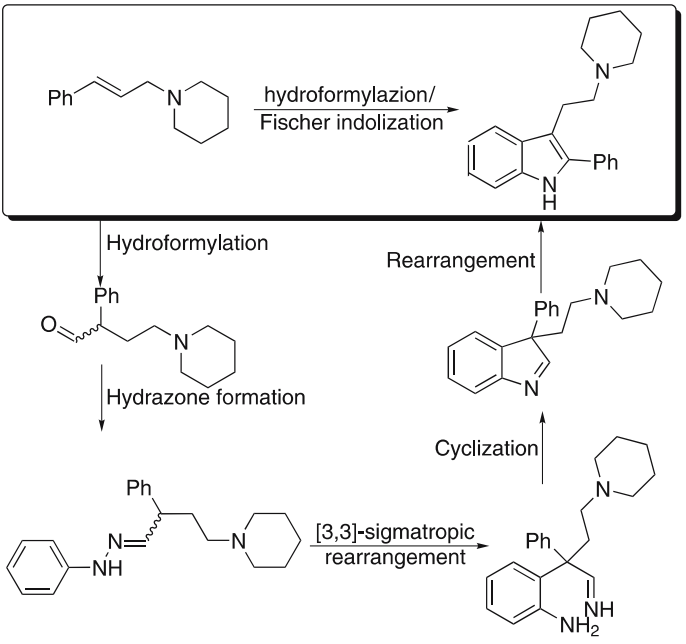

Scheme 39 Rearrangement involved in hydroformylation/Fischer indole synthesis – Access to 2-aryl tryptamines.

Table 4 Pharmacologically relevant indole derivatives via hydroformylation/Fischer indole synthesis

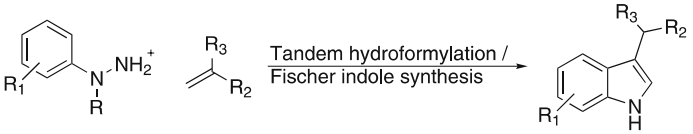

Hydrazine	Olefin	Product	Yield
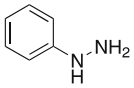	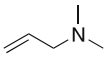	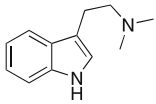	quant.
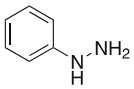	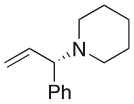	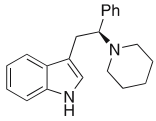	54%, 95% ee
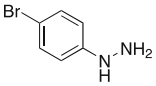	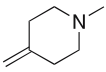	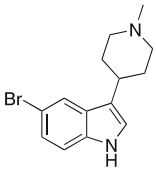	quant.
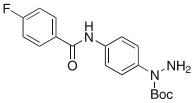	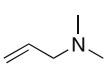	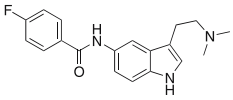	44%
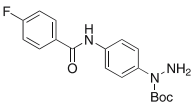	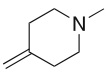	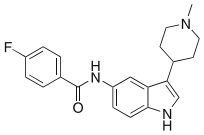	95%
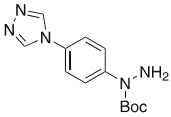	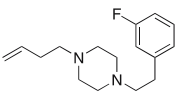	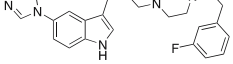	51%
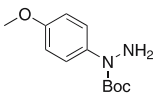	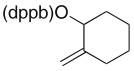	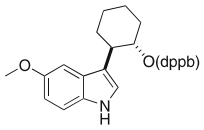	44%, *dr* > 95 : 5
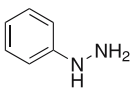	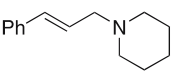	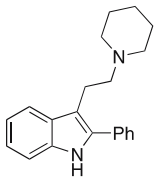	60%

4 Conclusions

In conclusion, the applicability of the transition metal catalyzed hydroformylation of easily accessible functionalized or non-functionalized unsaturated compounds is expanded by its implementation in reaction sequences, tandem reactions or domino reactions. The hydroformylation can be combined with simple functional group transformations, such as reduction or isomerization, or with *C*,*O*-, *C*,*N*- and, most importantly, *C*,*C*-bond forming reactions. It can be expected that more interesting examples and applications will be presented in the future.

References

1. Bohnen HW, Cornils B (2002) Adv Catal 47:1
2. Cornils B (1999) J Mol Catal A-Chem 143:1
3. Beller M, Cornils B, Frohning CD, Kohlpaintner CW (1995) J Mol Catal A-Chem 104:17
4. Cornils B, Herrmann WA, Kohlpaintner CW (1994) Angew Chem Int Ed Engl 33:2144
5. Cornils B, Herrmann WA (1996) Applied Homogeneous Catalysis with Organometallic Compounds. Wiley-VCH, Weinheim
6. van Leeuwen PWNM, Claver C (2000) Rhodium-Catalyzed Hydroformylation. Kluwer, Dordrecht
7. Burke SD, Cobb JE, Takeuchi K (1990) J Org Chem 55:2138
8. Breit B, Zahn SK (1998) Tetrahedron Lett 39:1901
9. Hornberger KR, Hamblett CL, Leighton JL (2000) J Am Chem Soc 122:12894
10. Breit B (2000) Chem Eur J 6:1519
11. Dreher SD, Leighton JL (2001) J Am Chem Soc 123:341
12. Liu P, Jacobsen EN (2001) J Am Chem Soc 123:10772
13. Breit B, Zahn SK (2001) J Org Chem 66:4870
14. Sun P, Sun C, Weinreb SM (2001) Org Lett 3:3507
15. Sun P, Sun CX, Weinreb SM (2002) J Org Chem 67:4337
16. Seepersaud M, Kettunen M, Abu-Surrah AS, Repo T, Voelter W, Al-Abed Y (2002) Tetrahedron Lett 43:1793
17. Weinreb SM (2003) Acc Chem Res 36:590
18. Gladiali S, Bayon JC, Claver C (1995) Tetrahedron: Asymmetry 6:1453
19. Eilbracht P (1995) In: Helmchen G, Hoffmann RW, Mulzer J (eds) Methoden der Organischen Chemie (Houben-Weyl), vol E 21c. Thieme, Stuttgart, p 2488
20. Agbossou F, Carpentier JF, Mortreux A (1995) Chem Rev 95:2485
21. Breit B, Seiche W (2001) Synthesis, p 1
22. Breit B (2003) Acc Chem Res 36:264
23. Patai S (1970) The Chemistry of the Carbonyl Group. Wiley, New York
24. Falbe J (1983) Methoden der Organischen Chemie (Houben-Weyl), vol E3. Thieme, Stuttgart
25. Tietze LF (1996) Chem Rev 96:115
26. Fogg DE, dos Santos EN (2003) Coord Chem Rev 284:2365

27. Eilbracht P, Bärfacker L, Buss C, Hollmann C, Kitsos-Rzychon B, Kranemann CL, Rische T, Roggenbuck R, Schmidt A (1999) Chem Rev 99:3329
28. Schmidt AM, Eilbracht P (2004) New Synthetic Applications of Tandem Reactions under Hydroformylation Conditions. In: Beller M, Bolm C (eds) Transition Metals for Organic Synthesis: Building Blocks and Fine Chemicals. Wiley, Weinheim, p 57
29. Schmidt AM, Eilbracht P (2004) Multiple Carbon-Carbon Bond Formations under Hydroformylation Conditions. In: Beller M, Bolm C (eds) Transition Metals for Organic Synthesis: Building Blocks and Fine Chemicals. Wiley, Weinheim, p 87
30. Parsons PJ, Penkett CS, Shell AJ (1996) Chem Rev 96:195
31. Nicolaou KC, Montagnon T, Snyder SA (2003) Chem Commun, p 551
32. Wuts PGM, Obrzut ML, Thompson PA (1984) Tetrahedron Lett 25:4051
33. Schmidt B, Costisella B, Roggenbuck R, Westhus M, Wildemann H, Eilbracht P (2001) J Org Chem 66:7658
34. Roggenbuck R, Schmidt A, Eilbracht P (2002) Org Lett 4:289
35. Ojima I, Moralee AC, Vassar VC (2002) Top Catal 19:89
36. Ojima I, Vidal ES (1998) J Org Chem 63:7999
37. Ojima I, Tzamarioudaki M, Eguchi M (1995) J Org Chem 60:7078
38. Eguchi M, Zeng Q, Korda A, Ojima I (1993) Tetrahedron Lett 34:915
39. Ojima I, Iula DM (1998) In: Pelletier SW (ed) The Alkaloids. Pergamon, London, p 371
40. Mizutani N, Chiou WH, Ojima I (2002) Org Lett 4:4575
41. Dixon DJ, Horan RAJ, Monck NJT (2004) Org Lett 6:4423
42. Bergmann DJ, Campi EM, Jackson WR, Patti AF (1999) Chem Commun, p 1279
43. Bergmann DJ, Campi EM, Jackson WR, Patti AF (1999) Aust J Chem 52:1131
44. Bergmann DJ, Campi EM, Jackson WR, Patti AF, Saylik D (1999) Tetrahedron Lett 40:5597
45. Campi EN, Jackson WR, McCubbin QJ, Trnacek AE (1994) Aust J Chem 47:1061
46. Campi EN, Jackson WR, Trnacek AE (1997) Aust J Chem 50:1031
47. Dong Y, Busacca CA (1997) J Org Chem 62:6464
48. Ucciani E, Bonfand AJ (1981) Chem Soc Chem Commun, p 82
49. Cannon JG (1981) J Med Chem 24:238
50. Siu J, Baxendale IR, Ley SV (2004) Org Biomol Chem 2:160
51. Douglas AW (1994) Tetrahedron Lett 35:6807
52. Teoh E, Campi EM, Jackson WR (2002) Chem Commun, p 978
53. Teoh E, Campi EM, Jackson WRN, Robinson AJ (2003) New J Chem 27:387
54. Teoh E, Jackson WR, Robinson AJ (2005) Aust J Chem 58:63
55. Botteghi C, Cazzolato L, Marchetti M, Paganelli S (1995) J Org Chem 60:6612
56. Rische T, Eilbracht P (1999) Tetrahedron 55:1915
57. Rische T, Müller KS, Eilbracht P (1999) Tetrahedron 55:9801
58. Botteghi C, Corrias T, Marchetti M, Paganelli S, Piccolo O (2002) Org Proc Res Develop 6:379
59. Donsbach M, Eilbracht P, Buss C, Mersch C (2000) DE 10033016 A1
60. Kranemann CL, Costisella B, Eilbracht P (1999) Tetrahedron Lett 40:7773
61. Kranemann CL, Eilbracht P (2000) Eur J Org Chem 2367
62. Angelovski G, Eilbracht P (2003) Tetrahedron 41:8265
63. Angelovski G, Costisella B, Kolaric B, Engelhard M, Eilbracht P (2004) J Org Chem 69:5290
64. Koç K, Eilbracht P (2004) Tetrahedron 60:8465
65. Koc F, Wyszogrodzka M, Eilbracht P, Haag R (2005) J Org Chem 70:2021
66. Jachimowicz F, Hansson A (1985) In: Augustine RL (ed) Catalysis of Organic Reactions. Dekker, New York, p 381

67. Jachimowicz F, Hansson A (1988) Can Patent 1231199
68. Jachimowicz F (1981) GE 3106139
69. Sunder A, Turk H, Haag R, Frey H (2000) Macromolecules 33:7682
70. Cornils B (1980) In: Falbe J (ed) New Syntheses with Carbon Monoxide. Springer, Berlin Heidelberg New York, p 1
71. Kranemann CL, Eilbracht P (1998) Synthesis, p 71
72. Bärfacker L (1999) Thesis, Dortmund University
73. Zacuto MJ, Leighton JL (2000) J Am Chem Soc 122:8587
74. O'Malley SJ, Leighton JL (2001) Angew Chem Int Ed 40:2915
75. Dreher SD, Leighton JL (2001) J Am Chem Soc 123:341
76. Zacuto MJ, O'Malley SJ, Leighton JL (2002) J Am Chem Soc 124:7890
77. Hoffmann RW, Brückner D, Gerusz VJ (2000) Heterocycles 52:121
78. Hoffmann RW, Brückner D (2001) New J Chem 25:369
79. Hoffmann RW, Kruüger J, Brückner D (2001) New J Chem 25:102
80. Dessole G, Marchetti M, Taddei MJ (2003) Comb Chem 5:198
81. Settambolo R, Savi S, Caiazzo A, Lazzaroni RJ (2000) Organomet Chem 601:320
82. Settambolo R, Caiazzo A, Lazzaroni R (2001) Tetrahedron Lett 42:4045
83. Settambolo R, Savi S, Caiazzo A, Lazzaroni RJ (2001) Organomet Chem 619:241
84. Hollmann C, Eilbracht P (1999) Tetrahedron Lett 40:4313
85. Hollmann C, Eilbracht P (2000) Tetrahedron 56:1685
86. Hollmann C (2000) Thesis, Dortmund University
87. Keränen MD, Hollmann C, Kot K, Eilbracht P (2004) Org Biomol Chem 2:3379
88. Keränen MD, Eilbracht P (2004) Org Biomol Chem 2:1688
89. Diaz AO, Augusti R, dos Santos EN, Gusevskaya EV (1997) Tetrahedron Lett 38:41
90. Roggenbuck R, Eilbracht P (1999) Tetrahedron Lett 40:7455
91. Köhling P, Schmidt AM, Eilbracht P (2003) Org Lett 5:3213
92. Ahmed M, Jackstell R, Seayad AM, Klein H, Beller M (2004) Tetrahedron Lett 45:869
93. Schmidt AM, Eilbracht P (2005) Org Biomol Chem 3:233
94. Köhling P, Schmidt AM, Eilbracht P (2006) Org Biomol Chem 4:302
95. Schmidt AM, Eilbracht P (2005) J Org Chem 70:5528
96. Schmidt AM (2005) Thesis, Dortmund University

Top Organomet Chem (2006) 18: 97–123
DOI 10.1007/3418_018

Published online: 25 May 2006

Hydroxy- and Alkoxycarbonylations of Alkenes and Alkynes

Philippe Kalck (✉) · Martine Urrutigoïty · Odile Dechy-Cabaret

Laboratoire de Catalyse Chimie Fine et Polymères,
Ecole Nationale Supérieure d'Ingénieurs en Arts Chimiques Et Technologiques (ENSIACET), 118 Route de Narbonne, 31077 Toulouse cedex, France
philippe.kalck@ensiacet.fr

1 Introduction 97

2 Hydroxycarbonylation Reactions 98
2.1 Hydroxycarbonylation of Alkenes 98
2.2 Hydroxycarbonylation of Alkynes 101

3 Alkoxycarbonylation Reactions 103
3.1 Alkoxycarbonylation of Alkenes 104
3.1.1 Intermolecular Alkoxycarbonylation of Alkenes 104
3.1.2 Intramolecular Alkoxycarbonylation of Alkenes 107
3.1.3 Asymmetric Alkoxycarbonylation 111
3.2 Alkoxycarbonylation of Alkynes 112
3.2.1 Intermolecular Alkoxycarbonylation of Alkynes 112
3.2.2 Intramolecular Alkoxycarbonylation of Alkynes 117

4 Conclusion 119

References 120

Abstract The use of Co building block in presence of water or an alcohol to functionalise alkenes by hydroxycarbonylation or alkoxycarbonylation reactions is reviewed in this chapter. The hydroxyl groups can be present in the substrate itself so cascade reactions can occur. Palladium precursors are largely involved in these reactions and this analysis of the literature focuses on the mechanisms involving Pd(0), $Pd(H)(X)L_2$, PdX_2 and an oxidant like CuCl systems. Introduction of chiral L or L_2 ligands or even the presence of chiral carbon atoms in the substrate lead to asymmetric carbonylation reactions.

Keywords Alkenes · Alkynes · CO building block · Lactonization · Palladium iodide

1 Introduction

Functionalization of various substrates to produce oxygenated compounds with high selectivity is a permanent challenge in metal-catalyzed organic synthesis. Most of these products present interesting biological properties. For instance polyether antibiotics contain often a furan or a pyran ring [1]. Simi-

larly, many lactones possess a biological activity [2]. Carbon monoxide, which is a cheap and abundant material from either fossil or renewable sources, appears as an attractive building block provided appropriate and selective tools have been elaborated [3]. Carbonylation reactions have been known since the early work of Reppe in the 1930s who used cobalt or nickel under drastic conditions [4–7]. Progress in coordination chemistry allowed us to reduce the operating conditions and to design the metal and its ligands so that selectivity has been gradually improved. In this regard the use of palladium by Chiusoli [8], Pino [9], and Knifton [10] was a real breakthrough. Today sophisticated late transition metal complexes are efficient precursors to catalyze the hydroxy- or alkoxycarbonylation reactions. The present work is devoted to the carbonylation of alkenes and alkynes.

2
Hydroxycarbonylation Reactions

The reactions are related to the incorporation of CO and H_2O into alkenes or alkynes leading to the corresponding saturated or unsaturated carboxylic acids. The general equation is shown below. Equation 1b is related to the synthesis of acrylic acid discovered by Reppe [11].

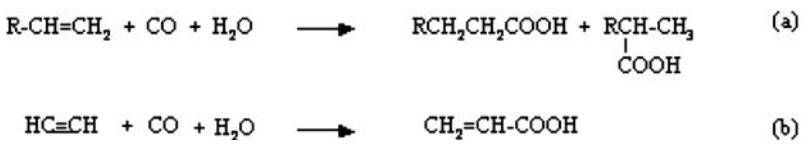

Equation 1

It is worth mentioning that sometimes this reaction is called hydrocarboxylation, which relates normally to the use of the H_2/CO_2 couple.

2.1
Hydroxycarbonylation of Alkenes

In 1969, von Kutepov and co-workers patented for BASF the hydroxycarbonylation of a terminal alkene using phosphine-containing palladium complexes [12]. Further studies by Fenton [13] showed that $PdCl_2/nPPh_3$ was a good precursor and the reaction parameters were optimized to combine high conversion rates and a good selectivity in the linear ester. At pressures ranging from 7 to 55 bar, temperatures near to 150 °C, with an excess of PPh_3, linear to branched ratios as high as 3.5 can be reached. As the conversion is largely improved when a hydrogen partial pressure is introduced, the ac-

tive catalytic species is presumably $[Pd(H)Cl(PPh_3)_2]$ and the catalytic cycle is shown in Scheme 1, in which "Pd" represents $[PdCl(PPh_3)_2]$.

Alper and co-workers discovered that the selectivity of the carbonylation reaction can be turned towards the branched acid by adding copper(II) chloride and hydrochloric acid to the palladium catalyst [14]. The working conditions become very mild since the reaction is performed at room temperature and at 1 bar of CO. Interestingly, also enantioselective carbonylations can be carried out from a prochiral terminal alkene. By addition of the (*R*)- or (*S*)-1,1′-binapthyl-2,2′-diylhydrogenophosphate (BNPPA) chiral ligand (Fig. 1), it was possible to reach an enantiomeric excess (ee) as high as 91% [15]. It is thus possible to transform *p*-isobutylstyrene into (*S*)-ibuprofen and 2-vinyl-6-methoxynaphtalene into (*S*)-naproxen, which both possess non-steroidal anti-inflammatory properties; the two (*R*)-isomers present a lower activity [16].

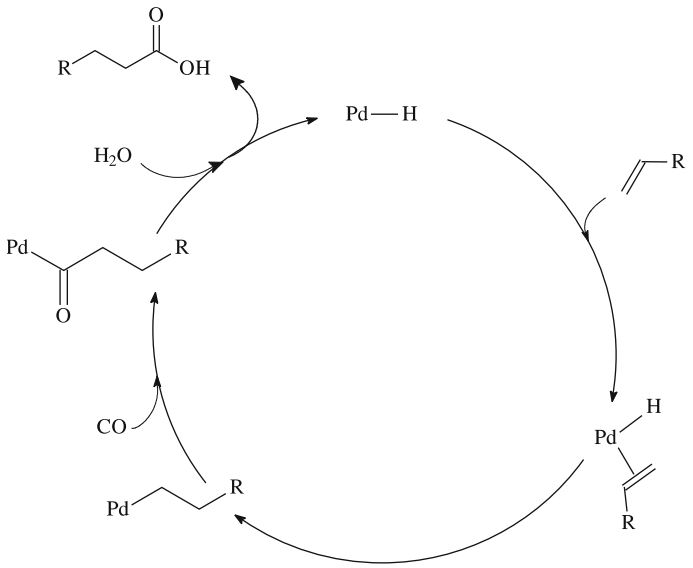

Scheme 1 Catalytic cycle of the Pd – H catalyzed hydroxycarbonylation of alkenes

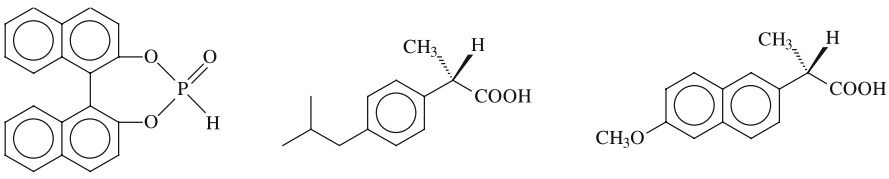

BNPPA (S)-ibuprofen (S)-naproxen

Fig. 1 Structures of BNPPA ligand, (*S*)-ibuprofen and (*S*)-naproxen

Similarly, high selectivity for the branched isomer has been achieved at 50 bar of CO using a palladium(II) tosylate complex containing a chelating anionic ligand such as 2-carboxylatopyridine that confers to the complex some solubility in water [17]. In the presence of LiCl or LiI as the promoter, styrene can be converted into 2-phenylpropanoic acid with an enantioselectivity of 99% and a turnover frequency (TOF) of 2600 h^{-1}. At 30 bar, in water 2-aminophenylthiolato ligands coordinated to $PdCl_2$ moieties allow van Koten et al. to obtain almost 100% of the branched acid, starting from styrene [18].

In order to keep the mild conditions, hydroxycarbonylation has been performed in biphasic media, maintaining the catalyst in the aqueous phase thanks to water-soluble mono- or diphosphine ligands. In the presence of the sodium salt of trisulfonated triphenylphosphine (TPPTS), palladium was shown to carbonylate efficiently acrylic ester [19], propene and light alkenes [20, 21] in acidic media. For heavy alkenes the reduced activity due to the mass transfer problems between the aqueous and organic phases can be overcome by introducing an inverse phase transfer agent, and particularly dimethyl-β-cyclodextrin [22, 23]. Moreover, a dicationic palladium center coordinated by the bidentate diphosphine ligand 2,7-bis(sulfonato)xantphos (Fig. 2) catalyzes, in the presence of tolylsulfonic acid for stability reasons, the hydroxycarbonylation of ethylene, propene and styrene and provides a ca. 0.34 : 0.66 molar ratio for the two linear and branched acids [24].

Bidentate chiral water-soluble ligands such as (*S*,*S*)-2,4-bis(diphenylsulfonatophosphino)butane BDPPTS (Fig. 2) or (*R*,*R*)-1,2-bis(diphenylsulfonatophosphinomethyl)cyclobutane have been prepared [25]. Their palladium complexes catalyze the synthesis of chiral acids from various vinylarenes and an ee of 43% has been reached for *p*-methoxystyrene with the BDPPTS ligand. Furthermore, recycling of the aqueous phase has shown that the regio- and enantioselectivity are maintained and that no palladium leaches.

In an opposite way, it is possible to reach high selectivity in linear acid by using a mixture of palladium acetate $Pd(OAc)_2$, 1,4-bis(diphenylphosphino)

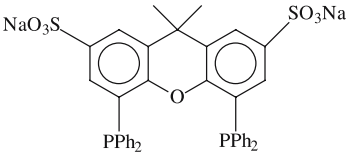

2,7-bis(sulfonato)-xantphos

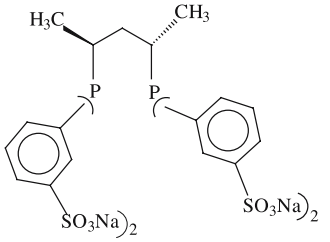

(S,S)-2,4-bis(diphenylsulfonatophosphinopentane) BDPPTS

Fig. 2 Structures of sulfonated bidentate phosphines

butane (dppb), and formic or oxalic acid. At roughly 7 bar of CO and 150 °C, high conversions and high linearities can be obtained: for instance α-methylstyrene gives 82 and 100%, or 2,4,6-trimethylstyrene gives 98 and 100%, respectively [26]. Labeling experiments have shown that the CO group incorporated in the acidic function is provided by carbon monoxide and not by formic or oxalic acid [27].

2.2 Hydroxycarbonylation of Alkynes

It is important to mention the pioneering work of Reppe and co-workers who discovered as early as 1938 the industrial preparation of acrylic acid by carbonylation of acetylene [28]. The reaction was conducted at 200–230 °C and 100 bar of CO and catalyzed by $Ni(CO)_4$ in the presence of a copper halide. Selectivity of 90 and 85% were reached in acrylic acid with regard to acetylene and carbon monoxide, respectively [29].

Later, Alper and his group reported that hydroxycarbonylation of alkynes can be performed under mild conditions (90 °C, 1 bar of CO), provided a phase transfer agent is added to the biphasic medium. Thus, starting from $Ni(CN)_2$, in the presence of cetyltrimethylammonium bromide, various substituted alkynes or diynes are converted into the corresponding unsaturated carboxylic acids [30]. When using the bimetallic system $CoCl_2$ and $Ni(CN)_2$ with KCN, saturated carboxylic acids are obtained with a good selectivity observed for the branched isomer [31]. Presumably, the introduction of cobalt in the catalytic system allows for the reduction of the intermediate unsaturated acids through the water-gas-shift reaction.

Similarly, allenes [32] and alkynols [33] were used as starting materials and their carbonylation provides β,γ-unsaturated acids and unsaturated diacids, respectively. The specific reactivity of alkynols is explained by three formal steps during nickel catalysis: (i) carbonylation of the triple bond leading to an acid containing an allylic alcohol moiety; (ii) second carbonylation of the double bond to provide a hydroxydiacid; and (iii) a dehydration step giving the corresponding unsaturated diacid (Scheme 2).

The authors show that the phase transfer agent exerts a strong influence on the stereochemistry observed in the final product since *E*-unsaturated diacids are the major products in the presence of polyethylene glycol (PEG-400), whereas *Z*-isomers are obtained when quaternary ammonium salts are added [34].

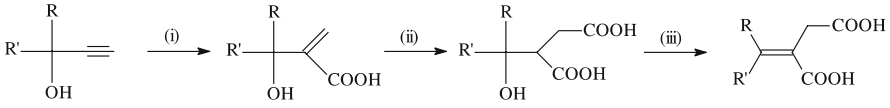

Scheme 2 Formation of a β,γ-unsaturated diacid from an alkynol

In the same research group the cationic hydridopalladium complex $[Pd(H)(H_2O)(PCy_3)_2][BF_4]$ has been shown to catalyze the hydroxycarbonylation of triple bonds. As a representative example the dehydration occurring to give the dienoic acid is displayed in Scheme 3 [35]. The same cationic complex is able to activate a carbon oxygen bond in α-allenic alcohols to provide dienoic acids but with the COOH group in the branched position (Scheme 3) [36].

It is worth mentioning that some precursors easily catalyze the reductive carbonylation of alkynes from the CO/H_2O couple. Here, the main role of water is to furnish hydrogen through the water-gas-shift reaction, as evidenced by the co-production of CO_2. In the presence of PdI_2/KI terminal alkynes have been selectively converted into furan-2-(5*H*)-ones or anhydrides when a high concentration in CO_2 is maintained. Two CO building blocks are incorporated and the cascade reactions that occur on palladium result in a cyclization together with the formation of an oxygen-carbon bond [37, 38]. Two examples are shown in Scheme 4.

Previous studies on various aliphatic and aromatic alkynes have evidenced that this type of furan-2-ones could also be produced in the presence of the rhodium carbonyl cluster $[Rh_4(CO)_{12}]$ [39–41]. Labeling experiments using D_2O allowed the authors to assign the origin of the hydrogen atoms (Scheme 6). Noteworthy, dicobalt octacarbonyl follows a different catalytic

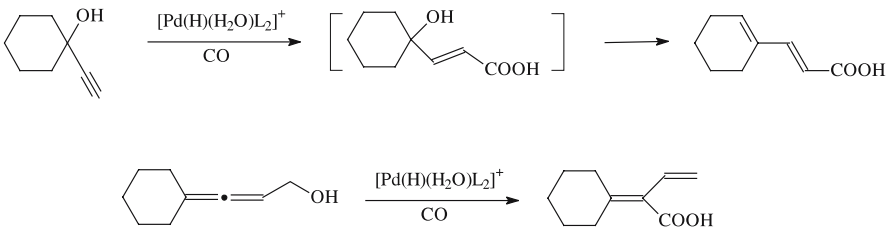

Scheme 3 Hydroxycarbonylation followed by a dehydration step (*L refers to the* PCy_3 *ligand*)

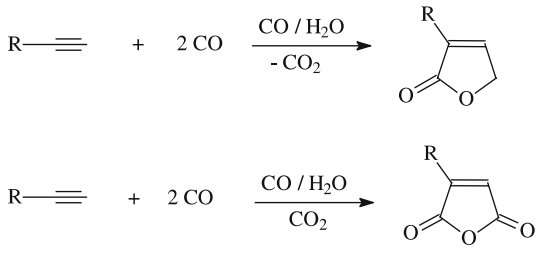

Scheme 4 Incorporation of two CO building-blocks into alkynes under water-gas-shift conditions

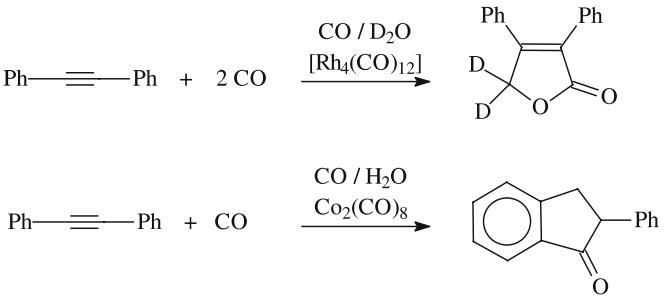

Scheme 5 Rh- or Co- catalyzed hydroxycarbonylation of diphenylacetylene

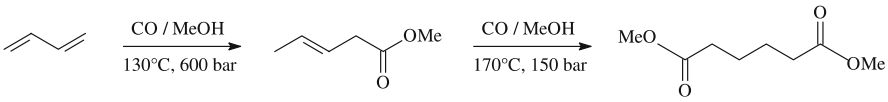

Scheme 6 The two-step methoxycarbonylation of butadiene

pathway providing indan-1-one by incorporation of only one CO moiety (Scheme 5) [42].

Carbonylation reactions under water-gas-shift conditions have been largely explored, alkynols giving saturated lactones and alkynyl amines giving saturated lactams [43]. Intramolecular alkoxycarbonylations of alkynols producing unsaturated lactones will be further described in the following paragraph.

3 Alkoxycarbonylation Reactions

This reaction involves the two reactants carbon monoxide and alcohol and produces esters, or lactones. The starting material, which will be considered here, is an alkene or an alkyne but it is also possible to start from activated halides (aryl- or allyl- iodides and bromides) to produce the same kind of organic products.

For this reaction, the early investigations of Reppe pointed out the need for catalyst precursors to operate at high pressure [2]. It is necessary to work at 150–300 bar of CO in order to stabilize the two catalytic species $[Co(H)(CO)_4]$ or $[Ni(H)(X)(CO)_2]$ that adopt a mechanism analogous to the cobalt-catalyzed hydroformylation [44, 45]. Many industrial applications have been reported [28, 46, 47] for the synthesis of plasticizers and detergents. Similarly, the two-step methoxycarbonylation of 1,3-butadiene has been explored by BASF and other companies to produce dimethyl 1,6-hexanedioate (adipate) directly from the C_4 cut [28, 48]. The first step operates at 130 °C and

600 bar of CO to give methyl-3-pentenoate, whereas the second step requires only 170 °C and 150 bar of CO. The catalyst is $[Co(H)(CO)_4]$ in the presence of pyridine (Scheme 6).

Recent investigations on octene have shown that the operating conditions can be decreased to 140 bar of CO provided a few amounts of water are added [49].

New generations of noble metal-based catalysts have been developed allowing the researchers to work under milder conditions and to improve yields and selectivity. Asymmetric versions can be envisioned by introduction of chiral ligands and/or substrates and thanks to the mild temperatures and pressures used.

3.1 Alkoxycarbonylation of Alkenes

3.1.1 Intermolecular Alkoxycarbonylation of Alkenes

Following the first observations by Heck that $Pd(OAc)_2$ can substitute a hydrogen atom in ethylene by a carbomethoxy group [50], Stille and James have discovered that the [Pd – Cu] couple catalyzes the incorporation of a COOMe group arising from carbon monoxide and methanol [51]. Most of the reactions with an alkene end up with a diester or a methoxyester, copper being used in stoichiometric quantities. Cyclic alkenes give preferentially diesters (Scheme 7).

Inomata and co-workers later reported that the same [Pd – Cu] system could also, in the presence of oxygen, drive the reaction towards the formation of the monoester with Cu(II) or diester with Cu(I) [52, 53]. Other Pd catalyst/oxidant systems have been used for the bisalkoxycarbonylation of alkenes; however the formation of by-products in the Pd-reoxidation process decreases ester yields dramatically [54].

In the absence of an oxidation agent, the reaction is derived to monoalkoxycarbonylation provided the Pd metal center is stabilized by surrounding ligands. This strategy, first illustrated in 1976 by Knifton with the complex $[PdCl_2(PPh_3)_2]$, has been extensively developed since then [55, 56]. Various terminal aliphatic alkenes are converted into the corresponding monoesters

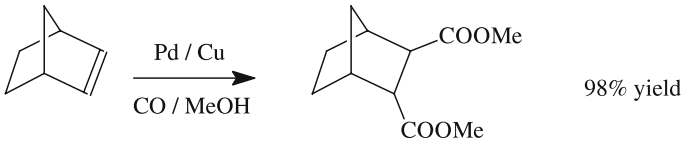

Scheme 7 An example of the methoxycarbonylation of a cyclic alkene leading to a diester

at 135 bar of CO and 70 °C and the selectivity of the carbonylation into the linear ester can be improved by introducing $SnCl_2$ as a co-catalyst. We have later shown that better selectivity with good yields can be achieved under milder conditions (100 °C, 40 bar of CO) provided an appropriate Pd/P/Sn ratio is respected [57]. This procedure has been successfully applied to the alkoxycarbonylation of monoterpenes, such as limonene [58], β-pinene, and camphene [59], leading to ester derivatives of abundant natural products that present potential application in perfumery, flavor and pharmaceutical industries. Noteworthy is the influence of reactive functionalities present in the substrate: whereas limonene gives the expected ester (Scheme 8), isolimonene leads to cyclopentanone because, even in the presence of methanol, coordination of the endocyclic C = C double bond occurs immediately after CO insertion [60, 61].

The selectivity in the linear ester can also be greatly improved by using bulky chelating diphosphines such as bis(di-*tert*-butylphosphinomethyl) benzene [62, 63] and bis(phosphaadamantyl)diphosphines [64]: high selectivity (> 95%) is achieved for both terminal and internal $C_6 - C_{12}$ alkenes; more modest selectivity, around 80%, is obtained in the case of heavier $C_{12} - C_{14}$ alkenes. Another example is given with palladium(II) complexes bearing the 1,1′-bis(diphenylphosphino)osmocene ligand which exhibits remarkable selectivity in the methoxycarbonylation of ethylene to methyl propanoate due to the formation of a dative Os – Pd bond as displayed by the X-ray crystal structure and NMR studies (Fig. 3) [65].

Concerning the mechanism of the reaction, two pathways have been considered [13, 54, 66–70] and are still proposed in the literature. The first involves an alkoxycarbonyl-palladium intermediate [Pd – COOR] on which

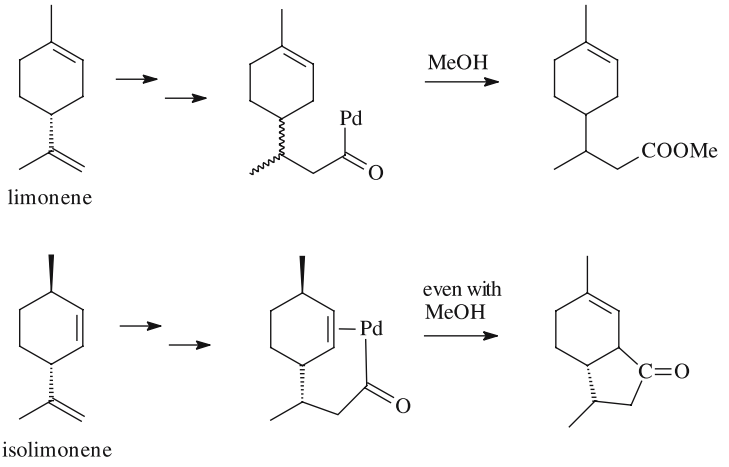

Scheme 8 Methoxycarbonylation of limonene and isolimonene

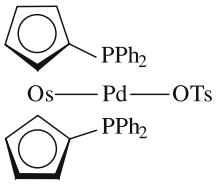

Fig. 3 Structure of a palladium(II) complex bearing the 1,1′-bis(diphenylphosphino) osmocene ligand

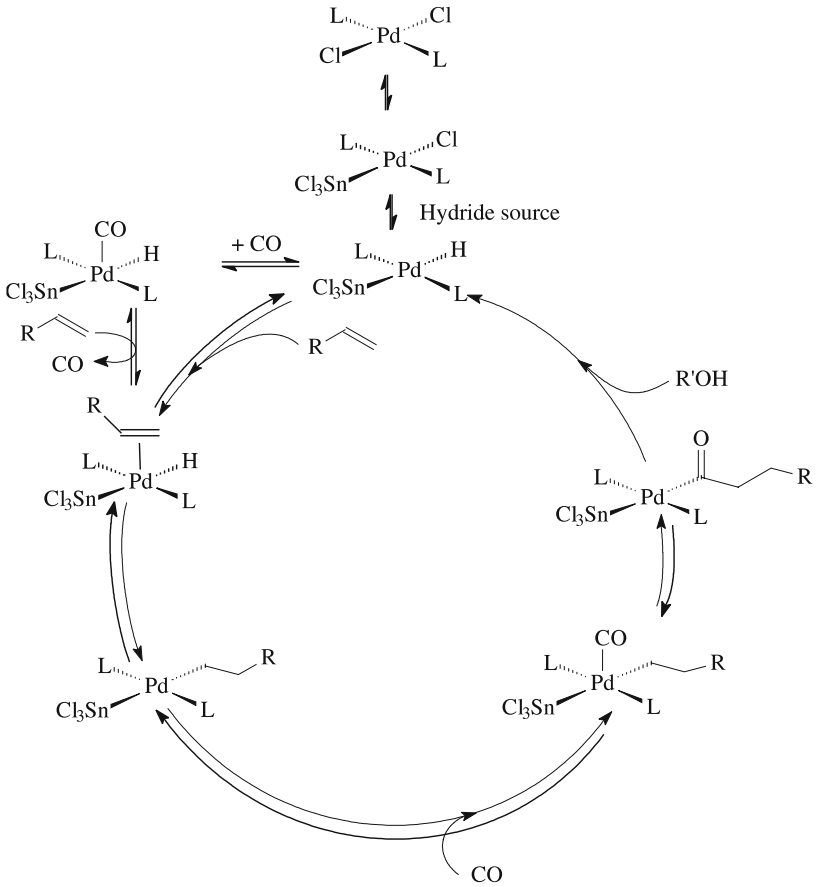

Scheme 9 Proposed hydridopalladium route for alcoxycarbonylation reaction

the alkene coordinates and a *cis*-migration step produces a palladium-alkyl moiety containing the ester group at its end. The second mechanism proceeds through a palladium-hydride active species [Pd – H] that gives, after coordination of the alkene, a palladium alkyl intermediate on which a migratory CO insertion occurs. The last step in each case concerns the direct

reaction of the alcohol to eliminate the ester and restore the active species. Recent studies have reported the characterization, and in some cases isolation, of hydrido-palladium complexes. Investigations include high-pressure NMR observations in the conditions of catalysis [71–74], or indirect evidences [75, 76].

Moreover, it has been evidenced that $SnCl_2$ acts as a ligand and that the active species is in fact $[Pd(H)(SnCl_3)(PR_3)_2]$ [71]. The catalytic cycle displayed in Scheme 9 shows the main steps that are admitted starting from $[PdCl_2L_2]/SnCl_2$.

3.1.2 Intramolecular Alkoxycarbonylation of Alkenes

Following the results obtained in the intermolecular carbonylation of alkenes in the presence of alcohols, it seemed conceivable that an alkene-bearing alcohol functionality would react in an intramolecular way giving a cyclic ester as the main product. Thus, the carbonylation (also referred to as cyclocarbonylation as a cyclization occurs simultaneously) of alkenols (or hydroxyalkenes) was investigated for the selective preparation of lactones.

The first attempts applying mild conditions were reported by Semmelhack and co-workers in 1984 [77]. Reactions were carried out in methanol, under 1 bar of CO, in the presence of catalytic $PdCl_2$ with $CuCl_2$ as a stoichiometric oxidant. No lactones were formed under these conditions; instead tetrahydrofuran or tetrahydropyran rings bearing a methoxyester moiety were selectively formed from various hydroxyalkenes as depicted in Scheme 10. Results are rationalized based on steric interactions within the appropriate reactant conformations. In fact, $PdCl_2$ coordinates the $C=C$ double bond so that the cyclization occurs first by a nucleophilic attack of the OH group. Steric effects prevail during this step (Scheme 10). Further reaction occurs through CO migratory insertion and attack of methanol to liberate the ester and produce a $Pd-H$ moiety. The active $PdCl_2$ species is restored because $CuCl_2$ is charged in excess with regard to the substrate, and retransforms $Pd(H)Cl$.

Further studies demonstrated the influence of the double-bond substitution on both the reactivity and the stereoselectivity of the reaction [78–81]. Tamaru and co-workers reported then that using the same $PdCl_2/CuCl_2/MeOH$ system on butenol derivatives, with the double bond in either the terminal or an internal position, furnished selectively γ-butyrolactones. This dicarbonylation process most probably includes (i) a lactonization step and (ii) a methoxycarbonylation step, as displayed in Scheme 11 in which we clarify some intermediate steps on a representative example [82, 83]. The use of propylene oxide as an additive promotes this Pd-catalyzed dicarbonylation by playing the role of an HCl quencher to maintain neutral conditions.

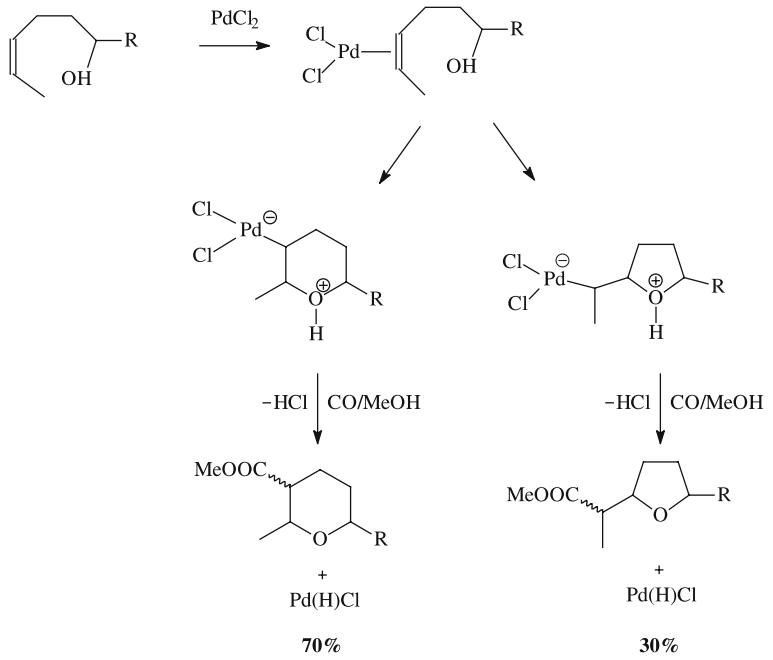

Scheme 10 Formation of tetrahydropyran or tetrahydrofuran rings in the alkoxycarbonylation of alkenols

In the early stages, Alper et al. described that α-alkyl-substituted γ-butylrolactones could be produced by carbonylation of 3-butenols and allylic alcohols in moderate yields, when treated by $PdCl/CuCl_2/CO$ in the presence of oxygen under acidic conditions, without methanol in the medium [84, 85]. Later, different palladium-based catalytic systems were used by the same group for cyclocarbonylation of allylic alcohols under neutral conditions and in the absence of an oxidant: thus, the simple combination of $Pd(OAc)_2$ or palladium dibenzylideneacetone ($Pd(dba)_2$) and dppb allowed for the preparation of lactones from secondary and tertiary allylic alcohols in 45 to 92% isolated yields [86]. With this catalytic system, β,γ-substituted allylic alcohols were converted into α,β-substituted-γ-butyrolactones in a stereoselective way, *trans*-disubstituted lactones being obtained from (*E*)-allylic alcohols [87]. By the same method, carbonylation of 2-allylphenols was reported to provide easy access to five-, six- or seven-membered lactones [88]. The $Pd(OAc)_2$/dppb catalytic system is also efficient for the preparation of both mono- and bis-lactones and has been extended to cyclocarbonylation of various substituted allylphenol and allylaniline derivatives [89–91]. As shown by Jutand and Amatore, $Pd(OAc)_2$ and phosphine ligands generate palladium(0) complexes [92]. Thus, the oxidative addition of the O – H

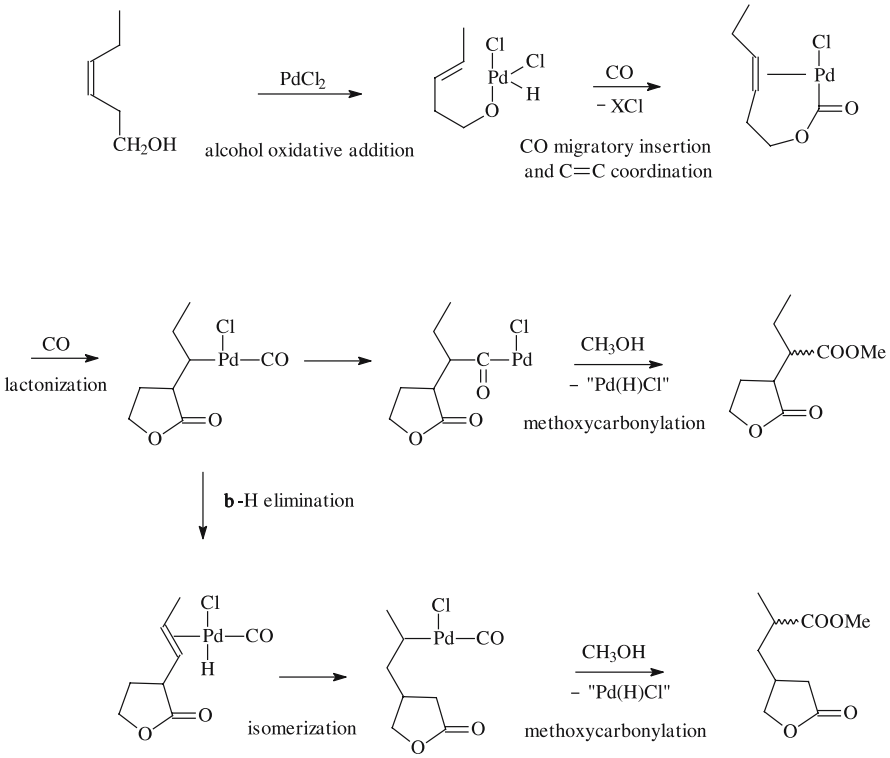

Scheme 11 Proposal of a mechanism for the intramolecular alkoxycarbonylation of a 3-butenol derivative

bond should be easy on a palladium(0) species and begin the catalytic cyclocarbonylation reaction.

The use of heterogeneous catalysts in this reaction has also been achieved: palladium-montmorillonite clays [93] or palladium/activated carbon [94] in the presence of dppb transformed 2-allylphenols into lactones, the regioselectivity of the reaction being largely dependant on the nature of the support. Very recently, palladium complexes immobilized onto silica-supported (polyaminoamido)dendrimers were used as catalysts in the presence of dppb for the cyclocarbonylation of 2-allylphenols, 2-allylanilines, 2-vinylphenols, and 2-vinylanilines affording five-, six-, or seven-membered lactones and lactams. Good conversions are realized and the catalyst can be recycled 3–5 times [95].

In order to obtain lactones from natural alkenols, we investigated the cyclocarbonylation of monoterpenic alcohols. The catalytic precursor is $[PdCl_2L_2]$ in the presence of a slight excess of tin chloride and phosphine ligands. Dihydromyrcenol, a representative acyclic terpene containing a termi-

nal C = C bond and a tertiary alcohol is functionalized into a nine-membered lactone with chemo- and regioselectivity of 100% and 98%, respectively [96, 97]. As the catalyst precursor provides in situ the $[Pd(H)(SnCl_3)L_2]$ active species liberating HCl in the medium the dehydration of the tertiary alcoholic function can be favored. We have shown that simple addition of molecular sieves to remove HCl and water co-produced, leads selectively to the lactone. Otherwise the carbonylation reaction provides the terminal unsaturated C_{11} acid from the dehydrated substrate and H_2O produced in the medium (Scheme 12).

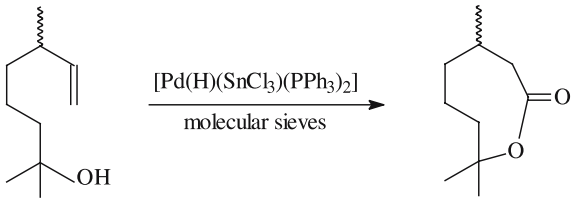

Scheme 12 Cyclocarbonylation of dihydromyrcenol

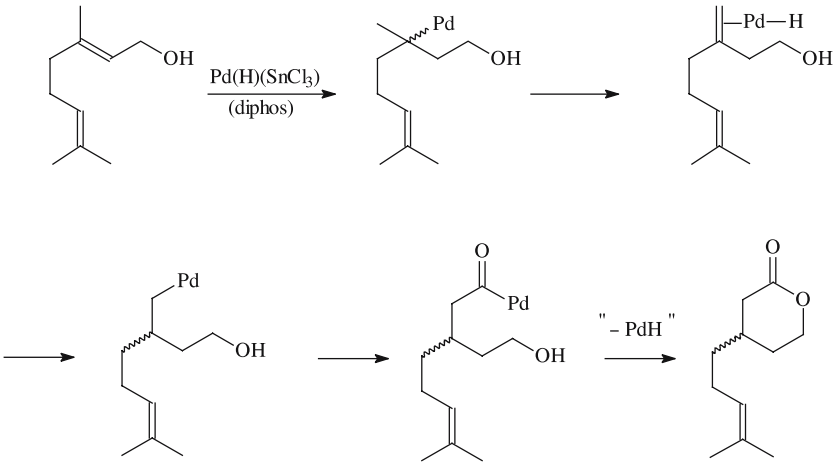

Scheme 13 Formation of a six-membered lactone in the cyclocarbonylation of geraniol

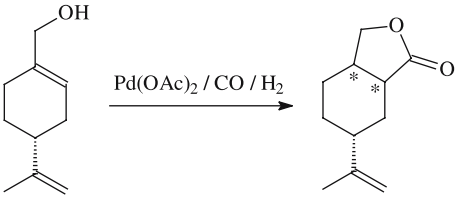

Scheme 14 Cyclocarbonylation of perillyl alcohol

Geraniol is an interesting substrate that presents a hindered terminal C = C bond and an allylic function. The carbonylation reaction gives, beside the acid, the six-membered lactone and not the butyrolactone; that means that initially an isomerization step occurred as depicted in Scheme 13. The most adapted ligand to obtain good selectivity in this lactone is dppb [98]. In the case of perillyl alcohol such an isomerization does not occur and the C_5-lactone is produced (Scheme 14) [99].

3.1.3 Asymmetric Alkoxycarbonylation

As the regio- and chemoselectivity of alkoxycarbonylations has been continuously improved and milder reaction conditions were applicable, it was attractive to develop an asymmetric version of this carbonylation reaction. Using $PdCl_2/CuCl_2$ in HCl/O_2 at room temperature and 1 bar of CO, Alper and Hamel introduced poly-L-leucine as a chiral ligand. Producing α-methyl-γ-butyrolactone by carbonylation of but-2-en-1-ol, moderate asymmetric induction with a 61% ee was observed [100]. Other chiral ligands were then introduced by several research groups and all the examples reported concern palladium-based catalysts. For example, various atropisomeric diphosphine ligands were tested by Consiglio et al. in the bismethoxycarbonylation of styrene [101] and aliphatic olefins [102]. Enantioselectivity up to 93% was achieved in the case of styrene whereas aliphatic olefins were converted with deceiving ee's. Another approach with palladium supported on clays in the presence of various chiral mono- or diphosphines gave poor enantioselectivity in the monomethoxycarbonylation of styrene [103]. Interestingly, norbornene was enantioselectively carbonylated to the exo (1*S*, 2*S*, 4*R*) ester with up to 92% ee in the presence of a carbohydrate-based diphosphine ligand [104].

The best enantioselectivity achieved so far was in intramolecular alkoxycarbonylation reactions. For example, using $Pd(OAc)_2$ with a chiral diphosphine ligand on β-substituted allylic alcohols containing dialkyl substituents at the α-position gave good enantioselectivity [105, 106]. More recent studies show that it is possible to carbonylate enantioselectively β,γ-substituted allylic alcohols [107]. Thus, following the observations achieved with nonchiral Pd(0)(dppb) complexes that *trans*-disubstituted lactones can be selectively produced from (*E*)-β,γ-substituted allylic alcohols [87], hindered chiral disphosphine ligands were introduced and led to high ee's for the resulting lactones. For instance, using the Pd/BICP [2*R*,2*R*′-bis-(diphenylphosphino)-1*R*,1*R*′-dicyclopentane] catalyst, a chiral γ-butyrolactone was formed in 98% ee from the allylic alcohol shown in Scheme 15 [108].

An alternative strategy to control the stereoselectivity is to introduce a chiral information on the substrate itself [109]. As far as alkoxycarbonylation is concerned, isopulegol is a representative example whose functionalization is

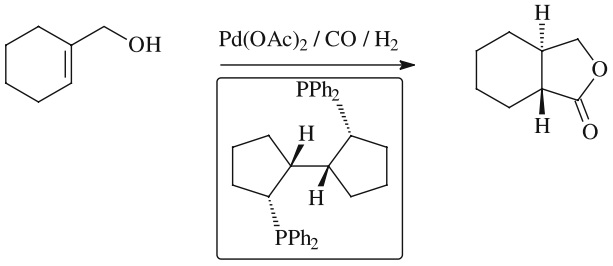

Scheme 15 Asymmetric cyclocarbonylation of an alkenol in the presence of the BICP chiral ligand

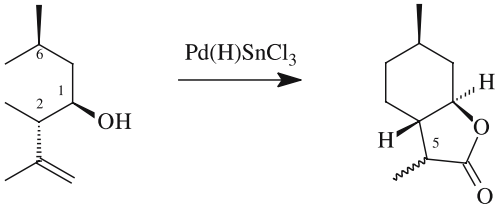

Scheme 16 Cyclocarbonylation of isopulegol

influenced by the presence of two pre-existing stereogenic centers (C_1 and C_2 in Scheme 16). Indeed, using $[Pd(H)(SnCl_3)L_2]$ as the catalyst, (+)DIOP or (–)DIOP L_2 ligands lead to the same stereoselectivity on C_5 (de of 62% in both cases), indicating that the chirality of the DIOP ligand does not play any role in the course of this reaction. In fact, the ligands intervene exclusively through their chelating effect and presumably their steric hindrance [110].

3.2 Alkoxycarbonylation of Alkynes

3.2.1 Intermolecular Alkoxycarbonylation of Alkynes

The first observations, done by Tsuji et al. in 1980 on substituted acetylenes, were reinvestigated by Brandsma in 1994 and concern the alkoxycarbonylation of these substrates, not to give an acrylate moiety, but instead acetylenic esters [111, 112]. The catalytic system involves $PdCl_2/CuCl_2/NaOAc$. Copper chloride introduced in stoichiometric amounts is responsible for the CH activation, maintaining the triple bond. Such an activation recalls that observed on allenyl- and propynylhalides that classically gives the allenylesters [113].

Later, using the same $PdCl_2/CuCl_2$ system without added base or acid and in less polar solvents, such as benzene, Jiang and his group de-

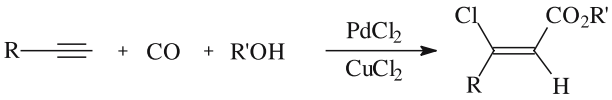

Scheme 17 Preparation of (*Z*)-chloroacrylate esters from terminal alkynes

veloped a method for the highly regio- and stereospecific synthesis of (*Z*)-3-chloroacrylate esters from terminal alkynes (Scheme 17). They explained that *cis*-addition of acetylenes on $PdCl_2$ produced a *cis*-chloropalladated intermediate. Then acylation and alcoholysis steps in the catalytic cycle afforded the corresponding chloroacrylate esters [114].

Under similar reaction conditions, γ-acetoxy-β-methoxyalkenoates are produced when propargylic acetates are carbonylated. The presence of the acetoxy moiety is indispensable; it plays the role of an ancillary ligand during the coordination of the triple bond to the palladium(II) species [115].

Conversion of alkynes into acrylate derivatives has been described by Drent et al. using a palladium(II) complex containing a 2-pyridylphosphine ligand in the presence of an acid whose conjugated base is a weakly coordinating ligand [116, 117]. Propyne was transformed into methyl methacrylate with 99.95% selectivity and TOF up to 50 000 h^{-1}. According to the authors, the catalytic cycle starts with a palladium(II)-methoxy species in which the 2-pyridylphosphine ligand plays either the role of a chelating P – N ligand or that of a mono-coordinating P ligand functioning as a "proton messenger" to the active palladium center as depicted in Scheme 18.

An alternative mechanism involving a palladium-hydride as the active species was proposed by Scrivanti et al. following their labeling experiments with CH_3OD and detection of a deuterated σ-vinylpalladium intermediate (Scheme 19) [118].

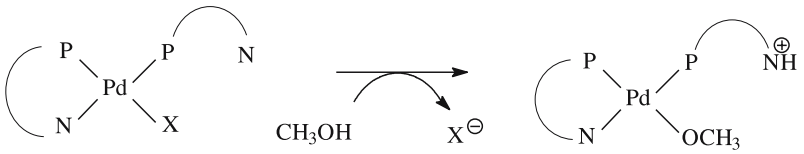

Scheme 18 Formation of the palladium(II) methoxy-species

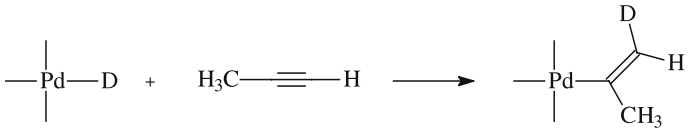

Scheme 19 Structure of the deuterated σ-vinylpalladium intermediate detected in labeling experiments

Another catalytic system based on $Pd(OAc)_2$/dppb transforms various alkynes into unsaturated esters in the presence of different alcohols such as tert-butanol and iso-propanol. High regioselectivity in branched esters was achieved but in moderate yields [119]. Later, addition of a catalytic amount of *p*-toluenesulfonic acid was found to enhance the reaction rate. Both terminal and internal alkynes are converted in good yields under milder conditions (1 bar of CO, 100 °C) [120]. An alternative approach is to simultaneously add *p*-toluenesulfonic acid and a hemilabile bidentate ligand such as pyridine carboxylic acid to improve catalytic activity [121]. Palladium-hydride was again privileged as the active species. Such a metal hydride pathway is also supported by studies on $[Pt(H)(Cl)(PPh_3)_2]$ showing that this complex and analogous platinum-hydride complexes are efficient precursors for the methoxycarbonylation of various terminal alkynes [122]. This study also underlines that $SnCl_2$ improves the catalytic activity or even is necessary to the reaction when starting from $[PtCl_2(PR_3)_2]$.

Incorporation of two CO building blocks can be obtained associating an oxidant to the palladium catalyst leading to a diester, or a reductant providing a lactone. $PdCl_2$ and more preferably PdI_2, stabilized by an excess of KI, transforms a terminal alkyne into the corresponding maleic esters in the presence of O_2 and a robust ligand like thiourea (Scheme 20) [123–125]. A rhodium-catalyzed double carbonylation of alkynes has been reported on aromatic internal alkynes leading to alkoxycarbonylindanones, provided the high pressure of CO (100 bar) and the high temperature (100 °C) are maintained (Scheme 20) [126].

Similarly, a double functionalization can be reached when an activating group is present in close vicinity to the triple bond. Tsuji et al. have discovered that with a diphosphine palladium(0) complex, a carbonate function in the α-position of the alkyne provides by decarboxylation a palladium methoxy species on which the alkyne moiety can be isomerized into an allenyl σ-bonded group. CO insertion in the Pd – C bond, reductive elimination with the methoxy group and further cyclization with incorporation of a second CO molecule give rise to the corresponding cyclopentenone as shown in Scheme 21 [127].

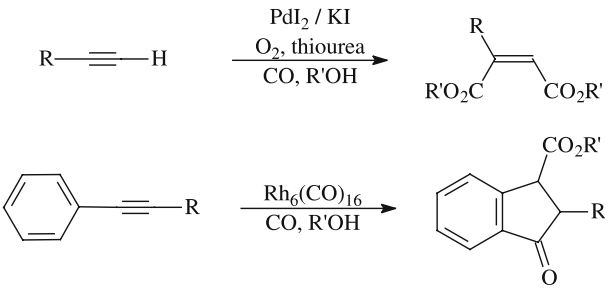

Scheme 20 Incorporation of two CO building-blocks into alkynes

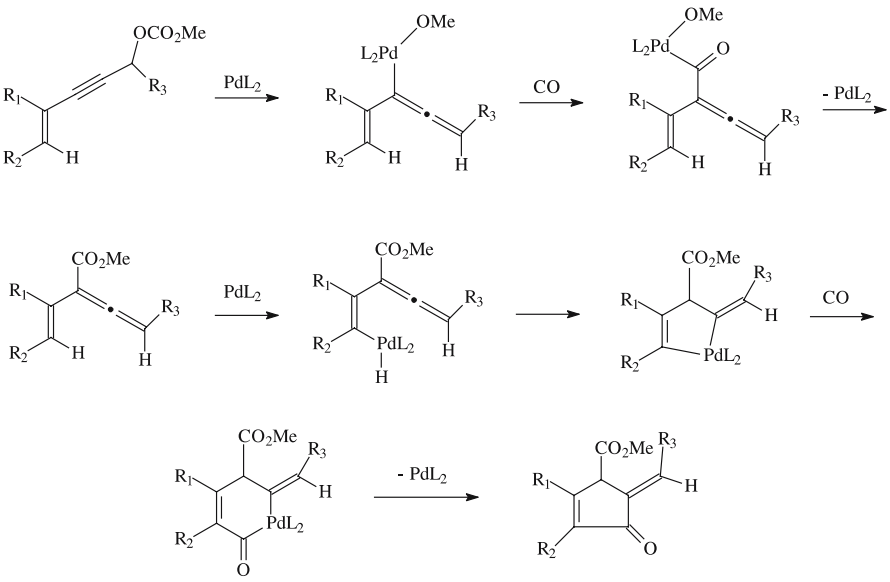

Scheme 21 Carbonylation of enynes bearing a carbonate function in the α-position of the triple bond

In an analogous approach explored by Dixneuf et al., a conjugated enynyl carbonate is converted into an oxolenone or a bicyclic lactone in significant yields via double carbonylation in the presence of methanol (Scheme 22) [128]. When a neighboring carbonyl group is present in the substrate, it can also participate in palladium-catalyzed cyclization-carbonylation. Indeed, 4-yn-1-ones lead to cyclic ketals that can be easily converted into 2-cyclopentenone carboxylates in an acidic medium (Scheme 22) [129].

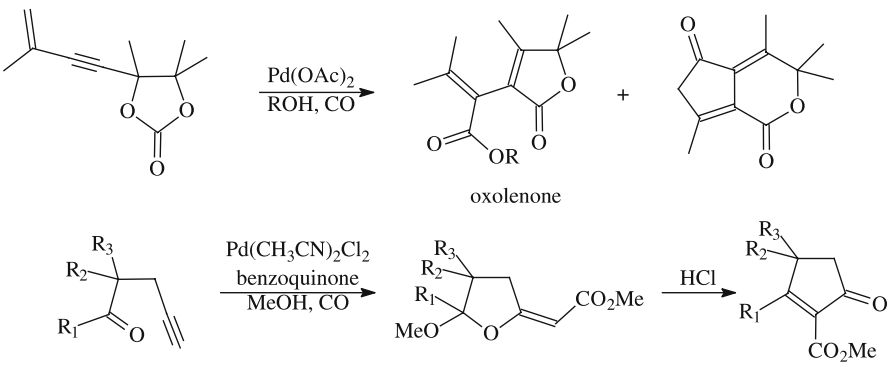

Scheme 22 Alkoxyarbonylation of alkynes bearing an activating group

In an alternative strategy functionalized phenols, such as iodophenol, were involved in palladium-catalyzed carbonylation of alkynes or allenes, producing coumarin or chromone derivatives (Scheme 23) [130–133]. After oxidative addition of the iodoarene to the Pd(0) catalyst the order of insertion of either CO or the unsaturated substrate mainly depends on the nature of the substrate. In fact, Alper et al. reported that CO insertion occurs prior to allene insertion leading to methylene- or vinyl-benzopyranone derivatives [130]. On the contrary, insertion of alkynes precedes insertion of CO, affording coumarine derivatives, as reported by Larock et al. According to the authors, this unusual selectivity can be explained by the inability of the acyl palladium species to further react with the alkyne, hence the decarbonylation step occurs preferentially [131–133].

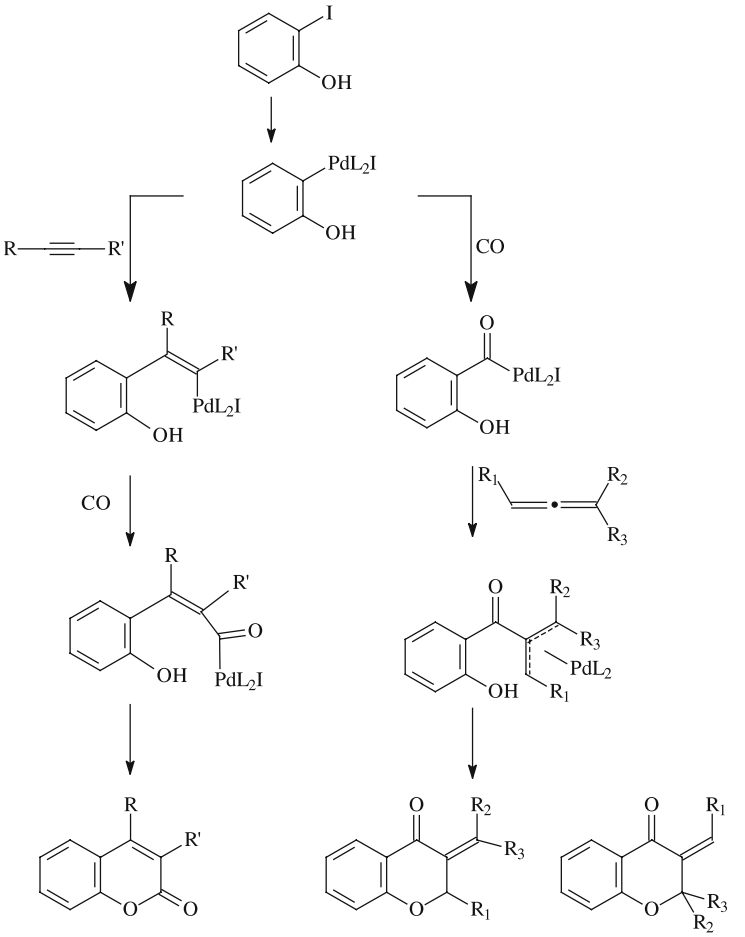

Scheme 23 Pd-catalyzed carbonylation of iodophenol with alkynes and allenes

3.2.2
Intramolecular Alkoxycarbonylation of Alkynes

Intramolecular alkoxycarbonylation of alkynols is parallel to what has been described for alkenols except that functionalization of the triple-bond produces a double bond. No lactone formation is observed in the Pd(II)-catalyzed oxidative cyclization-carbonylation of alkynes. Instead [(methoxycarbonyl)methylene]tetrahydrofurans are selectively formed [134, 135]. Moreover, starting from an enynol, furan-2-acetic ester is obtained resulting from a final aromatization step [136].

Dialkoxycarbonylation has been reported using a Pd-catalyst/oxidant system on propynols or butynols furnishing respectively β- or γ-lactone derivatives with α-(alkoxycarbonyl)ethylene chains (Scheme 24) [83, 137, 138]. This reaction occurs in a stereospecific way leading exclusively to *cis*-dicarbonylated products in fair to excellent yields (25–97%). Noteworthy, a butynol bearing an alkyl or an aryl substituent instead of a TMS one undergoes a different course of reaction under the same conditions: here *trans*-alkoxycarbonylation takes place selectively (Scheme 25).

Unsaturated lactones can be obtained from alkynols and according to the substrate and/or the catalyst as well as to the reaction conditions, the double bond can be endo- or exocyclic. Thus, we will distinguish the two modes of synthesis.

Methylene lactones deserve special interest due to their presence in many biologically active natural products [139]. Norton et al. have developed an

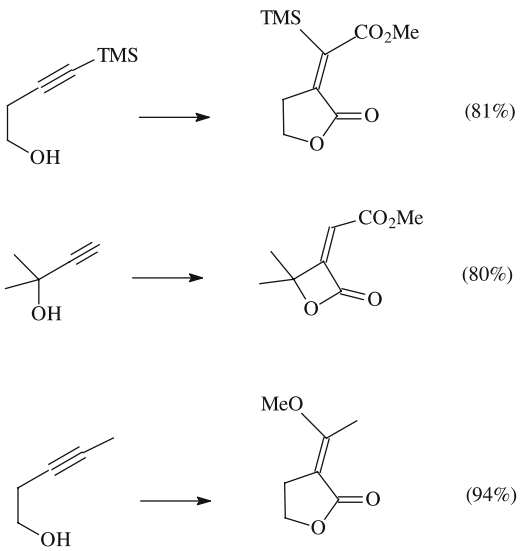

Scheme 24 Double carbonylation of various butynols or propynols

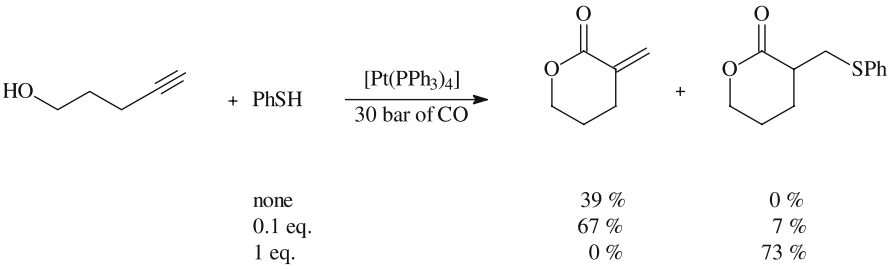

Scheme 25 Cyclocarbonylation of an alkynol in the presence of thiols

efficient tool to carbonylate alkynols into α-methylene lactones under mild conditions [140, 141]. Different palladium precursors can be used for this reaction such as $PdI_2/PBu_3/CH_3CN$ or $PdCl_2/PPh_3/SnCl_2/CH_3CN$. In the absence of comparative experiments with either Pd – H or Pd – COOR active species, the mechanism remains under debate. The alkoxycarbonylpalladium species which is privileged by the authors requires the cleavage of the O – H bond of the terminal alcohol [142]. However, this oxidative reaction on a palladium(II) metal center seems to us less evident than on a Pd(0) species. Recent studies on the use of ionic liquids to separate easily the organic phase from the catalytic phase started from $Pd(OAc)_2$ and pyridyldiphenylphosphine [143]. α-Methylene lactones are efficiently produced in isolated yields up to 80%; however, we know that such a catalytic system evolves rapidly towards $Pd(0)L_2$ complexes. Moreover, $[Pt(PPh_3)_4]$ has also been shown to catalyze the lactonization of 5-hydroxy-1-pentyne with yields improved by the presence of thiols (Scheme 25) [144]. In the absence of thiol, the production of the methylene lactone should also result from the oxidative addition of the substrate O – H bond. Addition of a few amounts of PhSH improves significantly the yields together with the formation of α-phenylthiomethyl-δ-lactone. Indeed, the oxidative addition of the S – H bond on platinum is easier than that of the O – H bond, and can trigger the catalytic cycle more efficiently. The α-phenylthiomethyl-δ lactone which may result from a Michael addition of ArSH on the methylene lactone, is exclusively formed when 1 equivalent of thiol is engaged.

Applying more drastic conditions (100 bar of CO; 175 °C), $[Rh_6(CO)_{16}]$ also catalyzes cyclocarbonylation of 2-alkynylphenols. The mechanism involves here also an O – H oxidative addition initial step. The α-methylene lactone is further reduced since rhodium catalyzes the water-gas-shift reaction and water is present in the medium [145].

Additionally, when Pd-catalyzed cyclocarbonylation of alkynols is carried out in the presence of a large excess of $CuCl_2$ (5 equivalents), (*Z*)-α-chloroalkylidene-β-lactones are obtained as depicted in Scheme 26 [146, 147]. As previously mentioned concerning the intermolecular alkoxycarbonyla-

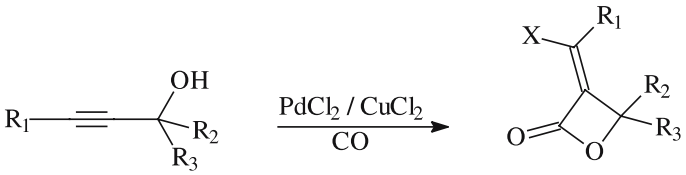

Scheme 26 Preparation of (*Z*)-α-chloroalkylidene-β-lactones from alkynol derivatives

tion, the introduction of the halide substituent is supposed to occur through a *cis*-chlorometalation on the triple bond coordinated on $PdCl_2$. (*Z*)-α-bromoalkylidene-β-lactones can be similarly obtained when using $Pd(OAc)_2$ and $CuBr_2$.

For unsaturated lactones containing an endocyclic double bond also the two previously described mechanisms are presumably involved and the regioselectivity of the cyclocarbonylation is governed by the presence of bulky substituents on the substrate. Inoue and his group have observed that the catalyst precursor needs to be the cationic complex $[Pd(PhCN)_2(dppb)]^+$ and not a neutral Pd(0) or Pd(II) complex [148, 149]. It is suggested that the mechanism involves a cationic palladium-hydride that coordinates to the triple bond; then a hydride transfer occurs through a *cis*-addition. Alper et al. have shown that addition of dihydrogen to the palladium(0) precursor $Pd_2(dba)_3$/dppb affords an "active" system, in our opinion a palladium-hydride species, that coordinates the alkyne [150].

To summarize this part, various palladium complexes efficiently catalyze the lactonization of alkynols. Many mechanistic studies remain to be carried out to have a clear understanding of the mechanism in order to anticipate the reactivity of such substrates. Nevertheless, the implication of palladium-hydride intermediates should take a large place in this catalysis.

4 Conclusion

Carbonylation of unsaturated substrates has been known for decades but the reaction selectivity has been progressively improved by tuning the coordination sphere of late transition metal-based catalysts. Palladium assumes a privileged place in this chemistry and its versatility allows the use of mild conditions for the selective incorporation of CO into acyclic and cyclic compounds. Further improvements open a path to more sophisticated reactions, particularly cascade reactions. Similarly, asymmetric versions of most of these carbonylations can be envisioned. Atom economy and the green character of the process will probably be the key criteria for evaluating any new catalytic system.

References

1. Boivin TL (1987) Tetrahedron 33:3309
2. Nicolaou KC, Sorensen EJ (eds) (1996) Classics in Total Synthesis. Wiley, Weinheim
3. Colquhoun HM, Thompson DJ, Twigg MV (eds) (1991) Carbonylation. Plenum Press, New York
4. Reppe W, Magin A, Schuster C, Keller R, Kroper H, Klein T, Kerchow FW, Blank G, Merchel K, Scheller H, Weschky L, Wolff K, Schwenckendiek W, Hecht W, Gassenmeier E, Simon A (1953) Liebigs Ann Chem 582:1
5. Reppe W, Kroper H, Pistor HJ, Schlenk H (1953) ibid 582:38
6. Reppe W, Kroper H, Von Kutepow N, Pistor HJ, Weissbarth O (1953) ibid 582:72
7. Reppe W, Schuster C, Keller R, Kroper H, Klein TH, Schlenk H, Reindl E, Schluhkecht W (1953) ibid 582:116
8. Chiusoli GP, Venturello C, Merzoni S (1968) Chem Ind 977 quoted by Gabriele B, Salerno G, Costa M, Chiusoli GP (2003) J Organmet Chem 687:219
9. Botteghi C, Consiglio G, Pino P (1973) Chimia 27:477 quoted by Nozaki K (1999) In: Jacobsen EN, Pfaltz A, Yamamoto H (eds) Comprehensive Asymmetric Catalysis. Springer, Heidelberg, p 382–409
10. Knifton JF (1976) J Org Chem 41:2885
11. Reppe W (1953) Liebigs Ann Chem, p 582
12. Von Kutepow V, Bittler K, Neubauer D (1969) US Patent, 3,437,676 to Badische Anilin and Soda-Fabrik
13. Fenton DM (1973) J Org Chem 38:3192 and references cited herein
14. Alper H, Woell JB, Despeyroux B, Smith DHJ (1983) J Chem Soc Chem Commun 1270
15. Alper H, Hamel N (1990) J Am Chem Soc 112:2803
16. Stahly GP, Starett RM (1997) In: Collins AN, Sheldrake GN, Crosby J (eds) Chirality in Industry II. Wiley, Chichester, West Sussex, p 19–40
17. Jayasree S, Seayad A, Chaudhari RV (2000) Organic Letters 2:203
18. Kruiz D, Ruiz N, Janssen MD, Boersma J, Claver C, Van Koten G (1998) Inorganic Chemistry Communications 1:295
19. Tilloy S, Monflier E, Bertoux F, Castanet Y (1977) New J Chem 21:529
20. Papadogiakis G, Verspui G, Maat L, Sheldon RA (1997) Catal Lett 47:43
21. Verspui G, Feiken J, Papadogiakis G, Sheldon RA (1999) J Mol Catal A: Chem 143:299
22. Monflier E, Tilloy S, Bertoux F, Castanet Y, Mortreux A (1997) New J Chem 21:857
23. Bertoux F, Monflier E, Castanet Y, Mortreux A (1999) J Mol Catal A: Chem 143:11
24. Goedheijt MS, Reck JNH, Kamer PCJ, Van Leeuwen PNM (1998) Chem Commun, p 2431
25. Miquel-Serrano M, Aghmiz A, Diéguez M, Masdeu-Bulto AM, Claver C, Sinou D (1999) Tetrahedron: Asymmetry 10:4463
26. El Ali B, Alper H (1992) J Mol Catal 77:7
27. El Ali B, Alper H (1993) J Mol Catal 80:377
28. Cornils B, Herrman WA (eds) (2002) In: Applied Homogeneous Catalysis with Organometallic Compounds. Second Completely Revised and Enlarged Edition. Wiley, Weinheim, pp 3–27
29. Weissermel K, Arpe JH (eds) (1997) In: Industrial Organic Chemistry. Third Completely Revised Edition. Wiley, Weinheim, p 290 (translated by C.R. Lindley)
30. Amer I, Alper H (1990) J Organomet Chem 383:573
31. Lee JT, Alper H (1991) Tetrahedron Lett 32:1769
32. Satyanarayana N, Alper H, Amer I (1990) Organometallics 9:284
33. Satyanarayana N, Alper H (1991) Organometallics 10:804

34. Zhou Z, Alper H (1996) Organometallics 15:3282
35. Huh KT, Orita A, Alper H (1993) J Org Chem 58:9656
36. Piotti ME, Alper H (1994) J Org Chem 59:3282
37. Gabriele B, Salerno G, Costa M, Chiusoli GP (1999) Tetrahedron Lett 40:989
38. Chiusoli GP, Costa M, Cucchia L, Gabriele B, Salerno G, Veltri L (2003) J Mol Catal A: Chem 204–205:133
39. Joh T, Doyama K, Onitsuka K, Takahashi S (1991) Organometallics 10:2493
40. Joh T, Nagata H, Takahashi S (1994) Inorg Chim Acta 220:45
41. Zhang SW, Sugioka T, Takahashi S (1999) J Mol Catal A: Chem 143:211
42. Joh T, Doyama K, Fujiwara K, Maeshima K, Takahashi S (1991) Organometallics 10:2493
43. Hirao K, Mori N, Joh T, Takahashi S (1995) Tetrahedron Lett 36:6243
44. Heck RF, Breslow DS (1963) J Am Chem Soc 85:2779
45. Sheldon RA (1983) In: Ugo R, James BR (eds) Chemical from Synthesis Gas. Reidel D Publishing Company, Dordrecht, pp 104–126
46. Pino P, Piacenti F, Bianchi M (1977) In: Wender I, Pino P (eds) Organic Synthesis via Metal Carbonyls. Wiley, New York, pp 233–296
47. Hoffman P, Kosswig K, Schafer W (1980) Ind Eng Chem Prod Res Dev 19:330
48. Beller M, Cornils B, Frohning CD, Kohlpaintner CW (1995) J Mol Catal A 104:17
49. Jacob C, Heaton BT, Iggo JA, Whytman R (2003) J Mol Catal A: Chem 204–205:149
50. Heck RF (1969) J Am Chem Soc 91:6707
51. James DE, Stille JK (1976) J Am Chem Soc 98:1810
52. Inomata K, Toda S, Kinoshita H (1990) Chem Lett 1567
53. Toda S, Miyamoto M, Kinoshita H, Inomata K (1991) Bull Chem Soc Jpn 64:3600
54. Beller M, Tafesh AM (2002) In: Cornils B, Herrman WA (eds) Applied Homogeneous Catalysis with Organometallic Compounds. Wiley, Weinheim, pp 182–194
55. Knifton JF (1976) J Org Chem 41:2885
56. Knifton JF (1978) J Am Oil Chem Soc 55:496
57. Cipres I, Jenk J, Kalck Ph (1990) J Mol Catal A 58:387
58. Chenal T, Cipres I, Jenk J, Kalck Ph, Perez Y (1993) J Mol Catal A 78:351
59. Da Rocha LL, Dias AO, Dos Santos EN, Augusti R, Gusevskaya E (1998) J Mol Catal A: Chem 132:149
60. Naigre R, Chenal T, Cipres I, Kalck Ph, Daran JC, Vaisserman J (1994) J Organomet Chem 480:91
61. Lenoble G, Lacaze-Dufaure C, Urrutigoïty M, Mijoule C, Kalck Ph (2004) Eur J Inorg Chem, p 791
62. Clegg W, Eastham GR, Elsegood MRJ, Tooze RP, Wang XL, Whiston K (1999) Chem Commun, p 1877
63. Rodriguez CJ, Foster DF, Eastham GR, Cole-Hamilton DJ (2004) Chem Commun, p 1720
64. Pugh RI, Drent E, Pringle PG (2001) Chem Commun, p 1476
65. Gusev OV, Kalsin AM, Petrovski PV, Lyssenko K, Oprunenko YF, Bianchini C, Meli A, Oberhauser W (2003) Organometallics 22:913
66. Bardi R, Del Pra A, Piazzesi AM, Toniolo L (1979) Inorg Chim Acta 35:L345
67. Cavinato G, Toniolo L (1979) Chimia 33:286
68. Cavinato G, Toniolo L (1979) J Mol Catal A 6:111
69. Cavinato G, Toniolo L (1981) J Mol Catal A 10:161
70. Cavinato G, Toniolo L (1990) J Mol Catal A 398:187
71. Nguyen DH, Coppel Y, Urrutigoïty M, Kalck Ph (2005) J Organomet Chem 690:2947
72. Eastham GR, Tooze RP, Kilner M, Foster DF, Cole-Hamilton DJ (2002) J Chem Soc Dalton, p 1613

73. Clegg W, Eastham GR, Elsegood MRJ, Heaton BT, Iggo IA, Tooze RP, Whyman R, Zacchini S (2002) J Chem Soc Dalton, p 3300
74. Liu J, Heaton BT (2004) Chem Commun, p 1326
75. Cavinato G, Vavasori A, Toniolo L, Benetollo F (2003) Inorg Chim Acta 343:183
76. Cavinato G, Toniolo L, Vavasori A (2004) J Mol Catal A: Chem 219:233
77. Semmelhack MF, Bodurow C (1984) J Am Chem Soc 106:1496
78. Semmelhack MF, Zhang N (1989) J Org Chem 54:4483
79. Semmelhack MF, Kim C, Zhang N, Bodurow C, Sanner M, Dobler W, Meier M (1990) Pure and Appl Chem 63:2035
80. Mac Cormick M, Monahan III R, Soria J, Goldsmith D, Liotta D (1989) J Org Chem 54:4485
81. White JD, Hong J, Robarge LA (1999) Tetrahedron Lett 40:1463
82. Tamaru Y, Hojo M, Yoshida Z (1987) Tetrahedron Lett 28:325
83. Tamaru Y, Hojo M, Yoshida Z (1991) J Org Chem 56:1099
84. Alper H, Leonard D (1985) Tetrahedron Lett 26:1463
85. Alper H, Leonard D (1985) J Chem Soc, Chem Commun, p 511
86. El Ali B, Alper H (1991) J Org Chem 56:1099
87. Brunner M, Alper H (1997) J Org Chem 62:7565
88. El Ali B, Okuro K, Vasapollo G, Alper H (1996) J Am Chem Soc 118:4264
89. Troisi L, Vasapollo G, El Ali B, Mele G, Florio S, Capriati V (1999) Tetrahedron Lett 40:1771
90. Vasapollo G, Scarpa A, Mele G, Ronzini L, El Ali B (2000) Appl Organometal Chem 14:739
91. Vasapollo G, Mele G, El Ali B (2003) J Mol Catal A: Chem 204–205:97
92. Amatore C, Jutand A, Khalil F, Barki MAM, Mottier L (1993) Organometallics 12:3168
93. Orejon A, Alper H (1999) J Mol Catal A: Chem 143:137
94. Maffei A, Mele G, Cicarella G, Vasapollo G, Crisafulli C, Scire S, La Mantia F (2002) Appl Organometal Chem 16:534
95. Touzani A, Alper H (2005) J Mol Catal A: Chem 227:197
96. Lenoble G, Urrutigoïty M, Kalck Ph (2001) Tetrahedron Lett 42:3697
97. Lenoble G, Urrutigoïty M, Kalck Ph (2002) J Organomet Chem 643–644:12
98. Nguyen DH, Hébrard F, Duran J, Polo A, Urrutigoïty M, Kalck Ph (2005) Appl Organometal Chem 19:30
99. El Ali B, Alper H (2000) Synlett 2:161
100. Alper H, Hamel N (1990) J Chem Soc, Chem Commun, p 135
101. Nefkens SC, Sperle M, Consiglio G (1993) Angew Chem Int Ed Engl 32:1719
102. Sperle M, Consiglio G (1999) J Mol Catal A: Chem 143:263
103. Nozaki K, Kantam ML, Horiuchi T, Takaya H (1997) J Mol Catal A: Chem 118:247
104. Zhou H, Lu S, Hou J, Chen J, Fu H, Wang H (1996) Chemistry Letters, p 339
105. Alper H, Leonard D (1985) J Chem Soc, Chem Commun, p 511
106. Alper H, Leonard D (1985) 26:5639
107. Yu WY, Bensimon C, Alper H (1997) Chem Eur J 3:417
108. Cao P, Zhang X (1999) J Am Chem Soc 121:7708
109. Kalck Ph, Urrutigoïty M (2004) Coord Chem Rev 248:2193
110. Lenoble G, Naigre R, Chenal T, Urrutigoïty M, Daran JC, Kalck Ph (1999) Tetrahedron: Asymm 10:929
111. Tsuji J, Takahashi M, Takahashi T (1980) Tetrahedron Lett 21:849
112. Vasilesky SF, Trofinov BA, Mal'kina AG, Brandsma L (1994) Synthetic Comm 24:85
113. Trieu ND, Elsevier CJ, Vrieze K (1987) J Organomet Chem 325:C23
114. LiI J, Jiang H, Feng A, Jia L (1999) J Org Chem 64:5984

115. Okumoto S, Nishihara S, Nakagawa H, Suzuki A (2000) Synlett 2:217
116. Drent E, Arnoldy P, Budzelaar PHM (1993) J Organomet Chem 455:247
117. Drent E, Arnoldy P, Budzelaar PHM (1994) J Organomet Chem 475:57
118. Scrivanti A, Beghetto V, Campagna E, Zanato M, Matteoli U (1998) Organometallics 17:630
119. El Ali B, Alper H (1991) J Mol Catal 67:29
120. Kushino Y, Itoh K, Miura M, Nomura M (1994) J Mol Catal 89:151
121. Jayasree S, Seayad A, Gupte SP, Chaudhari RV (1999) Catalysis Lett 58:213
122. Scrivanti A, Menchi G, Matteoli U (1995) J Mol Catal A: Chem 96:223
123. Gabriele B, Salerno G, Costa M, Chiusoli GP (1995) J Organomet Chem 503:21
124. Gabriele B, Salerno G, Costa M, Chiusoli GP (2003) J Organomet Chem 687:219
125. Bonardi A, Costa M, Gabriele B, Salerno G, Chiusoli GP (1994) J Chem Soc, Chem Commun, p 2429
126. Yonedo E, Kaneko T, Hang SW, Onitsuko K, Takahashi S (1999) Tetrahedron Lett 40:7811
127. Mandai T, Tsuji J, Tsujiguchi Y (1993) J Am Chem Soc 115:5865
128. Darcel C, Bruneau C, Dix-neuf PH (1990) Synlett, p 218
129. Kato K, Yamamoto Y, Akita H (2002) Tetrahedron Lett 43:4915
130. Okuro K, Alper H (1997) J Org Chem 62:1566
131. Kadnikov DV, Larock RG (2000) Organic Lett 2:3643
132. Kadnikov DV, Larock RG (2003) J Org Chem 68:9423
133. Kadnikov DV, Larock RG (2003) J Organomet Chem 687:425
134. Gabriele B, Salerno G, Di Pascali F, Costa M, Chiusoli GP (1999) J Org Chem 64:7693
135. Gabriele B, Salerno G, Di Pascali F, Costa M, Chiusoli GP (2000) J Organomet Chem 593–594:409
136. Gabriele B, Salerno G, Di Pascali F, Sciano GT, Costa M, Chiusoli GP (1997) Tetrahedron Lett 38:6817
137. Gabriele B, Salerno G, Costa M, Chiusoli GP (1994) J Chem Soc, Chem Commun, p 1429
138. Gabriele B, Salerno G, Di Pascali F, Costa M, Chiusoli GP (1997) J Chem Soc Perkin Trans 1:147
139. Avizee S, Yerzhanov KB, Al Aziz Al Quntar A, Dembitsky VM (2004) Tetrahedron 60:5499
140. Murray TF, Norton JR (1979) J Am Chem Soc 101:4107
141. Murray TF, Samsel EG, Varma V, Norton JR (1981) J Am Chem Soc 103:7520
142. Consorti CS, Ebeling G, Dupont J (2002) Tetrahedron Lett 38:6817
143. Ogawa A, Kawabe K, Kawakami J, Mihara M, Hirao T, Sonoda N (1998) Organometallics 17:311
144. Yoneda E, Sugiski T, Hirao K, Zhang SW, Takahashi S (1998) J Chem Soc Perkin Trans 1:477
145. Yoneda E, Sugioka T, Hirao K, Zhang SW, Takahashi S (1998) J Chem Soc Perkin Trans 1:477
146. Ma S, Wu B, Zhao S (2003) Org Lett 5:4429
147. Ma S, Wu B, Jiang X, Zhao S (2005) J Org Chem 70:2568
148. Matsushita K, Komori T, Oi S, Inoue Y (1994) 35:5889
149. Tezuka K, Ishizaki Y, Inoue Y (1998) J Mol Catal A: Chem 129:206
150. Yu WY, Alper H (1997) J Org Chem 62:5684

Top Organomet Chem (2006) 18: 125–164
DOI 10.1007/3418_019

Published online: 22 July 2006

Carbonylation of Ethene in Methanol Catalysed by Cationic Phosphine Complexes of Pd(II): from Polyketones to Monocarbonylated Products

Gianni Cavinato[1] · Luigi Toniolo[2] (✉) · Andrea Vavasori[2]

[1]University of Padua, Department of Chemical Sciences, Via Marzolo 1, 35131 Padova, Italy

[2]University of Venice, Department of Chemistry, Dorsoduro 2137, 30123 Venezia, Italy
toniolo@unive.it

1 Introduction 126

2 Mechanistic Aspects of the $CO–C_2H_4$ Copolymerisation 128
2.1 General Aspects 128
2.2 Alternating Chain Propagation 131
2.3 Chain Transfer (Termination–Initiation) 134
2.3.1 Protonolysis 134
2.3.2 Methanolysis 135
2.3.3 Shift From the Hydride Mechanism to the Carbomethoxy Mechanism and Vice Versa 136
2.4 Kinetic Studies 136

3 Control of Chain Growth 138
3.1 General Aspects 138
3.2 Influence of the Counter-Anion 140
3.3 Influence of the Ligand 141
3.3.1 High Molecular Weight Polyketones 141
3.3.2 From Cooligomers to Low Molecular Weight Products 144

4 Selective Synthesis of Monocarbonylated Products 147
4.1 Synthesis of Methyl Propanoate 147
4.1.1 Monophosphine Catalysts 148
4.1.2 Diphosphine Catalysts 151
4.2 Selective Synthesis of Diethyl Ketone 156

5 Conclusions and Outlook 158

References 160

Abstract This review article describes the advances on the carbonylation of ethene in methanol since the discovery of highly active cationic *cis*-chelating diphosphine-Pd(II) catalysts for the production of perfectly alternating high molecular weight polyketones, which led to the recent development of efficient catalysts for the synthesis of monocarbonylated products. After dealing with the activation of the catalyst precursor and with mechanistic aspects of the catalytic cycles, the influence of the operating conditions, the nature of the counter anion, the acidity of the reaction medium and the nature of the ligand on both the rate and the selectivity is delineated. In particular, it is shown that the

catalytic activity can be finely tuned by varying the electronic, bite angle and steric bulk properties of the ligand and that, within a series of related ligands, the selectivity mainly depends on the steric bulk.

Keywords Carbonylation · Ethene · Methanol · Monocarbonylation · Palladium · Phosphines · Polyketones

Abbreviations

dppp	1,3-bis(Diphenylphosphino)propane
dppe	1,2-bis(Diphenylphosphino)ethane
dppb	1,4-bis(Diphenylphosphino)butane
dapp	1,3-bis[bis(2-Methoxyphenyl)phosphino]propane,1,3 bis(dianysilphosphino) propane
dppm	1,1-bis(Diisobutylphosphino)methane
dibpp	1,3-bis(Diisobutylphosphino)propane
dippe	1,2-bis(Diisopropylphosphino)ethane
dtbpe	1,2-bis(Di-*t*-butylphosphino)ethane
dtbpp	1,3-bis(Di-*t*-butylphosphino)propane
dtbpx	1,2-bis[(Di-*tert*-butyl)phosphinomethyl]benzene
dppf	1,1′-bis(Diphenylphosphino)ferrocene
dppo	1,1′-bis(Diphenylphosphino)osmocene
dppomf	1,1′-bis(Diphenylphosphino)octamethylferrocene
dba	*Trans,trans*-dibenzylidenacetone
HOMs	Methanesulfonic acid
TFA	Trifluoroacetic acid
TFA^-	Trifluoroacetate anion
HOTf	Trifluoromethanesulfonic acid
HOTs	4-Toluenesulfonic acid
DEK	Diethylketone
MP	Methylpropanoate
BQ	Benzoquinone
NQ	Naphtoquinone
OX	Oxidant

1 Introduction

The discovery in the early 1980s that cationic palladium-phosphine complexes catalyse the copolymerisation of carbon monoxide with ethene or a higher α-olefin to yield perfectly alternating polyketones has since attracted continuous increasing interest [1, 2]. This is because the monomers are produced in large amounts at a low cost and because polyketones represent a new class of thermoplastics of physical-mechanical and chemical properties that have wide applications [3–6]. In addition, easy functionalisation can open the way to a large number of new materials [7]. The copolymerisation has

been extended to other olefins, such as cyclic alkenes, dienes, styrenes, and functionalised α-olefins and also to terpolymerisation. The introduction of a second olefin in the CO-ethene backbone lowers the melting point and makes the terpolymer more easily processable. The development of highly active palladium-diphosphine catalysts has opened the way to the commercialisation of the CO-ethene-propene terpolymer [2, 8–10].

Early disclosing of the results in some articles and reviews is still a basic guideline [1, 6, 11–16]. Perfectly alternating polyketones form because consecutive insertion of two molecules of CO is not allowed for thermodynamic reasons and two consecutive insertions of ethene do not occur for kinetic reasons [11–13]. Cationic palladium-diphosphine catalysts (typically dppp) are far superior, as far as both rate of copolymerisation and molecular weight of the polyketone, to catalysts having the metal coordinated by a monophosphine, such as PPh_3. This striking difference was explained as the result that the diphosphine is always *cis*-chelate, so that the other two coordination sites of the d^8-square planar palladium centre, one occupied by the growing polymer chain and the other by the monomer, are also always *cis* to each other, which is ideal in favouring the chain growth through migratory insertions of the monomers. Differently, Pd(II) coordinated by a monophosphine can assume both *cis* and *trans* geometry, so that chain growth is relatively slow compared to chain termination [14–16]. Since then many articles have been published. Research efforts have been focused towards the deeper understanding of the key factors that rule the catalysis. The subject has been extensively and excellently reviewed up to very recently [17–21]. The last review deals in particular the structure and physicochemical and mechanical properties of copolymers of less common olefins, such as higher olefins and styrenes, dienes, cyclic dienes and functionalised olefins. In addition the stereochemical copolymerisation has also been reviewed [22, 23], as well as theoretically investigated [24].

Several types of bidentate ligands, different from diphosphines, for example bipyridines and phenantrolines, have been proven to give active catalysts, particularly in the CO-styrene copolymerisation [25], but, particularly with ethene, diphosphines give higher performances.

The carbonylation of ethene has a wider interest as it can lead to the production not only of polyketones, but also to many other products ranging from low molecular weight cooligoesters, down to methyl propanoate (MP) and also cooligodiesters, cooligodiketones down to diethyl ketone (DEK). The insertion of the monomers into MeOH is schematized by Eq. 1, n ranging from 1 to even more that 10 000:

$$n\mathrm{CO} + n\mathrm{CH_2{=}CH_2} + \mathrm{CH_3OH} \longrightarrow \mathrm{H}\left(\mathrm{CH_2CH_2CO}\right)_n\mathrm{OCH_3} \qquad (1)$$

Mixtures of low molecular weight products and DEK can find large uses as low volatility “green” solvents [18, 26].

MP is a potential intermediate to methyl methacrylates, an important monomer produced annually on a multimillion tonne scale worldwide [27–29].

Highly active, selective and stable catalysts for the production of MP [30–33] and DEK [33] with sterically demanding basic diphosphine ligands have also been developed. In addition, these type of catalysts selectively convert internal olefins to linear esters for the production of detergents, plasticizers and nylon intermediates [32, 34].

The alkoxycarbonylation of olefins has also been reviewed recently [35].

Hereafter, the factors ruling the activity and selectivity of Pd(II)-phosphine catalysts for the carbonylation of ethene in MeOH are presented. In order to make the exposition clearer some of the concepts already discussed in other reviews will be shortly resumed. It will deal first with copolymerisation because it includes more general aspects, several of which are involved also in the catalysis to monocarbonylated non-polymeric products. The literature search covers all up to 2004.

2
Mechanistic Aspects of the CO–C_2H_4 Copolymerisation

2.1
General Aspects

The most active and selective catalysts for both the copolymerisation process and for the apparently simpler ethene carbonylation to monocarbonylated products MP or DEK are cationic square planar Pd(II) complexes in which the metal centre is *cis*-coordinated by a bidentate P – P ligand, by a ligand involved in the initial step of the catalysis or in the process of forming the product and with the fourth "vacant" site coordinated by CO or ethene or a keto group of the growing chain or MeOH (or H_2O, always present in the solvent even when not added on purpose) or even by a weakly coordinating anion.

In general, when using an active Pd-diphosphine catalyst, the end groups of the perfectly alternating CO – C_2H_4 polymer chains are couples of EtCO- (keto, K) and -COOMe (ester, E) or K – K or E – E groups [14]. When using a monodentate ligand, such as PPh_3, only K – E cooligomers form, together with MP. In this case it has been proposed that the hydride mechanism only is operative (Eq. 3) [11]. Polymers with K – E end groups form through initial insertion of CO into a Pd – OCH_3 bond, followed by sequential insertions of the monomers and ends by protonolysis by MeOH of a Pd-alkyl bond with reformation of the initiating species; it can also form starting from a Pd – H^+ species and end by methanolysis of a Pd-acyl bond, with regeneration of the starting species. The polymer E – E forms from Pd – $OCH_3{}^+$ and

ends through methanolysis of a Pd-acyl bond, with formation of a $Pd-H^+$ species, different from the starting one. In turn $Pd-H^+$ can start the process that leads to the polymer K – K, if the termination occurs via protonolysis of a Pd-alkyl bond with formation of $Pd-OCH_3^+$, different from the species that initiates this cycle (in Eqs. 2–5 and in the following ones, $Pd-OCH_3^+$, $Pd-H^+$, Pd^{2+}, etc., are also coordinated by a P – P ligand or two monophosphines). The last two cycles can be interconnected and, when they occur at comparable rates, the E – E and K – K chains should balance and the expected K/E ratio should be 1/1 [14].

$$Pd\text{-}OCH_3^+ \xrightarrow{CO,\ CH_2=CH_2} Pd\text{-}CH_2CH_2CO\sim\sim COOCH_3^+ \xrightarrow{CH_3OH} K\text{-}E + Pd\text{-}OCH_3^+ \quad (2)$$

$$Pd\text{-}H^+ \xrightarrow{CH_2=CH_2,\ CO} Pd\text{-}COCH_2CH_2\sim\sim COCH_2CH_3^+ \xrightarrow{CH_3OH} E\text{-}K + Pd\text{-}H^+ \quad (3)$$

$$Pd\text{-}OCH_3^+ \xrightarrow{CO,\ CH_2=CH_2} Pd\text{-}COCH_2CH_2\sim\sim COOCH_3^+ \xrightarrow{CH_3OH} E\text{-}E + Pd\text{-}H^+ \quad (4)$$

$$Pd\text{-}H^+ \xrightarrow{CH_2=CH_2,\ CO} Pd\text{-}CH_2CH_2CO\sim\sim COCH_2CH_3^+ \xrightarrow{CH_3OH} K\text{-}K + Pd\text{-}OCH_3^+ \quad (5)$$

However, this is not always the case. Excess of K – K has been found to occur during the initial stage of the copolymerisation when the cooligomer chain bound to the metal is still soluble and catalysis occurs in the homogeneous phase [36]. This may also occur when protonolysis involves H_2O in place of MeOH, with formation of a $Pd-OH^+$ species, which regenerates $Pd-H^+$ by insertion of CO to $Pd-COOH^+$ followed by CO_2 evolution. Thus in each catalytic cycle one molecule of CO is not incorporated into the polymer chain, but is consumed as CO_2:

$$Pd\text{-}H^+ \xrightarrow{CH_2=CH_2,\ CO} Pd\text{-}CH_2CH_2CO\sim\sim COCH_2CH_3^+ \xrightarrow{H_2O} K\text{-}K + Pd\text{-}OH^+ \quad (6)$$

$$Pd\text{-}OH^+ + CO \longrightarrow Pd\text{-}COOH^+ \longrightarrow Pd\text{-}H^+ + CO_2 \quad (7)$$

Excess of polymer E – E has also been found and in some cases only E – E forms, for instance during the initial stage of catalysis by $Pd(dapp)^{2+}$ in the presence of an oxidant, usually benzoquinone or naphtoquinone (BQ, NQ) [37]. The oxidant favours the formation of $Pd-OCH_3^+$ at the expense of $Pd-H^+$ [15] and in the copolymerisation process one molecule of oxidant is

consumed in each catalytic cycle:

$$Pd\text{-}H^+ + CH_3OH + OX \longrightarrow Pd\text{-}OCH_3^+ + OXH_2 \quad (8)$$

$$2CH_3OH + (n+1)CO + nC_2H_4 + OX \longrightarrow CH_3OCO\left(CH_2CH_2CO\right)_n OCH_3 + OXH_2 \quad (9)$$

The catalyst is not introduced into the reaction medium as the $Pd-OCH_3^+$ or $Pd-H^+$ species. These form in situ by reactions of a relatively stable "cationic" catalyst precursor with MeOH or a hydride source. In turn, the precursor can be prepared by adding to a $Pd(AcO)_2$ solution a solution of the P – P ligand (1/1) and then a solution of a strong acid HX, whose conjugate base may be a weakly or a non-coordinating anion, like $CF_3SO_3^-$, BF_4^-, TsO^-, CF_3COO^-, or from preformed $[PdCl_2(P-P)]$ by metathetical exchange with AgX or salts of metals that have a stronger affinity for Cl^- than palladium [38]; it can also be preformed $[PdX_2(P-P)]$ or $[PdX_{2-n}L_n(P-P)]X_n$ (n = 1 or 2, L = easily displaceable ligand such as H_2O or CH_3CN). Alumoxanes have also been used to abstract the acetate or chloride ligands [39].

The species that initiate the catalysis form in situ according to the reactions:

$$Pd^{2+} + CH_3OH \longrightarrow Pd\text{-}OCH_3^+ + H^+ \quad (10)$$

$$Pd\text{-}OCH_3^+ \longrightarrow Pd\text{-}H^+ + HCHO \quad (11)$$

$$Pd^{2+} + H_2O + CO \xrightarrow{-H^+} Pd\text{-}COOH^+ \longrightarrow Pd\text{-}H^+ + CO_2 \quad (12)$$

$$Pd^{2+} + CH_3OH + C_2H_4 \longrightarrow Pd\text{-}H^+ + CH_2{=}CHOCH_3 + H^+ \quad (13)$$

$$Pd^{2+} + H_2O + C_2H_4 \longrightarrow Pd\text{-}H^+ + CH_3CHO + H^+ \quad (14)$$

$$Pd\text{-}OCH_3^+ \xrightarrow{CO,\ CH_3OH} Pd\text{-}H^+ + (CH_3O)_2CO \quad (15)$$

$$Pd^{2+} + HCOOH \xrightarrow{-H^+} Pd\text{-}O_2CH^+ \longrightarrow Pd\text{-}H^+ + CO_2 \quad (16)$$

Equation 11 occurs via β – H abstraction by Pd(II) [33, 40–42]; Eq. 12 is related to the water–gas shift reaction (WGSR) [43–45]; Eq. 13 and Eq. 14 are related to the oxidation of C_2H_4 to acetaldehyde by Pd(II) in the presence of H_2O in the Wacker process [46]. Equation 15 has been shown to occur with octamethylferrocene-phosphine complexes [47]. Formic acid can also be a source of hydride species [48].

$Pd-Me^+$, $Pd-COR^+$ complexes, $Pd-Ar^+$ related to the $Pd-H^+$ catalytic cycle, and $Pd-COOCH_3^+$ complexes, related to the other cycle, can be also used to start the catalysis [11, 39, 49–60].

In MeOH, Pd – H^+ species are unstable and have the tendency to deprotonate with reduction to less active dimeric Pd(I) and Pd(0) complexes, which may lead to degeneration of the catalyst with formation of inactive palladium metal and free ligands, which in turn may give less active bis-chelate complexes $[Pd(P-P)_2]^{2+}$ [55, 61]. Possible deactivation paths have been delineated in [17]. In order to maintain or improve the catalytic activity, the precursor is used together with an oxidant and an excess of acid (usually BQ/Pd = 100 – 200 and acid/Pd = 10 – 20) [15, 47].

Furthermore, even the ligand, necessary to stabilize the catalyst, can reduce Pd(II) to Pd(0) complexes and formation of phosphine oxides [62–64]. In the preparation of $[Pd(AcO)_2(dppp)]$, from $Pd(AcO)_2$ and dppp in MeOH, phosphine oxides have been found to form together with methyl acetate and palladium metal [65]. The reaction can be schematized as follows:

$$Pd(AcO)_2 + H_2O + P\text{-}P \longrightarrow Pd_{metal} + 2AcOH + P\text{-}P{=}O \qquad (17)$$

Equations 12, 14 and 17 require the presence of H_2O. Thus H_2O plays an important role in promoting the catalytic activity, but can also cause deactivation. Catalysis will be more efficient when all the reactions directly involved in the catalytic cycle are faster than the side reactions subtracting active species. Deactivation is related to the requirement of the palladium centre to have a "vacant" coordination site to ensure high catalytic activity. However, palladium tends to achieve the usual coordination number four, for example through dimerisation. Dimerisation/deactivation can be prevented by coordination of labile ligands, like H_2O, which acts also as an efficient hydride source. Also deprotonation leads to dimerisation/deactivation; an acid can prevent it.

Thus, it has been found that H_2O and TsOH have a beneficial effect on the catalytic system $Pd(AcO)_2$/dppp/TsOH, first reported by Drent, as the copolymerisation rate significantly increases (with respect to the use of "anhydrous" MeOH) about five times and passes through a maximum in the presence of ca. 1000 ppm of H_2O and when Pd/TsOH = 1/8 (ca. 12 000 g polymer(g Pd·h)$^{-1}$ at 90 °C, 60 bar, CO/ethene = 1/1) [66].

2.2
Alternating Chain Propagation

The process of chain growing involves alternating reversible CO insertions and irreversible ethene insertions [13, 15, 67]. As already mentioned, consecutive insertion of two molecules of CO does not occur for thermodynamic reasons and consecutive insertion of two molecules of ethene does not occur because the insertion of CO is much faster than that of ethene [11–13, 67]. It was subsequently proposed that coordination through the oxygen atom of a carbonyl group of the growing chain with formation of β- and γ-chelates

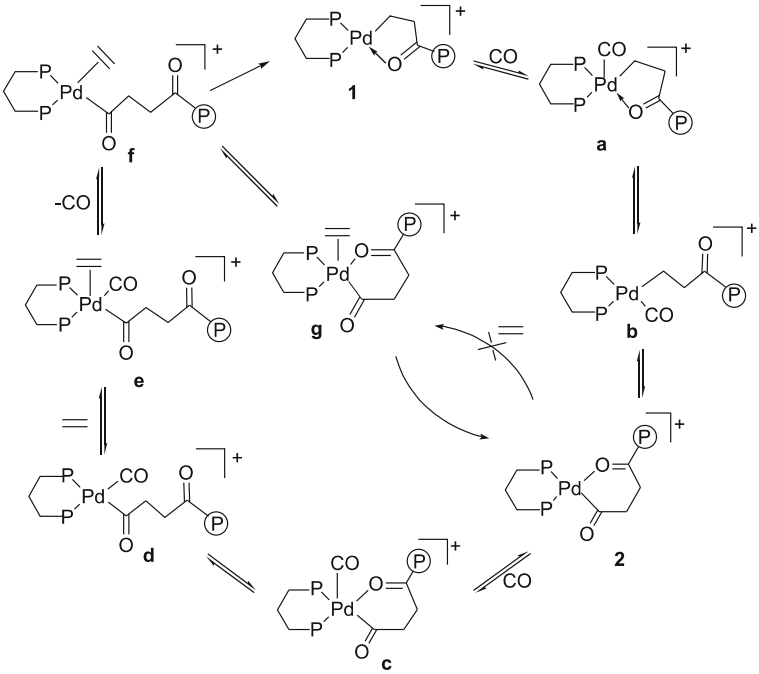

Fig. 1 Proposed alternating chain growing process, with observed intermediates, **1** and **2**, and proposed ones, **a–f**. Adapted from [51]

(Fig. 1) contributes to the perfect alternation. Because of its higher binding affinity, CO inserts into a five-membered β-chelate to give a six-membered γ-chelate. Since a five-membered ring is more stable that a six-membered one, further propagation occurs with the insertion of ethene and formation of the next five-membered ring [15].

By the use of polarization modulation reflection absorption infrared spectroscopy (PM-RAIRS), Drent and colleagues monitored in the microcrystalline state the single insertion steps catalysed by [Pd(CH_3)(OTf)(dppp)] and the presence of β- and γ-chelates **1** and **2**. It was proposed that substitution of the chelating cheto group by ethene is CO-assisted and occurs in two steps, associative substitution of the chelating keto group by CO (**2** → **c** → **d**) followed by associative substitution of CO by ethene (**d** → **e** → **f**), and that the substitution of the chelating keto group by CO is more facile than by ethene for steric reasons. It was also found that the total abundance of **1** and **2** and their ratio remain constant, so that both are resting states of the catalyst [51].

Such chelates have been detected also by variable temperature multinuclear NMR spectroscopy, which showed that basically the above mechanism is also operating in solution [47, 55, 58].

For a series of model alkyl complexes of the type $[Pd(R)(CO)(P-P)]^+$ (R = Me, Et) it has been found that the CO Eqs. 18 and 19 are reversible

and that the energy barriers, in the range of 14–18 kcal/mol, decrease with increasing P – Pd – P angles and steric bulk of the ligands [52, 54–56, 68]. However, a rate-enhancing effect was observed with ligands 1,*n*-bis(diphenyl)phosphinoalkanes in the order $n = 4 > n = 3 > n = 2$ [69].

For a series of model acyl of the type $[Pd(COMe)(C_2H_4)(P-P)]^+$ it has been found that the insertion of ethene into the Pd-acyl bond with formation of a β-chelate (Eq. 20) is irreversible and that the energy barrier is ca. 12 kcal/mol [52, 55, 56]. From thermodynamic and kinetic data, Schultz et al. calculated that the insertion of ethene into a Pd-alkyl bond (double ethene insertion) could occur every ca. 10^5 CO insertions into the same bond [52], which accounts for the strict alternating chain growing.

In addition, it has been established that the energy barriers of the β-chelate opening by CO (Eq. 21) decrease by increasing the length of the chain bridging the two P atoms and hence with increasing P – Pd – P bite angles, and that there is correlation between the intrinsic catalytic activity and the energy barrier Eq. 21 [55, 56]. It is noteworthy to report that ethene insertion into a β-chelate has never been observed, in spite of the fact that these model reactions have been studied in the absence of free CO, so that, at least in principle, ethene could insert, since double ethene insertion is known to occur in the absence of CO. Moreover, under actual catalytic conditions, imperfect alternating copolymers with ethene content > 50%, risen from multiple ethene insertions, have been obtained by increasing the ethene/CO ratio using *o*-alkoxy derivatives of diphenylphosphinobenzene sulfonic acid acting as P – O ligands [70].

On the basis of these studies both in solid and in solution, even under actual catalytic conditions, the importance of the chelates in controlling both the strict alternating chain growing and the chain propagation rate is well ascertained [19, 47, 51, 58].

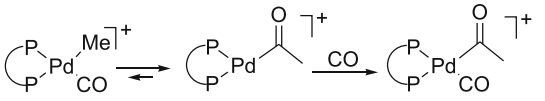

(18)

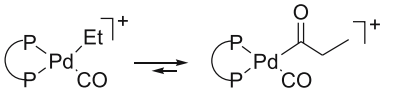

(19)

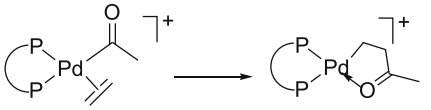

(20)

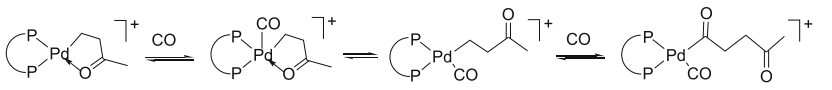

(21)

2.3
Chain Transfer (Termination–Initiation)

Ideally, the $Pd-OCH_3^+$ or $Pd-H^+$ species that initiate the catalytic cycle regenerate at the termination step of the chain propagation process. Chain transfer occurs via protonolysis or methanolysis.

2.3.1
Protonolysis

Protonolysis involves the reaction of a β-chelate moiety with methanol and produces a polymer with keto end group and a $Pd-OCH_3^+$ species. The mechanism proposed to explain deuterium enrichment in the 2-position with respect to 1-position involves a pre-equilibrium of the β-chelate with its enolate isomer by a β-H elimination/hydride migration and protonation to the more nucleophilic oxygen atom to give an enol, which rearranges to the ketone [49, 71]. This mechanism is operative also in the hydroacylation of ethene to DEK [72]. When protonolysis occurs by H_2O, the binuclear complex $[Pd(\mu\text{-}OH)(P-P)]_2^{2+}$, which may form if excess acid is not used, reacts with CO with regeneration of a $Pd-H^+$ species after CO_2 evolution (Eq. 7) [73]. In turn the hydride may undergo deprotonation with formation of a less active dimer as shown in Fig. 2 [47, 55, 56]. Efficient catalytic activity is achieved by using the precursor in combination with a quinone and an acid [47].

A lowering of the molecular weight upon increasing acid concentration could be expected, but this is not the case [74]. For several ligands enolate formation was found to be much slower than protonation. It was concluded that enolate formation is the rate-determining step [49].

The effect of bite angle of P – P ligands on the rate of protonolysis of β-chelates has been investigated with model complexes $[Pd(CH_2CH_2COCH_3)(P-P)]^+$. The rate slightly increases with increasing bite angles [75]. However, under actual copolymerisation conditions it was found that the rate of the β-chelate with dppf ligand is slower than the one of the β-chelate with dppe or dppp, which have a smaller bite angle than dppf [55, 56, 76, 77].

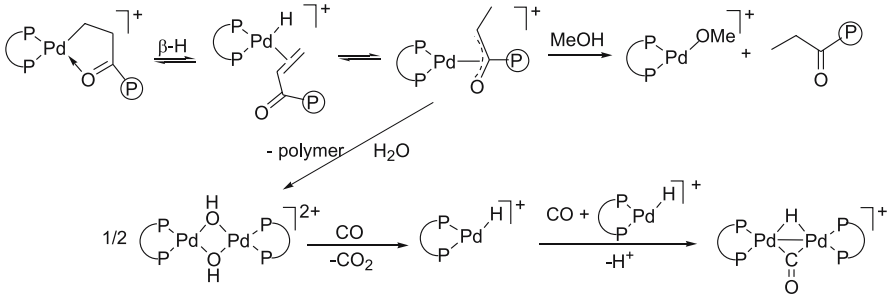

Fig. 2 Termination by protonolysis, with formation of dimeric species

2.3.2 Methanolysis

Methanolysis can occur via inter- or intramolecular nucleophilic attacks by MeOH at the carbon atom of a Pd-acyl moiety and produces an ester end group and a Pd – H^+ species. Again, the hydride may deprotonate with formation of less active Pd(0) and dimeric species (Fig. 3) [47, 57].

The rate of methanolysis is expected to be dependent on the nature of the alcohol. Indeed, the relative rate of termination versus the rate of chain growing catalysed by a cationic Pd(II) – PPh_3 system reported by Sen et al. is in the order of methanol > ethanol > *i*-propanol > *t*-butyl alcohol, which is the order of increasing steric bulk [12]. The same order has been observed for the rate of alcoholysis of the Pd-acyl bond of model complexes of the type $[Pd(COMe)(P-P)]^+$ to alkyl acetate [57]. Studies on the methanolysis of complexes of this type, in which the ligand is *trans* or *cis* coordinated, led to the conclusions that (1) ester elimination is prevented when the ligand adopts *trans* geometry, (2) complexes that have a *trans* structure but can adopt also a *cis* structure or complexes that have only a *cis* geometry do react with methanol to form methyl acetate, (3) methanolysis requires a "vacant" coordination site to coordinate MeOH *cis* to the acyl ligand and occurs via a migratory elimination or a 1,2-shift of the alkoxy group from palladium to the acyl carbon atom, and (4) the rate of methanolysis increases with increasing steric bulk [57].

That coordination of MeOH to palladium is an essential prerequisite to methanolysis and has been evidenced also by studying the effect of solvent, counter-anion and occupancy of the fourth site on $[Pd(dibpp)(COCH_3)L]^{n+}$ ($n = 0$ or 1; L = counter-anion or CH_3CN, CO) [78].

However, the complex $[Pd(dppomf)(COCH_3)]^+$ undergoes immediate methanolysis at room temperature and even though (1) the dppomf acts as a tridentate η^3-P, P, Fe ligand, with *trans* P atoms, and (2) ethene does not insert, which is indicative that a coordination site is not easily available. Thus, in this case, methanolysis either occurs via a five-coordinate transition state or it can occur also intermolecularly [47]. This might be also the case for the methoxycarbonylation of ethene catalysed by the osmocene analogue of dppf (Sect. 3.3.2) [79].

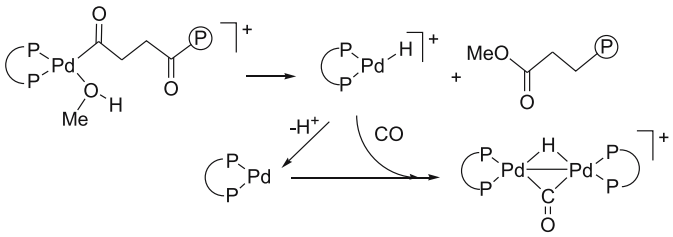

Fig. 3 Termination by methanolysis with formation of Pd(0) and dimeric complexes

2.3.3
Shift From the Hydride Mechanism to the Carbomethoxy Mechanism and Vice Versa

As already mentioned, $Pd-H^+$ generated at the methanolysis step may transform into $Pd-OCH_3{}^+$ by the action of a quinone. Vice versa, $Pd-OCH_3{}^+$ generated in the protonolysis step may undergo $\beta-H$ elimination with formation of $Pd-H^+$, as it occurs for the hydroacylation of ethene to DEK [33]. Direct shift from the hydride mechanism to the carbomethoxy mechanism has been demonstrated by Iggo et al. [58] (Sect. 3.3.2).

2.4
Kinetic Studies

Of the reports that have appeared [37, 72, 80–90], only a few deal with more quantitative studies. In [86, 89] the copolymerisation kinetics have been studied using the precursor [Pd(TsO)(H_2O)(dppp)](TsO) in MeOH over a temperature range of 70–90 °C and total pressure up to 70 bar. The rate increases linearly by increasing catalyst loading, the orders with respect to dissolved CO and ethene are 0.63 and 0.72, respectively; the apparent activation energy is 11.7 kcal/mol.

Table 1 reports different rate equations fitting the data, as functions of the activities of the monomers because their behaviour significantly differs from ideality. They are based on one- or two-"vacant" sites models (Fig. 4). In the one-site model the palladium centre is coordinated by the bidentate ligand, the growing chain, and has the fourth coordination site occupied by one of the monomers (like species **b**, **d** or **f** of Fig. 1). It can be also four-coordinated β- or γ-chelate like **1** or **2**, having the fifth site available for the coordination of the monomers, like species **a**, **c** or **g**. In the two-sites model palladium is coordinated by the bidentate ligand, the growing chain, and has the fourth and fifth sites available for coordination of the monomers, like species **e**. MeOH or the counter-anion can occupy the "vacant" site also, but this has not been taken into account, because their concentration has been considered constant. It is interesting to note that the rate equations are of the type that can be derived from the Hougen-Watson model for solid catalysts. Indeed the copolymerisation process occurs with the palladium centre attached to the polymer, which becomes insoluble after the chain has grown of ca. 13–25 (CH_2CH_2CO) units [37].

The one-site model fits the rate data better than the other.

In the work of Belov et al. the kinetic model that has been developed quantitatively describes the initial rate of copolymerisation, the kinetic curves of the consumption of the two monomers and the molecular weight characteristics of the resulting copolymers and their composition as mixture of ketoesters, diesters, diketones as function of the total pressure up to 40 bar,

Table 1 Proposed rate equations and mechanism

	Kinetic equations	Proposed mechanism
I	$r_{\text{pol}} = \frac{k_r K_{\text{CO}} K_{\text{et}} AB}{\left(1+K_{\text{CO}}A\right)\left(1+K_{\text{et}}B\right)}$	The two sites on Pd atom are non-equivalent; one can coordinate to only CO and the other to only ethene. The rate-determining step is the insertion of one monomer from an intermediate having both monomers simultaneously coordinated
II	$r_{\text{pol}} = \frac{k_r K_{\text{CO}} K'_{\text{et}} A\, B}{\left(1+K_{\text{CO}}A+K_{\text{et}}B\right)^2}$	The two sites on Pd atoms are equivalent and can be occupied by any of the monomers. The rate-limiting step is the insertion of one monomer from an intermediate in which both sites are occupied
III	$r_{\text{pol}} = \frac{k_r K_{\text{CO}} K'_{\text{et}} AB}{\left(1+K_{\text{CO}}A+K_{\text{et}}B\right)\left(1+K'_{\text{CO}}A+K'_{\text{et}}B\right)}$	The two sites on Pd atom are non-equivalent but can be occupied by any of the monomers. The rate-determining step is again the insertion of one monomer from an intermediate in which both sites are occupied by monomers
IV	$r_{\text{pol}} = \frac{k_2 k_4 K_1 AB[Pd]}{k_4+k_4 k_1 A+k_2 k_1 B}$	CO rapidly occupies the free sites on the Pd atom, and the rate-limiting step is reaction 2. Reactions 3 and 5 are very fast, making steps 2 and 4 practically irreversible
V	$r_{\text{pol}} = \frac{K_3 K_4 K_6 AB[Pd]}{K_4 A+K_4 K_6 AB+K_3 K_6 B}$	Intermediate **1** coordinates CO only, intermediate **2** can coordinate CO or ethene. The rate-determining step is reaction 3
VI	$r_{\text{pol}} = \frac{k_5 k_6 k_4 AB[Pd]}{k_6 B+k_6 k_4 AB+k_5 k_4 A}$	As in equation V, but here, the rate-determining step is reaction 5
VII	$r_{\text{pol}} = \frac{k_3 k_4 k_6 AB[Pd]}{k_4 A+k_4 k_6 AB+k_3 k_6 B+k_4 k_1 A^2}$	As in equation V, but here, CO can occupy both sites
VIII	$r_{\text{pol}} = K_{\text{obs}} A^{\alpha} B^{\beta}$	Empirical power law model

A = liquid phase activity of CO, kmol/m^3
B = liquid phase activity of ethane, kmol/m^3
k_r = reaction rate constants used in kinetic equations, kmol/(m^{3}s)
K_{CO} = equilibrium constant for CO coordination on Pd atom, m^3/kmol
K_{et} = equilibrium constant for ethene coordination on Pd atom, m^3/kmol
K_i = equilibrium constant for the ith reaction
k_i = pseudorate constant for the ith reaction
[Pd] = catalyst concentration, kmol/m^3

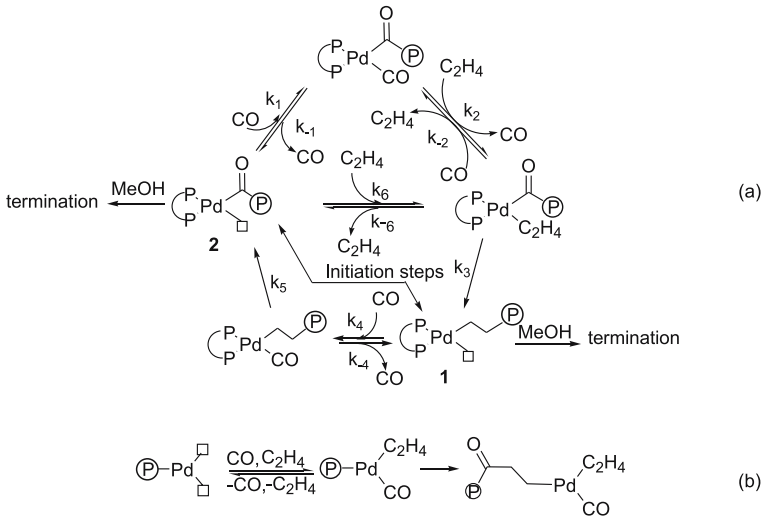

Fig. 4 One-site model (**a**), two-sites model (**b**)

CO/ethene = 1/1, using the catalyst system $Pd(AcO)_2$/dppp/TFA in the ratio 1/1/2 at 90 °C [90].

3
Control of Chain Growth

3.1
General Aspects

The products of the carbonylation of ethene in MeOH range from high molecular weight polyketones, to cooligomers down to low molecular weight oxygenates like dimethyl succinate, diethyl ketone and MP, which can be considered the lowest member of the copolymerisation process. Their abundance in the product mixture depends on the relative rate of the process of chain growing and of chain termination. For any given catalytic system, these are influenced mainly by temperature, pressure, monomers ratio, solvent; the molecular weight of the polyketone depends also on the batch time (Sect. 3.3.1).

The overall energy barrier for chain growing is lower than that for chain termination, thus, if a lower molecular weight product is desired, the copolymerisation should be carried out at higher temperature. In the copolymerisation process, the insertion of ethene is the slow step [13–15], thus upon increasing the pressure of the olefin, as well as the total pressure, it is reasonable to expect an increase in the molecular weight. The nature of the

solvent also influences the chain growing process. An alcohol is a chain transfer agent, the lower the steric bulk or the nucleophilicity of the alcohol, the faster the chain termination. Thus in *t*-BuOH or in CF_3CH_2OH a copolymer of higher molecular weight can be obtained than when using MeOH. Also the use of an aprotic solvent may be a better choice when a product of higher molecular weight is desired [1, 11, 55, 56].

The $Pd-PPh_3$ system is particularly instructive. In $CHCl_3$ the catalyst prepared in situ from $[Pd(CH_3CN)_4](BF_4)_2$ and PPh_3 gives a high molecular weight polyketone. It was proposed that catalysis starts from a $Pd-H^+$ species formed from adventitious H_2O and CO. The high molecular weight did not allow the identification of the end groups [11]. Under similar conditions, (rt, 45 bar, CO/ethene = 1/1), but using the complex *cis*-$[Pd(H_2O)_2(PPh_3)_2](TsO)_2 2H_2O$, a copolymer having average $n = 27$ with only keto end groups forms together with concomitant evolution of CO_2 [59]. These findings support the suggestion that catalysis initiates via a $Pd-H^+$ species; termination occurs via protonolysis by H_2O, with formation of a $Pd-OH^+$ species which re-enters the catalytic cycle by insertion of CO followed by CO_2 evolution (see Sect. 2.3.1 and Eqs. 6 and 7). The use of the aquo complex introduces enough water to lower significantly the molecular weight. The same system in MeOH, at 70 °C, 70 bar, CO/ethene = 1/1, yields low molecular weight products according to Eq. 1, with $n = 1–5$, together with a minor amount of higher polyketo esters with $n > 6$. In *t*-BuOH only polyketo esters with $n > 5$ are obtained. By lowering the pressure, chain propagation is slower and the only product is the propanoate ester. At higher temperature (100–110 °C) the "cationic" complex $[Pd(TsO)_2(PPh_3)_2]$, in the presence of PPh_3 and TsOH (Pd/P/TsOH = 1/6/8), is an efficient catalyst for the production of MP in MeOH [35, 91]. The chloride analogue is expected to give also MP, because the coordinating anion competes for chain propagation. Rather surprisingly, we have found that under similar conditions the main product is a polyketone. Only at a higher temperature and in the presence of relatively large amounts of PPh_3 (115 °C, Pd/P/HCl = 1/30/20), the main product is MP [14].

It is noteworthy to report also the results obtained using the $Pd(AcO)_2$ precursor in combination with an excess of PPh_3 or with the monosulfonated derivative PPh_2PhSO_3H, in acetic acid and in the presence of TsOH (Pd/P/TsOH = 1/8/80–800, 90 °C, 1–50 bar). The reaction switches from monocarbonylation with formation of propionic acid to oligocarbonylation products and to polyketones as the pressure and concentration of TsOH increase. The yield in polyketones also increases upon increasing the acidity [82, 87]. A similar acid effect has been found with the dtbpe-based catalyst in MeOH for the production of DEK in the presence of excess acid, as the selectivity lowers from 99% DEK to ca. 33%, ca. 60% being cooligomers (see Sect. 3.2 and Sect. 4.2).

The effect of the anion and of the ligand deserves a separate consideration.

3.2 Influence of the Counter-Anion

As already mentioned the anion has to be weakly coordinating in order to favour the coordination of the monomers and chain growing. The coordinating capacity depends not only on the nature of the anion, but also on that of the solvent. Polar solvents help the dissociation of the anion from the cationic active catalyst, thus favouring the polymerisation process. This is well illustrated by comparing the activity of the catalysts $[PdX_2(dppp)]$ (X = TfO, TsO, TFA^-, AcO, Cl). In MeOH the activity is comparable when X is weakly coordinating like TfO, TsO, TFA^- (ca. 7000–6000 g polymer(g Pd·h)$^{-1}$ at 90°, 45 bar, CO/ethene = 1/1). When X = AcO or Cl the catalyst is ineffective [14], but becomes very active when used in H_2O – AcOH, ca. 40–50% molar ratio (27 000 g polymer(g Pd·h)$^{-1}$, under the conditions just reported), in spite of the lower solubility of the monomers in this medium [92, 93]. In H_2O – AcOH the copolymerisation process occurs with concomitant evolution of CO_2 and the polyketone presents keto end groups only, suggesting that Pd – H^+ initiates the catalysis and that termination occurs via protonolysis by H_2O or H_3O^+ with formation of Pd – OH^+ or Pd – OH_2^{2+}, which regenerate the starting Pd – H^+ species upon interaction with CO followed by evolution of CO_2 (see Eqs. 6 and 7). Thus in H_2O – AcOH the AcO^- or Cl^- do not prevent coordination of the monomers and chain growing, probably because they are dissociated from the metal centre. The high activity may be due to the possibility that the acid and H_2O prevent deprotonation/dimerisation of the active hydride with formation of dimeric species of the type shown in Figs. 2 and 3, thus ensuring a relatively high concentration of the most active species. Moreover, the acid might destabilize the β- or γ-chelates through protonation of the oxygen atom of the coordinating keto group, thus favouring the insertions of the monomers.

It has also been reported that the precursor $Pd(AcO)_2$/dppp in combination with HCOOH, though having relatively high p*K*a = 3.75, becomes an efficient catalytic system provided the acid is used in relatively large excess (ca. 7500 g polymer/g Pd/h, HCOOH/Pd = 3000/1, under the conditions reported above) [48].

The activity of water-soluble catalysts based on the hydrophilic bidentate phosphines is also significantly influenced by the nature of the anion [94–100]. Thus for example, using the catalyst formed in situ from $[Pd(TsO)_2(NCMe)_2]$ and the *metha*-sulphonated analogue of dppp under conditions close to the ones reported above, but in water as solvent and with an excess of acid (acid/Pd = 500/1), the productivity is ca. 3900, 3600 or 2250 g polymer(g Pd·h)$^{-1}$, when the acid is TsOH, TFA or AcOH, respectively, under usual conditions [96]. If one considers that the monomers are a little soluble in H_2O, very high productivity and molecular weight are obtained using $[Pd(CH_3)(NCCH_3)$(dapp-s)](OTf) (dapp-s =

metha-sulphonated analogue of dapp): 32.2 kg · (gPd · h)$^{-1}$, molecular weight 125 kg/mol, at 90 °C, 60 bar, $C_2H_4/CO = 1/1$ at very low catalyst concentration, [Pd] ca. 10^{-5} mol/l [99].

For catalysts which promote the formation of low molecular weight products, the anion might make the difference, as in the case of the catalyst with C_2-bridged diphosphine ligand **23** (Fig. 5), which gives a low molecular weight polymer or MP when the counter-anion is MsO^- or propanoate, respectively [101].

However, there is a limit to operating conditions such as temperature, pressure and also the choice of solvent is rather restricted, particularly for commercial exploitations, and also batch time cannot be more that 6–8 hours, because generally the productivity lowers with time, and also the choice of the anion is not limitless. It is the ligand that can make the difference.

3.3 Influence of the Ligand

3.3.1 High Molecular Weight Polyketones

The influence of the nature of the ligand on the catalytic activity was first studied by Drent et al. using $Ph_2P(CH_2)_nPPh_2$ ligands ($n = 1 - 6$) [15]. The highest productivity, molecular weight and selectivity is obtained when $n = 3$; when $n = 4$ the catalyst is moderately active; when $n = 2$ the productivity is around one order of magnitude lower; when $n = 1$ the catalyst is ineffective. Considering the requirement of *cis*-coordination for fast chain growing in both ground and transition states, it was suggested that the activation energy is lower when the bite angle is close to 90°, which is better satisfied when $n = 3$ [15]. The *ortho*-methoxy substituted analogue with $n = 3$, dapp, used in the commercial production of the CO/ethene/propene terpolymer, gives a particularly high performance for both productivity and molecular weight (see below).

Noteworthy is the activity of the catalyst with the zwitter-ionic ligand **4**, in which the P atoms are also separated by 3 atoms [102].

Even though these results might be rationalised in terms of bite angle effects [103], further studies evidenced that other factors have to be considered, like steric hindrance induced by stereochemical rigidity of the ligand [55, 56, 60, 76, 77, 104]. Ligands **2**, **3**, **5–7**, shown in Fig. 5, which have methyl substituents at the chain backbone, give catalysts that are more active than the unsubstituted ones, particularly that with methyl groups at 1- and 3-carbon atoms of the bridging chain in *meso*-position in ligand **2**. It was suggested, also on the basis conformational consideration and of kinetic and thermodynamic studies, that a higher rigidity of the ligand backbone in the *meso*-ligand forces the phenyl substituents on the phosphorous atom to adapt

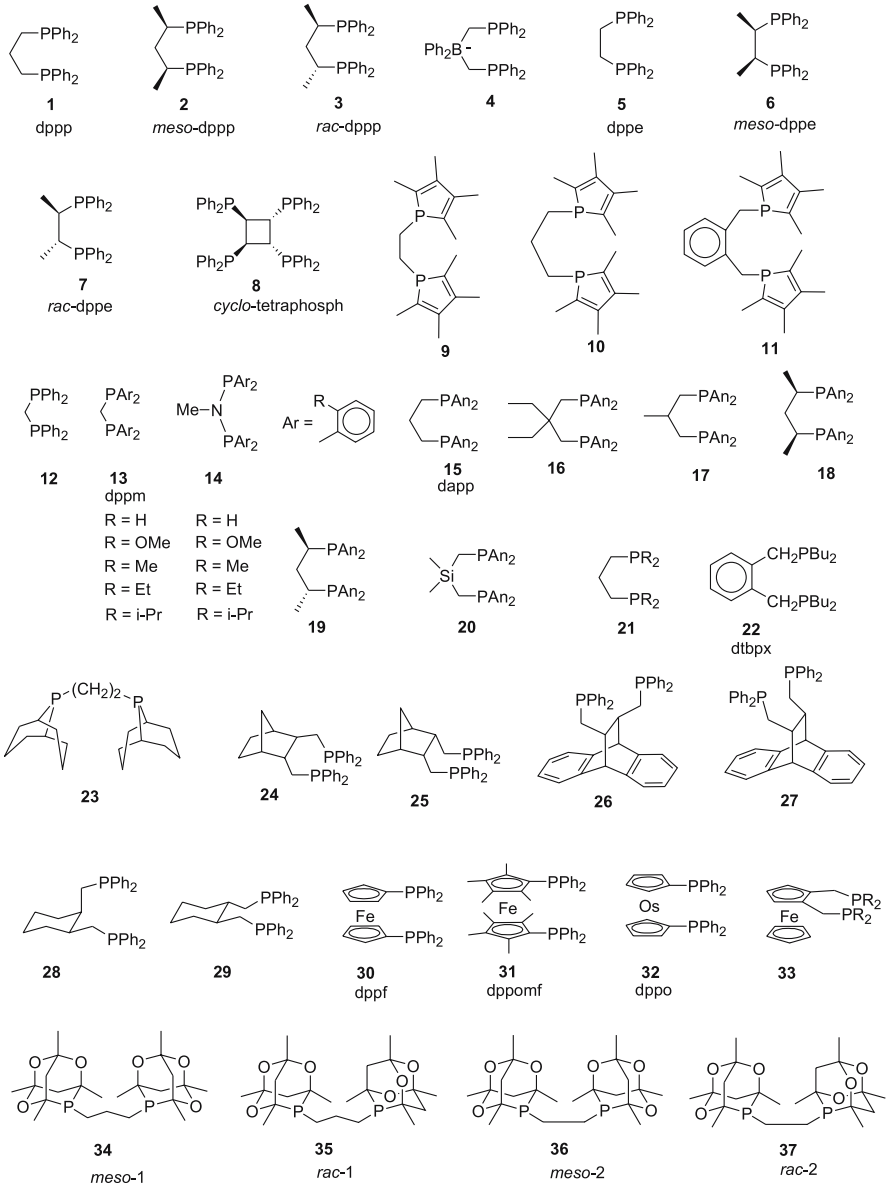

Fig. 5 Ligands in the text (An = Anisyl)

a conformation of higher steric hindrance which causes a higher destabilization of the β-chelate ring thus favouring the propagation step [55, 56, 60, 76, 77]. The *meso*-effect related to steric rigidity is more general as it has been found also in the bridge substituted dapp ligand (see below). The same has

been found with the ligand "*cyclo*-tetraphos" **8**, which gives a catalyst more efficient than the one with dppe by one order of magnitude [60].

A correlation between catalytic activity and backbone rigidity has been also established for the diphosphine ligands **9**–**11**. The rigid ligand **9** gives a more active catalyst than ligand **10**; ligand **11** gives poor results [104].

That steric bulk plays a role of paramount importance is suggested by the fact that the ineffective dppm-based catalyst becomes highly active in CH_2Cl_2 when the phenyl rings are *ortho*-substituted with bulky alkyl groups (ligands **13**). Polymerisation rate, catalyst stability and polymer molecular weight all increase with increasing steric bulk of the aryl *ortho* substituent [105, 106]. The catalyst can be prepared in situ from $Pd(AcO)_2$ and the ligand by activation through the borane method with $B(C_6F_5)_3$ which forms a $Pd-C_6H_5^+$ species that initiates the catalysis [107], which is bulkier than $Pd-COCH_3^+$ and $Pd-H^+$, which usually initiate the catalysis. Rather than acting as a *cis*-coordinating bidentate, the dppm ligand (**12**) prefers bridging two palladium atoms with mutually *trans* P atoms on each metal [108], which may explain the poor performance for the production of polyketones. Bulky *ortho*-substituted ligand **13** may inhibit dimerisation giving rise to a catalyst in which the ligand acts preferentially as a *cis*-coordinating bidentate on one metal centre. Another possible explanation is that dppm, when acting as a *cis*-coordinating bidentate ligand, leaves too much extra space at the "vacant" site on the metal centre, so that the insertion of the monomers into the species that initiate the catalysis and the subsequent insertions of the chain growing process are not favoured. Upon increasing the steric bulk of the ligand the monomers are "pushed" to give insertions in such a way that fast chain growing can occur. It is note worthy to observe that in MeOH, under the usual conditions, the catalyst is poorly active.

Steric bulk has a similar effect also for the methylamino-bridged diphosphines ligands **14** in CH_2Cl_2, which give catalysts even of superior performances [105, 109, 110], again with poor activity in MeOH.

Recently, some important aspects on the development of more efficient catalysts have been disclosed [37]. These studies are hereafter summarized, taking as a base of comparison the dppp-based catalyst.

Electron-donating substituents at the phenyl ring enhance the activity, whereas there is no clear correlation for the molecular weight, which in any case is affected. The productivity and the molecular weight are the highest with the *o*-MeO-substituent (at 90 °C, 50 bar CO/C_2H_4 = 1/1, dapp **15**: 12.7 $kg \cdot (gPd \cdot h)^{-1}$, LVN = 1.58 dL/g; dppp **1**: 7.1 $kg \cdot (gPd \cdot h)^{-1}$, LVN = 1.05 dL/g).

Even though the distinction between the electronic and the steric effects cannot be made so sharp, the close performance with *o*- and *p*-MeO-substituent suggests that the main effect is of electronic nature. However, X-ray structure shows that the oxygen atom of the *o*-MeO groups interact with palladium. In addition, NMR studies reveal an electrostatic interaction

of the *o*-aryl protons with the filled dz^2-orbital of the metal. It has been suggested that the higher productivity might be due to the lowering of the intramolecular interaction of the β-chelate moiety with palladium.

Variation of the length of the bridging chain $-(CH_2)_n-$ shows that both the productivity and molecular weight decrease in the order $n = 3 > n = 2 > n = 1$, as found for the unsubstituted analogues.

Alkyl substitution in the bridging chain enhances the catalytic activity. The highest productivity is obtained with two ethyl-substituents at the central carbon atom, though the molecular weight is higher with the unsubstituted dapp ligand (at 90 °C, 50 bar, $CO/C_2H_4 = 1/1$, ligand **16**: 42.7 kg · (gPd · h)$^{-1}$, LVN ca. 1.20 dL/g, compared to 12.7 kg · (gPd · h)$^{-1}$, LVN = 1.58 dL/g for ligand **15**). A similar effect of substitution is observed with dppp, though the increase of productivity is smaller (at 90 °C, 50 bar, $CO/C_2H_4 = 1/1$, ca. 12.4 kg · (gPd · h)$^{-1}$, LVN = 0.72 dL/g for *meso*-dppp (ligand **2**) compared to 7.1 kg · (gPd · h)$^{-1}$, LVN = 0.72 dL/g for **1**).

In addition, the catalyst undergoes a sharp lowering in activity during the first minutes (from about 25 to a constant rate of 8–10 kg · (gPd · h)$^{-1}$). The deactivation is not due to the formation of less active dimeric species of the type $[(dapp)Pd(\mu\text{-}H)(\mu\text{-}CO)Pd(dapp)]^+$, $[(dapp)Pd(\mu\text{-}CO)_2Pd(dapp)]^{2+}$, $[Pd(dapp)]_2^{2+}$ or $[(dapp)Pd(\mu\text{-}OH)_2Pd(dapp)]^{2+}$, nor to the formation of bis-chelate $[Pd(dapp)_2]^{2+}$, as it occurs for the dppp system [17]. Initially the growing chain is soluble in MeOH, so that the attached catalyst works in "homogeneous phase", whereas, as the chains grow to 13–25 (CH_2CH_2CO) units, the catalyst precipitates. Moreover, the polymer presents a bimodal molecular weight distribution, one of Flory–Schultz (FS) type, typical for a homogeneous polymerisation, and a Wesslau (W) type distribution, typical for a heterogeneous polymerisation. In addition, it was found that the molecular weight and particle size increase with time and that larger particles contain a larger fraction of chain with W distribution. It was suggested that the heterogeneous catalyst is present in two different environments, in part absorbed on the surface of the particles, producing the copolymer with FS distribution, and in part inside the micropores of the particles, producing the copolymer with W distribution [37].

The kinetics were also studied. The productivity increases regularly with the pressure of C_2H_4, whereas it passes through a maximum at p_{CO} = ca. 15 bar. This trend suggests that CO and C_2H_4 compete for coordination to palladium and that CO impedes coordination of C_2H_4 [37].

3.3.2 From Cooligomers to Low Molecular Weight Products

The general rule earlier proposed by Drent et al., that Pd(II)-diphoshine complexes, better with a bite angle near 90°, capable of maintaining *cis*-coordination throughout the copolymerisation process, give high molecular

weight polyketones with high productivity, whereas monophosphine ligands are more suitable to give MP [14–16], has been found, by the same proposers, to have important exceptions. For ligands **21** of the type $RR'P(CH_2)_3PRR'$ (R,R' = *n*-Bu, *n*-Bu or *n*-Bu, cyclohexyl or cyclohexyl, cyclohexyl or *t*-Bu, *t*-Bu) in which the alkylsubstituents differ only slightly in electron-donating properties, but differ significantly for the steric bulk: R,R' = *n*-Bu, *n*-Bu < *n*-Bu, cyclohexyl < cyclohexyl, cyclohexyl < *t*-Bu, *t*-Bu, it was found that productivity and molecular weight decrease when steric bulk increases to the point that with the last ligand the main product is MP (97.4% selectivity, TOF = 25 000 h^{-1} at 120 °C, 40 bar, CO/ethene = 2/1) [30, 33]. An even higher performance was obtained by Tooze et al. with ligand **22** dtbpx (99.98% selectivity, TOF = 50 000 h^{-1} under milder conditions, 80 °C, 10 bar, CO/ethene = 1/1, see Sect. 4.1.2) [31, 111]. At first, it was suggested that this diphosphine does not maintain *cis*-chelation, but opens one coordination arm thus acting as a monophosphine [111].

The same was previously suggested also by Doherty et al., which found that the Pd(II)-diphosphine of type **24** [112] and type **26** [113] produce low molecular weight oligomers of average length 13–20 monomer units and MP and that intermediate products having a low number of monomer units were not present. It was proposed that two different catalytic species are operating, one having the expected identity coordination producing the oligomers, the other with one arm of the diphosphine dissociated and effectively acting as a monodentate ligand producing MP. The catalyst with ligand **28** gives only oligomers. The bite angles of ligands **24** and **28** are similar (102°), however, close examination of the structures of the palladium complexes shows that the ligand backbones are oriented in different ways and that the phenyl rings in **24** provide a higher steric bulk [112]. This may be a key factor in determining the chemoselectivity.

As a matter of fact, it was proven, by variable temperature multinuclear NMR studies, that in the dtbpx-based catalyst, which is the most efficient in producing MP, the ligand maintains *cis*-coordination in all the identified intermediates well above room temperature [42, 114, 115] (see below).

In general, catalysts that promote the cooligomerisation to low molecular weight products promote also the formation of MP. However, apparently slight changes in the bridging chain or in the substituents the P atoms may cause quite different chemoselectivity, as already reported above. Another interesting case is that of dppf- and dppomf-based systems (ligands **30** and **31**) [47, 116]. The first presents a *cis*-κ^2-P,P coordination mode and promotes the formation of several low molecular weight products, from MP to alternating cooligomers, the other exclusively MP. The methyl substituents in dppomf induce significant changes in the coordination mode which changes to κ^3-P,P, Fe and in the secondary structure of the complexes (P – Pd – P bond angles (96° in $[Pd(H_2O)_2(dpff)]^{2+}$, 102° in the other), dihedral angles between the (P, Fe, P) and (P, Pd, P) planes, deviations of the phosphorous atoms from

the planes of the Cp rings). The selective production of MP might be due to the higher steric hindrance of dppomf and consequent greater propensity of dppomf versus dppf to give a Fe – Pd bond, thus forcing the P atoms to adopt a *trans* geometry, and yielding Pd-acyl species that do not react with ethene in MeOH to form β-chelates, which could continue the cooligomerisation process [47].

Quite interestingly the osmocene analogue of dppf (ligand **32**) catalyses the methoxycarbonylation of ethene selectively (TOF = 400 h^{-1} at 85 °C, 45 bar, CO/ethene = 1/1, Pd/TsOH = 1/40). Multinuclear NMR spectroscopy of complexes [PdX(dppo)](TsO) (X = TsO, Me, COMe) is consistent with the presence of Os – Pd bonds, which has been confirmed by NMR and X-ray studies on $[Pd(CH_3CN)(dppo)](TsO)_2$. The coordination geometry around palladium is that of a slightly distorted square planar with *trans* P atoms, a P – Pd – P angle of 164.9(1)° and a strong bonding Os – Pd interaction distance (2.840(1) A°) [79].

If the ligands dppomf and dppo maintain *trans*-coordination throughout the catalytic cycle, it will be interesting to establish how the insertions of CO and ethene and methanolysis to MP occur.

An example of how selectivity can subtly depend on the different steric bulk introduced upon varying the length of the backbone, or even when using different diastereoisomers, is the one found for the methoxycarbonylation of ethene or of higher olefins catalysed by in situ generated Pd(II) complexes of *meso/rac* adamantyl diphosphines (ligands **34–37**). Normally C_3-bridged diphosphines-based catalysts promote the copolymerisation, but the catalyst derived from C_3-bridged *meso/rac*-**1**, because of the steric hindrance adamantly moiety, catalyses the methoxycarbonylation of ethene (TOF = 10^4 h^{-1}, selectivity > 99% at 90 °C, ethene = 20 bar, CO = 30 bar, $Pd(AcO)_2$/P – P/TfOH = 1/1.5/2.5), whereas the C_2-bridged *meso/rac*-**2**-based system, inducing less steric hindrance, promotes the formation of polyketones of relatively low molecular weight [32, 117].

Liu et al. delineated the initiation, propagation and termination steps of the carbomethoxy of the hydride cycles for the catalyst $[Pd(CH_3CN)_2(dibpp)](TfO)_2$, which promotes both the formation of cooligomers and MP [58]. To generate a $Pd - OCH_3^+$ species of the carbomethoxy cycle, a base was added, but normally catalytic carbonylation is carried out in the presence of an excess of acid. However, protonolysis, by MeOH in the presence of CO, of a Pd-alkyl intermediate of the hydride cycle, provided an entry to the carbomethoxy cycle (through the shift from the hydride cycle to the carbomethoxy one), without the necessity of using a base. The methyl complex **1′** was used to start the hydride cycle, because the hydride could not be prepared separately [58]. All the species indicated were detected, including β- and γ-chelates. The cycles are closely related to the one shown to occur in the solid state [51].

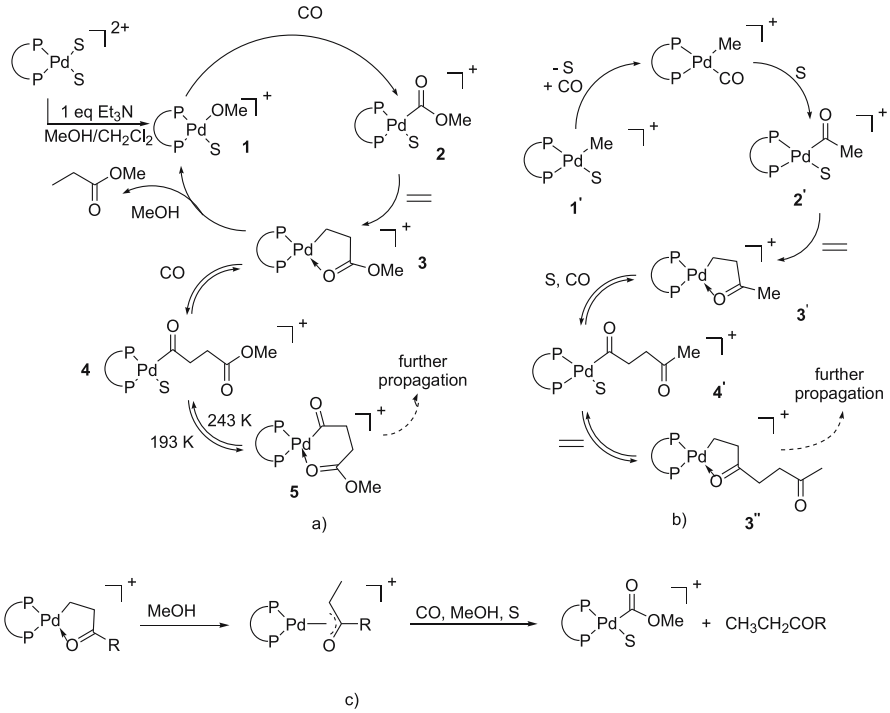

Fig. 6 The carbomethoxy cycle (**a**), the hydride cycle (**b**) and the shift of the hydride mechanism to the other (**c**) ($S = CH_3CN$). Adapted from [58]

It is interesting to point out that with this catalyst formation of MP occurs also through the carbomethoxy cycle, whereas it will be shown that most catalysts that are highly selective to MP operate through the hydride mechanism (see Fig. 6).

4
Selective Synthesis of Monocarbonylated Products

4.1
Synthesis of Methyl Propanoate

From what is reported above, it is evident that the CO-ethene copolymerisation and the methoxycarbonylation of ethene are closely related. In principle the mechanisms discussed for the copolymerisation process are valid also for the case when termination occurs after the insertion of just one molecule of each monomer into the species that initiate the catalysis, $Pd-OCH_3^+$ or $Pd-H^+$. These species can form as schematized by Eqs. 10–16. The copoly-

merisation occurs via both the so-called hydride and carbomethoxy mechanisms, as unambiguously proven by the end group analysis when both are ester end groups or keto end groups.

In the alkoxycarbonylation, the hydride mechanism initiates through the olefin insertion into a Pd – H bond, followed by the insertion of CO into the resulting Pd-alkyl bond with formation of an acyl intermediate, which undergoes nucleophilic attack of the alkanol to give the ester and the $Pd - H^+$ species, which initiates the next catalytic cycle [35, 40, 57, 118]. Alternatively, it has been proposed that a ketene intermediate forms from the acyl complex via β-hydride elimination, followed by rapid addition of the alcohol [119]. In principle the alkyl intermediate may form also by protonation of the olefin coordinated to a Pd(0) complex [120, 121].

In the other mechanism, the catalytic cycle initiates through the insertion of CO into a Pd-alkoxy bond, with formation of a Pd-carboalkoxy intermediate, which inserts the olefin with formation of an alkylcarboalkoxy β-chelate, which undergoes protonolysis by the alkanol through the intermediacy of its enolate isomer (see Sect. 2.3.1), yielding the ester and the Pd-alkoxy species, which then initiates a new catalytic cycle [122–125].

4.1.1 Monophosphine Catalysts

The hydride mechanism is the most likely to be operative. In favour of this mechanism there is the fact that after running the alkoxycarbonylation of an olefin catalysed by the precursor *trans*-$[PdCl_2(PPh_3)_2]$, the acyl complex *trans*-$[Pd(COR)Cl(PPh_3)_2]$ is isolated [126, 127]. The acyl complex reacts with an alcohol to give the expected ester in an almost stoichiometric amount and catalyses the alkoxycarbonylation of a different olefin to give the expected ester and a stoichiometric amount of the ester derived from the acyl ligand. This proves that the acyl complex is sufficiently stable to be isolated while being reactive enough to enter the catalytic cycle. Together with the acyl complex, a carboalkoxy complex also forms. However, the latter complex fails to give an ester in reaction with an olefin in the alkanol.

Moreover, catalysis is enhanced when carried out in the presence of HCl, which does not favour the formation of the carboalkoxy complex because of Eq. 22. In addition, no catalysis is observed when carried out in the presence of a base such as NEt_3, which favours the formation of the carboalkoxy complex; in this case there is formation of inactive Pd(0) complexes [127].

$$Pd^{2+} + ROH + CO \rightleftharpoons Pd\text{-}COOR^+ + H^+ \qquad (22)$$

In a subsequent study, it was found that a hydride source like H_2O, an acid (TsOH) or molecular hydrogen have an enhancing effect on the catalytic activity of the "cationic" precursor $[Pd(TsO)_2(PPh_3)_2]$. Water, in combination with CO, generates the hydride [91] and reforms it if $Pd - H^+$ consuming side

reactions occur during the course of catalysis (see below). The acid can re-oxidise the inactive Pd(0), which otherwise inevitably forms; palladium can activate molecular hydrogen via heterolytic splitting [33, 72]. Moreover, in the presence of hydrogen, there is concomitant formation of ethane, which can form only via a $Pd-H^+$ species. It was also found that catalysis is inhibited when carried out in the presence of BQ, which transforms a hydride species into a $Pd-OCH_3^+$ species (Eq. 8) and that decomposition to Pd(0) complexes and even to palladium metal occur in the presence of a base such as NEt_3 [91].

Using the "cationic" precursor just reported, the carbomethoxy and the acyl complexes *trans*-$[Pd(COEt)(TsO)(PPh_3)_2]$ and *trans*-$[Pd(COOMe)(H_2O)(PPh_3)_2](TsO)$ have been also isolated after methoxycarbonylation experiments [128, 129]. Similarly to what has been suggested for the corresponding neutral chlorides, only the acyl complex is the one most likely directly involved in the catalytic cycle. It reacts with MeOH giving MP in an almost stoichiometric amount and it catalyses the alkoxycarbonylation of a different olefin with almost quantitative formation of MP. In contrast, the carbomethoxy complex dissolved in MeOH, saturated with C_2H_4, at rt, does not yield the ester, even in the presence of TsOH, which has a promoting effect when the acyl complex is used as a catalyst. Catalysis occurs only upon heating at the usual temperature in order to observe significant catalytic activity (70–80 °C), in which case there is evolution of CO_2 in an amount equivalent to the carbomethoxy complex. After catalysis, in place of the starting complex, the acyl complex is recovered. It has been proposed that H_2O displaces MeOH from the carbomethoxy complex, with formation of a $Pd-COOH^+$ species, which upon evolution of CO_2 gives the hydride that starts the catalytic cycle which undergoes through an acyl type intermediate. This might explain the promoting effect of H_2O, which would bring the less active $Pd-COOMe^+$ species, which might form during the catalysis, back to the catalytic cycle (see Fig. 7).

In addition, it has been observed that, even when starting from the acyl complex, CO_2 forms during the catalysis. In principle, this should not occur because at any catalytic cycle, the regenerated hydride should continue the catalysis. Thus some $Pd-H^+$ consuming side reactions occur before the hydride is trapped by C_2H_4. As a matter of fact, when the acyl complex is used as precursor in the presence of an excess of acid, it is recovered as $[Pd(TsO)_2(PPh_3)]$. This is brought back to the catalytic cycle through a reaction related to the WGSR. This is another way through which H_2O might contribute to enhance the catalytic activity. The acid partially consumes the phosphine (see below), but it may prevent the formation of $[Pd(\mu\text{-}OH)(PPh_3)_4]^{2+}$ or may stabilize the hydride preventing its deprotonation to $[(PPh_3)_2Pd(\mu-H)(\mu-CO)Pd(PPh_3)_2]^+$ [130] or to inactive Pd(0) complexes, and, when these form, they can be reactivated by the acid. In addition the acid, through protonation at the O atom of the acetyl ligand, may enhance its electrophilicity and hence the methanolysis step [57].

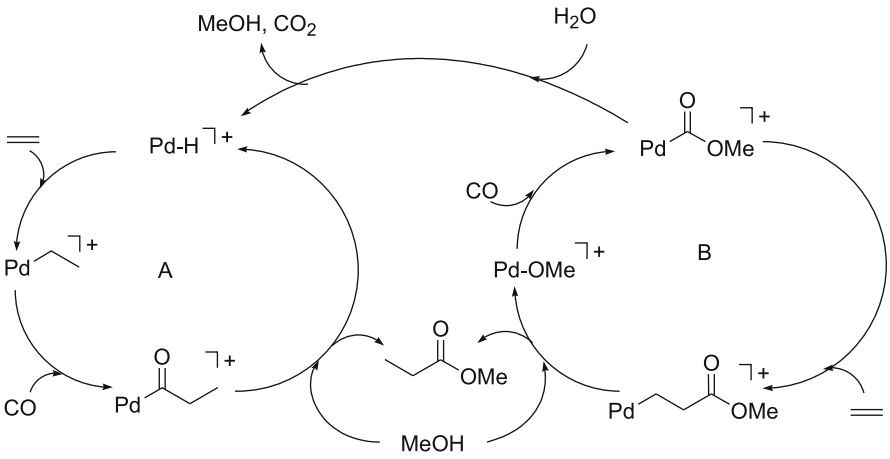

Fig. 7 The hydride (**A**) and the carbomethoxy (**B**) cycles, with shift from the latter to the first through the action of H_2O

The isolation of acyl and carboalkoxy complexes proves that the insertion of CO into both a Pd-alkyl and into a Pd – OR species occurs easily. Quite interestingly, it has been found that CO inserts only into the Pd – OCH_3 bond of the complex [$Pd(CH_3)(OCH_3)(P-P)$] and that after insertion methyl acetate eliminates with the formation of [$Pd(CO)_2(P-P)$] [131].

Although the isolation and reactivity of acyl complexes strongly support the hydride mechanism, the other mechanism cannot be excluded. For example H_2O, the acid or molecular hydrogen, which can act as a hydride source, can promote the Pd – C splitting of the Pd-alkylcarboalkoxy intermediate in the alkoxy cycle as well. More convincing for the hydride route is the fact that the acid, which does not promote the formation of a Pd – OCH_3^+ species, has a promoting effect on the catalysis and can activate a Pd(0) complex, otherwise inactive, whilst a base, which not only promotes the formation of this species, but also deprotonates a Pd – H^+ species to Pd(0), suppresses the catalysis.

Phosphine degradation side reactions with formation of phosphonium cations such as $MePPh_3^+$, $EtPPh_3^+$ and $EtCOCH_2CH_2PPh_3^+$, isolated as TsO^- salts, provide further evidences for the hydride path. The last two have been shown to form by metal mediated pathways and are products of the hydride route. It has been proposed that the 3-oxopentyltriphenylphosphonium cation forms via interruption of the palladium catalysed chain growth of CO-ethene oligomers arising from further insertion of ethene into the Pd-acyl intermediate [132].

It is worthy to note that these monophophine systems must be used in the presence of a free ligand, with a Pd/P ratio even up to 1/20, because the

acid partially consumes the phosphine and drives its dissociation from Pd(II), eventually with the degradation to Pd metal.

4.1.2 Diphosphine Catalysts

As already mentioned, for a long time it was generally accepted that monophosphine catalysts were more suitable to promote the formation of MP selectively. Luckly, it has been found that some diphosphines give catalysts that are highly active and selective to MP. The case of dtbpx deserve further presentation, because it gives the most active, selective and stable catalyst reported up to now (Sect. 3.3.2) and because it has been studied more in detail.

Catalysis undergoes via the hydride pathway [111, 114, 115, ?, 115]. The active Pd(II)-hydride catalyst [PdH(MeOH)(dtbpx)](TfO) can be easily prepared by mixing [Pd(dtbpx)(dba)] with 2–5 equivalents of TfOH, in MeOH and in the presence of an oxidant, BQ or O_2. The formation of the hydride occurs through a multistep process. Protonation of the starting complex gives [Pd(dtbpx) (dbaH)](TfO), which is readily oxidised by BQ or O_2 to give [Pd(dtbpx)(η^2-TfO)](TfO), from which the coordinated anion is displaced by the solvent. In the last step hydride formation occurs via irreversible β-hydride elimination from coordinated MeOH (or another primary or secondary alcohol). The hydride can also be obtained by dissolving [Pd(dtbpx)$(TfO)_2$] in a primary or secondary alcohol.

The hydride is stable in MeOH, deprotonation does not occur, probably because the basicity of the ligand makes the palladium centre more nucleophilic, nor partial deprotonation to (μ-H) dimeric species occurs, probably because of the high steric bulk of the ligand. Though the hydride is very reactive, its formation is quantitative and selective, so that its concentration is the highest possible, which is ideal for catalysis. The Pd(II)/PPh_3/TsOH catalytic precursor in MeOH is only partially transformed into an active Pd(II)-hydride, as several other species are present in solution, such as [Pd(μ-OH)$(PPh_3)_2]_2^{2+}$ and [Pd_2(μ-H)(μ-CO)$(PPh_3)_4]^+$ [130].

The hydride reacts immediately with ethene to give the expected ethyl complex selectively and quantitatively, which again is ideal for the catalytic activity. The hydride is very unstable when CO is bubbled into MeOH solution, even at low temperature [115]; at room temperature it reacts immediately with ethene giving a cationic ethyl complex. In the presence of both CO and ethene, like under catalytic conditions, decomposition does not occur because the hydride reacts much faster with ethene than with CO. Once the ethyl intermediate is formed, fast insertion of CO occurs with formation of an acyl intermediate, which in turn reacts with MeOH yielding MP with quantitative regeneration of the starting hydride to continue the catalytic cycle [114, 115]. The formation of the ethyl and of the acyl intermediates involves facile equi-

libria shifted toward them, whereas the methanolysis of the acyl complex is irreversible and is probably the rate-determining step (see Fig. 8) [115].

A detailed VT multinuclear NMR study has allowed the solution structure and dynamic properties of all the intermediates to be established. The hydride $[PdH(MeOH)(dtbpx)]^+$ is static, the two P atoms remain coordinated and do not become equivalent through solvent exchange until well above room temperature. The ethyl complex presents a strong β-agostic C – H interaction, which is remarkably stable and it is not displaced even in strongly coordinating solvents such as EtCN. C_α and C_β of the ethyl group become equivalent via a stereospecific interchange involving $[PdH(\eta^2\text{-}C_2H_4)(dtbpx)]^+$ without making the two P atoms equivalent; at higher temperature (ca. 80 °C) the two P atoms become equivalent, maintaining *cis*-coordination, probably via a T-shaped intermediate [115].

The β-agostic ethyl complex is similar to a transition state intermediate in the step of the ethene insertion into the Pd – H bond. This might be also relevant to the high catalytic activity of this catalyst.

For the acyl complex [Pd (COEt)(dtbpx)(solvent)]$^+$ (solvent = THF, EtCN) there is no β-agostic C – H interaction and the two P atoms become equivalent even below room temperature via movement of the intact acyl group. The MeOH analogue is too unstable to be characterised, it gives MP and the starting hydride quantitatively. The product forming step is too fast to follow by NMR, even at low temperature, thus it is not possible under catalytic conditions (80 °C, 10 bar, $CO/C_2H_4 = 1/1$) to distinguish between alternative pathways such as whether it proceeds by reductive elimination from the $[Pd(dtbpx)(COEt)(MeOH)]^+$ complex to give MP and Pd(0) species with release of a proton, which subsequently adds to Pd(0) to give the starting

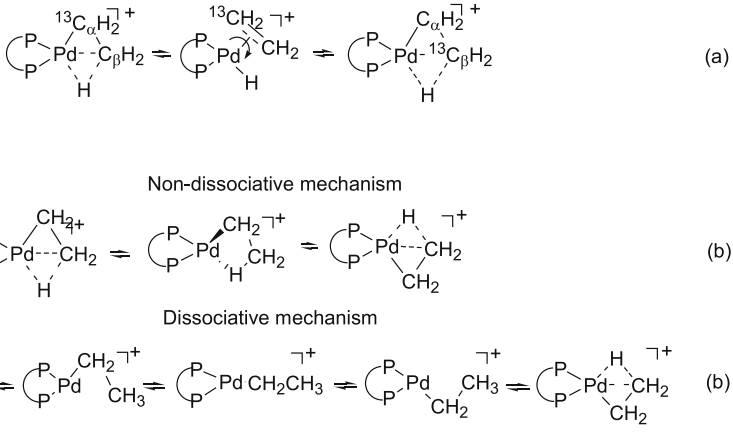

Fig. 8 Proposed mechanisms for scrambling the two carbons of the ethyl ligand (**a**); for making equivalent the two P atoms (**b**). Adapted from [115]

hydride, or whether reductive elimination and protonation proceed concertedly [115].

Another peculiarity of the acyl complex is that it prefers solvent coordination, even when the solvent has weakly coordinating ability such as THF, rather than CO coordination, even in the presence of free CO. This also can contribute to the high activity observed for these systems, as MeOH has not to compete with CO for coordination before the product-forming step. It is noteworthy that the carbonylation of the closely related complex $[Pd(Me)(Et_2O)(dippe)]^+$ in Et_2O or $[Pd(OTf)(CH_3)(dibpp)]$ results in the complex $[Pd(COMe)(CO)(dippe)]^+$ containing coordinated CO instead of solvent [133].

Further evidence for the hydride mechanism that exclude the other path have been provided by carrying out the catalysis in CH_3OD under conditions of chemical control of the rate of reaction or of CO g/l mass-transfer control [134]. In the first case a mixture of monodeuterated products $CH_2DCH_2CO_2Me$ and CH_3CHDCO_2Me in approximately 1/1 ratio formed, together with low levels of undeuterated MP and of $CH_2DCHDCO_2Me$, with no H incorporated into the CH_3OD. This can be explained if a hydride mechanism operates with rapid reversible migration of the hydride to coordinated ethene and coordination of CO occurring at a much higher rate than exchange of Pd – H with MeOD. It also suggests that coordination of ethene is essentially irreversible since otherwise significant amounts of undeuterated MP would be formed from loss of C_2H_3D from intermediate **1** in Fig. 9, followed by coordination–insertion of ethene into the Pd – H bond. Under conditions of CO starvation multiple labeled products would arise from Pd – H exchange with MeOD in intermediate **1**.

The formation of monodeuterated MP can be explained also by a carbomethoxy mechanism if, after migratory insertion of ethene into the Pd – COOMe bond, β-H abstraction occurs in intermediate **2** to give **3** (see Fig. 10). Deuteration of **2** and **4** by MeOD would then lead to the two products observed. Again, the termination, relative to Pd – H/CH_3OD exchange, has to be rapid, otherwise multiple deuterated products would form. Under conditions of CO starvation these products would arise from the reversible exchange between intermediates **2**, **3**, and **4**, through exchange of Pd – H with MeOD in **3**. However, this mechanism cannot explain the formation of large amounts of undeuterated MP, which form in the early stages of the reaction since the termination step must always transfer a D atom from the CH_3OD to end up on one of the ethyl carbon atoms of MP. It was concluded that the methoxycarbonylation of ethene occurs by a hydride mechanism in which the rate-determining step comes after the insertion of ethene into the Pd – H bond and that the carbomethoxy path is not operating.

That the carbomethoxy is unlikely to be operative is suggested also by the fact that in an attempt to synthesize a carboalkoxy derivative, $[PdCl_2(dtbpx)]$ was allowed to react with EtOH in the presence of NEt_3, or with $Na(OCH_3)$, in

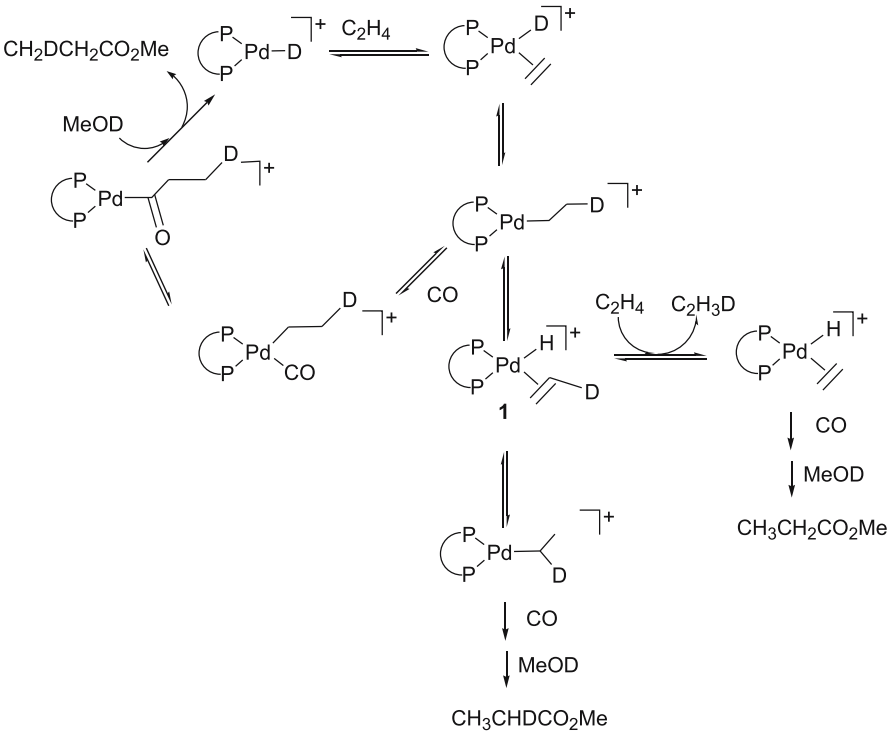

Fig. 9 Proposed hydride mechanism for the formation of d^{0-5} – MP. Adapted from [134]

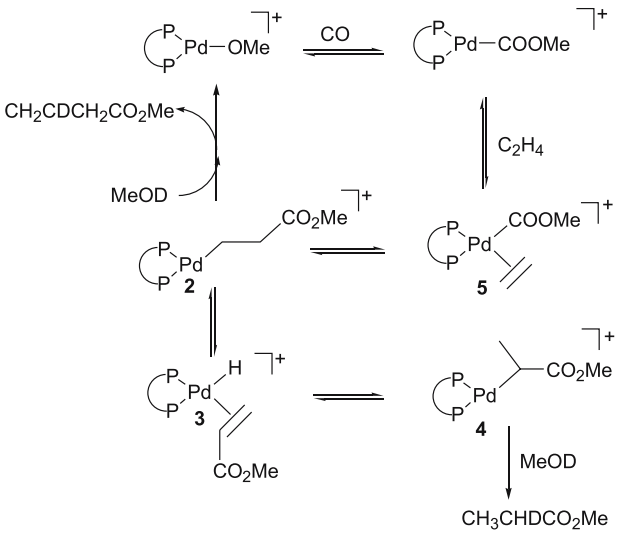

Fig. 10 Proposed carbomethoxy mechanism for the formation of monodeuterated $CH_2DCH_2CO_2Me$ and CH_3CHDCO_2Me. Adapted from [134]

both cases in the presence of CO. In place of the anticipated carboalkoxy complex [Pd(COOR)Cl(dtbpx)] [135, 136], the Pd(0) complex [Pd(CO)(dtbpx)] was obtained [136]. Attempts to convert the carbonyl complex to the hydride $[PdH(dtbpx)(MeOH)]^+$ by treatment with CF_3SO_3H failed [137], probably because of the instability of the hydride in the presence of CO [115].

In MeOH the hydride reacts with higher α-olefins, propene, 1-hexene and 1-hexadecene with formation of only the linear insertion product, probably for steric reasons. In all the insertion products, the alkyl ligand presents the β-agostic interaction. At room temperature, the insertion of ethene is quantitative whereas with propene an appreciable amount of the hydride is present, with 1-hexene the hydride prevails, with 1-hexadecene only the hydride is present. The fact that the position of the insertion equilibrium strongly depends on the chain length of the alkyl substituent is probably connected with the high steric hindrance of the ligand [115].

$$[PdH(dtbpx)(MeOH)]^+ \overset{CH_2=CHR}{\rightleftharpoons} [Pd(CH_2CH_2R)(dtbpx)(MeOH)]^+ \quad (23)$$
$$R = H, (CH_2)_nCH_3 \quad (n = 3 \text{ or } 13)\,.$$

It is noteworthy that the ethyl complex does not react even with the least hindered olefin to give higher alkyl complexes or ethene oligomerisation products; nor the acyl intermediate inserts another molecule of ethene to give intermediates that could lead to a cooligomerisation process, but it reacts immediately with MeOH to give the MP and the hydride back to the next catalytic cycle. It is worthwhile to note that the *i*-Pr, Cy or Ph analogues yield MP with only 20–30% selectivity and that the main product is a mixture of oligomers [111]. Not only, aryl substitution with electron-donating (MeO) and electron-withdrawing (NO_2) groups at the aryl ring of dtbpx have little effect on the rate and selectivity of the methoxycarbonylation of ethene [111]. Thus this unique chemistry of the dtbpx-based catalyst is most likely due to the highly restrictive steric demand of the ligand, which controls the insertion of only one molecule of monomer and then allows the methanolysis step. The relatively large bite angle of the ligand found by X-ray analysis of [Pd(COEt)Cl(dtbpx)] (103.08(3)°) [115] enhances the steric bulk.

In spite of this, the hydride catalyses the isomerisation of higher α-olefins to an equilibrium mixture of all the possible internal isomers and catalyses also the methoxycarbonylation of α-olefins and of internal olefins to the linear esters with 99% regioselectivity.

Preliminary mechanistic studies on the methoxycarbonylation of 1-octene showed that two pathways to methyl nonanoate occur, one involving the direct carbonylation of 1-octene to the linear ester, the other the alkene isomerisation in competition with the first one. Subsequently, the linear product forms by tandem isomerisation of the internal alkenes, with the terminal alkyl intermediate being trapped by migration to CO at a higher rate than any branched alkyl species. This has been confirmed by the analysis of products

obtained from reactions carried out in CH_3OD, which can be explained by a hydride mechanism [34, 138].

Recently, it has been reported that Pd(II) complexes with ferrocenyldiphosphines **33**, are also efficient catalysts for the selective methoxycarbonylation of ethene with activity comparable to that of the dtbpx-based system (initial TOF = 30 000 h^{-1}, TON = 60 000, at 100 °C, 10 bar) [139, 140].

4.2 Selective Synthesis of Diethyl Ketone

Because of its nature, DEK must form via a hydride mechanism. Up to the formation of a Pd-acyl intermediate, the paths leading to MP or DEK are similar. DEK forms if the insertion of a second molecule of ethene into the Pd-acyl bond is followed by protonolysis of the Pd – C bond of the resulting Pd-alkylacyl intermediate.

The first effective catalyst for this reaction has been reported by Zudin et al. [141]. The catalytic system was made in situ from $Pd(AcO)_2$, PPh_3 and aqueous CF_3COOH. In the absence of ethene, this catalyst promotes the formation of the WGSR. In the presence of ethene, the evolution of H_2 is inhibited and the reaction takes a different path, as DEK forms together with an equimolecular amount of CO_2. The source of hydrogen is H_2O [141]. The reaction can be depicted as follows:

$$2C_2H_4 + 2CO + H_2O \rightarrow DEK + CO_2 \qquad (24)$$

A significant increase of the catalytic activity occurs when the reaction is carried out in the presence of molecular hydrogen (TOF = 35 h^{-1} at 70 °C, 1 bar, $C_2H_4/CO/H_2 = 2/1/1$, Pd/P = 1/10). In this case CO_2 forms only in trace amounts [72]. The same active hydride $[PdHL_3]X$ is operative in both cases. In the absence of H_2 the hydride forms via a reaction closely related to the WGSR, in the other case it forms via heterolytic activation of H_2 by Pd(II). Deuterium studies using H_2/D^+ and D_2/D^+ systems elucidated the nature of the product forming steps, which occurs via keto-enol isomerisation of the alkylacyl β-chelate intermediate, followed by protonolysis [72], as shown to occur also for the analogous termination steps of the CO-ethene copolymerisation process.

More recently, Pugh and Drent found that $Pd(AcO_2)$/dtbpe/TfOH (Pd/P – P/TfOH = 1/1.2/2.5) is very active to catalyse the formation of DEK in MeOH and in the absence of H_2O (TOF = 4500 h^{-1} at 120 °C, 40 bar, CO/ethene = 1/1, 90% selectivity, 7.3% $CH_3CH_2COCH_2CH_2COOMe$, 1.5% MP), at variance with an analogous system based on the C_3-bridged analogue dtbpp (97.4% to MP, 2.6% to DEK, TOF = 25 000 h^{-1}) [33]. The source of hydrogen is MeOH [33]:

$$2C_2H_4 + CO + MeOH \longrightarrow DEK + HCHO \qquad (25)$$

When the reaction is carried out in the presence of hydrogen and excess acid (20 bar of H_2, Pd/TfOH = 1/50) the selectivity and TOF jump up to 98% and 90 000 h^{-1}. The mechanism proposed is shown in Fig. 11. After formation of the acyl intermediate **3**, the insertion of a second molecule of ethene is faster than methanolysis. Protonolysis by MeOH of the β-chelate gives the product and a $Pd-OCH_3^+$ species, which undergoes β-H elimination with regeneration of the active $Pd-H^+$ species **1**. Direct hydrogenolysis of **4** or of the $Pd-OCH_3$ bond may explain the promoting effect of H_2.

Differently from the dtbpp or the dtbpx systems, in the case of the dtbpe after the formation of intermediate **3,** insertion of a second molecule of ethene wins over termination by methanolysis to MP as, possibly, a consequence of the larger space at the "vacant" side because of the smaller bite angle of the C_2-bridged diphosphine.

Quite interestingly, excess acid changes the selectivity, as a significant amount of copolymer is produced (DEK 33%, oligomers/copolymers ca. 60%). Protonation at the oxygen atom of the β-chelate may open the five-membered (and the subsequent six-membered ring of a γ-chelate) and makes easier the insertion reactions to copolymers. A similar acid effect has been found using the monosulfonatedmonophosphine PPh_2PhSO_3H for the carbonylation to ethene in H_2O (Sect. 3.1) [82, 87].

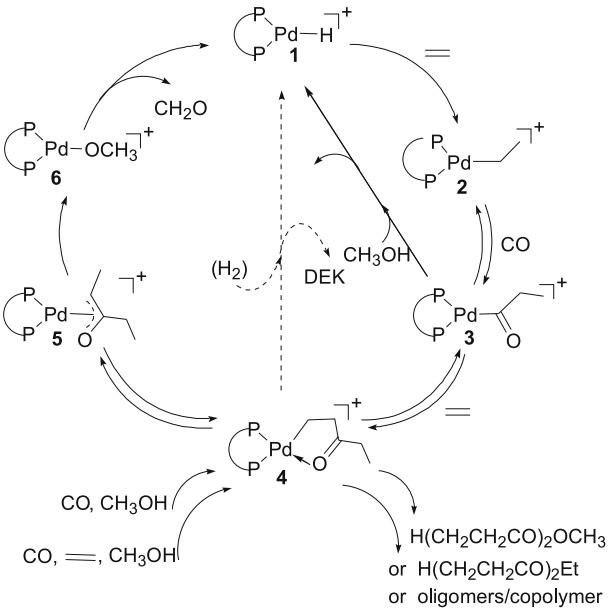

Fig. 11 Proposed mechanism for the formation of DEK. Adapted from [33]

5 Conclusions and Outlook

The most active Pd(II) catalysts for the carbonylation of ethene to high molecular weight polyketones, cooligomers or monocarbonylated products are cationic complexes of bidentate phosphines. *Cis*-coordination is ideal for promoting the insertion reactions and also methanolysis. Copolymerisation can occur through both the hydride and the carbomethoxy mechanism, whereas the formation of MP is likely to occur via the first mechanism only. The operating conditions, the nature of the counter-anion, the acidity and the nature of the solvent can influence both the rate of reaction and selectivity. But it is the ligand that can make the most significant difference.

After the promising results obtained with the C_3-bridged dppp ligand, which has a bite angle of 90°, believed to be optimal to make lower the activation energy of the copolymerisation process, systematic investigations on steric and electronic influence of modified dppp ligands led to the development of the dapp-type ligands, suitable for commercial exploitation, and also to the discovery of the dtbpp-based catalysts, highly active and selective for the production of MP.

The sharp change in selectivity from high molecular weight polyketones to MP occurring when the phenyl groups in dppp are replaced by bulkier *t*-Bu groups cannot be explained only on the basis of bridging chain length and bite angles. Nor can bite angle considerations alone explain the different selectivity between the C_4-bridged dtbpx and dppb-based catalyst, though their bite angles are significantly different, 104° and 98°, respectively.

Steric bulk considerations may provide a sound basis to explain the different activity. In the dtbpx catalyst ethene insertion into the Pd – H bond is fast as is the subsequent CO insertion into the Pd-acyl intermediate, because both the hydride and the CO ligands are small. Steric bulk impedes one more insertion of ethene, CO insertion does not occur because of thermodynamic reasons, thus propagation cannot occur. The acyl complex can react only with *cis*-coordinated MeOH, giving MP and the hydride back to the catalytic cycle. The larger the steric bulk, the faster methanolysis. The relatively large bite angle of dtbpx magnifies the steric bulk of *t*-Bu group, this may account for the exceptionally high selectivity to MP (99.98%) and also for the high reaction rate (TOF = 50 000 h^{-1} at 80 °C, 10 bar, CO/ethene = 1/1). The dtbpp ligand also gives a highly selective catalyst to MP, though slightly less efficient, probably because of the slightly lower steric bulk due to the shorter bridging chain. With less sterically hindering dppp type ligands, fast ethene insertion to β-chelates and fast multiple alternating insertions of CO and ethene occur before the relatively slow termination, which produces a high molecular weight polyketone.

By replacing the *t*-Bu groups with the smaller *s*-Bu in the C_3-bridged diphosphine, the selectivity changes from MP to DEK. Keeping the same sub-

stituents at the P atoms, the steric bulk can be varied by varying the length of the bridging chain. From dtbpp to less bulk dtbpe the selectivity changes from MP to DEK. After formation of the Pd – COEt intermediate, the less sterically hindering *s*-Bu-substituted diphosphine and the C_2-bridged dtbpe ligand allow the insertion of a second molecule of ethene with formation of an alkylacyl β-chelate intermediate, which undergoes protonolysis by MeOH to monocarbonylated DEK. When the catalysts are used in combination of an excess of acid, there is significant formation of oligomers/copolymers. It might be possible that protonation of the oxygen atom of the chelate destabilizes it and/or increases the electrophilicity of the chelate moiety, thus favouring further insertions.

Though mainly of electronic nature, the higher steric bulk of the dapp ligand, compared to dppp, may also contribute to enhance the performance of dapp. Also the increase of the steric constrains introduced by alkyl substitution in the bridging chain of both ligands may be involved in the increased productivity. The higher steric bulk and constraints may destabilize the β-chelates thus favouring the insertion of ethene, the low step of the copolymerisation process.

Steric bulk may play a role of paramount importance in making the catalysts based on the dppm type ligands **13** and **14** with bulky substituents at the *ortho*-position of the phenyl rings highly active for the copolymerisation to high molecular polyketones, whereas dppm itself is ineffective. The different selectivities observed using ligands **30** and **31** and **34–37** may also be related to steric bulk.

Ligands with intermediate steric bulk give cooligomers together with lower molecular weight products down to DEK and MP. Monophosphine catalysts also give these products. The P – Pd – P angle in *cis*-$[Pd(H_2O)_2(PPh_3)_2]^{2+}$ is 97°, close to the bite angle of dppb, but two PPh_3 have a higher steric bulk, which may explain the different selectivity shown by the two systems. In addition, the lower activity of the PPh_3-based catalyst system may be related to the fact that it undergoes *cis–trans* isomerisation and that it can undergo insertion and termination reactions only when in the *cis* geometry.

Though important results have already been obtained in the carbonylation of olefins, the field still remains open. Development of more active, efficient and stable catalysts based also on less expensive metals will make the carbonylation processes more attractive. Carbonylation of less common olefins, including functionalised ones, has to be explored in more depth. Other important targets are the efficient living copolymerisation, the multiple olefin insertion producing non-alternating copolymers and the selective synthesis of unsaturated products like acrylates and methacrylates.

Acknowledgements The authors are indebted to the undergraduate and graduate students we collaborated with, in particular to Federico Dall'Acqua who is at the beginning of his doctoral studies on the field of carbonylation of olefins and which helped us in the preparation of the manuscript.

References

1. Sen A, Lai TW (1982) J Amer Chem Soc 104:3520
2. Drent E (1984) EP 121965
3. Del Nobile MA, Mensitieri G, Nicolais L, Sommazzi A, Garbassi F (1993) J Appl Polym Sci 50:1261
4. Weinkauf DH, Kinneberg PA, Ash CA (1995) Proc of the ANTEC Conf, Boston, Massachusetts
5. Wakker A, Kormelink HG, Verbeke P, Jordaan JCM (1995) Plast Eur Kunststoffe September 110
6. Sommazzi A, Garbassi F (1997) Prog Polym Sci 22:1547
7. Sen A (1986) Adv Polymer Sci 73:125
8. van Broekhoven JAM, Wife RL (1988) EP 257663
9. Shell (1994) Carillon Thermoplastic Polymers, Information Sheet
10. European Plastics (1995) October
11. Lai TW, Sen A (1984) Organometallics 3:866
12. Sen A, Chen JT, Vetter WM, Whittle RR (1987) J Amer Chem Soc 109:148
13. Sen A (1993) Acc Chem Res 26:303
14. Drent E, van Broekhoven JAM, Doyle MJ (1991) J Organomet Chem 417:235
15. Drent E, Budzelaar PHM (1996) Chem Rev 96:663
16. Drent E, van Broekhoven JAM, Budzelaar PHM (1996) In: Cornils A, Herrmann WA (eds) Applied Homogeneous Catalysis with Organometallic Compounds, vol 1. VHC, Weinheim, p 333
17. Bianchini C, Meli A (2002) Coord Chem Rev 225:35
18. Robertson RAM, Cole-Hamilton DJ (2002) Coord Chem Rev 225:67
19. Bianchini C, Meli A, Oberhauser W (2003) J Chem Soc Dalton Trans 2627
20. Sen A (ed.) (2003) Catalytic Synthesis of Alkene-Carbon Monoxide Copolymers and Cooligomers. Kluwer Academic, Dordrecht
21. Belov GP, Novikova EV (2004) Russ Chem Rev 73:267
22. Consiglio G, Milani B (2003) In: Sen A (ed) Catalytic Synthesis of Alkene-Carbon Monoxide Copolymers and Cooligomers, chap. 6. Kluwer Academic, Dordrecht, p 189
23. Nosaki K (2003) In: Sen A (ed) Catalytic Synthesis of Alkene-Carbon Monoxide Copolymers and Cooligomers, chap. 7. Kluwer Academic, Dordrecht, p 217
24. Margl P, Michalak A, Ziegler T (2003) In: Sen A (ed) Catalytic Synthesis of Alkene-Carbon Monoxide Copolymers and Cooligomers, chap. 9. Kluwer Academic, Dordrecht, p 266
25. Scarel A, Dilani B, Zangrando E, Stener E, Furlan S, Fronzoni G, Mestroni G, Gladiali S, Carfagna C, Mosca L (2004) Organometallics 23:5593
26. Cole-Hamilton DJ, Robertson RAM (2003) In: Sen A (ed) Catalytic Synthesis of Alkene-Carbon Monoxide Copolymers and Cooligomers, chap. 3. Kluwer Academic, Dordrecht, p 37
27. Othmer K (1995) Encyclopedia of Chemical Technology, vol. 16, 4th edn. Wiley, New York, p 487

28. Chem Week (1999) November 10th, p. 14
29. New MMA Technology, European Chemical News (2000) October 30–November 5, p. 20
30. Drent E, Kragtwijk E (1992) EP 495548
31. Tooze RP, Eastham GR, Whiston K, Wang XL (1996) WO 96/19434
32. Suykerbuyk JCLJ, Drent E, Pringle PG (1998) WO 98/42717
33. Pugh RI, Drent E (2002) Adv Synth Catal 344:837
34. Jimenez C, Eastham GR, Cole-Hamilton DJ (2004) GB 003383
35. Kiss G (2001) Chem Rev 101:3435
36. Mul WP, Drent E, Jansens PJ, Kramer AH, Sonnemans MHW (2001) J Amer Chem Soc 123:5350
37. Mul WP, van der Made AW, Smaardijk AA, Drent E (2003) In: Sen A (ed) Catalytic Synthesis of Alkene-Carbon Monoxide Copolymers and Cooligomers, chap. 4. Kluwer Academic, Dordrecht, p 87
38. Luo HK, Li DG (2001) J Mol Catal A Chem 171:23
39. Koide Y, Bett SG, Barron AR (1996) Organometallics 15:2213
40. Grushin VV (1996) Chem Rev 96:2011
41. Bryndza HE, Tam W (1998) Chem Rev 88:1163
42. Clegg W, Eastham GR, Elsegood MRJ, Heaton BT, Iggo JA, Tooze RP, Whyman R, Zacchini S (2002) J Chem Soc Dalton Trans 3300
43. Zudin VN, Likholobov VA, Yermakov YI, Yeremenko NK (1997) Kinet Katal 18:524
44. Laine RM, Crawford EJ (1988) J Mol Catal 44:357
45. Likholobov VA, Yermakov YI (1980) Kinet Katal 21:904
46. Henry PM (1964) J Amer Chem Soc 86:3246
47. Bianchini C, Meli A, Oberhauser W, van Leeuwen PWNM, Zuideveld MA, Freixa Z, Kamer PJ, Spek AL, Gusev OV, Kal'sin M (2003) Organometallics 22:2409
48. Vavasori A, Cavinato G, Toniolo L (2003) J Mol Catal A Chem 191:209
49. Zuideveld MA, Kamer PCJ, van Leeuwen PWNM, Klusener PAA, Stil HA, Roobeek CF (1998) J Amer Chem Soc 120:7977
50. Schwarz J, Herdtweck E, Herrmann WA, Gardiner MG (2000) Organometallics 19:3154
51. Mul WP, Oosterbeek H, Beitel GA, Kramer GJ, Drent E (2000) Angew Chem Int Ed 39:1848
52. Shultz S, Ledford J, DeSimone JM, Brookhart M (2000) J Amer Chem Soc 122:6351
53. Zuideveld MA, Swennenhuis BHG, Kamer PCJ, van Leeuwen PWNM (2001) J Organomet Chem 637:805
54. Ledford J, Shultz CS, Gates DP, White PS, DeSimone JM, Brookhart M (2001) Organometallics 20:5266
55. Bianchini C, Lee HM, Meli A, Oberhauser W, Peruzzini M, Vizza F (2002) Organometallics 21:16
56. Bianchini C, Meli A, Oberhauser W, Passaglia E (2002) Organometallics 21:4965
57. Van Leeuwen PWNM, Zuideveld MA, Swennenhuis BHG, Freisa Z, Kamer PCJ, Goubitz K, Fraanje J, Lutz M, Spek AL (2003) J Amer Chem Soc 125:5523
58. Liu J, Heaton BT, Iggo JA, Whyman R (2004) Angew Chem Int Ed 43:90
59. Cavinato G, Vavasori A, Toniolo L, Dolmella A (2004) Inorg Chim Acta 357:2737
60. Bianchini C, Lee HM, Meli A, Oberhauser W, Vizza F, Brueggeller P, Haid R, Langes C (2000) J Chem Soc Chem Commun 777
61. Bianchini C, Meli A, Oberhauser W (2003) Organometallics 22:4281
62. Amatore C, Jutand A, M'Barki MA (1992) Organometallics 11:3009
63. Amatore C, Carré E, Jutand A, M'Barki MA (1995) Organometallics 14:1818

64. Amatore C, Jutand A, Thuilliez A (2001) Organometallics 20:3241
65. Benetollo F, Bertani R, Bombieri G, Toniolo L (1995) Inorg Chim Acta 233:5
66. Vavasori A, Toniolo L (1996) J Mol Catal A: Chemical 110:13
67. Sen A (2003) In: Sen A (ed) Catalytic Synthesis of Alkene-Carbon Monoxide Copolymers and Cooligomers, chap. 8. Kluwer Academic, Dordrecht, p 237
68. Toth I, Elsevier CJ (1993) J Amer Chem 115:10388
69. Dekker GPCM, Elsevier CJ, Vrieze K, van Leeuwen PWNM (1992) Organometallics 11:1598
70. Drent E, van Dijk R, van Ginkel R, van Oort B, Pugh RI (2002) J Chem Soc Chem Commun 964
71. Van Leeuwen PWNM (2003) In: Sen A (ed) Catalytic Synthesis of Alkene-Carbon Monoxide Copolymers and Cooligomers, chap. 5. Kluwer Academic, Dordrecht, p 141
72. Zudin VN, Chinakov VD, Nekipelov VM, Rogov VA, Likholobov VA, Yermakov YI (1989) J Mol Catal 52:27
73. Bianchini C, Lee HM, Meli A, Moneti S, Platinec V, Petrucci G, Vizza F (1999) Macromolecules 32:3859
74. Tschanen W (1990) Dissertation, ETH, Zurich
75. Zuideveld MA, Kamer PCJ, van Leeuwen PWNM (2001) J Amer Chem Soc 123:5350
76. Bianchini C, Lee HM, Meli A, Monetti S, Vizza F, Fontani M, Zanello P (1999) Macromolecules 32:4183
77. Bianchini C, Lee HM, Barbaro P, Meli A, Monetti S, Vizza F (1999) New J Chem 23:929
78. Liu J, Heaton BT, Iggo JA, Whyman R (2004) J Chem Soc Chem Commun 1326
79. Gusev OV, Kal'sin AM, Petrovskii PV, Lyssenko KA, Oprunenko YF, Bianchini C, Meli A, Oberhauser W (2003) Organometallics 22:913
80. Zhao AX, Chien JCW (1992) J Polym Sci A Polym Chem 30:2735
81. Belov GP, Chepaikin EG, Bezruchenko AP, Smirnov VI (1993) Polym Sci Ser A 35:1323
82. Chepaikin EG, Bezruchenko AP, Leshcheva AA, Boiko GN (1994) Russ Chem Bull 43:360
83. Belov GP, Golodkow ON, Dzhabieva ZM (1995) Macromol Symp 89:455
84. Koide Y, Barron AR (1996) Macromolecules 29:1110
85. Belov GP, Golodkov ON, Novikova EV (1998) Polym Sci Ser A 40:240
86. Fatutto D, Toniolo L, Chaudhari RV (1999) Catal Today 48:49
87. Chepaikin EG, Bezruchenko AP, Leshcheva AA (1999) Kinet Katal 40:313
88. Pivovarov AP, Novikova EV, Belov GP (2000) Russ J Coord Chem 26:38
89. Toniolo L, Kulkarni SM, Fatutto D, Chaudhari RV (2001) Ind Eng Chem Res 40: 2037
90. Belov GP, Psikha BL (2003) Polym Sci Ser A 45:752
91. Vavasori A, Cavinato G, Toniolo L (2001) J Mol Catal A Chem 176:11
92. Vavasori A, Toniolo L, Cavinato G, Visentin F (2003) J Mol Catal A Chem 204:295
93. Vavasori A, Toniolo L, Cavinato G (2004) J Mol Catal A Chem 215:63
94. Jiang Z, Sen A (1994) Macromolecules 27:7215
95. Verspui G, Papadogianakis G, Sheldon RA (1998) J Chem Soc Chem Commun 401
96. Verspui G, Feiken J, Papadogianakis G, Sheldon RA (1999) J Mol Catal A Chem 146:299
97. Bianchini C, Meli A, Vizza F (1998) WO 98/22482
98. Verspui G, Schaussema F, Sheldon RA (2000) Appl Catal A General 198:5
99. Verspui G, Schaussema F, Sheldon RA (2000) Angew Chem Int Ed 39:804

100. Lindner E, Schmid M, Wald J, Queisser JA, Geprags M, Wegner P, Nachtigal C (2000) J Organomet Chem 602:173
101. Pugh RI, Drent E (2003) In: Sen A (ed) Catalytic Synthesis of Alkene-Carbon Monoxide Copolymers and Cooligomers, chap. 2. Kluwer Academic, Dordrecht, p 9
102. Lu CC, Peters JC (2002) J Amer Chem Soc 124:5272
103. van Leeuwen PWNM, Diekers P (1999) J Chem Soc Dalton Trans 1518
104. Doherty S, Eastham GR, Tooze RP, Scanlan TH, Williams D, Elsegood MRJ, Clegg W (1999) Organometallics 18:3558
105. Dossett SJ, Gillon A, Guy Orpen A, Fleming JS, Pringle PG, Wass DF, Jones MD (2001) J Chem Soc Chem Commun 699
106. Dosset SJ (2000) WO 00/06299
107. Barlow GK, Boyle JD, Cooley NA, Ghaffar T, Wass DF (2000) Organometallics 19:1470
108. Puddephatt RJ (1983) Chem Soc Rev 12:99
109. Dossett J (1997) WO 97/37765
110. Dossett J, Fleming JS, Pringle PG (2000) WO 00/03803
111. Clegg W, Eastham GR, Elsegood MRJ, Tooze RP, Wang XL, Whiston K (1999) J Chem Soc Chem Commun 1877
112. Knight JC, Doherty S, Harriman A, Robins EG, Bertham M, Eastham GR, Tooze RP, Elsegood MRJ, Champlin PA, Clegg W (2000) Organometallics 19:4957
113. Doherty S, Robins EG, Knight JC, Newman CR, Rhodes B, Champlin PA, Clegg W (2001) J Organomet Chem 640:182
114. Eastham GR, Heaton BT, Iggo JA, Tooze RP, Whyman R, Zacchini S (2000) J Chem Soc Chem Commun 609
115. Clegg W, Eastham GR, Elsegood MRJ, Heaton BT, Iggo JA, Tooze RP, Whyman R, Zacchini S (2002) Organometallics 21:1832
116. Gusev OV, Kal'sin AM, Peterleitner MG, Petrovskii PV, Lyssenko KA, Akhmedov NG, Bianchini C, Meli A, Oberhauser W (2002) Organometallics 21:3637
117. Pugh RI, Drent E, Pringle PG (2001) J Chem Soc Chem Commun 1476
118. Knifton J (1976) J Org Chem 41:2885
119. Kudo K, Oida Y, Mitsihashi K, Mori S, Komatsu K, Sugita N (1996) Bull Chem Soc Jpn 69:1337
120. Conroy-Lewis FM, Mole L, Redhouse AD, Litster SA, Spencer JL (1991) J Chem Soc Chem Commun 1601
121. Crascall LE, Spencer JL (1992) J Chem Soc Dalton Trans 3445
122. Kalia O, Temkin ON, Mechriakova IG, Flid PM (1971) Dokl Akad Nauk SSSR 199:1321
123. Otsuka S, Nakamura A, Yoshida T, Naruto M, Ataka K (1973) J Amer Chem Soc 5:3180
124. Fenton DM (1973) J Org Chem 38:3192
125. Milstein D (1988) Acc Chem Res 21:428
126. Bardi R, Del Pra A, Piazzasi AM, Toniolo L (1979) Inorg Chim Acta 35:L345
127. Cavinato G, Toniolo L (1990) J Organomet Chem 398:187
128. Cavinato G, Toniolo L, Vavasori A (2004) J Mol Catal A Chem 219:233
129. Cavinato G, Vavasori A, Toniolo L, Benetollo F (2003) Inorg Chim Acta 343:183
130. Seayad A, Jayasree S, Damodaran K, Toniolo L, Chaudhari RV (2000) J Organomet Chem 601:100
131. Toth I, Elsevier CJ (1993) J Chem Soc Chem Commun 529
132. Tooze RP, Whiston K, Malyan AP, Taylor MJ, Wilson NW (2000) J Chem Soc Dalton Trans 3441

133. Fryzuk MD, Clentsmith GKB, Retting SJ (1998) J Chem Soc Dalton Trans 2007
134. Eastham GR, Tooze RP, Kilner MK, Foster DF, Cole-Hamilton DJ (2002) J Chem Soc Dalton Trans 1613
135. Hidai M, Kokura M, Uchida Y (1973) J Organomet Chem 52:431
136. Smith CD, Hanson BE, Merola JS, Waller FJ (1993) Organometallics 12:568
137. Bellabarba RM, Tooze RP, Slawin AMZ (2003) J Chem Soc Chem Commun 1916
138. Jimenez Rodriguez C, Eastham GR, Cole-Hamilton DJ (2004) J Chem Soc Chem Commun 1720
139. Butler IR, Horton PN, Fortune KM, Morris K, Greenwell CH, Eastham GR, Hursthouse MB (2004) Inorg Chem Commun 7:923
140. Butler IR, Baker PK, Eastham GR, Fortune KM, Horton PN, Hursthouse MB (2004) Inorg Chem Commun 7:1049
141. Zudin VN, Ill'inich GN, Likholobov VA, Yermakow YI (1984) J Chem Soc Chem Commun 545

Top Organomet Chem (2006) 18: 165–178
DOI 10.1007/3418_020

Published online: 10 June 2006

The Pauson–Khand Reaction

Dirk Strübing · Matthias Beller (✉)

Leibniz-Institut für Katalyse e.V. an der Universität Rostock,
Albert-Einstein-Straße 29a, 18059 Rostock, Germany
matthias.beller@ifok-rostock.de

1 Introduction 166

2 The Catalytic Pauson–Khand Reaction 168

3 Synthetic Applications 170

4 Stereoselective Pauson–Khand Reactions 173

5 Pauson–Khand Transfer Carbonylation Reactions 174

6 Conclusions and Outlook 176

References 176

Abstract The transition metal mediated conversion of alkynes, alkenes, and carbon monoxide in a formal [2 + 2 + 1] cycloaddition process, commonly known as the Pauson–Khand reaction (PKR), is an elegant method for the construction of cyclopentenone scaffolds. During the last decade, significant improvements have been achieved in this area. For instance, catalytic PKR variants are nowadays possible with different metal sources. In addition, new asymmetric approaches were established and the reaction has been applied as a key step in various total syntheses. Recent work has also focused on the development of CO-free conditions, incorporating transfer carbonylation reactions. This review attempts to cover the most important developments in this area.

Keywords Pauson–Khand reaction · Homogeneous catalysis · Cycloaddition · Transfer carbonylation · Cyclopentenones

Abbreviations

acac	Acetylacetonate
BINAP	2,2′-Bis(diphenylphosphino)-1,1′-binaphthyl
BSA	Bis(trimethylsilyl)acetamide
Bu	Butyl
^{t}Bu	*tert*-Butyl
cod	Cyclooctadiene
Cp	Cyclopentadienyl
dba	Dibenzylideneacetone
DMAc	*N*,*N*-Dimethylacetamide
DME	1,2-Dimethoxyethane
DMSO	Dimethyl sulfoxide

dppb	1,4-Bis(diphenylphosphino)butane
dppp	1,3-Bis(diphenylphosphino)propane
EBTHI	Ethylene-1,2-bis(η^5-4,5,6,7-tetrahydro-1-indenyl)
ee	Enantiomeric excess
Me	Methyl
Ph	Phenyl
PKR	Pauson–Khand reaction
Py	Pyridine
SDS	Sodium dodecyl sulfate
Tf	Trifluoromethanesulfonyl
TMANO	Trimethylamine *N*-oxide
tolBINAP	2,2′-Bis(di-4-tolylphosphino)-1,1′-binaphthyl
TPPTS	Triphenylphosphine trisulfonate

1 Introduction

An important procedure for the synthesis of cyclopentenones is the so-called Pauson–Khand reaction, which constitutes a formal [2 + 2 + 1] cycloaddition of an alkene, an alkyne, and carbon monoxide. Due to the increase in structural diversity of the available starting materials, the reaction has become an attractive target for scientific investigations [1–8]. The first successful example was reported by Pauson, Khand et al [9] in 1973 for the conversion of norbornene with the phenylacetylene–hexacarbonyldicobalt complex to give the corresponding cyclopentenone in 45% yield (Eq. 1).

A proposed mechanism of this reaction was reported by Magnus and Principle [10], which is nowadays widely accepted (Scheme 1). Recently, negative-ion electrospray collision experiments have confirmed this mechanism in detail [11]. Starting with the formation of the alkyne–$Co_2(CO)_6$ complex **2**, olefin **3** coordination and subsequent insertion takes place at the less hindered end of the alkyne. The in situ formed metallacycle **4** reacts rapidly under insertion of a CO ligand **5** and reductive elimination of **6** proceeds to liberate the desired cyclopentenone **7**. It is important to note that all the bond-forming steps occur on only one cobalt atom. The other cobalt atom of the complex is presumed to act as an anchor which has additional electronic influences on the bond-forming metal atom via the existing metal–metal bond [12].

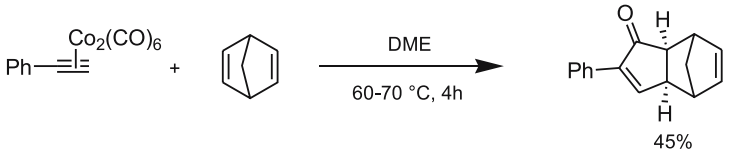

Equation 1

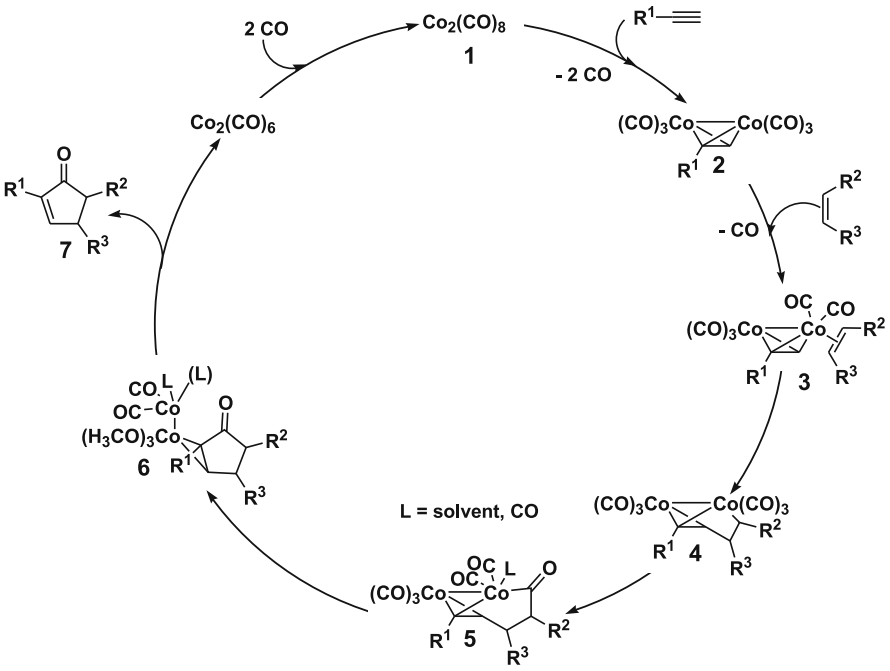

Scheme 1 Mechanistic proposal for the Pauson–Khand reaction

After its discovery the method was affected by various problems. For instance, a stoichiometric amount of catalyst and the use of strained olefins were necessary to obtain useful yields. Furthermore, if unsymmetrical alkynes and alkenes were used, the reactions typically gave a mixture of regioisomers. In addition, many early examples reported the need for long reaction times and high temperatures to obtain full conversion.

An important advance was reported by Schore and Croudace [13], who showed for the first time that carbon-tethered enyne precursors undergo an intramolecular Pauson–Khand reaction (PKR) in good yields with complete control of regioselectivity. In this connection, it was not essential to use strained olefins as starting materials.

In addition to $Co_2(CO)_8$, subsequently other metal complexes such as molybdenum hexacarbonyl [14], iron pentacarbonyl [15, 16], tungsten pentacarbonyl [17], and zirconium [18] or heterobimetallic cobalt/tungsten complexes [19] were reported to facilitate the PKR. Although various metals furnish the stoichiometric PKR, $Co_2(CO)_8$ has become the catalyst of choice due to its several advantages, e.g., the complex tolerates a broad range of functional groups, reveals activity toward both terminal and internal alkynes, and is relatively cheap. With regard to problems like high temperatures and CO pressures, as well as long reaction times, significant progress was reported independently by the groups of Jeong [20] and Schreiber [21], who reported

the application of *N*-methylmorpholine *N*-oxide and trimethylamine *N*-oxide as PKR accelerating agents. Using *N*-oxides, cyclopentenones were obtained in good yields even at room temperature. It is likely that the promoting effect of *N*-oxides is based on the oxidative liberation of the CO ligands of the metal complex. Therefore, the following oxidative alkene addition, known as the rate-determining step in the PKR, can now proceed very fast.

Other reagents such as silica gel [22, 23], molecular sieves [24, 25], alkyl methyl sulfides [26], or primary amines [27] were also reported to facilitate the reaction, but seem not to work as generally as *N*-oxides.

2 The Catalytic Pauson–Khand Reaction

PKR with stoichiometric amounts of $Co_2(CO)_8$ are still often used as the key step in various total syntheses. However, with regard to environmental friendliness, catalytic procedures are desirable. This chapter will deal with recent approaches in the development of the catalytic PKR.

The first catalytic PKR was reported by Rautenstrauch et al. [28], who described the conversion of heptyne using a mixture of 40 bar ethylene and 100 bar CO to form the resulting cycloaddition adduct in a yield of 48%. A more practicable procedure was later reported by Jeong et al. [29], who realized the PKR in good yields at 3 atm of CO and 110 °C by stabilization of the cobalt catalyst with triphenylphosphite as ligand. Apart from $Co_2(CO)_8$, other Co sources were also successfully applied within the reaction. For example, Sugihara and Yamaguchi [30] described the employment of methylidynetricobalt nonacarbonyl clusters $Co_3(CO)_9(\mu^3 - CH)$, which are advantageous due to the catalyst productivity (1–2 mol %). Furthermore, the system catalyzes both the intra- and intermolecular PKR with remarkably good yields (78–91%). Lee and Chung [31] examined the use of $Co(acac)_2/NaBH_4$ as cycloaddition catalyst. In this case, yields were observed in a range of 33–85%. Successful conversions needed high CO pressures (40 atm) and long reaction times (up to several days). The first example of a catalytic conversion under atmospheric pressure of carbon monoxide was reported by Rajesh and Periasamy [32]. Here, a combination of 0.4 eq. $CoBr_2$ and 0.43 eq. Zn was chosen to facilitate the intermolecular PKR. Isolated yields were obtained in the range of 30–88% at 110 °C. Supplementary to reactions in organic solvents, procedures applying supercritical fluids have become more and more attractive in industry and academic research. So it is not surprising that Jeong's group reported the use of supercritical CO_2 as alternative solvent [33]. Using $Co_2(CO)_8$ as catalyst, 112 atm of CO_2 and 15–30 atm of CO were required at 37 °C to obtain cyclopentenones in yields up to 91%.

In addition to the accelerating effect of sulfides and amines in the stoichiometric $Co_2(CO)_8$-mediated procedure, Hashimoto et al. showed that phos-

phane sulfides are able to promote the $Co_2(CO)_8$-catalyzed reaction [34]. Even at atmospheric CO pressure and moderate temperature of 70 °C, the desired products were isolated in almost quantitative yields (ca. 90%).

Due to the easier recycling of heterogeneous catalysts, Chung et al. developed an easy system that is based on the immobilization of 12 wt % metallic cobalt on commercially available charcoal [35]. The resulting yields were obtained in the range of 61–98%. After simple filtration the catalyst was reused up to ten times without significant loss of activity.

Although Co carbonyl complexes have been used most often in catalytic PKR, a variety of other transition metal complexes are able to catalyze this reaction. For instance, $Cp_2Ti(PMe_3)_2$ [36] and Ni(0) catalysts [37] have been reported to afford iminocyclopentenes by the use $^tBuMe_2SiNC$ instead of CO. Subsequent hydrolysis provides the desired cyclopentenones. Unfavorably, the isolated product yield decreases significantly when applying this reaction sequence.

Buchwald et al. have shown that 5–20 mol % $Cp_2Ti(CO)_2$ facilitates the PKR at 18 psi CO and 90 °C, giving yields in between 58 and 95% [38]. Moreover, Mitsudo et al. [39] and Murai et al. [40] reported independently on the employment of $Ru_3(CO)_{12}$ as active catalyst. Cyclopentenones were isolated in moderate to excellent yields (41–95%). In addition, rhodium catalysts were successfully examined for use in the PKR. Narasaka et al. [41] carried out reactions at atmospheric CO pressure using the dimeric $[RhCl(CO)_2]_2$ complex. Also, in the presence of other rhodium complexes like Wilkinson catalyst $RhCl(PPh_3)_3$ and $[RhCl(CO)(dppp)]_2$ [42] in combination with silver salts, cyclopentenones were obtained in yields in the range of 20–99%. Some representative examples of the catalytic PKR are shown in Eq. 2.

In contrast to the development of general procedures for intramolecular PKR, the realization of comparable intermolecular procedures was afflicted

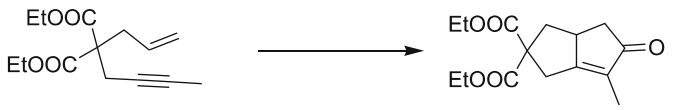

a: 90% e: 78%
b: 91% f: 91%
c: 98% g: 96%
d: 58%

conditions:

a: 3 mol% $Co_2(CO)_8$, $P(OPh)_3$, DME, 3 atm, [29]
b: 3 mol% $Co_2(CO)_8$, 11 atm CO_2 at 36°C, 30 atm CO, 94°C, 24h [33]
c: 12 wt%Co supported on charcoal, 20 atm CO, THF, 18 h, [35]
d: 10 mol% $Cp_2Ti(PMe_3)_2$, ^tBuMe SiNC, additional hydrolysis, [36]
e: 5 mol% $Ru_3(CO)_{12}$, DMAc, 15 atm CO, 140°C, 20 h, [39]
f: 1 mol% $[RhCl(CO)_2]_2$, 1 atm CO, Bu_2O, 130 °C, 18 h, [41]
g: 2.5 mol% *trans*-$[RhCl(CO)(dppp)]_2$, 1 atm CO, 110 °C, 24 h, toluene, [42]

Equation 2

with various problems. With exception of ethylene and strained alkenes, reactions employing simple olefins gave only poor yields because of their low reactivity. Furthermore, the observed regioselectivities were also disappointing. The pioneering work of Krafft et al. [43–45] revealed that the introduction of coordinating heteroatoms, such as nitrogen or sulfur, attached to the alkene leads to a strong enhancement of reactivity and regioselectivity. Hence, further work was dedicated to developing an easily removable directing group, which would open the way to increasing the synthetic potential of the intermolecular PKR. In this connection, Itami et al. [46, 47] developed an interesting system, which included a 2-pyridyldimethylsilyl group tethered to the alkene part (Eq. 3). As a major advantage, this directing group enabled the regioselective synthesis of cyclopentenones at the 4- and 5-position, respectively. The pyridylsilyl group is removed after product formation caused by residual water. Looking at different catalysts, $Ru_3(CO)_{12}$ gave the best results even under a remarkably low pressure of 1 atm CO. Here, yields were obtained in the range of 40–91%.

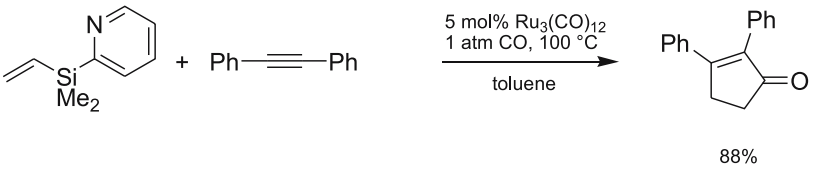

Equation 3

3 Synthetic Applications

In addition to the use of the simple enyne precursors, several groups examined the PKR of related systems, which would broaden the scope of the method. Pursuing this strategy, Wender et al. elaborated dienyl-type PKR [48]. Conversion proceeded smoothly even at room temperature under an atmospheric pressure of CO by applying $[RhCl(CO)(PPh_3)_2]$ as catalyst. Yields ranging from 43 to 96% were obtained. Interestingly, the chosen system tolerates a variety of substitution patterns on the alkyne dienyl moiety (Eq. 4).

Recently, Shibata et al. reported on the successful conversion of allenynes [49]. By employing $[IrCl(CO)(PPh_3)_2]$ as active catalyst (Eq. 5), reactions were carried out under a very low pressure of carbon monoxide affording yields up to 91%.

Without doubt, multicomponent reactions have become an attractive tool for the synthesis of biologically active molecules. In this regard, Jeong et al. reported an interesting domino synthesis of bicyclopentenones [50]. They employed a bimetallic system consisting of $[Pd_2(dba)_3(CHCl_3)]$ and

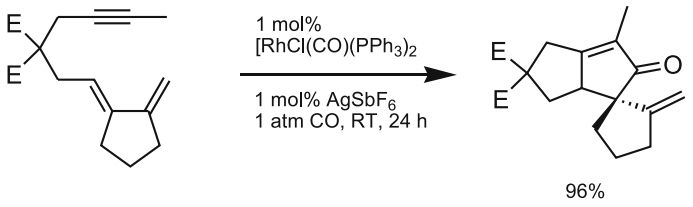

Equation 4

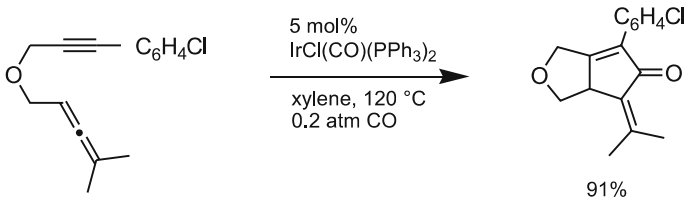

Equation 5

[{RhClCO(dppp)}$_2$] for the sequential construction of an enyne precursor, starting from a malonic acid derivative and allylic acetate, which was converted in situ to the cycloaddition product with excellent yields. Obviously, the Pd complex catalyzes the allylic substitution reaction, while the rhodium catalyst is responsible for the PKR (Eq. 6).

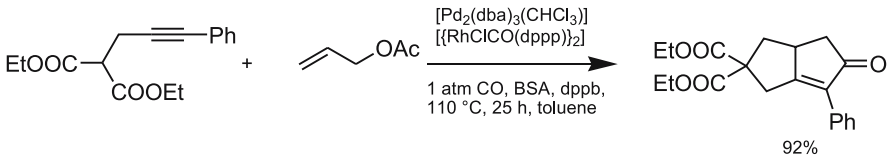

Equation 6

Because of the remarkable increase of molecular complexity, the PKR serves as a useful methodology for various natural product syntheses. Numerous examples of synthetic applications have been reported during the last two decades. For instance, the PKR was successfully employed in the total syntheses of β-cupraenone [51], loganin [52], hirsutene [53], and (+)-epoxydictymene [54]. Just to comment on recently published examples, Nomura and Mukai [55] reported on the total synthesis of (±)-8α-hydroxystreptazolone (Eq. 7). This target molecule achieved attention due its antibiotic and antifungal activity. In this case, the PKR was used to build up the required tricyclic framework. The successful conversion was facilitated by the employment of an equimolar amount of $Co_2(CO)_8$ and TMANO as promoting reagent. The resulting cyclopentenone derivative was isolated in 51% yield.

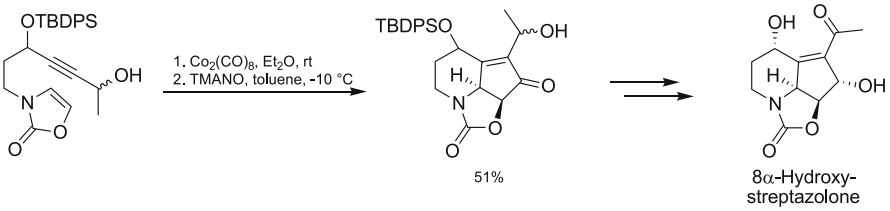

Equation 7

More recently, the total synthesis of isocarbacyclin, a therapeutically useful agent against numerous vascular diseases, was reported by Saito et al. [56]. Again, the crucial cycloaddition step was carried out using a stoichiometric amount of $Co_2(CO)_8$. The reaction was completed within 3 h and gave 78% yield of the desired cyclopentenone (Eq. 8).

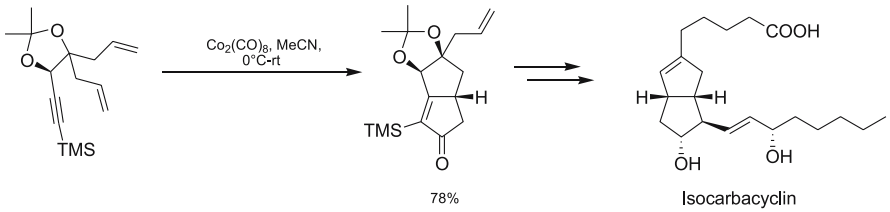

Equation 8

With regard to the known activity of cyclopentenone-containing prostaglandins, which serve, for instance, as anti-inflammatory and antineoplastic ingredients [57], Brummond et al. elaborated the total synthesis of 15-deoxy-$\Delta^{12,14}$-prostaglandin J_2 by applying an allenic PKR [58]. As a special feature, screening for a suitable catalyst system gave the best results when employing $Mo(CO)_6$. The reaction was accomplished in a moderate yield of 38%, producing a mixture of E/Z isomers in a ratio of 1 : 2 with respect to the unwanted Z isomer. Additional reisomerization of the undesired isomer, by photolysis or treatment with boron trifluoride/propanedithiol, increased the yield of the target isomer (Eq. 9).

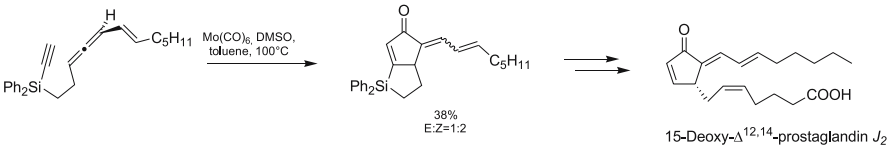

Equation 9

4
Stereoselective Pauson–Khand Reactions

The virtue of performing the PKR in an enantioselective manner has been extensively elaborated during the last decade. As a result, different powerful procedures were developed, spanning both auxiliary-based approaches and catalytic asymmetric reactions. For instance, the use of chiral *N*-oxides was reported by Kerr et al., who examined the effect of the chiral brucine *N*-oxide in the intermolecular PKR of propargylic alcohols and norbornadiene [59]. Under optimized conditions, ee values up to 78% at – 60 °C have been obtained (Eq. 10). Chiral sparteine *N*-oxides are also able to induce chirality, but the observed enantioselectivity was comparatively lower [60].

The application of chiral auxiliaries is an alternative route to obtain enantiomerically pure compounds. This approach has been frequently used in the total syntheses of natural products like hirsutene [53] and (+)-15-norpentalene [61].

Although this procedure often provides excellent diastereoselectivities, a major drawback is the expensive synthesis of the PKR precursor. Hence, the application of chiral transition metal catalysts is a more convenient method for the synthesis of enantiomerically pure cyclopentenones. The first successful results were reported by Buchwald and Hicks, who showed that the chiral titanocene complex (*S*,*S*) –(EBTHI)Ti$(CO)_2$ is a useful system for that purpose [62, 63]. Various enynes were converted under 14 psig CO pressure and 90 °C reaction temperature. Yields were often good (72–96%), and the obtained enantioselectivities were also good to excellent (70–94%). In addition, RhCl$(CO)_2$ in combination with AgOTf and (*S*)-BINAP was reported to facilitate enantioselective PKR [64]. Values of ee were observed in between 22 and 99% and isolated yields were in the range of 22–96%. Moreover, it was shown that chiral iridium diphosphine complexes catalyze such cycloaddition reactions [65]. Using a comparatively large amount of 10 mol %

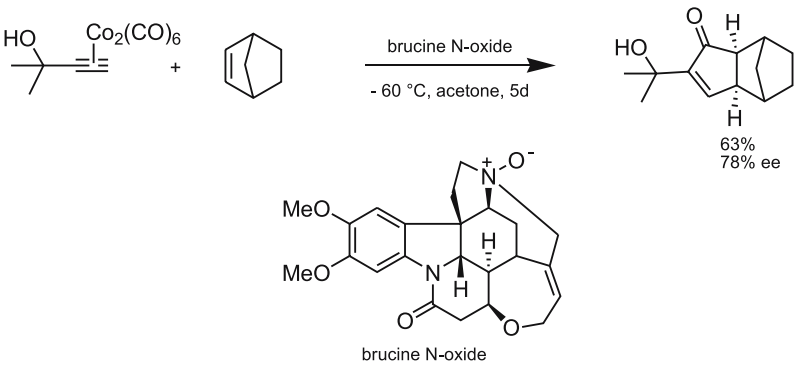

Equation 10

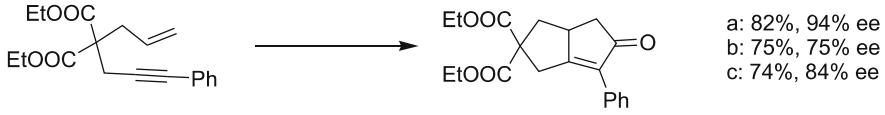

conditions:

a: 7.5 mol% (*S*,*S*)(EBTHI)Ti$(CO)_2$, 14 psig CO, toluene, 12h, 90 °C, [62, 63]
b: 6 mol% $Co_2(CO)_8$, 10 mol% ligand, toluene, 1 atm CO, 24 h, 95 °C, [67]
c: 5 mol% $[Ir(cod)Cl]_2$ + 10 mol% (*S*)-tolBINAP, 1 atm CO, refluxing xylene, 72h, [65]

Equation 11

$[Ir(cod)Cl]_2$, reactions afforded enantiomerically enriched cyclopentenones when (*S*)-tolBINAP was employed as ligand. The corresponding cyclopentenones were obtained in yields up to 85% and ee values ranging from 82 to 98%. Interestingly, $Co_2(CO)_8$ in combination with a chiral bisphosphite also gives access to chiral Pauson–Khand products [66]. Here, yields were observed up to 97%; however, in most cases the ee was rather low (< 20%). Equation 11 summarizes some representative examples of enantioselective PKR.

5
Pauson–Khand Transfer Carbonylation Reactions

During the last few years, the PKR has been developed as a straightforward and practicable method for the synthesis of highly substituted cyclopentenones. But for many synthetic chemists, the employment of poisonous CO still represents a disadvantage. Hence, different strategies focused on the replacement of carbon monoxide within the reaction sequence. Recent successful examples are based on results from the early 1960s, which dealt with the transition metal catalyzed decarbonylation of organic oxo compounds [67].

In Scheme 2 the general mechanism of this transformation is shown. Clearly, the in situ formation of CO by a decarbonylation process takes advantage of the formation of metal carbonyls, which are known to be the key intermediates in the PKR.

Morimoto, Kakiuchi, and co-workers were the first to show that aldehydes are a useful source of CO in the catalytic PKR [68]. Based on ^{13}C-labeling experiments, it was proposed that after decarbonylation of the aldehyde, an active metal catalyst is formed. This was proven by the absence of free carbon monoxide. As a consequence CO, which is directly generated by previous aldehyde decarbonylation, is incorporated in situ into the carbonylative coupling. The best results were obtained using C_5F_5CHO and cinnamaldehyde as CO source in combination with $[RhCl(cod)]_2$/dppp as the catalyst system. In the presence of an excess of aldehyde the corresponding products were isolated in the range of 52–97%.

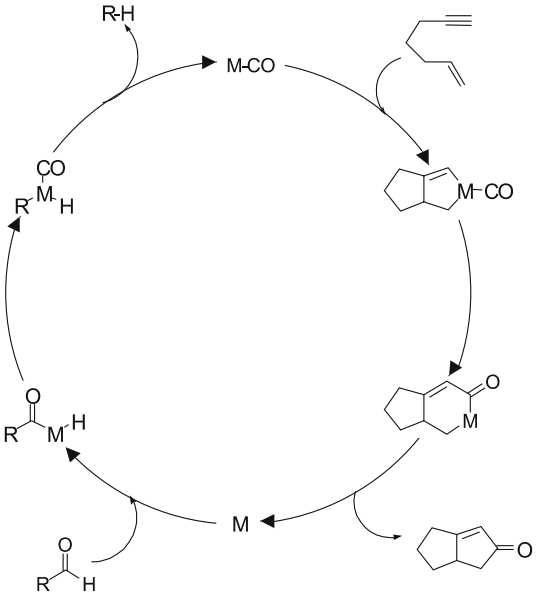

Scheme 2 Proposed catalytic mechanism for PK transfer carbonylations

Later, Shibata et al. reported PK-type transfer carbonylation reactions in the absence of solvent and employing a large excess of aldehyde [69]. Also in this case, the reactions went smoothly yielding cyclopentenones in the range of 56–96%. Interestingly, it was also demonstrated that this methodology provides access to chiral products. By applying the chiral catalyst system $[RhCl(cod)]_2$/tolBINAP, ee values of 45–90% were observed. Another convincing approach to carrying out PK-type transfer carbonylation reactions was again reported by Kakiuchi et al. [70]. Herein, formaldehyde was employed as decarbonylating agent in the presence of a micelle-containing aqueous system. It was proposed that the decarbonylation and carbonylation reactions take place in different phases. More precisely, the water-

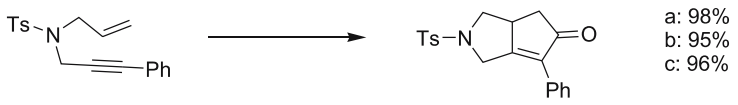

conditions:

a: 5 mol% $Rh(dppp)_2Cl$, 20 eq. cinnamaldehyde, 2h, 120 °C, [69]
b: 5 mol% $[RhCl(cod)]_2$, 11 mol%. dppp, 2 eq. C_6F_5CHO, xylene, 4h, 130 °C [68]
c: 5 mol% $[RhCl(cod)]_2$, 10 mol% dppp, 10 mol% TPPTS, 2 eq. SDS, 10 eq. HCHO, 2h, refluxing water [70]

Equation 12

soluble formaldehyde is decarbonylated in the aqueous phase, enabled by the $[RhCl(cod)]_2$/TPPTS system, while carbonylation takes place in a micelle formed by the surfactant SDS. Also, in this case the yields obtained were good to quantitative (67–96%). Recently, the same group reported on the first asymmetric version of this procedure [71]. By applying the catalyst system $[RhCl(cod)]_2$/(*S*)-tolBINAP, the reactions resulted in ee values of 74–95% and yields up to 83%. Selected examples of PK-type transfer carbonylation reactions are shown in Eq. 12.

6
Conclusions and Outlook

Recent developments have impressively enlarged the scope of Pauson–Khand reactions. Besides the elaboration of strategies for the enantioselective synthesis of cyclopentenones, it is often possible to perform PKR efficiently with a catalytic amount of a late transition metal complex. In general, different transition metal sources, e.g., Co, Rh, Ir, and Ti, can be applied in these reactions. Actual achievements demonstrate the possibility of replacing "external" carbon monoxide by transfer carbonylations. This procedure will surely encourage synthetic chemists to use the potential of the PKR more often in organic synthesis. However, apart from academic research, industrial applications of this methodology are still awaited.

References

1. Schore NE (1988) Chem Rev 88:1081
2. Schore NE (1991) Organ React 40:1
3. Schore NE (1991) In: Trost BM, Fleming I (eds) Comprehensive organic synthesis, vol 5. Pergamon, Oxford, pp 1037–1064
4. Schore NE (1995) In: Hegedus LS (ed) Comprehensive organometallic chemistry II, vol 12. Pergamon, Oxford, pp 703–739
5. Geis O, Schmalz HG (1998) Angew Chem Int Ed 37:911
6. Innate ST, Marco-Contelles J (1988) Org Prep Proc Int 30:121
7. Brummond KM, Kent JL (2000) Tetrahedron 56:3263
8. Gibson SE, Stevenazzi A (2003) Angew Chem Int Ed 42:1800
9. Khand IU, Knox GR, Pauson PL, Watts WE, Foreman MI (1973) J Chem Soc Perkin Trans 1 977
10. Magnus P, Principle LM (1985) Tetrahedron Lett 26:4851
11. Gimbert Y, Lesage D, Milet A, Fournier F, Greene AE, Tabet JC (2003) Org Lett 5:4073
12. Yamanaka M, Nakamura E (2001) J Am Chem Soc 123:1703
13. Schore NE, Croudace MC (1981) J Org Chem 46:5436
14. Jeong N, Lee SJ, Lee BY, Chung YK (1993) Tetrahedron Lett 34:4027
15. Pearson AJ, Dubbert RA (1991) J Chem Soc Chem Commun 202
16. Pearson AJ, Dubbert RA (1994) Organometallics 13:1656

17. Hoye TR, Suriano JA (1993) J Am Chem Soc 115:1154
18. Negishi EI, Takahashi T (1994) Acc Chem Res 27:124
19. Rios R, Pericás MA, Moyano A (2002) Tetrahedron Lett 42:4903
20. Jeong N, Chung YK, Lee BY, Lee SH, Yoo SE (1991) Synlett, p 204
21. Shambayati S, Crowe WE, Schreiber SL (1990) Tetrahedron Lett 31:5289
22. Smit WA, Gybin AS, Shaskov AS, Strychkov YT, Kyzmina LG, Mikaelian GS, Caple R, Swanson ED (1986) Tetrahedron Lett 27:1241
23. Smit WA, Simonyan SO, Tarasov GS, Mikaelian GS, Gybin AS, Ibragimov II, Cable R, Froen O, Kraeger A (1989) Synthesis, p 472
24. Pérez-Serrano L, Casarrubios L, Domínguez G, Pérez-Castells (1999) Org Lett 1:1187
25. Pérez-Serrano L, Blanco-Urgoiti, Casarrubios L, Domínguez G, Pérez-Castells (2000) J Org Chem 65:3513
26. Sugihara T, Yamada M, Yamaguchi M, Nishizawa M (1999) Synlett 6:771
27. Sugihara T, Yamada M, Ban H, Yamaguchi M, Kaneko C (1997) Angew Chem Int Ed 36:2801
28. Rautenstrauch V, Megard P, Conesa J, Kuster W (1990) Angew Chem Int Ed 29:1413
29. Jeong N, Hwang SH, Lee Y, Chung YK (1994) J Am Chem Soc 116:3159
30. Sugihara T, Yamaguchi M (1998) J Am Chem Soc 120:10782
31. Lee NY, Chung YK (1996) Tetrahedron Lett 37:3145
32. Rajesh T, Periasamy M (1999) Tetrahedron Lett 40:817
33. Hwang SH, Lee YW, Lim JS, Jeong N (1997) J Am Chem Soc 119:10549
34. Hayashi M, Hashimoto Y, Yamamoto Y, Usuki J, Saigo K (2000) Angew Chem Int Ed 39:631
35. Son SU, Lee SI, Chung YK (2000) Angew Chem Int Ed 39:4158
36. Berk SC, Grossman RB, Buchwald SL (1993) J Am Chem Soc 115:4912
37. Zhang M, Buchwald SL (1996) J Org Chem 61:4498
38. Hicks FA, Kablaoui NA, Buchwald SL (1996) J Am Chem Soc 118:9450
39. Kondo T, Suzuki N, Okada T, Mitsudo T (1997) J Am Chem Soc 119:6187
40. Morimoto K, Chatani N, Fukumoto Y, Murai S (1997) J Org Chem 62:3762
41. Koga Y, Kobayashi T, Narasaka K (1998) Chem Lett 249
42. Jeong N (1998) Organometallics 17:3642
43. Krafft ME (1988) J Am Chem Soc 110:968
44. Krafft ME, Juliano CA, Scott IL, Wright C, McEachin MD (1991) J Am Chem Soc 113:1693
45. Krafft ME, Juliano CA (1992) J Org Chem 57:5106
46. Itami K, Mitsudo K, Yoshida J (2002) Angew Chem 114:3631
47. Itami K, Mitsudo K, Fujita K, Ohashi Y, Yoshida J (2004) J Am Chem Soc 126:11058
48. Wender PA, Deschamps NM, Gamber GG (2003) Angew Chem Int Ed 42:1853
49. Shibata T, Kadowaki S, Hirase M, Takagi K (2003) Synlett 4:573
50. Jeong N, Seo SD, Shin JY (2000) J Am Chem Soc 122:10220
51. Castro J, Moyano A, Pericàs MA, Riera A, Greene AE, Alvarez-Larena A, Pinella JF (1996) J Org Chem 61:9016
52. Jeong N, Yoo SE, Lee SJ, Lee SH, Chung YK (1991) Tetrahedron Lett 32:2137
53. Castro J, Sörensen H, Riera A, Morin M, Moyano A, Pericàs MA, Greene AE (1990) J Am Chem Soc 112:9388
54. Jamison TF, Shambayati S, Crowe WE, Schreiber SL (1994) J Am Chem Soc 116:5505
55. Nomura I, Mukai C (2004) J Org Chem 69:1803
56. Ishikawa T, Ishii H, Shimizu K, Nakao H, Urano J, Kudo T, Saito S (2004) J Org Chem 69:8133
57. Straus DS, Glass CK (2001) Med Res Rev 21:185

58. Brummond KM, Sill PC, Chen H (2004) Org Lett 6:149
59. Kerr WJ, Lindsay DM, Rankin EM, Scott JM, Watson SP (2000) Tetrahedron Lett 41:3229
60. Derdau V, Laschat S, Jones PG (1998) Heterocycles 48:1445
61. Tormo J, Moyano A, Pericàs MA, Riera A (1997) J Org Chem 62:4851
62. Hicks FA, Buchwald SL (1996) J Am Chem Soc 118:11688
63. Hicks FA, Buchwald SL (1999) J Am Chem Soc 121:7026
64. Jeong N, Sung BK, Choi YK (2000) J Am Chem Soc 122:6771
65. Shibata T, Takagi K (2000) J Am Chem Soc 122:9852
66. Sturla SJ, Buchwald SL (2002) J Org Chem 67:3398
67. Beck CM, Rathmill SE, Park YJ, Chen J, Crabtree RH, Liable-Sands LH, Rheingold AL (1999) Organometallics 18:5311
68. Morimoto T, Fuji K, Tsutsumi K, Kakiuchi K (2002) J Am Chem Soc 124:3806
69. Shibata T, Toshida N, Takagi K (2002) J Org Chem 67:7446
70. Fuji K, Morimoto T, Tsutsumi K, Kakiuchi K (2003) Angew Chem Int Ed 42:2409
71. Fuji K, Morimoto T, Tsutsumi K, Kakiuchi K (2004) Tetrahedron Lett 45:9163

Top Organomet Chem (2006) 18: 179–205
DOI 10.1007/3418_021

Published online: 25 May 2006

Acetic Acid Synthesis by Catalytic Carbonylation of Methanol

Anthony Haynes

Department of Chemistry, University of Sheffield, Dainton Building, Brook Hill, Sheffield S3 7HF, UK
a.haynes@sheffield.ac.uk

1 Introduction 180
1.1 Process Considerations 181

2 Rhodium-Catalysed Carbonylation 183
2.1 Catalytic Mechanism 183
2.2 The Use of Iodide Salts 185
2.3 Promotion by Phosphine Ligands and Derivatives 186
2.4 Model Studies of Reaction Steps with Non-phosphine Ligands 192
2.5 Polymer-Supported Catalysts 194

3 Iridium-Catalysed Carbonylation 196
3.1 Catalytic Mechanism 197
3.2 Effect of Promoters 198
3.2.1 Promotion of the Catalytic Reaction 198
3.2.2 Promotion of the Stoichiometric Carbonylation of $[Ir(CO)_2I_3Me]^-$ 199
3.2.3 Role of Promoters in the Catalytic Process 200

4 Conclusions 202

References 203

Abstract Acetic acid synthesis via the carbonylation of methanol is one of the most important industrial applications of catalysis using organometallic compounds. All the group 9 metals are active, with processes based on cobalt, rhodium and iridium having been developed since the 1960s. This paper surveys some of the more recent approaches employed for improving the performance of the rhodium- and iridium-based catalytic systems. Particular emphasis is placed on how understanding the fundamental organometallic chemistry is crucial for process development. A number of strategies for enhancing the stability and activity of rhodium-based catalysts are discussed, including (i) promotion by iodide salts, (ii) promotion by group 15 and 16 donor ligands and (iii) heterogenisation by ionic attachment of the catalyst to a polymeric support. Both iodide salts and heterogenisation can improve process performance and economics by maintaining catalyst stability at reduced water concentration. The most significant recent development is the commercialisation by BP Chemicals of the iridium-based Cativa^{TM} process. Enhanced stability of iridium catalysts also allows operation at lower water concentration. Mechanistic studies of iridium-catalysed carbonylation are described, and the crucial role of iodide-accepting promoters in enhancing activity is discussed.

Keywords Carbonylation · Catalysis · Rhodium · Iridium · Mechanism

Abbreviations

Ac	Acetyl
Ar	Aryl
bpy	2,2′-Bipyridyl
dppe	Bis(diphenylphosphino)ethane
dppeo	Bis(diphenylphosphino)ethane oxide
dppm	Bis(diphenylphosphino)methane
dppmo	Bis(diphenylphosphino)methane oxide
dppms	Bis(diphenylphosphino)methane sulfide
dppp	Bis(diphenylphosphino)propane
Et	Ethyl
HPIR	High pressure infrared
Me	Methyl
Mes	Mesityl
NHC	*N*-Heterocyclic carbene
Ph	Phenyl
i-Pr	Isopropyl
WGS	Water gas shift

1 Introduction

It is now nearly 40 years since the introduction by Monsanto of a rhodium-catalysed process for the production of acetic acid by carbonylation of methanol [1]. The so-called Monsanto process became the dominant method for manufacture of acetic acid and is one of the most successful examples of the commercial application of homogeneous catalysis. The rhodium-catalysed process was preceded by a cobalt-based system developed by BASF [2, 3], which suffered from significantly lower selectivity and the necessity for much harsher conditions of temperature and pressure. Although the rhodium-catalysed system has much better activity and selectivity, the search has continued in recent years for new catalysts which improve efficiency even further. The strategies employed have involved either modifications to the rhodium-based system or the replacement of rhodium by another metal, in particular iridium. This chapter will describe some of the important recent advances in both rhodium- and iridium-catalysed methanol carbonylation. Particular emphasis will be placed on the fundamental organometallic chemistry and mechanistic understanding of these processes.

Acetic acid is an important bulk commodity chemical, with world annual production capacity of ca. 7 million tonnes. The principal use (ca. 40%) of acetic acid is in the manufacture of vinyl acetate, a monomer of great importance in the polymer industry. A variety of other acetate esters are also

significant derivatives, and acetic acid also finds a major use as a solvent for the oxidation of xylene to terephthalic acid. Other derivatives include cellulose acetate (from acetic anhydride) and monochloroacetic acid (important in pesticides).

Methanol carbonylation has been the subject of several reviews, including Denis Forster's seminal studies at Monsanto [4–10]. This chapter will not seek to repeat all the information included in those reviews but will focus on the role of organometallic chemistry in recent process development.

1.1 Process Considerations

The carbonylation reaction (Eq. 1) involves formal insertion of carbon monoxide into the C – O bond of methanol:

$$MeOH + CO \rightarrow MeCO_2H\,. \tag{1}$$

In a working catalytic system, however, the principal solvent component is acetic acid, so esterification (Eq. 2) leads to substantial conversion of the substrate into methyl acetate. Methyl acetate is activated by reaction with the iodide co-catalyst (Eq. 3):

$$MeOH + AcOH \rightarrow MeOAc + H_2O \tag{2}$$

$$MeOAc + HI \rightarrow MeI + AcOH\,. \tag{3}$$

Transition metal catalysed carbonylation of methyl iodide then gives acetyl iodide (Eq. 4), which is rapidly hydrolysed to the product acetic acid (Eq. 5). The net result of the reactions described in Eqs. 2–5 is the carbonylation of methanol (Eq. 1):

$$MeI + CO \rightarrow MeCOI \tag{4}$$

$$MeCOI + H_2O \rightarrow AcOH + HI\,. \tag{5}$$

As well as playing a role in some of the organic transformations outlined above, excess water is also present as a significant component of the solvent mixture, which helps to maintain catalyst stability (as discussed later).

A typical configuration for a methanol carbonylation plant is shown in Fig. 1. The feedstocks (MeOH and CO) are fed to the reactor vessel on a continuous basis. In the initial product separation step, the reaction mixture is passed from the reactor into a "flash-tank" where the pressure is reduced to induce vapourisation of most of the volatiles. The catalyst remains dissolved in the liquid phase and is recycled back to the reactor vessel. The vapour from the flash-tank is directed into a distillation train which removes methyl iodide, water and heavier by-products (e.g. propionic acid) from the acetic acid product.

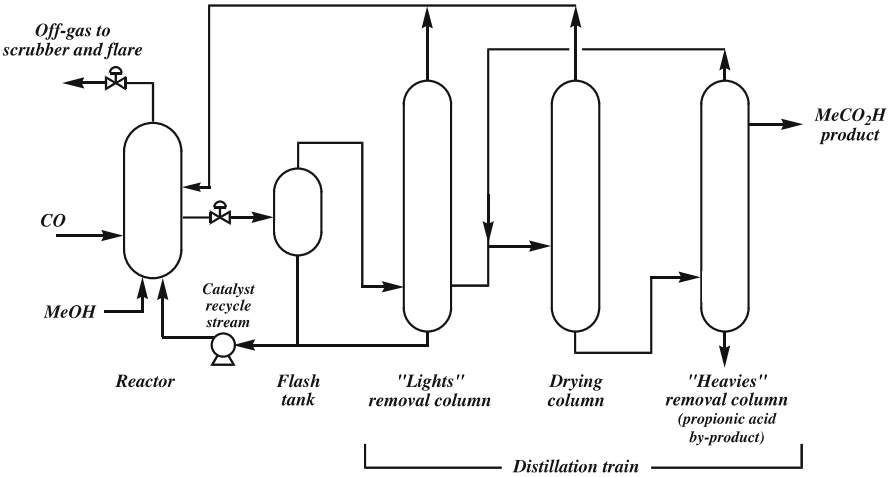

Fig. 1 Schematic diagram of methanol carbonylation plant

Exposure of the reaction mixture to reduced carbon monoxide pressure in the flash-tank has implications for catalyst stability. Since the metal catalyst exists principally as iodocarbonyl complexes (e.g. $[Rh(CO)_2I_2]^-$ and $[Rh(CO)_2I_4]^-$ for the Rh system), loss of CO ligands and precipitation of insoluble metal species (e.g. RhI_3) can be problematic. It is found that catalyst solubility is enhanced at high water concentrations but this results in a more costly separation process to dry the product. The presence of water also results in occurrence of the water gas shift (WGS) reaction (Eq. 6), which can be catalysed by Rh and Ir iodocarbonyls, in competition with the desired carbonylation process, resulting in a lower utilisation of CO:

$$H_2O + CO \rightarrow CO_2 + H_2 \,. \tag{6}$$

From a commercial viewpoint potential benefits can accrue from operating the methanol carbonylation process at low water concentration, provided that catalyst stability can be maintained. Strategies to achieve this include (i) addition of iodide salts to stabilise the Rh catalyst, (ii) heterogenisation of the Rh catalyst on a polymer support to restrict the catalyst to the reactor and (iii) replacement of Rh by a more robust Ir catalyst. These strategies, along with others for improving catalyst activity, will be discussed in the following sections.

2
Rhodium-Catalysed Carbonylation

2.1
Catalytic Mechanism

The Monsanto catalyst system has been the subject of numerous studies (for leading references see [4–10]). The kinetics of the overall carbonylation process are zero-order in both reactants (MeOH and CO) but first order in rhodium catalyst and methyl iodide co-catalyst. This behaviour is interpreted on the basis of the well-established catalytic cycle shown in Scheme 1, comprising a sequence of reactions of anionic rhodium complexes. The active catalyst (identified by in situ high-pressure infrared (HPIR) spectroscopy [11]) is the square-planar Rh(I) complex, *cis*-$[Rh(CO)_2I_2]^-$. Oxidative addition of methyl iodide to this complex is the rate-determining step of the cycle, consistent with the observed kinetics. Rate measurements on the stoichiometric reaction of $[Rh(CO)_2I_2]^-$ with MeI have confirmed this to be second-order, with activation parameters comparable to those for the overall carbonylation process [12]. The octahedral Rh(III) methyl complex resulting from oxidative addition is short-lived and undergoes rapid methyl migration to give an acetyl complex. The reactive methyl complex, $[Rh(CO)_2I_3Me]^-$ was not observed in the original studies by Forster. However, Haynes et al. found that this key intermediate could be detected spectroscopically by using very

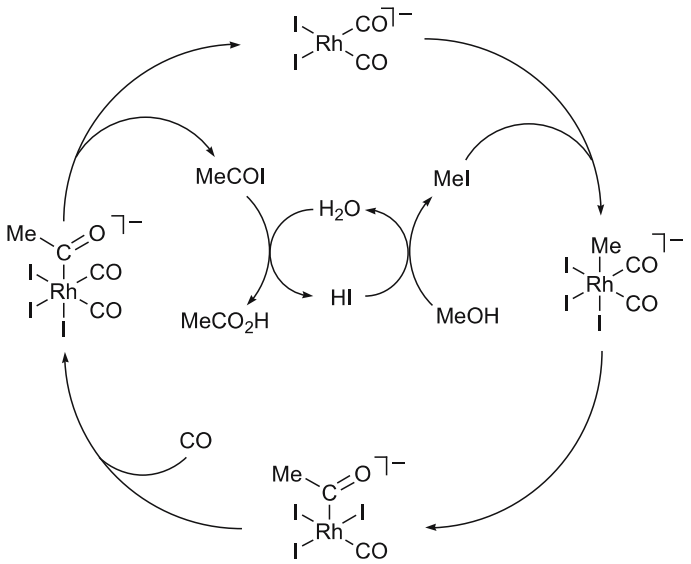

Scheme 1 Catalytic cycle for Rh-catalysed methanol carbonylation

high [MeI] to increase its steady state concentration during the stoichiometric reaction of $[Rh(CO)_2I_2]^-$ with MeI [13, 14]. This enabled the rate of the subsequent methyl migration reaction to be quantified.

The acetyl complex, $[Rh(CO)I_3(COMe)]^-$, exists as an iodide bridged dimer $[\{Rh(CO)I_2(\mu-I)(COMe)\}_2]^{2-}$ in the solid state [15] (and in non-coordinating solvents) but is easily cleaved to monomeric species ($[Rh(CO)(sol)I_3(COMe)]^-$ or $[Rh(CO)(sol)_2I_2(COMe)]$) in coordinating solvents [16, 17]. Coordination of CO to $[Rh(CO)I_3(COMe)]^-$ is rapid, giving the *trans*-dicarbonyl acetyl species, $[Rh(CO)_2I_3(COMe)]^-$, which can eliminate acetyl iodide to regenerate the active Rh(I) species. The *cis*-dicarbonyl isomer of $[Rh(CO)_2I_3(COMe)]^-$ can also be formed by oxidative addition of acetyl iodide to $[Rh(CO)_2I_2]^-$, subsequent geometrical isomerisation leading to the thermodynamically preferred *trans* isomer [18]. The observation that acetyl iodide readily adds to $[Rh(CO)_2I_2]^-$ shows that, for the overall catalytic reaction to be driven forward, the acetyl iodide must be scavenged by hydrolysis. An alternative to sequential reductive elimination and hydrolysis of acetyl iodide is direct reaction of water with a Rh acetyl complex to give acetic acid. The relative importance of these two alternative pathways has not yet been fully determined, although the catalytic mechanism is normally depicted as proceeding via reductive elimination of acetyl iodide from the rhodium centre. In addition to the experimental studies of the catalytic mechanism, some theoretical studies have also appeared in the recent literature [19–24].

It has already been noted in the Introduction that the WGS reaction occurs in competition with methanol carbonylation. The mechanism of the WGS reaction involves oxidation of Rh(I) to Rh(III) by reaction with HI, as shown in Scheme 2 [25].

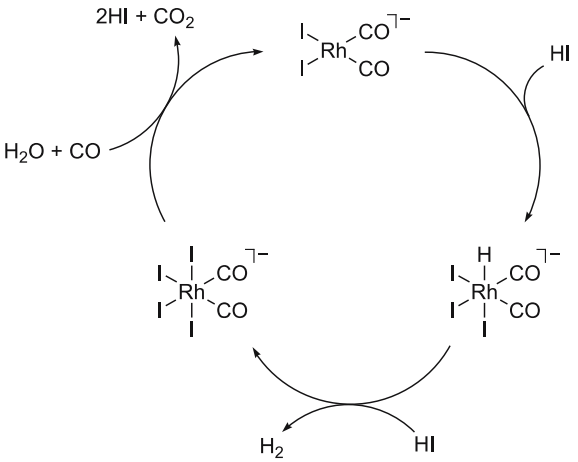

Scheme 2 Cycle for the rhodium-catalysed WGS reaction

Reaction of $[Rh(CO)_2I_2]^-$ with HI initially gives the hydride, $[Rh(CO)_2I_3H]^-$ [26] but this reacts readily with a second equivalent of HI to release H_2 and form the tetraiodide complex, $[Rh(CO)_2I_4]^-$. As in the case of the acetyl complex, $[Rh(CO)_2I_3(COMe)]^-$, both the hydride and the tetraiodide are more stable as the *trans*-dicarbonyl isomers. Addition of I_2 to *cis*-$[Rh(CO)_2I_2]^-$ initially gives *cis*-$[Rh(CO)_2I_4]^-$ and a kinetic study of the *cis–trans* isomerisation suggested a mechanism involving loss of a CO ligand [27]. In situ HPIR measurements revealed the presence of $[Rh(CO)_2I_4]^-$ alongside $[Rh(CO)_2I_2]^-$ under conditions of low water concentration [28] and during the anhydrous carbonylation of methyl acetate to acetic anhydride [29]. The tetraiodide is regarded as an inactive form of the catalyst and it is desirable to tune conditions to minimise its concentration. Loss of CO from $[Rh(CO)_2I_4]^-$, in regions of reduced CO pressure, is also thought to lead to $[Rh(CO)(sol)I_4]^-$, a precursor to precipitation of insoluble rhodium species. Increasing the water concentration results in acceleration of the reduction of $[Rh(CO)_2I_4]^-$ back to the active Rh(I) catalyst, completing the WGS reaction cycle, as depicted on the left hand side of Scheme 2. Thus, high water concentration helps both to keep the Rh catalyst in its active form and to prevent catalyst precipitation. Related to this, the rate of rhodium-catalysed carbonylation shows a dependence on water concentration which increases and then reaches a plateau above ca. 10 wt % H_2O.

2.2 The Use of Iodide Salts

One approach which enables lower water concentrations to be used for rhodium-catalysed methanol carbonylation is the addition of iodide salts, especially lithium iodide, as exemplified by the Hoechst-Celanese *Acid Optimisation* (AO) technology [30]. Iodide salt promoters allow carbonylation rates to be achieved at low (< 4 M) $[H_2O]$ that are comparable with those in the conventional Monsanto process (where $[H_2O] > 10$ M) while maintaining catalyst stability. In the absence of an iodide salt promoter, lowering the water concentration would result in a decrease in the proportion of Rh existing as $[Rh(CO)_2I_2]^-$. However, in the iodide-promoted process, a higher concentration of methyl acetate is also employed, which reacts with the other components as shown in Eqs. 3, 7 and 8:

$$MeOAc + LiI \rightarrow MeI + LiOAc \quad (7)$$

$$LiOAc + HI \rightarrow LiI + AcOH\,. \quad (8)$$

Raising the methyl acetate concentration results in a lowering of the HI concentration via these equilibria, which slows down the reaction of HI with $[Rh(CO)_2I_2]^-$ in the WGS cycle. This inhibits conversion of $[Rh(CO)_2I_2]^-$ into

$[Rh(CO)_2I_4]^-$, which is beneficial for catalytic activity and also suppresses the WGS reaction significantly.

Evidence has been presented that iodide salts can promote the oxidative addition of MeI to $[Rh(CO)_2I_2]^-$, the rate-determining step in the Rh cycle [12]. The precise mechanism of this promotion remains unclear; formation of a highly nucleophilic dianion, $[Rh(CO)_2I_3]^{2-}$, has been suggested, although there is no direct spectroscopic evidence for its detection. Possible participation of this dianion has been considered in a theoretical study [23]. An alternative nucleophilic dianion, $[Rh(CO)_2I_2(OAc)]^{2-}$, has also been proposed [31, 32] on the basis that acetate salts (either added or generated in situ via Eq. 7) can promote carbonylation. Iodide salts have also been found to be effective promoters for the anhydrous carbonylation of methyl acetate to acetic anhydride [33]. In the absence of water, the catalyst cannot be maintained in its active form ($[Rh(CO)_2I_2]^-$) by addition of LiI alone, and some H_2 is added to the gas feed to reduce the inactive $[Rh(CO)_2I_4]^-$.

2.3 Promotion by Phosphine Ligands and Derivatives

On the basis that the rate-determining step for rhodium/iodide-catalysed methanol carbonylation is the oxidative addition of MeI to Rh(I), numerous attempts have been made to improve catalytic activity by introduction of strongly donating ligands that increase the nucleophilicity of the Rh centre. These studies have typically employed phosphine ligands and their derivatives. For example, Rankin et al. demonstrated that the very basic triethylphosphine ligand, combined with a rhodium/iodide catalyst system, resulted in initial catalytic carbonylation activity almost double that found in the absence of phosphine [34]. The reaction was first order in MeI and zero order in CO, consistent with rate-determining oxidative addition of MeI to Rh(I). Kinetic studies showed that the increased electron density on the metal centre imparted by the PEt_3 ligands results in much higher nucleophilicity, with oxidative addition of MeI to *trans*-$[Rh(CO)(PEt_3)_2I]$ occurring 57 times faster than to $[Rh(CO)_2I_2]^-$ at 25 °C. The Rh(III) methyl product, $[Rh(CO)(PEt_3)_2I_2Me]$, has sufficient stability to be isolated and crystallographically characterised, in contrast to the very reactive $[Rh(CO)_2I_3Me]^-$. Carbonylation of $[Rh(CO)(PEt_3)_2I_2Me]$ to give $[Rh(CO)(PEt_3)_2I_2(COMe)]$ is 38 times slower than methyl migration in $[Rh(CO)_2I_3Me]^-$, which can be ascribed to the effect of increased back-donation from Rh to CO, combined with a stronger Rh – Me bond. Despite the high initial activity, catalyst degradation occurs via loss of phosphine ligand (to give Et_3PI^+, Et_3PH^+, Et_3PMe^+ and Et_3PO), the rhodium catalyst reverting to $[Rh(CO)_2I_2]^-$.

The problem of phosphine ligand dissociation and degradation is a common in attempts to modify the rhodium carbonylation catalyst. This arises from the relatively harsh conditions employed (i.e. aqueous acetic acid, HI,

150–200 °C, high pressure CO), which necessitate extremely robust complexes for prolonged use as catalysts.

Several studies have taken advantage of the chelate effect in attempts to stabilise the ligand–metal interactions. Wegman and coworkers found that the bidentate phosphine oxide ligand, $Ph_2PCH_2CH_2P(O)Ph_2$ (dppeo), gave a rhodium catalyst that had good activity for methanol carbonylation under relatively mild conditions [35]. Mechanistic studies indicated that the dppeo ligand exhibited hemi-labile behaviour, with the oxygen donor being quite easily displaced from Rh(I) by CO as shown in Scheme 3. The resulting *cis*-dicarbonyl with a monodentate dppeo ligand was the only Rh species observed by in situ HPIR spectroscopy under catalytic conditions with no evidence for $[Rh(CO)_2I_2]^-$. Reaction of $[Rh(CO)_2(\kappa^1\text{-dppeo})Cl]$ with MeI was found to lead rapidly to acetyl iodide. When dppeo (which forms a six-membered chelate ring) was replaced by the shorter chain analogue $Ph_2PCH_2P(O)Ph_2$ (dppmo), the corresponding chelate complex was found to be less easily disrupted, with only traces of $[Rh(CO)_2(\kappa^1\text{-dppmo})Cl]$ being detectable when $[Rh(CO)(\kappa^2\text{-dppmo})Cl]$ was placed under 3 atm CO.

Despite the promising catalytic activity exhibited by the dppeo ligand under mild conditions, it gave only a marginal rate improvement compared with $[Rh(CO)_2I_2]^-$ when tested by Baker et al. under conditions closer to those used commercially [36]. Likewise, neither dppmo nor $Ph_2PN(Ph)P(S)Ph_2$ proved particularly effective at 185 °C. By contrast, substantial acceleration of catalysis was obtained when using the diphosphine sulfide ligand, $Ph_2PCH_2P(S)Ph_2$ (dppms), which gave rates up to 8.5 times faster than the non-ligand promoted rhodium catalyst. The highest activity was found for a ligand:Rh ratio of 1 : 1 and in situ HPIR spectroscopy identified [Rh(CO)(dppms)I] as the only detectable species under catalytic conditions. An X-ray crystallographic study of the chloride analogue revealed a square planar geometry with the CO *trans* to the sulfur donor atom of the bidentate dppms ligand. Initial mechanistic studies showed that [Rh(CO)(dppms)I] reacts readily with MeI to give the acetyl complex $[Rh(dppms)I_2(COMe)]$ but the presumed intermediate Rh(III) methyl species was not detected by NMR spectroscopy. Addition of CO to $[Rh(dppms)I_2(COMe)]$ gives two isomers of $[Rh(CO)(dppms)I_2(COMe)]$ that can reductively eliminate acetyl iodide to complete the catalytic cycle shown in Scheme 4. In contrast to the dppeo system, no evidence for hemi-labile behaviour was found for the dppms ligand. Analogous catalytic cycles were

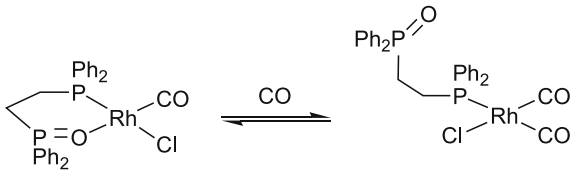

Scheme 3 Hemi-labile behaviour of [Rh(CO)(dppeo)Cl]

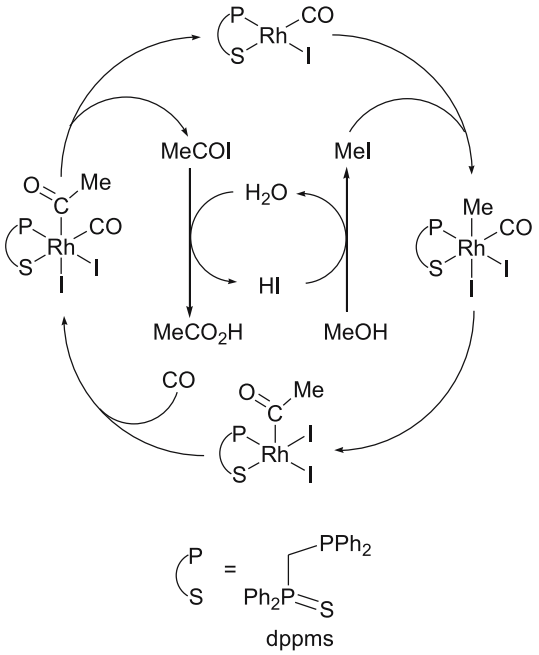

Scheme 4 Catalytic cycle for catalytic carbonylation with [Rh(CO)(dppms)I]

proposed for reactions employing the P,S chelating phosphino-thiother ligands, $Ph_2PCH_2CH_2SMe$ and $Ph_2PC_6H_4$-2-SMe, which also displayed enhanced catalytic activity relative to $[Rh(CO)_2I_2]^-$ [37].

Further detailed studies of the dppms system were undertaken by Gonsalvi et al. [38, 39]. As expected, kinetic measurements showed that oxidative addition of MeI to [Rh(CO)(dppms)I] is substantially (ca. 40 times) faster than to $[Rh(CO)_2I_2]^-$ at 25 °C. The rate enhancement arises from the good electron donor properties of the dppms ligand, and is similar to that found in the same study for [Rh(CO)(dppe)I] and by Rankin et al. for $[Rh(CO)(PEt_3)_2I]$ [34]. Using the same strategy as that employed previously to detect $[Rh(CO)_2I_3Me]^-$, it was shown that the reactive Rh(III) methyl intermediate $[Rh(CO)(dppms)I_2Me]$ could be detected during the stoichiometric reaction of [Rh(CO)(dppms)I] with high concentrations of MeI. The observation of this intermediate allowed its rate constant for methyl migration to be estimated. Surprisingly, the rate of methyl migration is an order of magnitude larger for $[Rh(CO)(dppms)I_2Me]$ than for $[Rh(CO)_2I_3Me]^-$. This contrasts with the normal retardation of methyl migration by phosphine ligands, as exemplified by $[Rh(CO)(dppe)I_2Me]$ which reacts an order of magnitude *slower* than $[Rh(CO)_2I_3Me]^-$ [34]. One explanation for the unexpectedly fast migratory CO insertion in $[Rh(CO)(dppms)I_2Me]$ was suggested by examination of X-ray crystal structures of dppms complexes (Fig. 2).

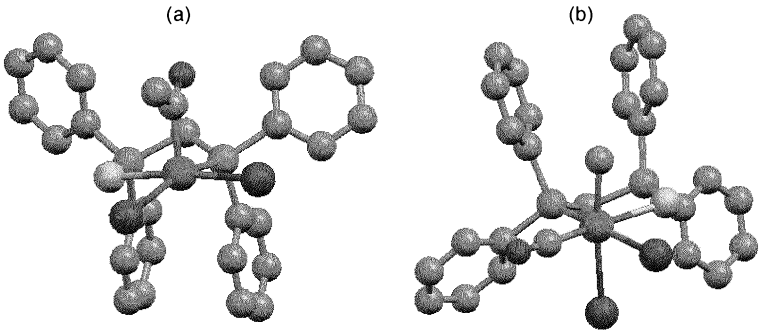

Fig. 2 X-ray structures of **a** [Rh(dppms)I_2(COMe)] and **b** [Ir(CO)(dppms)I_2Me]

Of particular interest in these structures was the conformation of the phenyl substituents on the phosphorus atoms. In the distorted square pyramidal [Rh(dppms)I_2(COMe)] two phenyls are stacked almost parallel, flanking the vacant coordination site *trans* to the acetyl ligand. Similar conformations of the dppms ligand are found in square planar complexes (e.g. [Rh(dppms)(CO)Cl] [36]) in which two phenyl groups tend to align so that approach to one face of the complex is hindered. In the octahedral [Ir(CO)(dppms)I_2Me] (a stable analogue of the reactive Rh species), there are no vacant coordination sites, and the two axial phenyls create a crowded pocket enclosing the methyl ligand. The presence of the methyl ligand causes the two axial phenyls to deviate from their preferred near-parallel arrangement. In the analogous Ir(III) ethyl complex, the ethyl ligand causes an even more substantial change in the conformation of the dppms ligand substituents. On the basis of these structural features, it was suggested that inter-ligand steric interactions destabilise [Rh(CO)(dppms)I_2Me] and provide a driving force for methyl migration to give the acetyl product. A reaction scheme depicting the proposed changes in ligand conformation during oxidative addition and migratory CO insertion steps is shown in Scheme 5.

Two separate computational investigations of the Rh/dppms catalyst and related systems have appeared in the literature. One study [40] concluded that steric effects were important in promoting migratory CO insertion in [Rh(CO)(dppms)I_2Me], while the other [41] proposed that an electronic effect, arising from the sulfur donor atom of dppms, was responsible. It is likely that a combination of steric and electronic effects result in the observed reactivity.

Dutta and coworkers used a functionalised triarylphosphine ligand, $PPh_2(C_6H_4$-2-$CO_2Me)$, which contains an *ortho*-ester substituent on one of the phenyl groups, with the potential for chelate formation [42]. Rhodium(I) complexes were synthesised containing one or two coordinated phosphines, as illustrated in Scheme 6. In the mono(phosphine) complex, chelation via the ester carbonyl group occurs to form a six-membered ring reminiscent of the structure formed by dppeo (Scheme 3) [35]. A crystal structure of

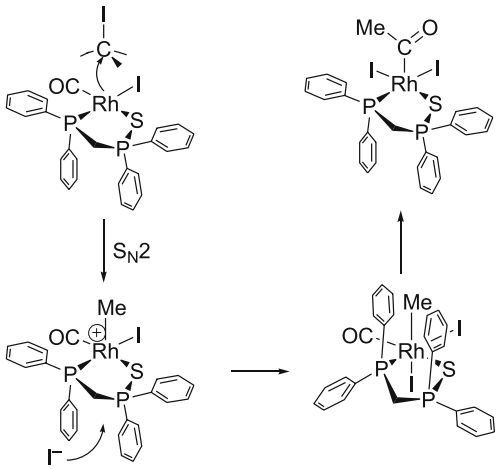

Scheme 5 Proposed mechanism for reaction of [Rh(CO)(dppms)I] with MeI

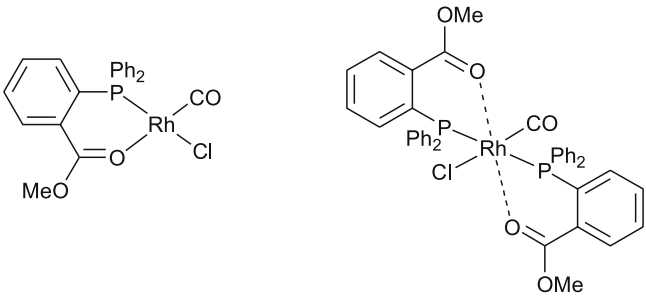

Scheme 6 Rhodium complexes of an ester-functionalised phosphine ligand

the bis(phosphine) complex indicates the presence of secondary Rh – O interactions with the ester groups of the phosphines. The ν(CO) frequencies reflect high electron density at the metal centre in both complexes, which were found to react readily with MeI to give Rh(III) acetyl products, *via* unstable Rh(III) methyl intermediates. When tested as catalysts for methanol carbonylation (at 135 °C), both complexes were more active than the PPh_3 analogue and the non-phosphine promoted $[Rh(CO)_2I_2]^-$ system. The chelate mono(phosphine) complex had the highest activity, but it is unclear whether the chelate structure is maintained throughout the catalytic reaction.

Diphosphine ligands (e.g. dppe, dppp) were originally found, by Wegman and coworkers [43], to be effective ligands in the rhodium-catalysed reductive carbonylation of methanol to give acetaldehyde (Eq. 9) or ethanol (Eq. 10):

$$MeOH + CO + H_2 \rightarrow MeCHO + H_2O \quad (9)$$

$$MeOH + CO + 2H_2 \rightarrow EtOH + H_2O\,. \quad (10)$$

The mechanism of these reactions is closely related to that for conventional methanol carbonylation, but with a rhodium acetyl intermediate being intercepted by H_2 to give acetaldehyde (which can subsequently be hydrogenated to ethanol). Pringle and coworkers tested a series of unsymmetrical fluorinated diphosphine ligands, $Ph_2PCH_2CH_2PAr^F{}_2$ for rhodium-catalysed methanol carbonylation (Scheme 7) [44]. These ligands were designed to mimic the unsymmetrical coordination characteristics of heterofunctional bidentate ligands such as dppeo and dppms discussed above. The unsymmetrical ligands gave catalysts with high selectivity to acetic acid and higher activity than a catalyst based on the symmetrical dppe ligand. However, all the catalysts tested were less active than the $[Rh(CO)_2I_2]^-$ system. In situ HPIR spectroscopy showed the absence of bands due to $[Rh(CO)_2I_2]^-$ and it was inferred that the diphosphine ligand remains coordinated to Rh during catalysis. In support of this, a Rh(III) complex [Rh(CO)(diphosphine)I_3] was isolated at the end of the catalytic experiment and characterised crystallographically for the diphosphine ligand with Ar^F = 3-F-C_6H_4.

Trans-chelating ligands have been developed by Süss-Fink et al. using condensation reactions of 2-diphenyl-phosphinobenzoic acid with appropriate diols or amino alcohols [9, 45]. The ligands were found to coordinate to square planar Rh(I) in a *trans*-chelating manner in [Rh(CO)(κ^2-diphosphine)Cl] or as a bridging ligands in a dinuclear complex, [{Rh(CO)(μ,κ^1,κ^1diphosphine)Cl}$_2$] (when the diphosphine has a longer linker group) as shown in Scheme 8. When tested in rhodium-catalysed methanol carbonylation, the ligands all gave enhanced activity relative to $[Rh(CO)_2I_2]^-$. For one of the ligands, two isomers of a dinuclear Rh(III) acetyl complex

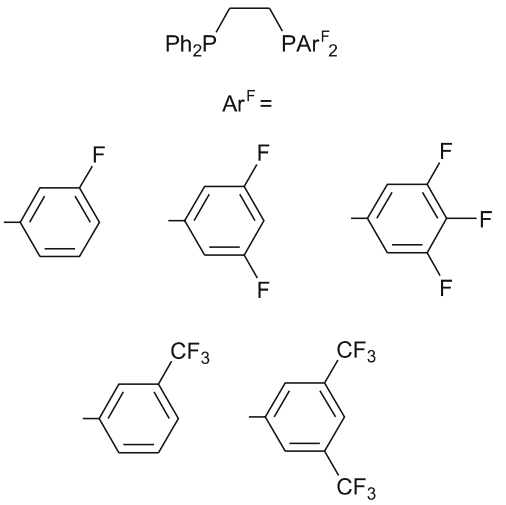

Scheme 7 Unsymmetrical fluorinated diphosphine ligands

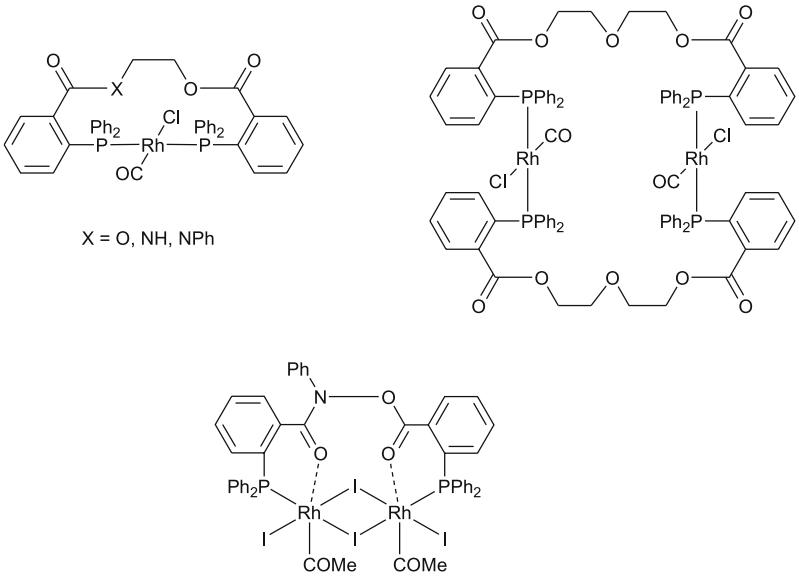

Scheme 8 Rhodium complexes of *trans*-chelating diphosphine ligands

were isolated from the catalytic reaction solution, or from the reaction of [Rh(CO)(diphosphine)Cl] with MeI. The *cisoid* isomer is shown in Scheme 8 and is bridged by a single diphosphine ligand and two iodides. Octahedral coordination about each Rh centre is completed by interaction with carbonyl oxygens on the diphosphine ligand backbone.

2.4
Model Studies of Reaction Steps with Non-phosphine Ligands

The influence of steric effects on the rates of oxidative addition to Rh(I) and migratory CO insertion on Rh(III) was probed in a study of the reactivity of a series of [Rh(CO)(α-diimine)I] complexes with MeI (Scheme 9) [46]. For α-diimine ligands of low steric bulk (e.g. bpy, $\mathbf{L}^1$, $\mathbf{L}^4$, $\mathbf{L}^5$) fast oxidative addition of MeI was observed (10^3–10^4 times faster than $[Rh(CO)_2I_2]^-$) and stable Rh(III) methyl complexes resulted. For more bulky α-diimine ligands (e.g. $\mathbf{L}^2$, $\mathbf{L}^3$, $\mathbf{L}^6$) containing ortho-alkyl groups on the *N*-aryl substituents, oxidative addition is inhibited but methyl migration is promoted, leading to Rh(III) acetyl products. The results obtained from this model system demonstrate that steric effects can be used to tune the relative rates of two key steps in the carbonylation cycle.

Steric effects were also found to be important for determining the reactivity of rhodium complexes containing *N*-heterocyclic carbene (NHC) ligands [47] (Scheme 10), which have been the subject of intense in-

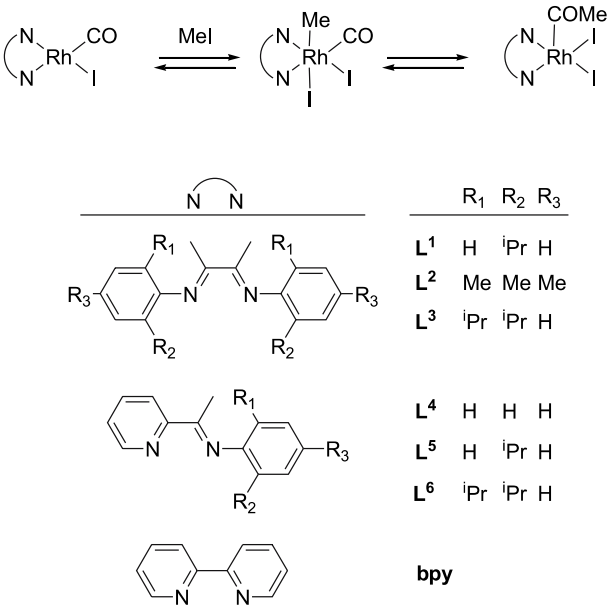

Scheme 9 Reactions of [Rh(CO)(α-diimine)I] complexes with MeI

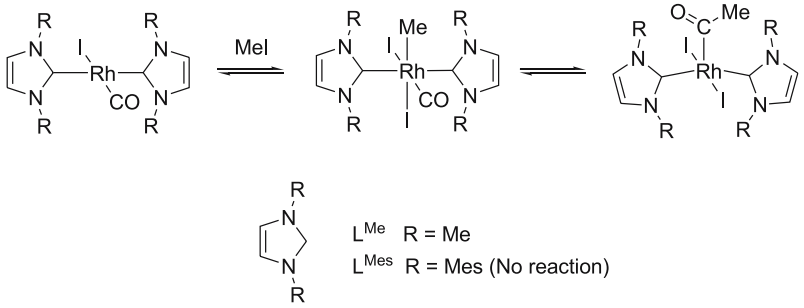

Scheme 10 Reactions of [Rh(CO)$(NHC)_2$I] complexes with MeI

terest in recent years. Methyl iodide reacts 3.5 times more slowly with *trans*-[Rh(CO)$(L^{Me})_2$I] (ν(CO) 1943 cm^{-1}) than with *trans*-[Rh(CO)$(PEt_3)_2$I] (ν(CO) 1961 cm^{-1}) despite the stronger electron donor power of the NHC ligand (as indicated by the IR frequencies). The nucleophilicity of the Rh centre is moderated by the *N*-methyl substituents on the NHC ligands, which tend to block the axial sites of the square planar reactant complex. As for the bulky bidentate diimine systems discussed above, steric effects of the L^{Me} ligands destabilise the Rh(III) methyl intermediate encouraging migratory CO insertion to give a Rh(III) acetyl product. For the very bulky L^{Mes} ligand, reaction of *trans*-[Rh(CO)$(L^{Mes})_2$I] with MeI was completely blocked.

Although the bonds formed between transition metals and NHC ligands are regarded as being very strong, it was found that *trans*-$[Rh(CO)(L^{Me})_2I]$ degraded under quite mild conditions. When tested for catalytic methanol carbonylation activity at 120 °C, HPIR spectroscopy showed that the complex lost its NHC ligands sequentially to give first $[Rh(CO)_2(L^{Me})_2I]$ and eventually $[Rh(CO)_2I_2]^-$. The NHC ligands are presumably protonated (or methylated) at the carbene carbon to give imidazolium cations.

2.5 Polymer-Supported Catalysts

An important requirement for all homogeneous catalytic processes is that the dissolved catalyst must be separated from the liquid product and recycled to the reactor without significant catalyst loss. One approach to aid this separation process is to immobilise (or "heterogenise") the homogeneous catalyst on a solid support in order to confine the catalyst to the reactor and overcome the need for a separate catalyst recycling step. A number of types of solid support have been employed to heterogenise rhodium catalysts for methanol carbonylation. These were reviewed by Howard et al. (1993) [6] and include activated carbon, inorganic oxides, zeolites and a range of polymeric materials. One frequent approach to catalyst immobilisation is covalent attachment, in which the support (e.g. carbon or polystyrene) is modified to contain a pendant group (usually a phosphine) capable of acting as a ligand for the metal complex. However, the susceptibility of covalently bound systems to metal–ligand bond cleavage (as discussed above for homogeneous rhodium complexes) makes irreversible leaching of the catalyst from the solid support a serious problem. This is particularly the case for methanol carbonylation, as pendant phosphines are prone to degradation by the aqueous acidic medium and quaternisation by methyl iodide.

An alternative strategy for catalyst immobilisation uses ion-pair interactions between ionic catalyst complexes and polymeric ion exchange resins. Since all the rhodium complexes in the catalytic methanol carbonylation cycle are anionic, this is an attractive candidate for ionic attachment. In 1981, Drago et al. described the effective immobilisation of the rhodium catalyst on polymeric supports based on methylated polyvinylpyridines [48]. The activity was reported to be equal to the homogeneous system at 120 °C with minimal leaching of the supported catalyst. The ionically bound complex $[Rh(CO)_2I_2]^-$ was identified by infrared spectroscopic analysis of the impregnated resin.

The ionic attachment strategy for catalytic methanol carbonylation has recently seen a resurgence of interest from both industry [49–53] and academic groups [54–57]. Most significantly, in 1998 Chiyoda and UOP announced their *Acetica*™ process, which uses a polyvinylpyridine resin tolerant of elevated temperatures and pressures [8, 58]. The process attains increased

catalyst loading in the reactor (due to removal of solubility constraints of the homogeneous system) and reduced by-product formation as a consequence of lower water concentration (3–7 wt %). Catalytic carbonylation rates comparable to the homogeneous high water system can be achieved. The ionic attachment is extremely effective with a very low Rh concentration (< 0.5 wt – ppm) in the effluent from the reactor.

A mechanistic study by Haynes et al. demonstrated that the same basic reaction cycle operates for rhodium-catalysed methanol carbonylation in both homogeneous and supported systems [59]. The catalytically active complex $[Rh(CO)_2I_2]^-$ was supported on an ion exchange resin based on poly(4-vinylpyridine-*co*-styrene-*co*-divinylbenzene) in which the pendant pyridyl groups had been quaternised by reaction with MeI. Heterogenisation of the Rh(I) complex was achieved by reaction of the quaternised polymer with the dimer, $[Rh(CO)_2I]_2$ (Scheme 11). Infrared spectroscopy revealed ν(CO) bands for the supported $[Rh(CO)_2I_2]^-$ anions at frequencies very similar to those observed in solution spectra. The structure of the supported complex was confirmed by EXAFS measurements, which revealed a square planar geometry comparable to that found in solution and the solid state. The first X-ray crystal structures of salts of $[Rh(CO)_2I_2]^-$ were also reported in this study.

The use of thin polymer films allowed the reaction of supported $[Rh(CO)_2I_2]^-$ with MeI to be monitored directly, by in situ IR spectroscopy. The reactivity was very similar to that found in solution, with oxidative addition of

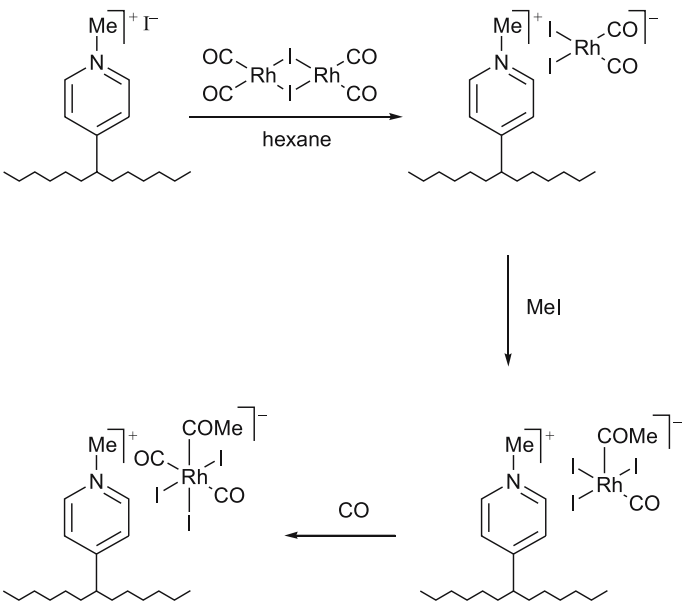

Scheme 11 Formation and reactions of polymer-supported $[Rh(CO)_2I_2]^-$

MeI followed by rapid migratory CO insertion to give $[Rh(CO)(COMe)I_3]_n^{n-}$ (which could be monomeric or dimeric). Kinetic measurements showed the reaction to be first order in both $[Rh(CO)_2I_2]^-$ and MeI and the observed pseudo-first order rate constants at a given MeI concentration were comparable with those in homogeneous solution. The close similarity in kinetic behaviour for homogeneous and heterogeneous reactions suggests that the permeability of the macroporous polymer to MeI is high, and that the reaction rate is not mass-transfer limited. Exposure of a polymer film containing supported $[Rh(CO)(COMe)I_3]_n^{n-}$ to CH_2Cl_2 saturated with CO resulted in rapid formation of IR bands due to the *trans*-dicarbonyl complex $[Rh(CO)_2(COMe)I_3]^-$. Over several hours, the dicarbonyl acetyl species decomposed slowly to give $[Rh(CO)_2I_2]^-$, presumably via reductive elimination of acetyl iodide. Thus the same organometallic steps of the homogeneous catalytic carbonylation cycle illustrated in Scheme 1 can be demonstrated under mild conditions in the supported system.

3 Iridium-Catalysed Carbonylation

It was discovered by Monsanto that methanol carbonylation could be promoted by an iridium/iodide catalyst [1]. However, Monsanto chose to commercialise the rhodium-based process due to its higher activity under the conditions used. Nevertheless, considerable mechanistic studies were conducted into the iridium-catalysed process, revealing a catalytic mechanism with similar key features but some important differences to the rhodium system [60].

In 1996, BP Chemicals announced a new methanol carbonylation process, *Cativa*™, based upon a promoted iridium/iodide catalyst which now operates on a number of plants worldwide [61–69]. Promoters, which enhance the catalytic activity, are key to the success of the iridium-based process. The mechanistic aspects of iridium-catalysed carbonylation and the role of promoters are discussed in the following sections.

A great advantage of iridium, compared to rhodium is that a broad range of conditions are accessible for the Ir catalyst without precipitation of IrI_3 occurring. The greater stability of the iridium catalyst can be ascribed to stronger metal–ligand bonding for the third-row metal, which inhibits CO loss from the Ir centre. Stronger back-donation from iridium to CO is evident from the lower ν(CO) values of iridium iodocarbonyl complexes compared to the rhodium analogues. The rate of iridium-catalysed carbonylation displays a rather complicated dependence on a range of process variables such as pCO, [MeI], [MeOAc] and $[H_2O]$. The catalytic rate displays a strong positive dependence on [MeOAc] but is is zero order in [MeI] above a limiting threshold and independent of CO partial pressure above ca. 10 bar.

A particularly interesting aspect is the dependence of rate on $[H_2O]$ which attains a maximum at ca. 5 wt % H_2O. The ability to operate at relatively low $[H_2O]$ results in a less costly product purification than the high-water rhodium system.

3.1 Catalytic Mechanism

Mechanistic studies of iridium/iodide-catalysed methanol carbonylation have been reported by Forster [60] and others [70–75]. The catalytic cycle involves the same fundamental steps as the rhodium system: oxidative addition of MeI to Ir(I), followed by migratory CO insertion to form an Ir(III) acetyl complex. On the basis of spectroscopic and kinetic observations, Forster proposed that two different (but linked) cycles exist, one involving neutral iridium complexes, and the other predominantly involving anionic species (Scheme 12). Similar cycles were also proposed for the competing WGS reaction. At low concentrations of water and iodide, the "neutral cycle" operates, with $[Ir(CO)_3I]$ as the resting state and rate-determining oxidative addition of MeI to $[Ir(CO)_2I]$. At higher iodide concentrations the "anionic cycle" predominates. Model kinetic studies [76, 77] have shown that addition of MeI to $[Ir(CO)_2I_2]^-$ is ca. 100 times faster than to $[Rh(CO)_2I_2]^-$, and gives a stable Ir(III) methyl complex, *fac,cis*-$[Ir(CO)_2I_3Me]^-$ which is the resting state of the

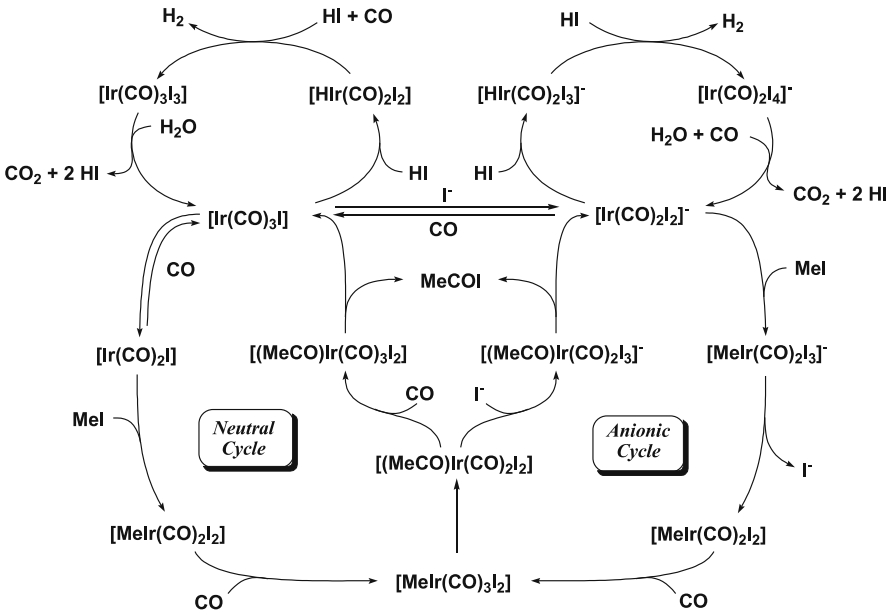

Scheme 12 Catalytic cycles for iridium-catalysed methanol carbonylation

catalyst in the anionic cycle. Under these conditions, the rate of catalysis is inhibited by ionic iodide and it was proposed that the rate-determining step involves dissociative substitution of I^- by CO in $[Ir(CO)_2I_3Me]^-$, followed by migratory CO insertion in the tricarbonyl, $[Ir(CO)_3I_2Me]$.

The neutral tricarbonyl was not observed by Forster, but was eventually characterised spectroscopically under CO pressure by Ghaffar et al. [73, 78]. HPIR and HPNMR experiments showed that $[Ir(CO)_3I_2Me]$ is formed by the reaction of the dimer, $[Ir(CO)_2I_2Me]_2$ with CO. The product has a *fac* arrangement of carbonyl ligands and is much more reactive toward migratory CO insertion than the anion, $[Ir(CO)_2I_3Me]^-$ (ca. 700 times faster at 85 °C). The increased reactivity can be ascribed to increased competition for backbonding in the tricarbonyl, which increases the electrophilicity of the CO ligands, encouraging intramolecular nucleophilic attack by the methyl ligand. A lower activation barrier for migratory CO insertion in $[Ir(CO)_3I_2Me]$ is supported by theoretical calculations [20, 23, 73].

3.2 Effect of Promoters

3.2.1 Promotion of the Catalytic Reaction

A range of compounds can enhance the activity of an iridium catalyst [61–64, 67–69, 73]. The promoters fall into two categories: (i) carbonyl or halocarbonyl complexes of W, Re, Ru and Os; and (ii) simple iodides of Zn, Cd, Hg, Ga and In. None of the promoters show any detectable catalytic activity in the absence of iridium catalyst (although ruthenium has been reported to catalyse methanol carbonylation under harsh conditions and with relatively low selectivity [79–84]). Addition of a promoter tends to increase the catalytic rate towards a plateau which is reached for a promoter:Ir mole ratio between 5 : 1 and 10 : 1. For example, the carbonylation rate is enhanced by factors of 2.6 and 1.8, respectively, for $[Ru(CO)_4I_2]$ and InI_3, with a promoter:Ir mole ratio of 5 : 1. By contrast, ionic iodides such as LiI and Bu_4NI are both strong catalyst *poisons*, reducing activity by factors of ca. 2 and 3 respectively, when added in a 1 : 1 molar ratio with Ir. A ruthenium promoter is effective over a range of water concentrations, the maximum rate again being attained at ca. 5 wt % H_2O.

In situ HPIR spectroscopy showed that the dominant Ir species under catalytic conditions are $[Ir(CO)_2I_3Me]^-$ and $[Ir(CO)_2I_4]^-$, both in the absence or presence of a promoter. A ruthenium promoter exists mainly as $[Ru(CO)_3I_3]^-$, in equilibrium with smaller amounts of $[Ru(CO)_3I_2(sol)]$ and $[Ru(CO)_2I_2(sol)_2]$.

3.2.2
Promotion of the Stoichiometric Carbonylation of $[Ir(CO)_2I_3Me]^-$

Kinetic studies of the stoichiometric carbonylation of $[Ir(CO)_2I_3Me]^-$ were conducted to model the rate-determining step of the catalytic cycle [73, 85]. The reaction can form both *fac,cis* and *mer,trans* isomers of $[Ir(CO)_2I_3(COMe)]^-$ (Scheme 13), the product ratio varying with the solvent and temperature used. An X-ray crystal structure was obtained for the *fac,cis* isomer. Carbonylation of $[Ir(CO)_2I_3Me]^-$ is rather slow and requires temperatures $> 80\,^{\circ}C$ in chlorinated solvents (e.g. PhCl). However, the presence of protic solvents (e.g. methanol) has a dramatic accelerating effect. This is interpreted in terms of the protic solvent aiding iodide dissociation by solvation.

The effect of metal promoter species on the rate of carbonylation of $[Ir(CO)_2I_3Me]^-$ was tested. Neutral ruthenium iodocarbonyl complexes such as $[Ru(CO)_3I_2]_2$, $[Ru(CO)_4I_2]$ or $[Ru(CO)_2I_2]_n$ were found to give substantial rate enhancements (by factors of 15–20 for a Ru : Ir ratio of 1 : 13 at 93 °C, PhCl). Indium and gallium triiodides and zinc diiodide had comparable promotional effects. By contrast, addition of *anionic* ruthenium(II) species $[Ru(CO)_3I_3]^-$ or $[Ru(CO)_2I_4]^{2-}$ did not lead to any appreciable promotion *or* inhibition. This behaviour indicates that the ability to accept an iodide ligand is a key property of the promoter. Indeed, it has been demonstrated that an iodide ligand can be transferred from $[Ir(CO)_2I_3Me]^-$ to neutral ruthenium or indium species [73, 74].

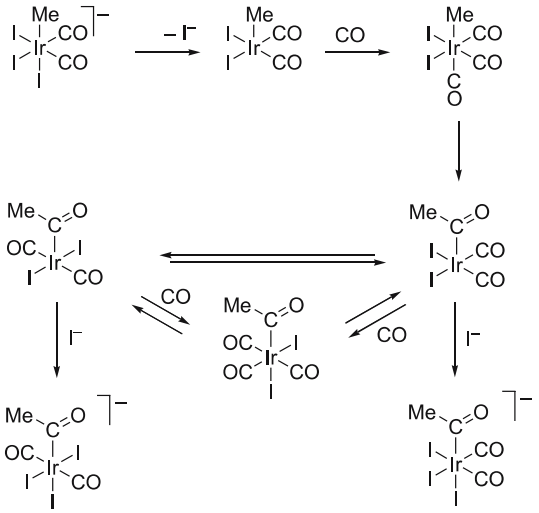

Scheme 13 Mechanism for formation of isomers of $[Ir(CO)_2I_3(COMe)]^-$ by carbonylation of $[Ir(CO)_2I_3Me]^-$

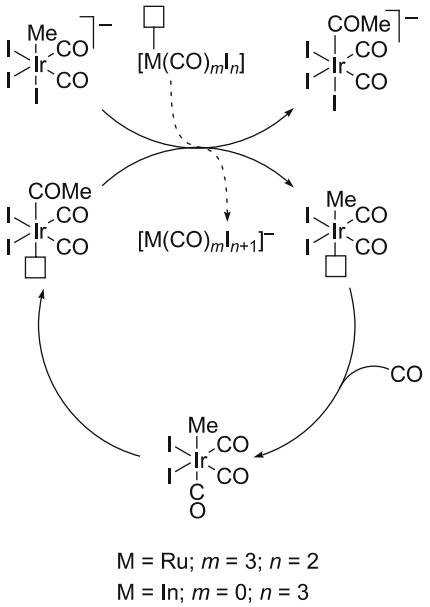

Scheme 14 Mechanism for promotion of carbonylation of $[Ir(CO)_2I_3Me]^-$ by iodide abstractors

A mechanism for the promotion of carbonylation of $[Ir(CO)_2I_3Me]^-$ is shown in Scheme 14. An iodide ligand is initially transferred from $[Ir(CO)_2I_3Me]^-$ to the promoter, allowing coordination of CO to Ir to give $[Ir(CO)_3I_2Me]$, which undergoes migratory insertion to form $[Ir(CO)_2I_2(COMe)]$. Iodide transfer from the promoter back to Ir at this point is unlikely, given that InI_3 is able to abstract iodide from $[Ir(CO)_2I_3(COMe)]^-$. Instead, iodide transfer between iridium centres can give $[Ir(CO)_2I_3(COMe)]^-$ and generate another molecule of $[Ir(CO)_2I_2Me]$. In this scenario, the initial iodide abstraction is an initiation step, as indicated by the dashed arrow in Scheme 13. This introduces an iodide "hole" which propagates the promotion, the anion $[InI_4]^-$ or $[Ru(CO)_3I_3]^-$ then acting as a spectator. In support of this, the effect of $[Ru(CO)_3I_2]$ or InI_3 can be mimicked by addition of the neutral iridium complex $[Ir(CO)_2I_2Me]_2$, which also promotes carbonylation of the anion $[Ir(CO)_2I_3Me]^-$. Thus, the key role of the promoter is to perturb the ratio of anionic and neutral iridium complexes. A more direct interaction between the promoter and the iridium centre does not appear to involved.

3.2.3 Role of Promoters in the Catalytic Process

A mechanism for the catalytic process is shown in Scheme 15, which comprises three sets of iridium complexes, namely Ir(I) species, Ir(III)-methyls

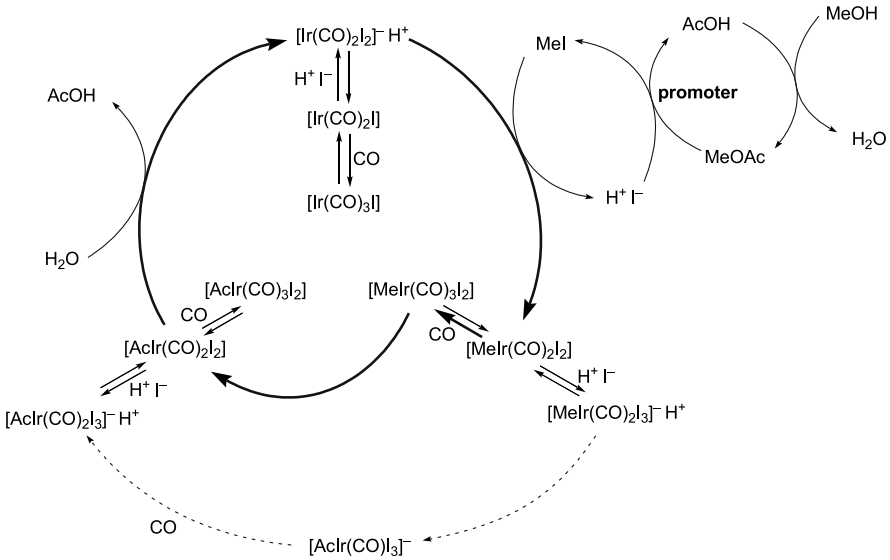

Scheme 15 Mechanism for promoted iridium-catalysed methanol carbonylation

and Ir(III)-acetyls. The three complexes within each set are linked by equilibria involving I^- and CO and the dominant route for catalytic turnover is indicated by the bold arrows. The interconversions of Ir species are essentially equivalent to Forster's mechanism (Scheme 11), but here the catalytic process is viewed as one cycle, rather than two. Varying the conditions results in build up of either $[Ir(CO)_3I]$ (at low $[I^-]$) or $[Ir(CO)_2I_3Me]^-$ (at higher $[I^-]$) as the catalyst resting state, corresponding to Forster's neutral and anionic cycles, respectively.

The iodide ($HI_{(aq)}$) concentration is also influenced by the water and methyl acetate concentrations (according to Eq. 11):

$$MeOAc + H_3O^+ + I^- \rightleftharpoons MeI + H_2O + AcOH\,. \tag{11}$$

Each turnover of the iridium cycle generates one molar equivalent of HI, which has to be recycled by reaction with methyl acetate to give methyl iodide, as shown in Eq. 11. The steady state concentration of iodide will therefore depend on the rate of this conversion. The iodide concentration is also crucial in governing the rate-determining step in the Ir cycle, which requires displacement of iodide in $[Ir(CO)_2I_3Me]^-$ by CO. It is thought that a key role of the promoter is to moderate the iodide concentration, which it achieves in two ways: firstly it acts as an iodide acceptor, for example to give $[Ru(CO)_3I_3]^-$, as demonstrated in the model studies; secondly, the presence of a high concentration of species such as $[Ru(CO)_3I_3]^-H_3O^+$ increases the Brønsted acidity and accelerates the reaction of methyl acetate with HI by acid catalysis (Scheme 16). This has been demonstrated in separate experiments

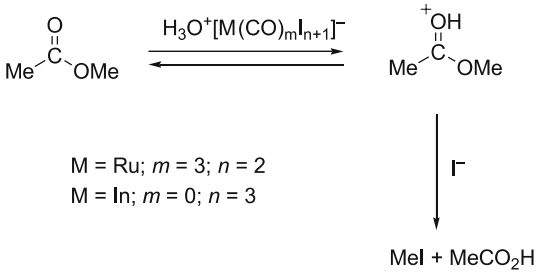

Scheme 16 Acid catalysis of conversion of methyl acetate into methyl iodide

in which $[Ru(CO)_3I_3]^-H_3O^+$ accelerates the exchange of isotopically labelled methyl groups between MeI and MeOAc.

4 Conclusions

The research and process development described in this paper illustrate how understanding fundamental patterns of organometallic reactivity is crucial for the design and improvement of industrial catalysts. The Monsanto acetic acid process stands as one of the major success stories of homogeneous transition catalysis, and for over 30 years rhodium-catalysed carbonylation was dominant due to its excellent activity and selectivity. It has been demonstrated, however, that careful choice of additives (e.g. iodide salts) and reaction conditions can significantly benefit the rhodium process by improving catalyst stability. Many attempts have been made to modify the rhodium catalyst by incorporation of other ligands (particularly phosphines). Although some interesting catalytic behaviour is observed, the long-term stability of metal–ligand interactions is a major issue. Nevertheless, the search continues for ligands with the appropriate electronic and steric characteristics to impart high activity, selectivity and stability. An alternative strategy, involving rhodium catalyst heterogenisation on polymer supports has also shown good potential.

The commercialisation of an iridium-based process is the most significant new development in methanol carbonylation catalysis in recent years. Originally discovered by Monsanto, iridium catalysts were considered uncompetitive relative to rhodium on the basis of lower activity, as often found for third row transition metals. The key breakthrough for achieving high catalytic rates for an iridium catalyst was the identification of effective promoters. Recent mechanistic studies have provided detailed insight into how the promoters influence the subtle balance between neutral and anionic iridium complexes in the catalytic cycle, thereby enhancing catalytic turnover.

Considerable challenges still remain in the development of new carbonylation processes for acetic acid manufacture. For example, all of the current processes use iodide compounds, leading to corrosive HI and the need for expensive materials for plant construction. An iodide-free system could potentially impart considerable benefit. Other long term goals include the selective direct conversion of syn-gas or oxidative carbonylation of methane to acetic acid. Organometallic chemists are certain to play a crucial role if these targets are to be achieved.

Acknowledgements Many colleagues at the University of Sheffield and collaborators at BP Chemicals have contributed to the studies mentioned in this article. Particular thanks are due to Peter Maitlis, Glenn Sunley and George Morris for many hours of fruitful discussion.

References

1. Paulik FE, Roth JF (1968) Chem Commun: 1578
2. Hohenschutz H, von Kutepow N, Himmle W (1966) Hydrocarbon Process 45:141
3. von Kutepow N, Himmle W, Hohenschutz H (1966) Chem-Ing-Tech 37:383
4. Forster D (1979) Adv Organomet Chem 17:255
5. Dekleva TW, Forster D (1986) Adv Catal 34:81
6. Howard MJ, Jones MD, Roberts MS, Taylor SA (1993) Catal Today 18:325
7. Maitlis PM, Haynes A, Sunley GJ, Howard MJ (1996) J Chem Soc, Dalton Trans: 2187
8. Yoneda N, Kusano S, Yasui M, Pujado P, Wilcher S (2001) Appl Catal A 221:253
9. Thomas CM, Süss-Fink G (2003) Coord Chem Rev 243:125
10. Torrence P (2002) Carbonylations: synthesis of acetic acid and acetic acid anhydride from methanol. In: Cornils B, Herrmann WA (eds) Applied homogeneous catalysis with organometallic compounds, vol 1, 2nd edn. Wiley, Weinheim, p 104
11. Forster D (1977) Ann NY Acad Sci 295:79
12. Fulford A, Hickey CE, Maitlis PM (1990) J Organomet Chem 398:311
13. Haynes A, Mann BE, Gulliver DJ, Morris GE, Maitlis PM (1991) J Am Chem Soc 113:8567
14. Haynes A, Mann BE, Morris GE, Maitlis PM (1993) J Am Chem Soc 115:4093
15. Adamson GW, Daly JJ, Forster D (1974) J Organomet Chem 71:C17
16. Adams H, Bailey NA, Mann BE, Manuel CP, Spencer CM, Kent AG (1988) J Chem Soc, Dalton Trans: 489
17. Haynes A, Maitlis PM, Stanbridge IA, Haak S, Pearson JM, Adams H, Bailey NA (2004) Inorg Chim Acta 357:3027
18. Howe L, Bunel EE (1995) Polyhedron 14:167
19. Griffin TR, Cook DB, Haynes A, Pearson JM, Monti D, Morris GE (1996) J Am Chem Soc 118:3029
20. Cheong M, Schmid R, Ziegler T (2000) Organometallics 19:1973
21. Ivanova EA, Gisdakis P, Nasluzov VA, Rubailo AI, Rösch N (2001) Organometallics 20:1161
22. Kinnunen T, Laasonen K (2001) J Organomet Chem 628:222
23. Kinnunen T, Laasonen K (2001) J Mol Struct (Theochem) 542:273
24. Kinnunen T, Laasonen K (2001) J Mol Struct (Theochem) 540:91

25. Baker EC, Hendriksen DE, Eisenberg R (1980) J Am Chem Soc 102:1020
26. Roe DC, Sheridan RE, Bunel EE (1994) J Am Chem Soc 116:1163
27. Haynes A, McNish J, Pearson JM (1997) J Organomet Chem 551:339
28. Eby RT, Singleton TC (1983) Appl Ind Catal 1:275
29. Schrod M, Luft G, Grobe J (1983) J Mol Catal 22:169
30. Smith BL, Torrence GP, Aguilo A, Alder JS (1991) US5001259 to Hoechst Celanese
31. Murphy MA, Smith BL, Torrence GP, Aguilo A (1986) J Organomet Chem 303:257
32. Smith BL, Torrence GP, Murphy MA, Aguilo A (1987) J Mol Catal 39:115
33. Zoeller JR, Agreda VH, Cook SL, Lafferty NL, Polichnowski SW, Pond DM (1992) Catal Today 13:73
34. Rankin J, Benyei AC, Poole AD, Cole-Hamilton DJ (1999) J Chem Soc, Dalton Trans: 3771
35. Wegman RW, Abatjoglou AG, Harrison AM (1987) J Chem Soc, Chem Commun: 1891
36. Baker MJ, Giles MF, Orpen AG, Taylor MJ, Watt RJ (1995) J Chem Soc, Chem Commun: 197
37. Dilworth JR, Miller JR, Wheatley N, Baker MJ, Sunley JG (1995) J Chem Soc, Chem Commun: 1579
38. Gonsalvi L, Adams H, Sunley GJ, Ditzel E, Haynes A (2002) J Am Chem Soc 124:13597
39. Gonsalvi L, Adams H, Sunley GJ, Ditzel E, Haynes A (1999) J Am Chem Soc 121:11233
40. Cavallo L, Sola M (2001) J Am Chem Soc 123:12294
41. Daura-Oller E, Poblet JM, Bo C (2003) Dalton Trans: 92
42. Dutta DK, Woollins JD, Slawin AMZ, Konwar D, Das P, Sharma M, Bhattacharyya P, Aucott SM (2003) Dalton Trans: 2674
43. Moloy KG, Wegman RW (1989) Organometallics 8:2883
44. Carraz CA, Ditzel E, Orpen AG, Ellis DD, Pringle PG, Sunley GJ (2000) Chem Commun: 1277
45. Thomas CM, Mafua R, Therrien B, Rusanov E, Stœckli-Evans H, Süss-Fink G (2002) Chem Eur J 8:3343
46. Gonsalvi L, Gaunt JA, Adams H, Castro A, Sunley GJ, Haynes A (2003) Organometallics 22:1047
47. Martin HC, James NH, Aitken J, Gaunt JA, Adams H, Haynes A (2003) Organometallics 22:4451
48. Drago RS, Nyberg ED, El A'mma A, Zombeck A (1981) Inorg Chem 3:641
49. Scates MO, Warner RJ, Torrence GP (1995) US5466874 to Hoechst Celanese
50. Watson DJ, Williams BL, Watt RJ (1994) EP0612712 to BP Chemicals
51. Minami T, Shimokawa K, Hamato K, Shiroto Y, Yoneda N (1994) US5364963 to Chiyoda
52. Shiroto Y, Hamato K, Asaoka S, Maejima T (1993) EP0567331 to Chiyoda
53. Marston CR, Goe GL (1988) EP0277824 to Reilly Tar
54. Sowden RJ, Sellin MF, De Blasio N, Cole-Hamilton DJ (1999) Chem Commun: 2511
55. De Blasio N, E T, Kaddouri A, Mazzocchia C, Cole-Hamilton DJ (1998) J Catal 176:253
56. De Blasio N, Wright MR, E T, Mazzocchia C, Cole-Hamilton DJ (1998) J Organomet Chem 551:229
57. Jiang DZ, Li XB, Wang EL (1996) Macromol Symp 105:161
58. Yoneda N, Minami T, Weiszmann J, Spehlmann B (1999) Stud Surf Sci Catal 121:93
59. Haynes A, Maitlis PM, Quyoum R, Pulling C, Adams H, Spey SE, Strange RW (2002) J Chem Soc, Dalton Trans: 2565
60. Forster D (1979) J Chem Soc, Dalton Trans: 1639
61. Garland CS, Giles MF, Sunley JG (1995) EP0643034 to BP Chemicals
62. Baker MJ, Giles MF, Garland CS, Rafeletos G (1996) EP0749948 to BP Chemicals

63. Garland CS, Giles MF, Poole AD, Sunley JG (1996) EP0728726 to BP Chemicals
64. Baker MJ, Giles MF, Garland CS, Muskett MJ, Rafeletos G, Smith SJ, Sunley JG, Watt RJ, Williams BL (1997) EP0752406 to BP Chemicals
65. Anon (1996) Chem Br 32:7
66. Anon (1996) Chem Ind (London): 483
67. Sunley GJ, Watson DJ (2000) Catal Today 58:293
68. Jones JH (2000) Platinum Metals Rev 44:94
69. Howard MJ, Sunley GJ, Poole AD, Watt RJ, Sharma BK (1999) Stud Surf Sci Catal 121:61
70. Mizoroki T, Matsumoto T, Ozaki A (1979) Bull Chem Soc Jpn 52:479
71. Matsumoto T, Mizoroki T, Ozaki A (1978) J Catal 51:96
72. Brodzki D, Denise B, Pannetier G (1977) J Mol Catal 2:149
73. Haynes A, Maitlis PM, Morris GE, Sunley GJ, Adams H, Badger PW, Bowers CM, Cook DB, Elliott PIP, Ghaffar T, Green H, Griffin TR, Payne M, Pearson JM, Taylor MJ, Vickers PW, Watt RJ (2004) J Am Chem Soc 126:2847
74. Whyman R, Wright AP, Iggo JA, Heaton BT (2002) J Chem Soc, Dalton Trans: 771
75. Gautron S, Giordano R, Le Berre C, Jaud J, Daran J-C, Serp P, Kalck P (2003) Inorg Chem 42:5523
76. Ellis PR, Pearson JM, Haynes A, Adams H, Bailey NA, Maitlis PM (1994) Organometallics 13:3215
77. Bassetti M, Monti D, Haynes A, Pearson JM, Stanbridge IA, Maitlis PM (1992) Gazz Chim Ital 122:391
78. Ghaffar T, Adams H, Maitlis PM, Sunley GJ, Baker MJ, Haynes A (1998) Chem Commun: 1023
79. Braca G, Sbrana G, Valentini G, Andrich G, Gregorio G (1978) J Am Chem Soc 100:6238
80. Braca G, Paladini L, Sbrana G, Valentini G, Andrich G, Gregorio G (1981) Ind Eng Chem Prod Res Dev 20:115
81. Braca G, Sbrana G, Valentini G, Cini M (1982) J Mol Catal 17:323
82. Gautier-Lafaye J, Perron R, Leconte P, Colleuille Y (1985) Bull Soc Chim Fr: 353
83. Jenner G, Bitsi G (1987) J Mol Catal 40:71
84. Kelkar AA, Kohle DS, Chaudhari RV (1992) J Organomet Chem 430:111
85. Pearson JM, Haynes A, Morris GE, Sunley GJ, Maitlis PM (1995) J Chem Soc, Chem Commun: 1045

Top Organomet Chem (2006) 18: 207–221
DOI 10.1007/3418_022

Published online: 10 June 2006

Carbonylations of Aldehydes

Axel Jacobi von Wangelin · Helfried Neumann · Matthias Beller (✉)

Leibniz-Institute for Catalysis e.V. an der Universität Rostock,
Albert-Einstein-Straße 29a, 18059 Rostock, Germany
matthias.beller@ifok-rostock.de

1 Introduction 207

2 Amidocarbonylations 208
2.1 Cobalt Catalysis 208
2.2 Palladium Catalysis 212

3 Hydro- and Silylformylations 214
3.1 Hydroformylation of Formaldehyde 214
3.2 Silylformylations 215

4 Hetero Pauson–Khand Reactions 216

5 Reactions with Acylanions 217

6 Miscellaneous 218
6.1 Benzofuranones 218
6.2 Reactions with Carbonium Ions 219
6.3 Other Reactions 219

References 220

Abstract Synthetically useful examples of carbonylations of aldehydes that enable the synthesis of structurally diverse carbonyl compounds such as α-amino acids, α-hydroxy carbonyl compounds, furanones, and lactones will be highlighted in this chapter.

Keywords Carbonylations · Aldehydes · Catalysis

1 Introduction

Carbonylations of aldehydes incorporate an inexpensive source of carbon, carbon monoxide, and can convert ubiquitously available aldehydes into various synthetically useful functionalities. This chapter deals with the most prominent applications of carbonylation methodology to aldehydes and is restricted to reactions where a direct bond is formed between the carbonyl moiety of the aldehyde (C or O) and carbon monoxide. Carbonylations of aldehydes mostly involve severe structural reorganizations of both reacting

carbonyl moieties. The neutral charge of the nucleophile CO requires the presence of another nucleophile/anion to trap the intermediate adduct as a stable species or subsequent bond reorganization. On the other hand, the direct carbonylation of aldehydes with CO is not known to proceed with significant levels of efficiency; carbonylations involving radical species have been reported in some cases. However, indirect carbonylations of aldehydes have very well been achieved upon in situ activation/transformation of the aldehyde moiety, often in the presence of metals. Such activated/masked aldehyde surrogates have been demonstrated to exhibit a higher propensity to undergo carbonylation by the rather poor nucleophile CO.

2
Amidocarbonylations

The amidocarbonylation of aldehydes provides highly efficient access to *N*-acyl α-amino acid derivatives by the reaction of the ubiquitous and cheap starting materials aldehyde, amide, and carbon monoxide under transition metal-catalysis [1, 2]. Wakamatsu serendipitously discovered this reaction when observing the formation of amino acid derivatives as by-products in the cobalt-catalyzed oxo reaction of acrylonitrile [3–5]. The reaction was further elaborated to an efficient cobalt- or palladium-catalyzed one-step synthesis of racemic *N*-acyl α-amino acids [6–8] (Scheme 1). Besides the range of direct applications, such as pharmaceuticals and detergents, racemic *N*-acetyl α-amino acids are important intermediates in the synthesis of enantiomerically pure α-amino acids via enzymatic hydrolysis [9].

2.1
Cobalt Catalysis

The active catalyst in the cobalt-catalyzed amidocarbonylation is $[Co(CO)_4]^-$, which is generated in situ from $Co_2(CO)_8$ (1–5 mol %) in the presence of CO/H_2 [10]. The reaction is carried out at 70–160 °C and syngas pressures of 50–200 bar (CO/H_2 = 1/1 to 4/1). Scheme 2 illustrates the proposed mechan-

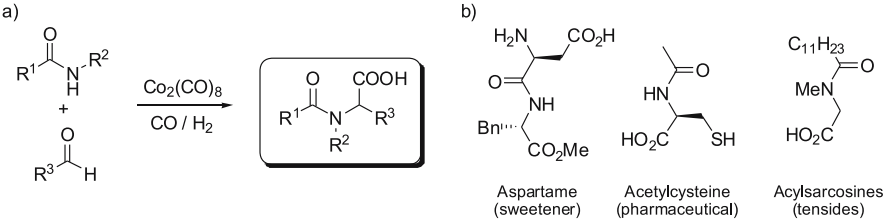

Scheme 1 **a** Amidocarbonylation of aldehydes; **b** Applications of *N*-acylamino acids

ism, which is believed to commence with the formation of alkyl complex **II**. Cobalt-centered carbonylation affords acyl complex **III** which can release the desired *N*-acyl α-amino acid via hydrolysis. The reaction proceeds with 100% atom utilization.

Numerous aldehydes have been used successfully for the synthesis of natural and unnatural amino acid derivatives, though the cobalt-catalyzed process is limited to α-hydrogen bearing aldehydes and formaldehyde. Diamidocarbonylation with a primary amide and two equivalents of formaldehyde affords *N*-acylamino diacetic acids, which are of potential use as glufosinate intermediates [11]. Cyclic and secondary amides, such as 2-pyrrolidinone, can only be amidocarbonylated with formaldehyde [12]. Lin reported on the catalytic performance of various cobalt/ligand systems in the synthesis of *N*-acetylglycine. Basic phosphines, such as PBu_3, were shown to allow low-pressure conditions (55 bar). The addition of Ph_2SO or succinonitrile resulted in improved selectivity and facilitated the catalyst recovery [13–15]. The addition of acid cocatalysts ($pK_a < 3$, e.g., TFA) allowed for low-temperature conditions and absence of hydrogen [16] (Scheme 3).

A broad range of olefins, acetals, epoxides, alcohols, and chlorides were demonstrated effective alternative starting materials. Cobalt and rhodium carbonyls and bimetallic complexes were shown to catalyze the domino hydro-

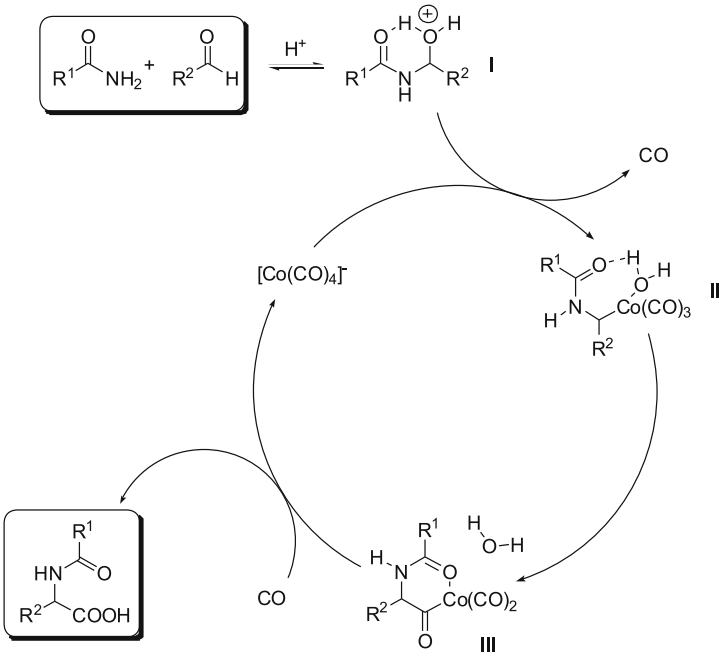

Scheme 2 Proposed mechanism for the cobalt-catalyzed amidocarbonylation

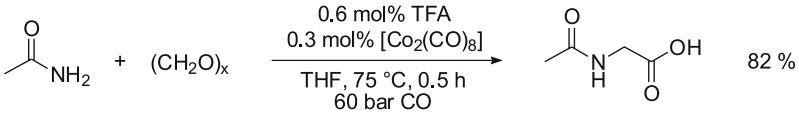

Scheme 3 Acid cocatalyst obviates the need for H_2

formylation-amidocarbonylation of olefins [17–22]. Addition of 0.1 mol % $Rh_6(CO)_{16}$ to the cobalt catalyst gave branched *N*-acetyltrifluorovaline which indicated that the hydroformylation step governs the regioselectivity of the domino process (Scheme 4) [22].

Interesting cyano, polyoxyethylene, and *O*-acetyl functionalized *N*-acylamino acid derivatives can be obtained from functionalized olefins (Table 1). Diamidocarbonylation products may also be synthesized in moderate yields from terminal diolefins [13–15].

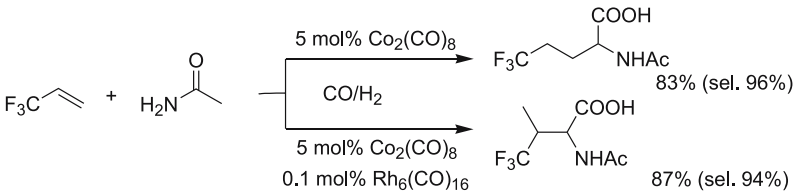

Scheme 4 Regioselectivity issues

Table 1 Amidocarbonylation of functionalized olefins

Olefin	*N*-Acylamino acid	Yield [%]	Application
NC	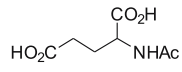	n.d.	glutaminic acid [21]
NC	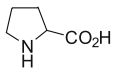	69	proline [21]
EtO_2C	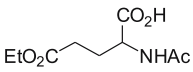	85	glutamate [22]
AcO	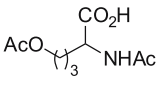	85	polyamide ester [13–15]

The in situ generation of the aldehyde can be achieved by a preceding rearrangement of epoxides and allyl alcohols. Ojima demonstrated the use of styrene oxide and propene oxide in the presence of [Ti(O*i*Pr)$_4$] or [Al(O*i*Pr)$_3$] as cocatalysts [19]. The transition metal-mediated isomerization of allylic alcohols (HRh(CO)(PPh$_3$)$_3$, Fe$_2$(CO)$_9$, RuCl$_2$(PPh$_3$)$_3$, PdCl$_2$(PPh$_3$)$_2$) was also shown compatible with amidocarbonylation conditions (Scheme 5) [23].

Amidocarbonylation methodology can also be applied to the synthesis of *N*-acetyl-(*D*,*L*)-phenylalanine, a key intermediate for aspartame (l-aspartyl-l-phenylalanine methylester), from styrene oxide (via isomerization to phenacetaldehyde) [24] or benzyl chloride [25] in good yields.

A two-step process for the reaction of paraformaldehyde with *N*-methyl fatty acid amides on a > 250 kg scale was developed at Hoechst AG [26, 27]. The *N*-methyl α-hydroxymethyl amide is generated in the presence of acid at 80 °C and subsequently carbonylated (50–70 °C, 10–50 bar CO) to afford the glycine derivative in high yields (> 98%) under very mild conditions. The key to this reaction lies in the higher activation energy for the methylol formation and the higher stability and selectivity of the cobalt catalyst at lower temperatures (Scheme 6). Glufosinate (phosphinotricine), a natural phosphinyl amino acid, exhibits herbicide and antibiotic activity (BASTA®) and can be manufactured by domino hydroformylation-amidocarbonylation of methylvinylphosphinate (Scheme 7) [28, 29].

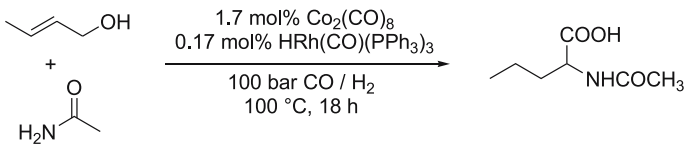

Scheme 5 Domino isomerization-amidocarbonylation of allylic alcohols

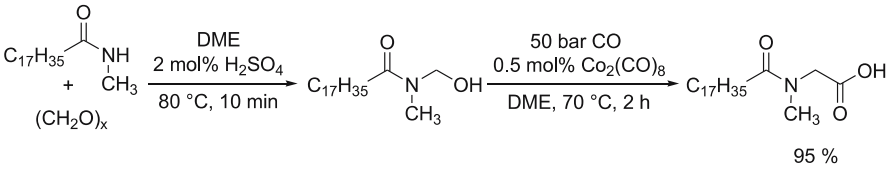

Scheme 6 Hoechst process for the manufacture of sarcosinates

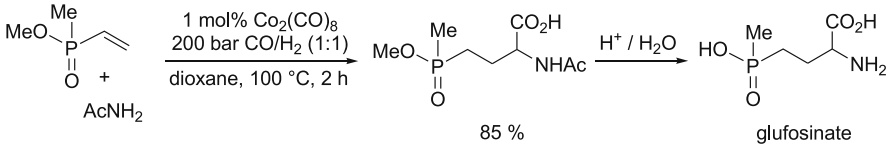

Scheme 7 Synthesis of BASTA®

To the best of our knowledge none of the cobalt-catalyzed amidocarbonylation procedures is applied on an industrial scale at present, largely due to the unsatisfactory catalytic activity (TON < 100) and relatively harsh conditions ($T > 100\,°C$; $p > 100$ bar).

2.2 Palladium Catalysis

In 1987, researchers at Hoechst found that palladium complexes are capable catalysts for the amidocarbonylation of aldehydes [30]. The reaction was typically run at 80–120 °C and 30–60 bar CO. Under optimized conditions, the desired *N*-acyl α-amino acids could be afforded with TON's of up to 60 000 (Scheme 8) [31–33]. The palladium-catalyzed reaction is not limited to aldehydes containing no α-hydrogens. The presence of halide ions is essential under palladium catalysis in order to facilitate the oxidative addition to palladium(0). However, the palladium catalysts are more tolerant to various functional groups. Recently, Beller et al. reported on an optimized set of conditions. While phosphine-free catalyst systems gave best yields at low CO pressure, phosphine-ligated palladium catalysts led to better yields at higher CO pressure. At low palladium loadings (< 0.1 mol %), unwanted condensation reactions of propionaldehyde were competitive [34, 35]. In recent mechanistic investigations, Kozlowski identified *N*-acyl imine and enamine species as key intermediates in the palladium-catalyzed amidocarbonylation [36].

The ureidocarbonylation reaction provides access to hydantoins containing diverse substituents in the 1-, 3-, and 5-positions with good selectivities (Table 2) [37]. With monosubstituted ureas, 3-substituted hydantoins are obtained.

The one-pot amidocarbonylation of commercially more attractive nitriles can be performed via preceding nitrile hydrolysis in cc. H_2SO_4 [38] or HCl/HCO_2H [39, 40] and was shown to afford the desired *N*-acylamino acids in good yields [41]. Systematic studies have shown that amidocarbonylation of benzaldehydes in the presence of palladium catalysts allows for the synthesis of functionalized, racemic *N*-acetyl-α-arylglycines (Table 3) [42]. Generally, electron-rich benzaldehydes react faster than those with electron withdrawing substituents, though useful yields could be achieved in all cases. *N*-alkyl and *N*-aryl *N*-acylamino acids can be prepared from secondary

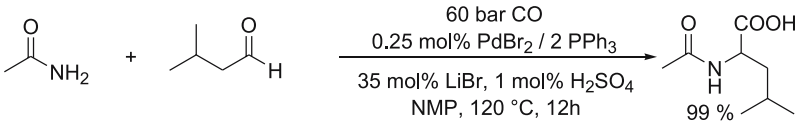

Scheme 8 Palladium-catalyzed amidocarbonylation of isovaleraldehyde

Table 2 Palladium-catalyzed ureidocarbonylation

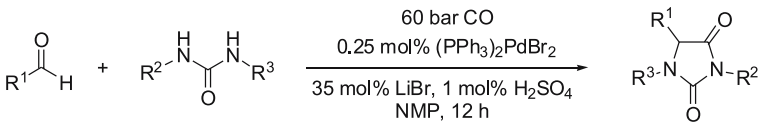

	R^1	R^2	R^3	T [°C]	Yield [%]	TON
1	Ph	Me	H	80	75	300
2	*i*-Bu	Me	Me	120	61	244
3	H	Ph	Ph	130	93	372
4	*m*-ClC_6H_4	Me	Me	100	79	316

Table 3 Palladium-catalyzed amidocarbonylation of benzaldehydes

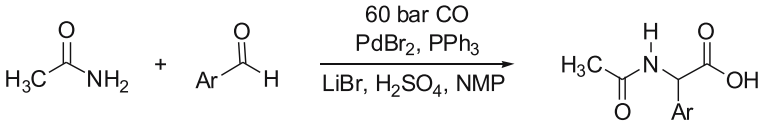

	Ar	T [°C]	t [h]	Yield [%]	TON
1	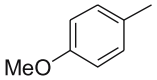	100	15	75	300
2		100	15	56	224
3	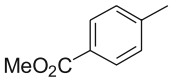	120	12	89	356
4		125	60	42	168

amides in moderate yields with Pd/C catalysts. The reaction of paracetamol® with paraformaldehyde gave *N*-acetyl-*N*-(4-hydroxyphenyl)glycine in 70% yield [43].

Table 4 Enzymatic hydrolysis of *N*-acylamino acids

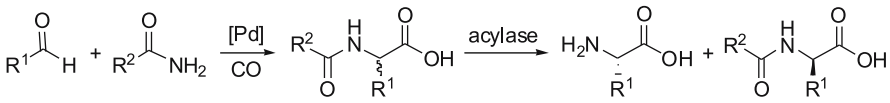

Amidocarbonylation				Enzymatic hydrolysis				
R,*S*-Acylamino acid		Yield	TON	enzyme	(*S*)-Amino acid		(*R*)-Amino acid	
R^1	R^2	[%]			Yield [%]	ee	Yield [%]	ee
p-ClBn	Me	75	300	AA	40	> 99	46	94
$MeSC_2H_4$	Me	75	300	PKA	32	> 99	40	86

AA: *Aspergillus spp.* acylase; PKA: pig liver acylase

The relevance of the palladium-catalyzed amidocarbonylation for natural product synthesis has been demonstrated with the multi gram-scale preparation of the central amino acid of chloropeptin I ((*S*)-3,5-dichloro-4-hydroxyphenylglycine) as well as methionine and *p*-chlorophenyl alanine via the combination of amidocarbonylation and enzymatic hydrolysis (Table 4) [44].

3
Hydro- and Silylformylations

3.1
Hydroformylation of Formaldehyde

Hydroformylation of hetero olefins such as carbonyl compounds is not known to proceed with significant levels of efficiency, whereas the hydroformylation of olefins has been developed to a sophisticated stage. Generally, aldehydes resultant from the latter process exhibit a low propensity to undergo further hydroformylation, with the exception of some activated aldehydes. The rhodium-catalyzed hydroformylation of formaldehyde is the key step in the synthesis of ethyleneglycol from synthesis gas. Chan et al. found

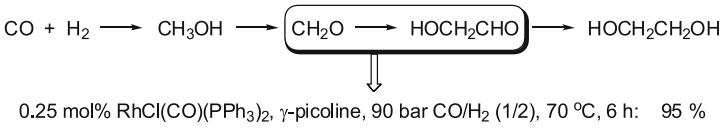

Scheme 9 Hydroformylation of formaldehyde

rhodium/phosphine catalysts and the presence of catalytic amounts of an amine to enhance the catalyst activity most effectively [45]. The nature of the employed ligand (e.g., PPh_3, $(p\text{-}CF_3C_6H_4)_3P$) and base (e.g., NEt_3, py) must be carefully balanced in order to facilitate deprotonation of the hydridorhodium species and prevent base-promoted aldol condensation of glycolaldehyde. Pyridines as solvents greatly enhanced the activity and selectivity of the catalyst; and with pyridines immiscible with water (4-pentylpyridine), 99% of the desired glycolaldehyde could be extracted into the aqueous phase (Scheme 9) [46].

3.2 Silylformylations

Unlike CC double bonds, the insertion of CO double bonds into a M – H species is generally disfavored. With $MH(SiR_3)$ species however, the high Si – O affinity enforces the formation of a metal-carbon bond which is consequently subject to CO insertion. Murai and coworkers reported the direct silylformylation of aliphatic aldehydes (3-fold excess) with diethylmethylsilane and carbon monoxide in the presence of catalytic $Co_2(CO)_8/PPh_3$ to afford α-siloxyaldehydes in moderate yields (100 °C, benzene) [47]. Wright demonstrated the superior selectivity of a rhodium-catalyzed variant [48]. With 0.5 mol % $[(cod)RhCl]_2$ and Me_2PhSiH, the silylformylation of aliphatic and aromatic aldehydes affords high yields of the α-siloxyaldehydes. The mild reaction conditions (17 bar CO, rt) permit discrimination of the starting aldehyde from the newly formed and bulkier siloxyaldehyde (Scheme 10). In related studies, Ojima found that aldehydes containing an acetylene moiety were exclusively silylformylated on the alkyne functionality [49].

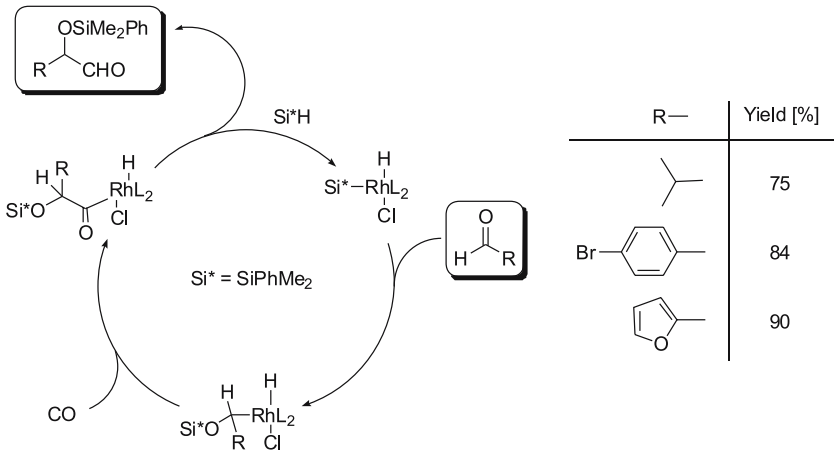

Scheme 10 Rhodium-catalyzed silylformylation of aldehydes

4
Hetero Pauson–Khand Reactions

Hetero Pauson–Khand reactions with an aldehyde or ketone component have been shown to afford synthetically versatile γ-butyrolactones. Buchwald [50] and Crowe [51] independently showed that aliphatic enones and enals react with CO under $Cp_2Ti(PMe_3)_2$ mediation (Scheme 11). CO insertion and thermal (or oxidative) decomposition gave diastereomerically pure bicyclic γ-butyrolactones and stable $Cp_2Ti(CO)_2$. Imines did not react under the reaction conditions.

o-Allyl acetophenones have been found capable of displacing CO on $Cp_2Ti(CO)_2$ via electron transfer processes and thus allowing catalytic reactions [52]. While the strong Ti – O bond renders a catalytic reaction difficult in most cases, the use of a late transition metal facilitates the realization of catalytic protocols. Murai reported on the cyclocarbonylation of ynals with CO to give bicyclic lactones in the presence of 2 mol % $Ru_3(CO)_{12}$. Two alternative mechanisms have been discussed, one commencing with oxidative addition of the aldehyde–CH bond to Ru, while the other involves the intermediacy of a metallacycle [53]. Kang developed a related reaction with allenyl aldehydes with CO to afford α-methyl-γ-butyrolactones in good yields (Scheme 12) [54].

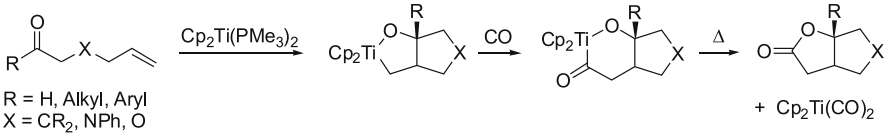

Scheme 11 Titanium-mediated hetero Pauson–Khand reaction

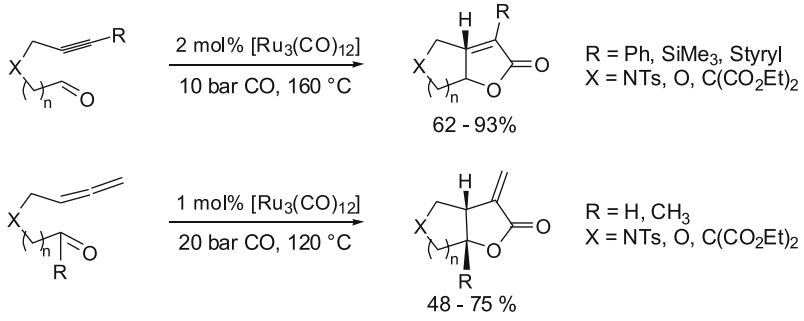

Scheme 12 Ruthenium-catalyzed hetero Pauson–Khand reactions with alkynes and allenes

5
Reactions with Acylanions

While various carbon-monoxide-free *Umpolung* approaches utilize the intermediacy of masked acylanion equivalents, alkyllithium species have been shown to undergo selective carbonylation at low temperatures (< – 110 °C) to form acylanions. Such in situ prepared acyllithium species have been demonstrated versatile reagents for the direct nucleophilic acylation of aldehydes [55, 56]. The resultant acyloins were obtained in good yields from reactions of *s*- and *t*-BuLi with aliphatic and aromatic aldehydes (< 95%, Scheme 13). However, simple alkylation of the aldehyde was observed with the sterically less hindered *n*-BuLi, except in the case of the highly hindered pivaldehyde which gave the desired α-hydroxy ketone in 62% yield. Generally, side reactions such as RLi addition to the carbonyl function and enolization are minimized at an equimolar ratio of alkyllithium/aldehyde. The methodology is limited by the commercial availability of organolithium substrates and the operational requirements of low temperatures and strict exclusion of moisture.

Murai and coworkers reported on operationally simple aldol reactions with lithium enolates generated from carbonylation of silylmethyl lithium species [57]. Upon 1,2-silicon shift, α-silyl acyllithium species can be stereoselectively converted to (*E*) lithium enolates that undergo addition to aldehydes to give β-hydroxy acylsilanes (Scheme 14).

Stable acylzirconocene chloride has been utilized by Hanzawa and coworkers [58] for the synthesis of α-hydroxy ketones. Consecutive hydrozirconation of terminal alkenes or alkynes with Schwartz' reagent and in situ carbonylation with gaseous CO at room temperature affords acylzirconocene

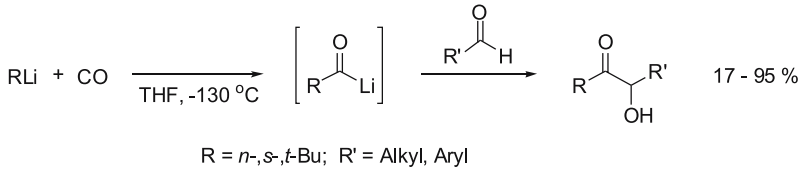

Scheme 13 Acyllithium addition to aldehydes

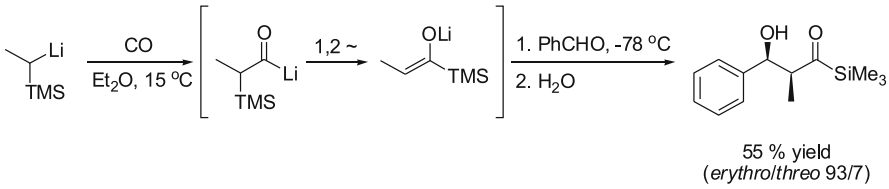

Scheme 14 1,2-Silicon shift toward lithium enolates

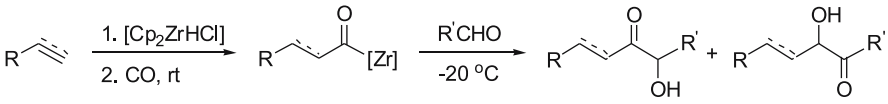

R = Alkyl, Aryl
R' = Alkyl, Aryl, Alkenyl

Alkene	R' =	I	Yield [%]	II
n-C_6H_{13}	Ph	79		-
n-C_6H_{13}	PhCH=CH	-		59
BnO	MeCH=CH	22		53

Scheme 15 Acylzirconocene addition to aldehydes

chloride. The yields of addition reactions to aldehydes were strongly dependent on the presence of a Lewis acid. Interestingly, the isomeric α-ketol was obtained in some reactions with alkenes when $BF_3 \cdot OEt_2$ was used (Scheme 15).

6
Miscellaneous

6.1
Benzofuranones

The three-component synthesis of benzo and naphthofuran-2(3*H*)-ones from the corresponding aromatic alcohol (phenols or naphthols) with aldehydes and CO (5 bar) can be performed under palladium catalysis (Scheme 16) [59, 60]. The mechanism involves consecutive Friedel–Crafts-type aromatic alkylation and carbonylation of an intermediate benzylpalladium species. The presence of acidic cocatalysts such as TFA and electron-donating substituents in *ortho*-position (no reaction with benzyl alcohol!) proved beneficial for both reaction steps.

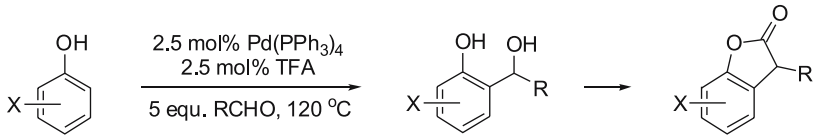

R = Alkyl, Aryl; X = H, -C_4H_4-, OR, Alkyl, Cl

Scheme 16 Cyclocarbonylation to furanones

6.2
Reactions with Carbonium Ions

The metal-free carbonylation of carbocationic intermediates with carbon monoxide under strongly acidic conditions (Koch–Haaf reaction) is used industrially to convert *i*-butene to pivalic acid [61]. Woo showed that α,β-unsaturated aldehydes can be carbonylated in conc. H_2SO_4 to give 3,4-dialkyl-2(5*H*)-furanones (70 bar CO, 50 °C) [62]. Although carbonylation occurs in conjugate fashion, secondary intramolecular carbonylation of the aldehyde-oxygen results in the formation of the furanone ring. Simple aldehydes can be converted to α,β-unsaturated aldehydes by rapid aldol condensation under the acidic reaction conditions and give only slightly lower yields (Scheme 17).

Under analogous conditions, carbonylation of chloral affords *cis* or *trans* 2,5-bis(trichloromethyl)-1,3-dioxolan-4-ones. The stereochemical outcome of the reactions can be controlled by the concentration of the employed sulfuric acid (90–99%) and the reaction time. The *cis* isomer is predominantly formed under more acidic conditions after 10 min (*cis*/*trans* 95/5; 48% yield), whereas complete isomerization to the *trans* isomer (*cis*/*trans* 0/100; 65% yield) takes place at lower acidity (90%) and prolonged reaction time (7 h) [63].

6.3
Other Reactions

Toniolo reported the carbonylation of aromatic aldehydes containing electron-donating substituents with a Pd/PPh_3 catalyst system in the presence of HCl to give phenylacetic acid derivatives [64]. No activity was observed in the absence of PPh_3 or HCl, and high yields could be achieved with alkanols as solvent (e.g., EtOH). It is believed that the mechanism involves HCl addition to the aldehyde, with the resultant chlorohydrin being subject to oxidative addition to Pd, CO insertion, and alcoholysis. Upon Cl ↔ OR substitution with the formed mandelic acid derivative, a second carbonylation takes place,

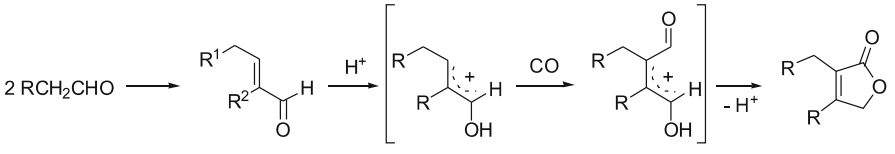

aldehyde	Yield [%]
R = Et	44
R^1 = H, R^2 = Me	55
R^1, R^2 = Me	52

Scheme 17 Acid-mediated conjugate carbonylation

which after decarboxylation of the resultant phenylmalonate gives the desired phenylacetic acid derivative in 70–75% yield.

Unsymmetrical vicinal diols can be prepared from a three-component reaction of aldehydes, CO, and aminotroponiminate-ligated titanium dialkyl complexes. Solutions of Me_2TiL_2 (L = *N*,*N*′-dimethylaminotroponiminate) react rapidly with CO at room temperature. Double methyl migration to CO produces an η^2-acetone complex which inserts the aldehyde to afford a titanadioxolane and releases the unsymmetrical diol upon hydrolysis [65].

An indirect carbonylation of aldehydes via photolysis of chromium alkoxycarbenes with aldehydes in the presence of Lewis acids was reported by Hegedus [66]. The formation of β-lactones was especially efficient when the aldehyde was incorporated into either chain of the carbene ligand resulting in an intramolecular process.

References

1. Beller M, Eckert M (2000) Angew Chem Int Ed 39:1010
2. Jacobi von Wangelin A, Neumann H, Gördes D, Beller M (2004) In: Beller M, Bolm C (eds) Transition metals for organic synthesis. Wiley, Weinheim, p 133
3. Wakamatsu H, Uda J, Yamakami N (1971) Chem Commun 1540
4. Wakamatsu H, Uda J, Yamakami N (1971) DE-B 2115 985
5. Wakamatsu H (1989) Kagaku 44:448
6. Knifton JF (1996) In: Cornils B, Herrmann WA (eds) Applied homogeneous catalysis with organometallic compounds. VCH, Weinheim, p 159
7. Ojima I (1988) Chem Rev 88:1011
8. Dyker G (2000) In: Schmalz HG (ed) Organic synthesis highlights IV. Wiley, Weinheim, p 53
9. Drauz K, Waldmann H (1995) Enzyme catalysis in organic synthesis. VCH, Weinheim
10. Ojima I, Zhang Z (1990) Organometallics 9:3122
11. Stern R, Reffet D, Hirschauer A, Commereuc D, Chauvin Y (1982) Synth Commun 12:1111
12. Lin JJ (1986) US Patent A 4 620 949
13. Lin JJ, Knifton JF (1991) J Organomet Chem 417:99
14. Knifton JF, Lin JJ, Storm DA, Wong SF (1993) Catal Today 18:355
15. Lin JJ, Knifton JF, Yeakey EL (1987) US Patent 4 918 222
16. Drent E, Kragtwijk E (1991) GB 2 252 770
17. Wakamatsu H (1974) Sekiyu Gakkaishi 17:105
18. Stern R, Hirschauer A, Commereuc D, Chauvin Y (1981) US Patent 4 264 515
19. Ojima I, Hirai K, Fujita M, Fuchikami T (1985) J Organomet Chem 279:203
20. Ojima I, Okabe M, Kato K, Kwon HB, Horvath IT (1988) J Am Chem Soc 110:150
21. Izawa K (1988) Yuki Gosei Kagaku Kyokaishi 46:218
22. Lin JJ (1988) US Patent 4 720 573
23. Hirai K, Takahashi Y, Ojima I (1982) Tetrahedron Lett 23:2491
24. Lin JJ, Knifton JF (1997) Catal Lett 45:139
25. de Vries JG, de Boer RP, Hogeweg M, Gielens EECG (1996) J Org Chem 61:1842
26. Beller M, Fischer H, Gross P, Gerdau T, Geissler H, Bogdanovic S (1995) DE-B 4415 712
27. Bogdanovic S, Geissler H, Beller M, Fischer H, Raab K (1995) DE-B 195 45 641 A1

28. Takigawa S, Shinke S, Tanaka M (1990) Chem Lett 1415
29. Sakakura T, Huang XY, Tanaka M (1991) Bull Chem Soc Jpn 64:1707
30. Jägers E, Koll HP (1989) EP-B 0 338 330 B1
31. Beller M, Eckert M, Vollmüller F, Geissler H, Bogdanovic S (1996) DE-B 196 27 717
32. Beller M, Eckert M, Vollmüller F, Bogdanovic S, Geissler H (1997) Angew Chem Int Ed 36:1494
33. Beller M, Eckert M, Vollmüller F (1998) J Mol Catal 135:23
34. Gördes D, Neumann H, Jacobi von Wangelin A, Fischer C, Drauz K, Krimmer HP, Beller M (2003) Adv Synth Catal 345:510
35. Jacobi von Wangelin A, Neumann H, Gördes D, Klaus S, Strübing D, Beller M (2003) Chem Eur J 9:4286
36. Freed DA, Kozlowski MC (2001) Tetrahedron Lett 42:3403
37. Beller M, Eckert M, Moradi W, Neumann H (1999) Angew Chem Int Ed 38:1454
38. Seeliger W, Hesse KD (1974) US Patent A 3846 419
39. Becke F, Gnad J (1968) Liebigs Ann Chem 713:212
40. Becke F, Fleig H, Pässler P (1971) Liebigs Ann Chem 749:198
41. Beller M, Eckert M, Moradi WA (1999) Synlett 108
42. Beller M, Eckert M, Holla EW (1998) J Org Chem 63:5658
43. Beller M, Moradi WA, Eckert M (1999) Tetrahedron Lett 40:4523
44. Beller M, Eckert M, Geissler H, Napierski B, Rebenstock HP, Holla EW (1998) Chem Eur J 4:935
45. Chan ASC, Carroll WE, Willis DE (1983) J Mol Cat 19:377
46. Okano T, Makino M, Konishi H, Kiji J (1985) Chem Lett 1793
47. Murai S, Kato T, Sonoda N, Seki Y, Kawamato K (1979) Angew Chem 91:421
48. Wright ME, Cochran BB (1993) J Am Chem Soc 115:2059
49. Ojima I, Tzamarioudaki M, Tsai CY (1994) J Am Chem Soc 116:3643
50. Kablaoui NM, Hicks FA, Buchwald SL (1996) J Am Chem Soc 118:5818
51. Crowe WE, Vu AT (1996) J Am Chem Soc 118:1557
52. Kablaoui NM, Hicks FA, Buchwald SL (1997) J Am Chem Soc 119:4424
53. Chatani N, Morimoto T, Murai S (1998) J Am Chem Soc 120:5335
54. Kang SK, Kim KJ, Hong YT (2002) Angew Chem 114:1654
55. Seyferth D, Weinstein RM, Hui RC, Wang WL, Archer CM (1992) J Org Chem 57:5620
56. Seyferth D, Weinstein RM, Wang WL, Hui RC (1983) Tetrahedron Lett 24:4907
57. Murai S, Ryu I, Iriguchi J, Sonoda N (1984) J Am Chem Soc 106:2440
58. Harada S, Taguchi T, Tabuchi N, Narita K, Hanzawa Y (1998) Angew Chem 110:1796
59. Satoh T, Tsuda T, Kushiäno Y, Miura M, Nomura M (1996) J Org Chem 61:6476
60. Satoh T, Tsuda T, Terao Y, Miura M, Nomura M (1999) J Mol Cat 143:203
61. Bahrman A (1980) In: Falbe J (ed) New synthesis with carbon monoxide. Springer, Berlin, p 372
62. Woo EP, Cheng FCW (1986) J Org Chem 51:3706
63. Mori S, Emura K, Kano M, Kudo K, Komatsu K, Sugita N (1995) Tetrahedron 51:8977
64. Cavinato G, Toniolo L (1991) J Mol Cat 69:283
65. Steinhuebel DP, Lippard SJ (1999) J Am Chem Soc 121:11762
66. Colson PJ, Hegedus LS (1994) J Org Chem 59:4972

Top Organomet Chem (2006) 18: 223–238
DOI 10.1007/3418_023

Published online: 23 June 2006

Carbonylation of Epoxides

Koji Nakano · Kyoko Nozaki (✉)

Department of Chemistry and Biotechnology, Graduate School of Engineering, The University of Tokyo, 7-3-1 Hongo, Bunkyo-ku, 113-8656 Tokyo, Japan
nozaki@chembio.t.u-tokyo.ac.jp

1 Introduction 223

2 Ring-expansion Carbonylation 224

3 Alternating Copolymerization 229

4 Formylation: Hydroformylation and Silylformylation 232

5 Alkoxycarbonylation and Aminocarbonylation 235

6 Concluding Remarks 237

References 237

Abstract Development in the field of transition metal-catalyzed carbonylation of epoxides is reviewed. The reaction is an efficient method to synthesize a wide range of β-hydroxy carbonyl compounds such as small synthetic synthons and polymeric materials. The reaction modes featured in this chapter are ring-expansion carbonylation, alternating copolymerization, formylation, alkoxycarbonylation, and aminocarbonylation.

1 Introduction

Carbonylation of epoxides provides direct access to a large variety of hydroxy carbonyl compounds, such as β-lactones, useful synthons in organic synthesis, and poly(3-hydroxyalkanoate), important biodegradable polyesters. Thus, the development of efficient catalysts for such carbonylations has been widely studied.

The carbonylation of epoxides to afford β-hydroxyesters or β-hydroxyaldehydes has been known since 1950s using $Co_2(CO)_8$ as a catalyst [1–6]. The original catalyst systems, however, required harsh reaction conditions. In order to improve the reaction efficiency, significant research efforts have been devoted, resulting in the recent rapid development of catalysts. In particular, cobalt catalysts have been found to show high catalytic activity. The key reaction in the cobalt-catalyzed carbonylations is the ring-opening of epoxides by the nucleophilic attack of the tetracarbonylcobaltate anion to one of the epoxide carbons (Scheme 1) [3, 7, 8]. This characterizes the regioselectivity and

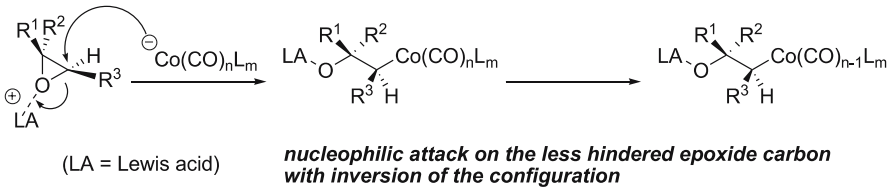

Scheme 1

stereospecificity in these carbonylations: in general the tetracarbonylcobaltate anion attacks on the less hindered epoxide carbon with inversion of the configuration. Here, in this chapter, we focused on the recent development in the metal-catalyzed carbonylation of epoxides. Although carbonylation reactions of other cyclic compounds with a heteroatom such as aziridines [9–11], oxetanes [12] and thietanes [13] have been reported, those reactions are omitted in this chapter.

2
Ring-expansion Carbonylation

The ring-expansion carbonylation of epoxides is the most widely studied field in the epoxide carbonylation chemistry since the product lactones are highly attractive targets: particularly, β-lactones are useful compounds due to their versatility in organic synthesis [14, 15] as well as their utilization as monomers to produce poly(3-hydroxyalkanoate)s, naturally occurring biodegradable polyesters [16–19].

The first successful example of a catalytic ring-expansion carbonylation was reported by Aumann et al. in 1970s [20, 21]. Here, isoprene oxide was allowed to react with CO in the presence of $[Rh(cod)Cl]_2$ to give an β,γ-unsaturated lactone (Scheme 2). Soon after their report, the carbonylation of styrene oxide to yield the corresponding β-lactone was demonstrated by using $RhCl(CO)(PPh_3)_2$ [22]. The scope of this method is, however, quite

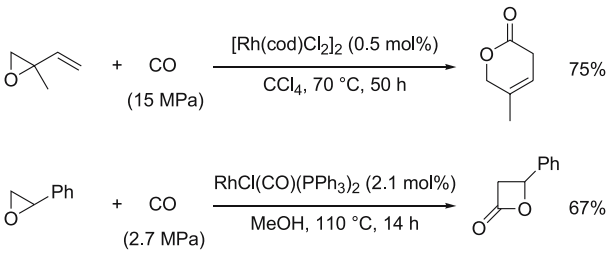

Scheme 2

limited; the reaction of stilbene oxide and aliphatic epoxides resulted in very low yields of the desired β-lactones.

Improved methods for the ring-expansion carbonylation were investigated in the last decade [23]. For example Alper et al. reported the regioselective carbonylation of epoxides by using $[PPN]Co(CO)_4$ [PPN = bis(triphenylphosphine)iminium] in conjugation with a Lewis acid such as $BF_3 \cdot OEt_2$ or $SnCl_4$ in DME (Scheme 3) [24]. The CO insertion occurred regioselectively at the unsubstituted C – O bond when monosubstituted epoxides were used as substrates, giving β-substituted β-lactones in good yields. Various functional groups such as alkenyl, haloalkyl, hydroxyalkyl, and ether groups tolerated the reaction condition, affording the corresponding β-lactones. The ring-expansion carbonylation of 1,2-disubstituted epoxides also proceeded by using $B(C_6F_5)_3$ in place of $BF_3 \cdot OEt_2$ as a Lewis acid while the yields were much lowered. Stereochemistry of the products was completely retained: hence, the reaction of *trans*- and *cis*-2,3-epoxybutane yielded *trans*- and *cis*-disubstituted β-lactone, respectively (Scheme 4). This configurational retentin is unusual in the cobalt-catalyzed carbonylation of epoxides where nucleophilic attack of tetracarbonylcobaltate anion usually results in the configurational inversion.

More recently, Coates et al. reported well-defined cobalt complexes with high catalytic activity and regioselectivity [25–27]. The key concept for the

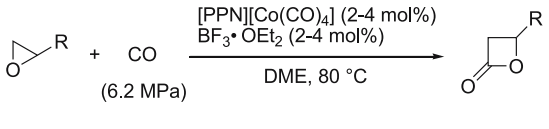

substrate	time (h)	yield (%)
R = Bu	24	66
	48	87
CH_2Cl	48	83
CH_2OH	24	57
CH_2O^iPr	48	86

Scheme 3

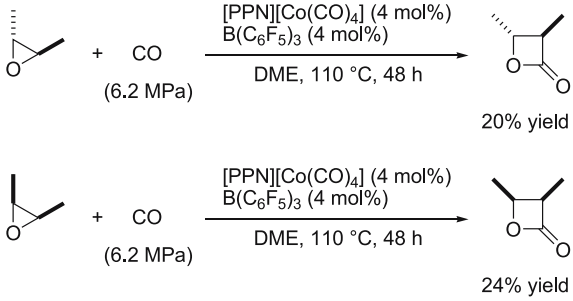

Scheme 4

design of the catalyst is a combination of [Lewis acid]$^+$ and $[Co(CO)_4]^-$, which was based on the proposed reaction mechanism (Scheme 5): the cationic Lewis acid coordinates and activates the epoxide for the nucleophilic attack of the cobaltate anion [steps (i) and (ii)]. After insertion of CO into the metal-alkyl bond and recoordination of CO to the cobalt center [step (iii)], the metal alkoxide attacks the acyl carbon intramolecularly to form a β-lactone and regenerates the original catalyst [Lewis acid]$^+[Co(CO)_4]^-$ [step (iv)]. The complexes $[(salph)Al(thf)_2][Co(CO)_4]$ (**1**), $[Cp_2Ti(thf)_2][Co(CO)_4]$ (**2**), and $[(TPP)Cr(thf)_2][Co(CO)_4]$ (**3**) were found to catalyze the ring-expansion carbonylation of a wide range of epoxides under the condition of relatively low CO pressure, low reaction temperature, and low catalyst loading. In general complex **3** was superior to the other two complexes with respect to the catalytic activity and the wide scope of the applicable substrates (Table 1). Carbonylation of monosubstituted epoxides proceeded regioselectively to afford the corresponding β-substituted β-lactones (runs 1–8). In the same way as the catalyst system of $[PPN][Co(CO)_4]$ described above, carbonylation with **1**, **2**, and **3** tolerated various functional groups (Table 1, runs 4–8). In addition, optically active epoxide, (*R*)-propylene oxide gave the (*R*)-β-butyrolactone with retention of the configuration (Table 1, run 3). These catalyst systems were also effective for the carbonylation of 1,2-disubstituted epoxides (Table 1, runs 9–16). In contrast to the case of using$[PPN][Co(CO)_4]$, *trans*- and *cis*-2,3-epoxybutanes yielded *cis*- and *trans*-disubstituted β-lactones, respectively (Table 1, runs 9–14). This stereochemistry is reasonably explained by back-side attack of the cobaltate anion described in the proposed mechanism (Scheme 5). Carbonylation of bicyclic epoxides such as cyclooctene oxide and cyclododecene oxide also proceeded to give the corresponding bicyclic β-lactones with inversion of the configuration at the α-carbon of the carbonyl (Table 1, runs 15, 16). Using cyclododecene oxide composed of 66% cis isomer

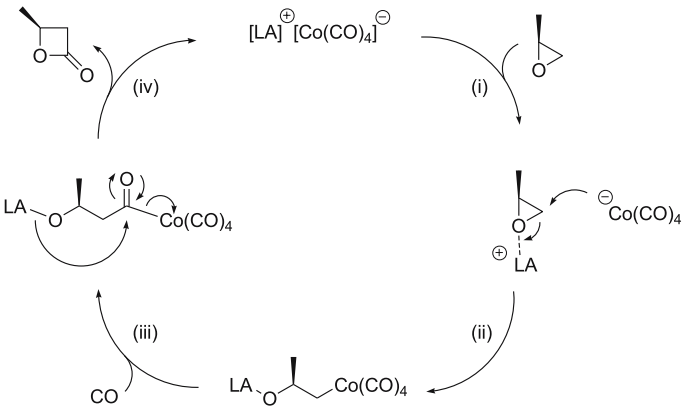

Scheme 5

Table 1

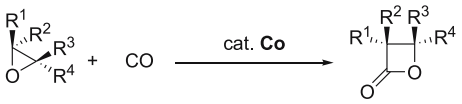

run	substrate	**Co**(substrate : **Co**)	condition	time (h)	yield (%)
1		**1**(100 : 1)	**A**	1	95
2		**2**(100 : 1)	**B**	4	95
3		**1**(100 : 1)	**A**	1	95
4	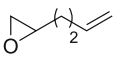	**1**(250 : 1)	**C**	6	40
5		**3**(250 : 1)	**C**	6	> 99
6	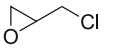	**1**(100 : 1)	**A**	9.5	73
7	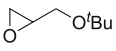	**1**(200 : 1)	**C**	6	> 99
8		**3**(200 : 1)	**C**	6	> 99
9		**1**(75 : 1)	**C**	6	20
10		**2**(50 : 1)	**B**	10	75
11		**3**(75 : 1)	**C**	6	56
12		**1**(75 : 1)	**C**	6	74
13		**2**(50 : 1)	**B**	10	99
14		**3**(75 : 1)	**C**	6	> 99
15		**3**(250 : 1)	**C**	6	> 99
16		**3**(450 : 1)	**C**	6	66

conditions **A**: CO (6.1 MPa), 50 °C, neat. **B**: CO (6.2 MPa), 60 °C, DME. **C**: CO (6.2 MPa), 60 °C, neat.

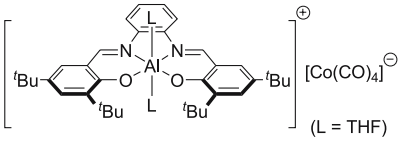

[(salph)Al(thf)$_2$][Co(CO)$_4$] (**1**)

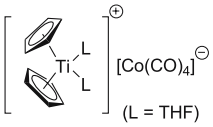

[Cp$_2$Ti(thf)$_2$][Co(CO)$_4$] (**2**)

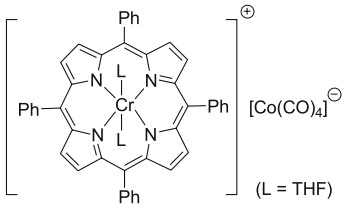

[(TPP)Cr(thf)$_2$][Co(CO)$_4$] (**3**)

as substrate, the cis isomer was found to be carbonylated much more readily than the trans isomer, resulting in the production of the β-lactone composed of 97% trans isomer in 66% yield (Table 1, run 16).

Carbonylative kinetic resolution of a racemic mixture of *trans*-2,3-epoxybutane was also investigated by using the enantiomerically pure cobalt complex $\{[(R,R)\text{-salcy}]Al(thf)_2\}[Co(CO)_4]$ (**4**) [28]. The carbonylation of the substrate at 30 °C for 4 h (49% conversion) gave the corresponding *cis*-β-lactone in 44% enantiomeric excess, and the relative ratio (k_{rel}) of the rate constants for the consumption of the two enantiomers was estimated to be 3.8, whereas at 0 °C, k_{rel} = 4.1 (Scheme 6). This successful kinetic resolution reaction supports the proposed mechanism where cationic chiral Lewis acid coordinates and activates an epoxide.

Two molecules of carbon monoxide were successively incorporated into an epoxide in the presence of a cobalt catalyst and a phase transfer agent [29]. When styrene oxide was treated with carbon monoxide (0.1 MPa), excess methyl iodide, NaOH (0.50 M), and catalytic amounts of $Co_2(CO)_8$ and hexadecyltrimethylammonium bromide in benzene, 3-hydroxy-4-phenyl-2(5*H*)-furanone was produced in 65% yield (Scheme 7). A possible reaction mechanism was proposed as shown in Scheme 8: Addition of an in situ

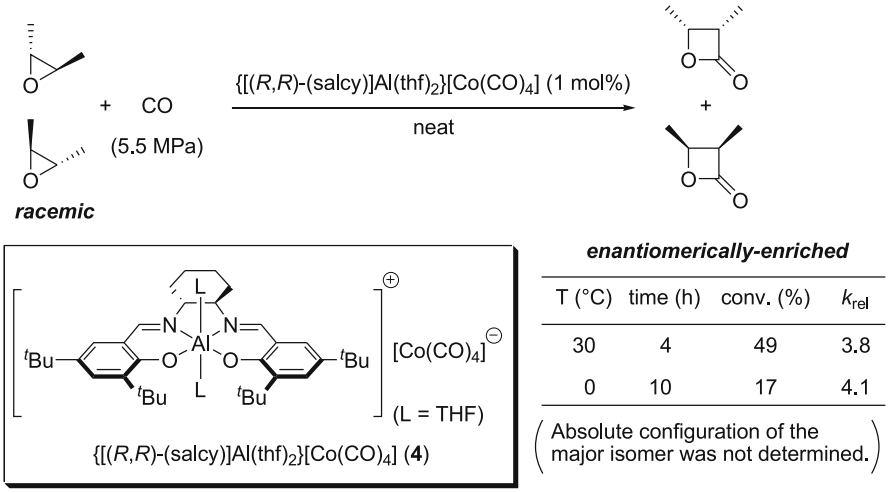

T (°C)	time (h)	conv. (%)	k_{rel}
30	4	49	3.8
0	10	17	4.1

(Absolute configuration of the major isomer was not determined.)

Scheme 6

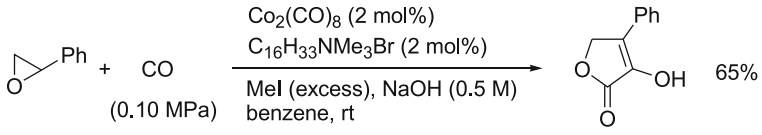

Scheme 7

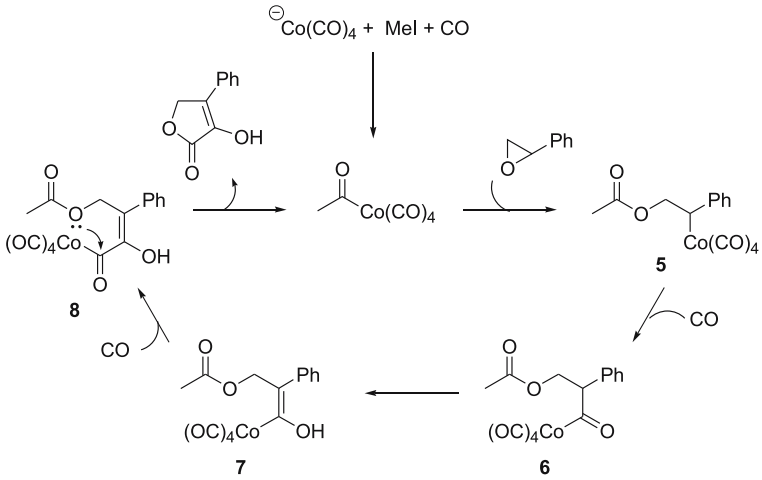

Scheme 8

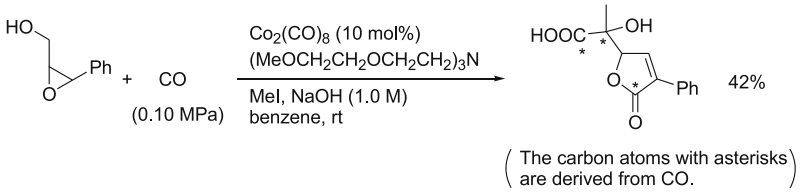

Scheme 9

generated acyl cobalt complex to the epoxide gives a benzylcobalt complex **5**, followed by CO insertion into the cobalt–carbon bond and recoordination of CO. Enolization of the resulting acylcobalt complex **6** to **7** is the key step in the double carbonylation, and the insertion of the second CO molecule gives complex **8**. Then, intramolecular cyclization results in the production of 2(5*H*)-furanone and the regeneration of the acylcobalt complex. Furthermore, triple carbonylation proceeded by employing 2-aryl-3-(hydroxymethyl)oxiranes as substrates and tris(3,6-dioxaheptyl)amine as a phase transfer catalyst (Scheme 9) [30].

3 Alternating Copolymerization

Poly(3-hydroxyalkanoate)s have potential for application to engineering plastics endowed with biodegradable nature. One of the synthetic approaches to the polyesters is the ring-opening polymerization of β-substituted β-lactones which can be effectively produced by ring-expansion carbonylation of epox-

ides described above. Meanwhile, the alternating copolymerization of epoxides with CO, which was first reported by Furukawa et al. in 1965 [31], should be a more efficient and direct route to produce them.

Recently, Rieger et al. [32–34] and Osakada et al. [35] independently studied the alternating copolymerization of epoxides with CO by using $Co_2(CO)_8$/3-hydroxypyridine catalyst system, which was originally discovered by Drent et al. [23]. The copolymerization of propylene oxide with CO proceeded with high regioselectivity to give poly(3-hydroxybutyrate). Racemic propylene oxide gave atactic polyester, while enaniomerically pure (*S*)-propylene oxide afforded isotactic polyester with retension of configuration (Scheme 10), indicating the ring-opening at the less hindered epoxide carbon through the back-side attack by the tetracarbonyl cobaltate. This is the same process as that in the carbonylation of epoxide (*vide supra*). On the contrary, the generated alkoxide form an ester group not intramolecularly but intermolecularly. The chain-elongation mechanism has not yet fully revealed [32–35]. Generally, molecular weight of the obtained copolymer was low ($M_n < 4000$ g/mol) due to several termination reactions. One possible termination reaction is suggested to be the hydrolysis of an acyl-cobalt complex, a growing chain-end, induced by a trace amount of water which contaminated in the reaction system or was produced by dehydration from the polymer chain-end (Scheme 11).

Although the dehydration is an unfavorable side reaction for the production of high molecular weight polyester, the copolymer containing a polymerizable olefinic terminal group should serve as a possible macromonomer. Nozaki et al. demonstrated the successful example of the selective synthesis of oligoesters bearing a crotonate terminal group through the alternating copolymerization of propylene oxide with CO by using $NaCo(CO)_4$ in the presence of an organic base (Scheme 12) [36].

A relatively high molecular weight copolymer can be synthesized by using an acyl-cobalt complex as an initiator: such a catalyst system is not accompanied by dehydration theoretically because the terminal group of a growing species is not a free alcohol but protected by an acyl group (Scheme 13).

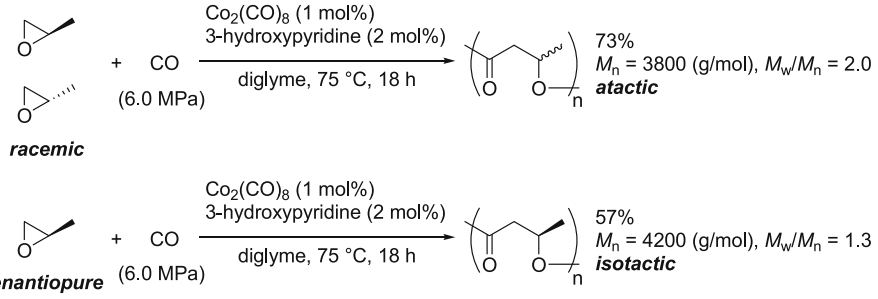

Scheme 10

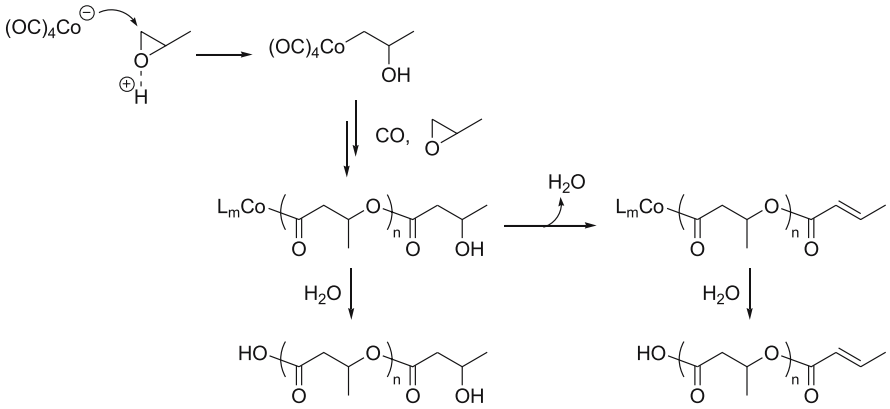

Scheme 11

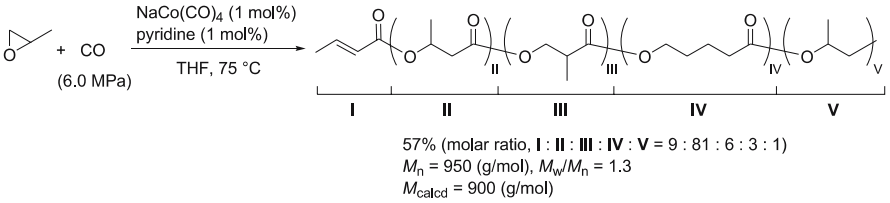

Scheme 12

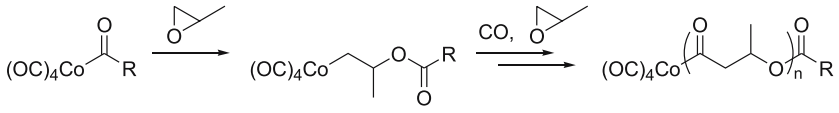

Scheme 13

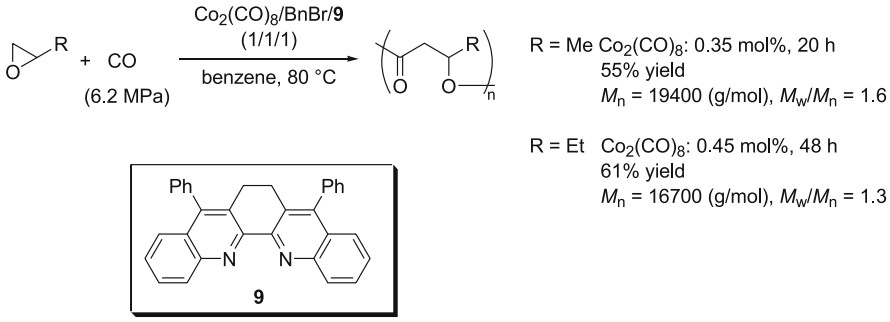

Scheme 14

An equimolar mixture of $Co_2(CO)_8$, benzyl bromide (BnBr), and dihydro-1,10-phenanthroline **9**, which generated $BnCOCo(CO)_4$ under the reaction conditions, copolymerized propylene oxide or 1,2-epoxybutane with CO to give the corresponding atactic polyesters with high regioregularities, perfectly alternating structures, and high molecular weights (Scheme 14) [37]. Isolated acyl cobalt complex $MeCOCo(CO)_3[P(o\text{-tolyl})_3]$ was also demonstrated to produce high molecular weight polyesters [38].

4 Formylation: Hydroformylation and Silylformylation

Hydroformylation of epoxides provides an elegant and inexpensive pathway to β-hydroxyaldehydes, which are formal cross-aldol products between two aliphatic aldehydes, and potentially useful intermediates in organic synthesis. In industry, hydroformylation of ethylene oxide is attractive because hydrogenation of the product 3-hydroxypropanal gives 1,3-propane diol which is an intermediate in the production of polyester fibers and films. To achieve this reaction, cobalt, rhodium, or iridium catalysts have been employed [5, 39–43]. However, during the development of the hydroformylation catalyst, the reaction has been found to often accompany some side reactions such as isomerization, hydrogenation of the resulting formyl group, and dimerization of the product β-hydroxyaldehyde. Thus, in order to establish the synthetic utility of hydroformylation of epoxides, a more sophisticated reaction system (catalyst, ligand, additive) is needed to suppress such side reactions.

One possible solution to suppress the side reactions is the in situ protection of the reactive functional groups (formyl and/or hydroxy group). A successful example of protection of the resulting formyl group is the cobalt-catalyzed hydroformylation of epoxides in the presence of trimethyl orthoformate reported by Nozaki et al.: the product β-hydroxyaldehydes were converted into its dimethyl acetal forms [44]. As shown in Table 2, hydroformylation-acetalization of various epoxides proceeded by using $Co_2(CO)_8$/iminophosphine **10** catalyst system in trimethyl orthoformate. Bicyclic *cis*-epoxides were efficiently converted into *trans*-β-hydroxyaldehyde dimethylacetals (Table 2, runs 1, 2), while the reaction of *trans*-4-octene oxide resulted in a low conversion (Table 2, run 3). When mono-substituted epoxides were employed, the terminal carbon was selectively carbonylated to give acetals of linear aldehydes as the major products (Table 2, runs 4–7). For example, the reaction with 1,2-epoxyoctane produced a mixture of linear and branched isomer (linear/branched = 4.5) in 69% isolated yield (Table 2, run 4). Functionalized terminal epoxides also gave the corresponding acetals (Table 2, runs 5–7). A single enantiomer of a protected oxyranylmethanol was converted into the corresponding linear product with complete retention of the configuration (Table 2, run 7).

Table 2

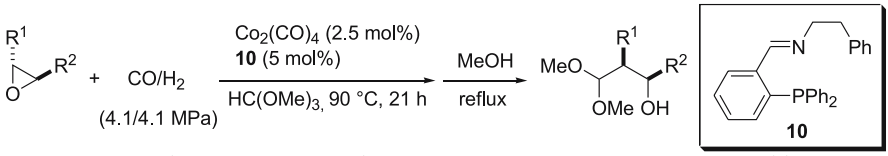

run	epoxide	product		yield (%)
1		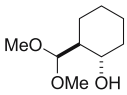		70
2		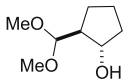		74
3		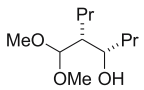		13
4		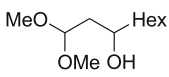 ***linear***	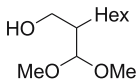 ***branched***	69 (l/b = 4.5)
5		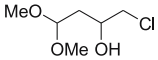		33
6	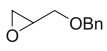	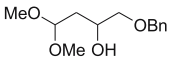		57
7	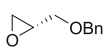	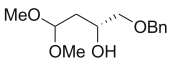		52

These results indicate that a nucleophilic attack of a tertacarbonylcobalt anion is taking place at an epoxide that is activated by a proton as illustrated in Scheme 15. Preferred formation of linear products from mono-substituted epoxides indicates the susceptibility of cobaltate nucleophile to steric hindrance in this catalytic reaction. This view is consistent with low reactivity of 1,2-disubsutituted epoxides such as *trans*-4-octene oxide. The high reactivity of bicyclic epoxides, in spite of their 1,2-disubstituted structure, is probably due to their ring-strain that overcomes the steric hindrance. Stereochemistry of the products supports that the nucleophilic ring-opening is likely proceeding through an S_N2 mechanism rather than S_N1 mechanism.

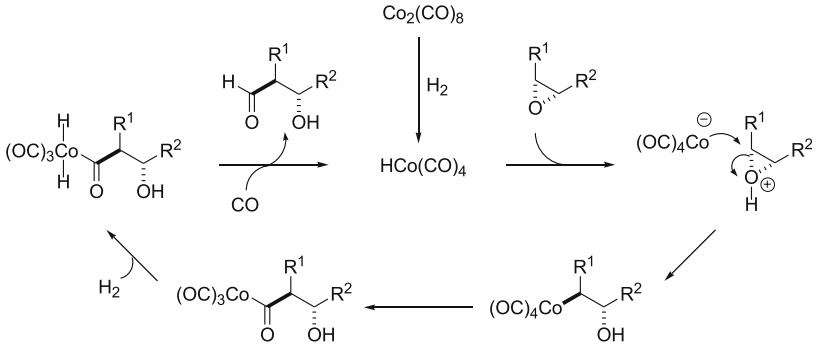

Scheme 15

Silylformylation is another successful catalytic formylation of epoxides involving the in situ protection of functional group. As a hydrosilane is deemed to behave much like a molecular hydrogen, formylation of epoxides can be carried out using a hydrosilane in place of hydrogen to give β-siloxyaldehydes [45–48]. Murai et al. reported silylformylation of epoxides by using rhodium catalysts [47]. Under the optimized conditions ($[RhCl(CO)_2]_2$: 2 mol %, 1-methylpyrazole: 40 mol %, CO: 5.1 MPa, $HSiMe_2Ph$: 1.2 equiv, CH_2Cl_2, 50 °C, 20 h), a wide range of epoxides were formylated in good yields (Table 3). The trend of regioselectivity and stereospecificity is similar to the hydroformylation described above. The authors proposed that the key catalytic species is $PhMe_2Si-Rh-H$ generated from oxidative addition of the silane to the rhodium complex (Scheme 16). The silylrhodium species interacts with the epoxide to generate a silyloxonium species and a rhodium anion which nucleophilically attacks the activated epoxide carbon. Carbonylation of the resulting carbon-rhodium bond and the subsequent reductive elimination of the aldehyde generate the product.

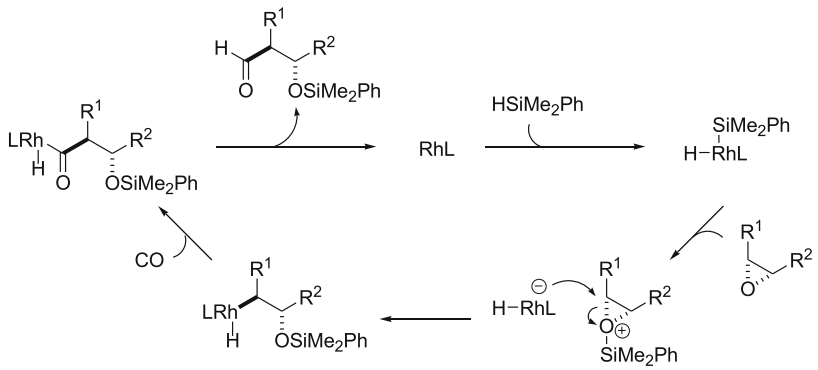

Scheme 16

Table 3

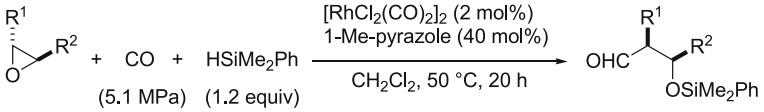

run	epoxide	product	yield (%)
1		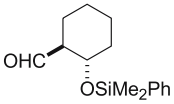	82
2		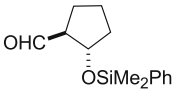	72
3		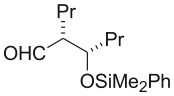	55
4		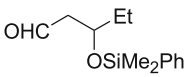 *linear* 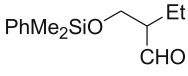 *branched*	60 (l/b = 3.3)

5
Alkoxycarbonylation and Aminocarbonylation

Carbonylation of epoxides in the presence of an alcohol gives β-hydroxyesters. This alkoxycarbonylation of epoxides with $Co_2(CO)_8$ catalyst has been known for a long time [2, 49–51]. However, the known catalyst systems required harsh reaction conditions, resulting undesired side reactions. In 1999, Jacobsen et al. demonstrated that methoxycarbonylation of epoxides proceeds effectively under relatively mild conditions by using $Co_2(CO)_8$/3-hydroxypyridine catalyst system in the presence of methanol (Scheme 17) [52]. In most cases, carbonylation occurred selectively at the less substituted epoxide carbon to afford β-hydroxyesters. Thus, enantiomerically pure mono-substituted epoxides, which are easily prepared by kinetic resolution via hydration of racemic epoxides reported by Jacobsen [53, 54], were transformed to the corresponding esters without any loss of enantiopurity. However, monosubstituted epoxides bearing an aryl or vinyl group (e.g., styrene oxide and vinyloxirane) underwent methoxycarbonylation in low yields.

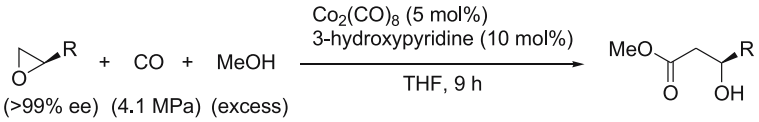

	substrate	T (°C)	yield (%)	ee (%)
R =	Me	65	92	>99
		60	95	>99
	CH_2Cl	55	96	>99
	COOMe*	60	91	>99

*CO pressure: 4.6 MPa

Scheme 17

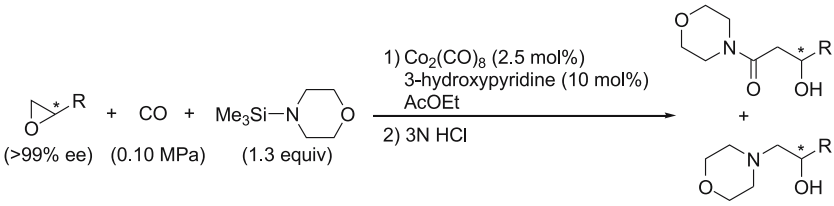

	substrate	T (°C)	time (h)	amide : amine	yield (%)	ee (%)
R =	Me	25	12	87 : 13	67	>99
		25	24	88 : 12	80	>99
	CH_2Cl	25	12	80 : 20	75	>99
	CH_2COOPr	50	12	80 : 20	56	>99

Scheme 18

Aminocarbonylation can also be carried out by use of CO and a silyl amide. Watanabe et al. reported the cobalt-catalyzed aminocarbonylation of epoxides [55]. Some silyl amides such as $PhCH_2NHSiMe_3$ and Et_2NSiMe_3 were applicable to the reaction to give the β-siloxyamide in good yields, whereas high reaction temperature was required. The use of 4-(trimethylsilyl) morpholine was found to be crucial for a milder and more efficient carboamination: here, the reaction proceeded at ambient temperature under 0.1 MPa of CO. However, *N*-(2-hydroxyalkyl)morpholines, a product without carbonylation, were yielded as by-products (Scheme 18) [56].

6 Concluding Remarks

The carbonylation of epoxides has been significantly improved in the last decade. The resulting products are of interest since β-hydroxycarbonyl compounds have potential application as useful building blocks for fine chemicals and polymer materials. Particularly, a combination of the regioselective and stereospecific carbonylation reactions and the recently developed methodology to prepare enantiopure epoxides should contribute to stereoselective organic synthesis. Meanwhile, asymmetric carbonylation of racemic or meso epoxides is still waiting to be explored as an alternative route toward enantiopure β-hydroxycarbonyl compounds. Thus, advance in stereoselectivity (kinetic resolution of racemic epoxides and desymmetrization of meso epoxides) as well as substrate scope and reaction efficiency constitute significant challenges for the future.

References

1. Séon M, Leleu J (1957) US Patent 2,782,226
2. Eisenmann JL, Yamartino RL, Howard JF Jr (1961) J Org Chem 26:2102
3. Heck RF (1963) J Am Chem Soc 85:1460
4. Takegami Y, Yokokawa C, Watanabe Y, Masada H (1964) Bull Chem Soc Jpn 37:672
5. Yokokawa C, Watanabe Y, Takegami Y (1964) Bull Chem Soc Jpn 37:677
6. Takegami Y, Yokokawa C, Watanabe Y (1964) Bull Chem Soc Jpn 37:935
7. Kreisz J, Ungváry F, Sisak A, Markó L (1991) J Organomet Chem 417:89
8. Molnar F, Luinstra GA, Allmendinger M, Rieger B (2003) Chem Eur J 9:1273
9. Khumtaveeporn K, Alper H (1995) Acc Chem Res 28:414
10. Jia L, Sun H, Travis Shay J, Allgeier AM, Hanton SD (2002) J Am Chem Soc 124:7282
11. Komine N, Tanaka S, Tsutsuminai S, Akahane Y, Hirano M, Komiya S (2004) Chem Lett 33:858
12. Getzler YDYL, Kundnani V, Lobkovsky EB, GW Coates (2004) J Am Chem Soc 126:6842
13. Furuya M, Tsutsuminai S, Nagasawa H, Komine N, Hirano M, Komiya S (2003) Chem Commun 2046
14. Pommier A, Pons JM (1993) Synthesis 441
15. Yang HW, Romo D (1999) Tetrahedron 55:6403
16. Müller HM, Seebach D (1993) 32:477
17. Hori Y, Suzuki M, Yamaguchi A, Nishishita T (1993) Macromolecules 26:5533
18. Le Borgne A, Pluta C, Spassky N (1994) Macromol Papid Commun 15:955
19. Rieth LR, Moore DR, Lobkovsky EB, Coates GW (2002) J Am Chem Soc 124:15239
20. Aumann R, Ring H (1977) Angew Chem Int Ed 16:50
21. Aumann R, Ring H, Kruger C, Goddard R (1979) Chem Ber 112:3644
22. Kamiya Y, Kawato K, Ohta H (1980) Chem Lett 1549
23. Drent E, Kragtwijk (1994) EP 577,206
24. Lee J, Thomas PJ, Alper H (2001) J Org Chem 66:5424
25. Getzler YDYL, Mahadevan V, Lobkovsky EB, Coates GW (2002) J Am Chem Soc 124:1174

26. Mahadevan V, Getzler YDYL, Coates GW (2002) Angew Chem Int Ed 41:2781
27. Schmidt JAR, Mahadevan V, Getzler YDYL, Coates GW (2004) Org Lett 6:373
28. Getzler YDYL, Mahadevan V, Lobkovsky EB, Coates GW (2004) Pure Appl Chem 76:557
29. Alper H, Arzoumanian H, Petrignani JF, Saldana-Maldonado M (1985) J Chem Soc, Chem Commun 340
30. Alper H, Eisenstat A, Satyanarayana N (1990) J Am Chem Soc 112:7060
31. Furukawa J, Iseda Y, Saegusa T, Fujii H (1965) Makromol Chem 89:263
32. Allmendinger M, Eberhardt R, Luinstra G, Rieger B (2002) J Am Chem Soc 124:5646
33. Allmendinger M, Eberhardt R, Luinstra G, Rieger B (2003) Macromol Chem Phys 204:564
34. Allmendinger M, Zintl M, Eberhardt R, Luinstra G, Molnar F, Rieger B (2004) J Organomet Chem 689:971
35. Takeuchi D, Sakaguchi Y, Osakada K (2002) J Polym Sci Part A: Polym Chem 40:4530
36. Nakano K, Kondo F, Nozaki K (2004) J Polym Sci Part A: Polym Chem 42:4666
37. Lee JT, Alper H (2004) Macromolecules 37:2417
38. Liu G, Jia L (2004) J Am Chem Soc 126:14716
39. Roos L, Goetz RW, Orchin M (1965) J Org Chem 30:3023
40. Rosenthal A, Kan G (1967) Tetrahdron Lett 8:477
41. Powell JB, Mullin SB, Weider PR, Eubanks DC, Arhancet JP (1998) US Patent 5,770,776
42. Weber R, Englert U, Ganter B, Keim W, Möthrath M (2000) Chem Commun 1419
43. Lee BN, Yang DJ, Byun YH (2002) US Patent 6,348,611 B1
44. Nakano K, Katayama M, Ishihara S, Hiyama T, Nozaki K (2004) Synlett 1367
45. Seki Y, Murai S, Yamamoto I, Sonoda N (1977) Angew Chem Int Ed 16:789
46. Murai S, Kato T, Sonoda N, Seki Y, Kawamoto K (1979) Angew Chem Int Ed 18:393
47. Fukumoto Y, Chatani N, Murai S (1993) J Org Chem 58:4187
48. Chatani N, Murai S (1996) Synlett 414
49. McClure JD, Fisher RF (1966) US Patent 3,260,738
50. Kawabata Y, Tanaka M, Hayashi T, Ogata I (1979) Nippon Kagaku Kaishi 635
51. Lee BN, Chen BS (2002) US Patent 6,348,632 B1
52. Hinterding K, Jacobsen EN (1999) J Org Chem 64:2164
53. Tokunaga M, Larrow JF, Kakichi F, Jacobsen EN (1997) Science 277:936
54. Schaus SE, Brandes BD, Larrow JF, Tokunaga M, Hansen KB, Gould AE, Furrow ME, Jacobsen EN (2002) J Am Chem Soc 124:1307
55. Tsuji Y, Kobayashi M, Okuda F, Watanabe Y (1989) J Chem Soc, Chem Commun 1253
56. Goodman SN, Jacobsen EN (2002) Angew Chem Int Ed 41:4703

Top Organomet Chem (2006) 18: 239–272
DOI 10.1007/3418_024

Published online: 20 May 2006

Oxidative Carbonylations

Bartolo Gabriele[1] (✉) · Giuseppe Salerno[2] · Mirco Costa[3]

[1]Dipartimento di Scienze Farmaceutiche, Università della Calabria, 87036 Arcavacata di Rende (Cosenza), Italy
b.gabriele@unical.it

[2]Dipartimento di Chimica, Università della Calabria, 87036 Arcavacata di Rende (Cosenza), Italy

[3]Dipartimento di Chimica Organica e Industriale, Università di Parma, 43100 Parma, Italy

1 General Overview 239

2 PdI_2-catalyzed Oxidative Carbonylations 255

References 265

Abstract The basic principles of the oxidative carbonylation reaction together with its synthetic applications are reviewed. In the first section, an overview of oxidative carbonylation is presented, and the general mechanisms followed by different substrates (alkenes, dienes, allenes, alkynes, ketones, ketenes, aromatic hydrocarbons, aliphatic hydrocarbons, alcohols, phenols, amines) leading to a variety of carbonyl compounds are discussed. The second section is focused on processes catalyzed by PdI_2-based systems, and on their ability to promote different kind of oxidative carbonylations under mild conditions to afford important carbonyl derivatives with high selectivity and efficiency. In particular, the recent developments towards the one-step synthesis of new heterocyclic derivatives are described.

Keywords Carbon monoxide · Carbonyl compounds · Heterocycles · Homogeneous catalysis · Palladium iodide

1 General Overview

Oxidative carbonylations have acquired a growing importance during the last few years, owing to the development of new and selective catalytic systems, mainly based on palladium, which are able to promote ordered sequences of transformations under mild conditions with formation of highly functionalized carbonyl compounds in one step starting from very simple building blocks.

By definition, an oxidative carbonylation is a process in which carbon monoxide is inserted into an organic substrate under the action of a metal undergoing a reduction of its oxidation state [the reduction Pd(II) → Pd(0)

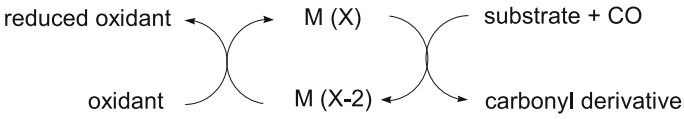

Scheme 1

is the most common case]. In order to achieve a catalytic reaction, some way must be provided to reconvert the metal in its original oxidation state (Scheme 1). In other words, an external oxidant is needed to allow a stoichiometric process (Eq. 1) to become a catalytic one (Eq. 2).

$$SH_2 + CO + M(X) \rightarrow S(CO) + M(X-2) + 2H^+ \quad (1)$$

$$SH_2 + CO + [OX] \xrightarrow{M\ cat} S(CO) + [OXH_2] \quad (2)$$

The metal reoxidation process has always been a major problem in oxidative carbonylation, in relation to which a large number of patents have been issued. Either organic or inorganic oxidants, such as benzoquinone (BQ) or copper chloride, have been used as reoxidizing agents (Eqs. 3, 4). In the case of $CuCl_2$, the resulting cuprous chloride in some cases has in its turn been reoxidized by means of oxygen (Eq. 5) or other oxidants such as alkyl nitrites. Direct reoxidation with O_2 is also possible (Eq. 6), and has proven particularly effective in the case of $Pd(0) \rightarrow PdI_4^{2-}$ reconversion (Eq. 7; see next Section).

$$M(X-2) + 2H^+ + BQ \rightarrow M(X) + H_2BQ \quad (3)$$

$$M(X-2) + 2CuCl_2 \rightarrow M(X) + 2CuCl + 2Cl^- \quad (4)$$

$$2CuCl + 2HCl + (1/2)O_2 \rightarrow 2CuCl_2 + H_2O \quad (5)$$

$$M(X-2) + 2H^+ + (1/2)O_2 \rightarrow M(X) + H_2O \quad (6)$$

$$Pd(0) + 2HI + 2I^- + (1/2)O_2 \rightarrow PdI_4^{2-} + H_2O \quad (7)$$

Another major problem in oxidative carbonylation is the presence in the reaction medium of water, which, as we have seen, is even formed as a co-product when oxygen is used as reoxidant for Cu(I) or for M(X-2). In fact, in the presence of water, competitive M-promoted oxidation processes, such as oxidation of CO to CO_2, may take place, which reduce the activity of the catalyst towards the desired carbonylation reaction. The oxidation of CO to CO_2 may be promoted by Ir(IV), Pt(IV, II), Rh(III), and especially by Pd(II), and can be stoichiometric (Eq. 8) or catalytic (working in the presence of an oxidant such as O_2, Cu(II) or quinone, Eq. 9). In the case of particularly water-sensible oxidative carbonylation processes, a dehydrating agent has proven necessary to achieve acceptable catalytic efficiencies and/or product yields. Several systems have been envisaged to eliminate water, such as acetals, enol ethers,

orthoformates, etc.

$$MX_2 + CO + H_2O \rightarrow M + CO_2 + 2HX \quad (8)$$

$$CO + H_2O + [OX] \rightarrow CO_2 + [OXH_2] \quad (9)$$

A wide range of organic substrates can undergo an oxidative carbonylation reaction. Depending on reaction conditions, **alkenes** have been converted into β-chloroalkanoyl chlorides (oxidative chloro-chlorocarbonylation) [1, 2], succinic diesters (oxidative dialkoxycarbonylation) [3–20], α,β-unsaturated esters [21, 22] (oxidative monoalkoxycarbonylation), or β-alkoxyalkanoic esters [11] (oxidative alkoxy-alkoxycarbonylation), according to Eqs. 10–13.

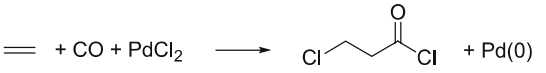

(10)

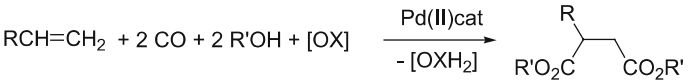

(11)

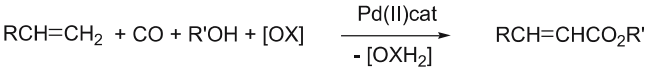

(12)

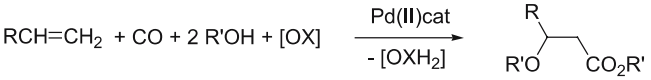

(13)

All these reactions are promoted by Pd(II) species, and can be stoichiometric (Eq. 10) or catalytic (Eqs. 11–13, in the presence of Cu(II) salts or other oxidizing agents). 3-Chloropropionyl chloride from ethylene is conceivably formed through $PdCl_2$ addition to the double bond followed by CO insertion and reductive elimination (Scheme 2).

Succinic diesters and acrylic esters are formed through insertion of the olefin into the Pd – C bond of an alkoxycarbonylpalladium species X – Pd – CO_2R (ensuing from the reaction between PdX_2, CO and an alcohol R′OH used as an external nucleophile, Scheme 3). Further carbon monoxide insertion, followed by nucleophilic displacement by R′OH, then leads to the succinic diester (Scheme 3, *path a*). β-H elimination may also take place to give the α,β-unsaturated ester (Scheme 3, *path b*). This latter pathway is followed at low carbon monoxide partial pressures.

On the other hand, β-alkoxyalkanoic esters are formed through a completely different mechanism, involving *anti* nucleophilic attack by R′OH on the coordinated double bond followed by alkoxycarbonylation (Scheme 4).

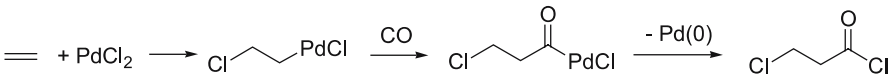

Scheme 2

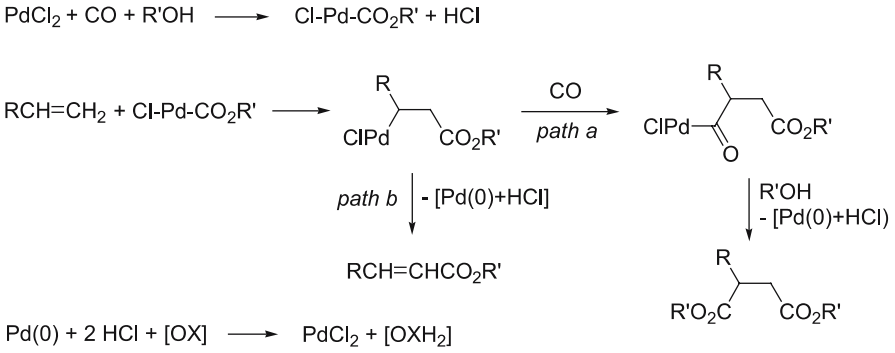

Scheme 3

Attack by other nucleophiles YH (such as amines, acids, carbanions) followed by alkoxycarbonylation has also been observed [23–28]. When the nucleophile is an organic anhydride, the final product is a β-acyloxyanhydride (Eq. 14) [29].

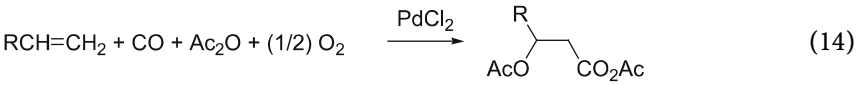

(14)

Ring closure with formation of heterocyclic derivatives may occur when a nucleophilic function is present in the starting alkene and it is suitably placed for cyclization [30–43]. Both kind of the mechanistic pathways shown in *path a* of Scheme 3 and in Scheme 4 may operate, as exemplified by Schemes 5–6 (Y = O, NR). Clearly, only in the first case carbon monoxide is incorporated into the heterocyclic ring (cyclocarbonylation).

With alkenes bearing two suitably placed nucleophilic groups, the two mechanisms may even occur in sequence, leading to a double cyclization product, as depicted in Scheme 7 [44–48].

π-Allyl palladium complexes, formed from the reaction between alkenes bearing an α-hydrogen and $PdCl_2$, can undergo alkoxycarbonylation to give β,γ-unsaturated esters (Scheme 8) [49, 50]. The overall reaction from the alkenes to the β,γ-unsaturated ester corresponds to a stoichiometric oxidative monoalkoxycarbonylation process.

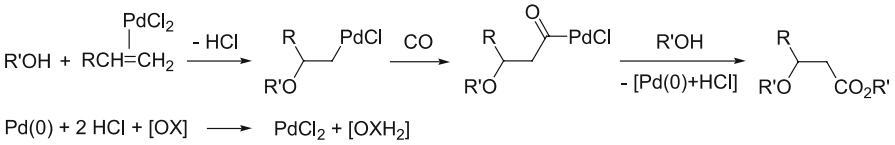

Scheme 4

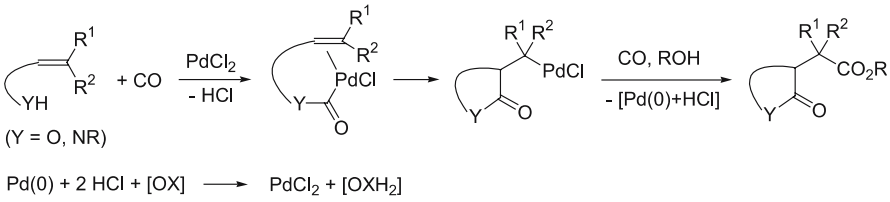

Scheme 5

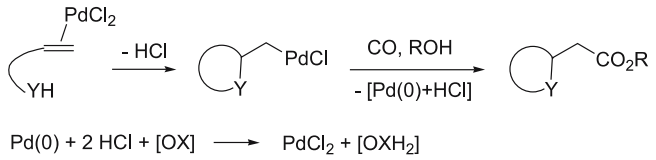

Scheme 6

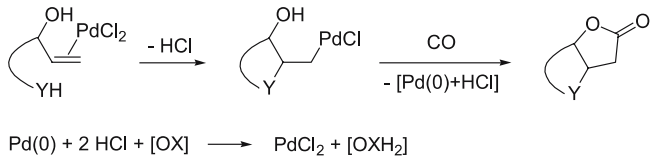

Scheme 7

β-Aminoacylpalladium complexes, obtained from the reaction between an olefin, $PdCl_2$, CO and a secondary amine, have also been reported to undergo carbonylation in the presence of piperidine to afford keto amides (Scheme 9) [51].

Conjugated dienes can also undergo Pd-catalyzed oxidative carbonylations. Thus, 1,3-butadiene has been converted into a mixture of 1,4-addition products, according to Eq. 15 [12].

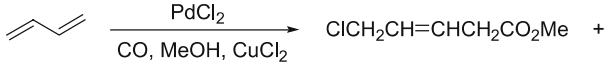

(15)

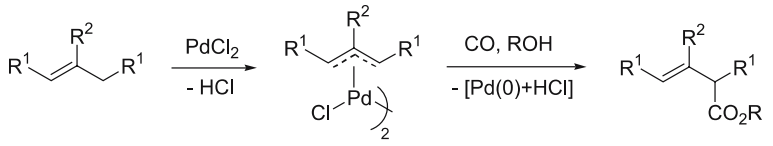

Scheme 8

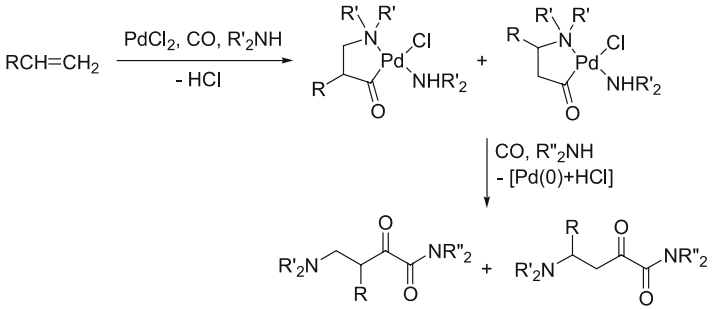

Scheme 9

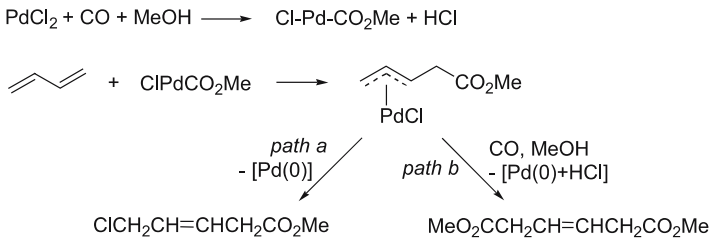

Scheme 10

The chloroester and the diester are formed through Cl – Pd – CO_2Me addition to the double bond followed by reductive elimination (Scheme 10, *path a*) or further methoxycarbonylation (Scheme 10, *path b*).

On the other hand, the methoxyester results from MeOH attack on coordinated double bond, followed by methoxycarbonylation (Scheme 11). In both cases, the formation of π-allylpalladium complexes directs the regiochemistry of the process. By optimizing the reaction conditions, it has been possible to obtain the unsaturated diester selectively. The latter compound is particularly important, since it can be easily transformed after hydrolysis and hydrogenation into adipic acid [52–54]. Selective alkoxy-alkoxycarbonylation of 1,3-dienes has also been achieved [55].

Penta-2,4-dienamides have been obtained by stoichiometric Ni(II)-promoted oxidative aminocarbonylation of 1,3-butadiene (Eq. 16) [56].

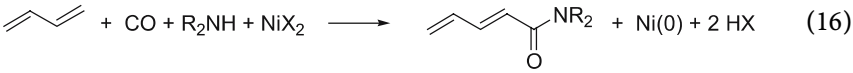

(16)

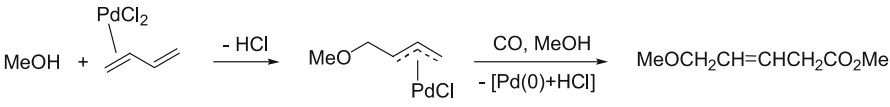

Scheme 11

Allene has been reported to undergo Pd-promoted oxidative dialkoxycarbonylation with a stoichiometric amount of $PdCl_2$ [57] (Eq. 17) and oxidative alkoxy-alkoxycarbonylation under catalytic conditions using $CuCl_2/O_2$ as the oxidizing agent [58, 59] (Eq. 18).

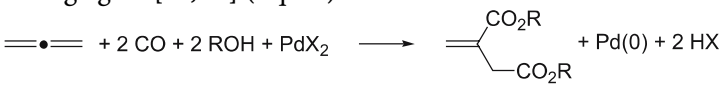

(17)

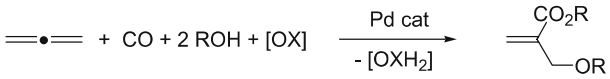

(18)

On the other hand, unsaturated β-aminoamides have been obtained by Ni(II)-promoted stoichiometric oxidative amino-aminocarbonylation of substituted allenes [60] (Eq. 19).

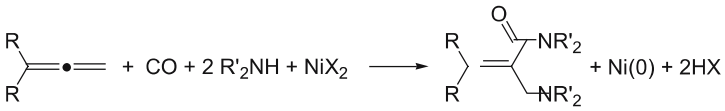

(19)

Pd(II)-catalyzed intramolecular nucleophilic attack by an oxygen [61–63] or a nitrogen [64–68] atom followed by alkoxycarbonylation has also been reported, and has allowed an easy entry to useful heterocyclic compounds (Scheme 12).

Depending on the metal promoter and reaction conditions, **alkynes** may undergo several different oxidative carbonylation reactions, most of which are promoted by Pd(II) species and are usually carried out in the presence of an oxidizing agent (such as $CuCl_2$ or O_2).

$PdCl_2$-promoted stoichiometric dichlorocarbonylation of acetylene (Eq. 20) is the first example of oxidative carbonylation of an alkyne that appeared in the literature [69, 70], and presumably occurs through the mechanism shown in Scheme 13, involving addition of $PdCl_2$ to the triple bond followed by CO insertion, reductive elimination, oxidative addition to the C – Cl bond, further CO insertion and reductive elimination (Scheme 13, *path a*).

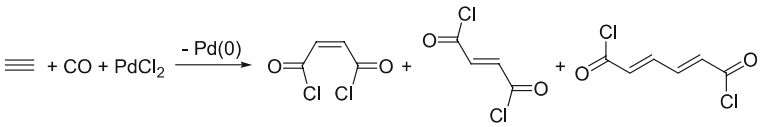

(20)

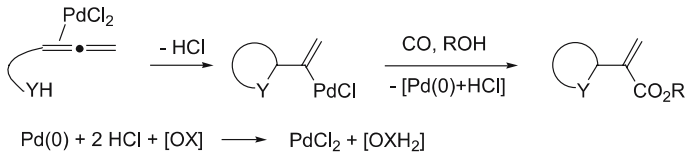

Scheme 12

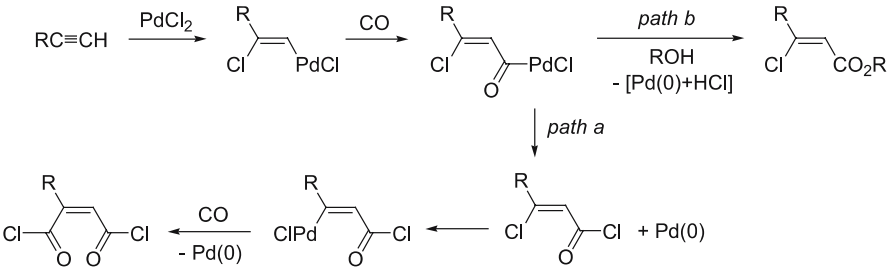

Scheme 13

It is conceivable that $PdCl_2$ addition occurs in a *syn* fashion, followed by partial isomerization. Insertion of a second molecule of acetylene before the first CO insertion is also possible and accounts for the formation of muconyl chloride. On the other hand, working in the presence of an alcohol under appropriate conditions, the β-chloroacryloylpalladium intermediate may undergo nucleophilic displacement with selective formation of (*Z*)-β-chloroacryloyl esters (Scheme 13, *path b*). In this latter case, the reaction of 1-alkynes has been made catalytic using $CuCl_2$ as oxidant [71]. The reaction has also been reported to occur with $PdBr_2$ as catalyst and $CuBr_2$ as oxidant to afford (*Z*)-β-bromoacrylates (Eq. 21) [72].

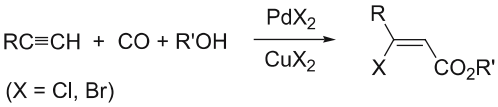

(21)

Pd(II)-catalyzed dialkoxy- or dihydroxycarbonylation of alkynes (Eq. 22, R′ = alkyl or H, respectively) with formation of maleic and fumaric esters or acids (and, in the case of acetylene, of muconic esters too), has been reported to occur in the presence of $CuCl_2$ and/or O_2 as oxidant [73–79]; electrochemical reoxidation of Pd(0) has also been described [80].

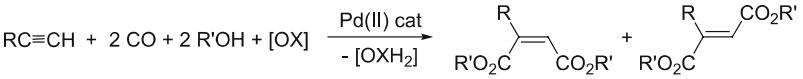

(22)

The mechanistic pathway, shown in Scheme 14, is similar to that already seen for olefin dialkoxycarbonylation (Scheme 3, *path a*). Oxydicarbonylative cyclization with formation of maleic anhydrides (Eq. 23, formally corresponding to dihydroxycarbonylation and cyclization with loss of H_2O) has been reported to occur working in the presence of water under appropriate conditions [81–86]. As can be seen in the next section, PdI_2-based catalysts have been found to be much more active with respect to other Pd(II) species, not only for alkyne dialkoxycarbonylation, but also for dihydroxycarbonyla-

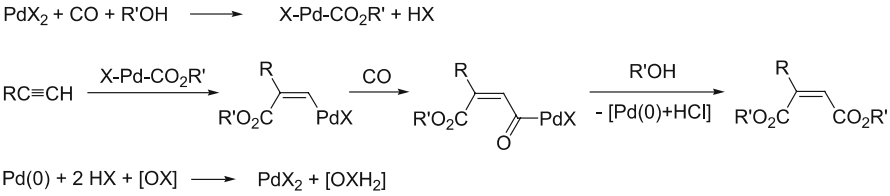

Scheme 14

tion and oxydicarbonylative cyclization.

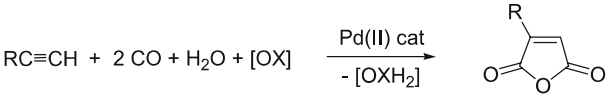

(23)

Alkyne diaminocarbonylation is also possible, and has been reported for internal alkynes using a secondary amine as the nucleophile and a stoichiometric amount of Ni(II) (Eq. 24) [87].

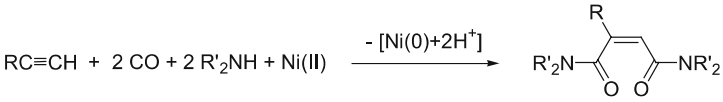

(24)

In contrast with olefins, alkoxy-alkoxycarbonylation of alkynes to give β-alkoxyacrylic esters is not a common reaction, and has occasionally been observed as a side reaction of the main reaction pathway leading to maleates and fumarates [77, 80]. However, with suitably functionalized alkynes bearing a coordinating group (such as α,α-disubstituted propargylic acetates) it may become the major reaction course (Scheme 15) [88].

On the contrary, monoalkoxycarbonylation of 1-alkynes to give 2-ynonate esters is a general reaction, which may occur either under basic conditions, favoring the formation of an alkynylpalladium species as intermediate (Scheme 16) [89–96] or under conditions allowing β-H elimination from an alkoxycarbonylvinylpalladium species (Scheme 17) [83].

Monoaminocarbonylation of 1-alkynes has also been reported, in the presence of a stoichiometric amount of a Ni(II) complex (Eq. 25) [97, 98] or of

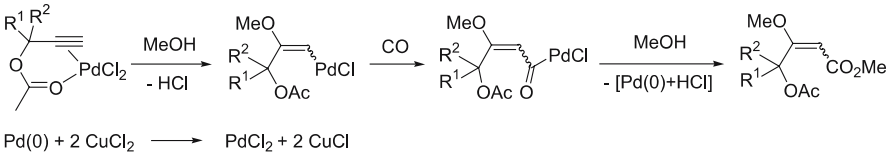

Scheme 15

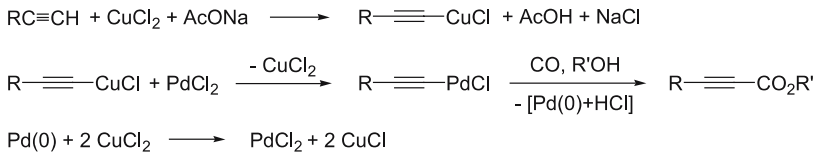

Scheme 16

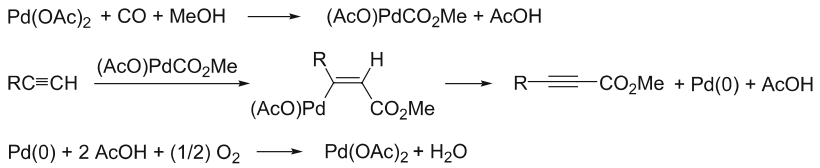

Scheme 17

catalytic amounts of PdI_2 – KI (see next Section) [99].

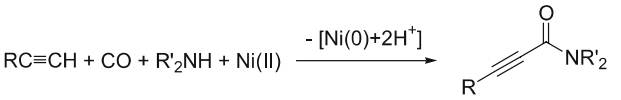

(25)

Alkynes bearing a nucleophilic group in suitable position for cyclization are excellent substrates for different kinds of oxidative carbonylation reactions leading to functionalized heterocyclic derivatives. Both oxidative cyclocarbonylation (with incorporation of CO into the cycle) and oxidative cyclization–carbonylation (without incorporation of CO ino the cycle) are possible. All these reactions are catalyzed by Pd(II) species. For example, alkynols and alkynamines have been successfully converted into β- and γ-lactones or lactams (cyclocarbonylation products) through the general pathways shown in Scheme 18 (X = Cl, I; Y = O or NR, NuH = external nucleophile, such as an alcohol or an amine) [39, 100–103]. Thus, insertion of the triple bond into the Pd – C bond of an X – Pd – CONu intermediate (formed from the reaction between PdX_2, CO and NuH) followed by CO insertion and intramolecular nucleophilic attack by YH on the acylpalladium complex may occur (Scheme 18, *path a*). Another possibility is the formation of an – YPdX intermediate (stabilized by triple bond coordination, Scheme 18, *path b*), which in its turn may undergo either CO insertion followed by triple bond insertion, further carbonylation and nucleophilic displacement by NuH (Scheme 18, *path c*) or external attack by NuH (with formation of a palladacycle complex) followed by CO insertion and reductive elimination (Scheme 18, *path d*).

Products deriving from cyclization–alkoxycarbonylation are instead formed through the general mechanism shown in Scheme 19, involving *exo* (*path a*) or *endo* (*path b*) intramolecular nuclophilic attack by YH to the triple bond coordinated to Pd(II) followed by CO insertion and nucleophilic

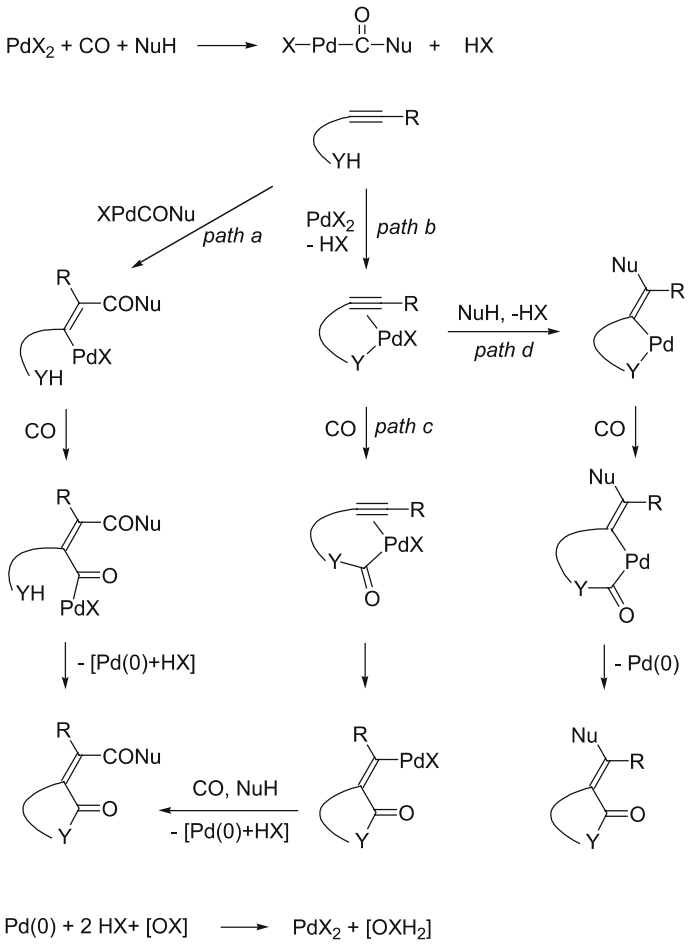

Scheme 18

displacement by NuH [104–121]. The *exo* mode has been observed more frequently with respect to the *endo* one.

Ketones can be oxidatively carbonylated at the α-carbon via enol intermediates using $PdCl_2$ as the catalyst and $CuCl_2$ as oxidant [122]. The initially formed carbonylation products correspond to α-chlorination and α-alkoxycarbonylation. Under the reaction conditions, these compounds undergo further transformations involving C – C cleavage eventually leading to a mixture of esters and an alkyl chloride or (in the case of cyclic ketones) to a diester and a chloroester (Schemes 20–21).

The oxidative carbonylation reaction of enolizable ketones follows the general routes already illustrated for simple alkenes. Thus, α-methoxycarbonylation may occur either by addition of a Cl – Pd – CO_2Me species to the enolic

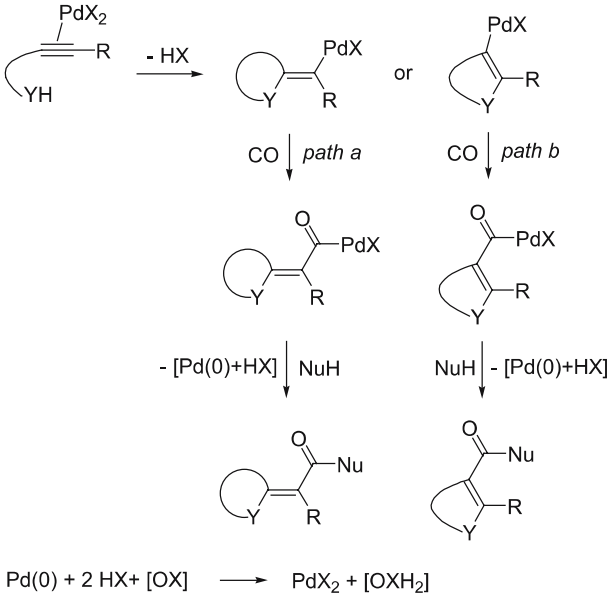

Scheme 19

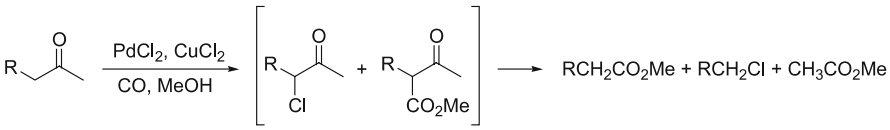

Scheme 20

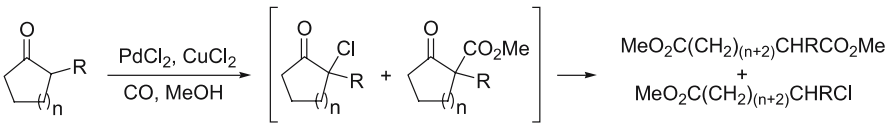

(n = 1-3; R = H or Me)

Scheme 21

double bond followed by [Pd(0) + HCl] elimination from the H – O – C – PdCl unit (Scheme 22, *path a*) or by MeOH attack on the enolic double bond followed by CO insertion, MeOH elimination and nucleophilic displacement by MeOH (Scheme 22, *path b*).

Some trimethylsilyl enol ethers, not able to undergo β-H elimination, have been stoichiometrically converted into α-alkoxycarbonyl ketones via the intermediate formation of oxa-π-allyl complexes (Scheme 23) [123, 124].

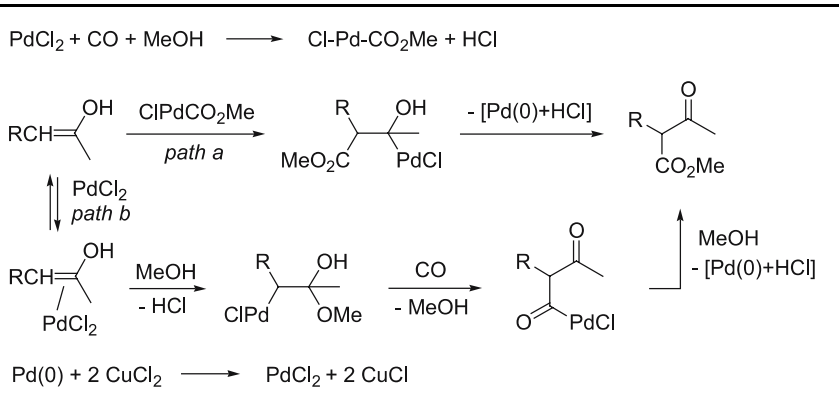

Scheme 22

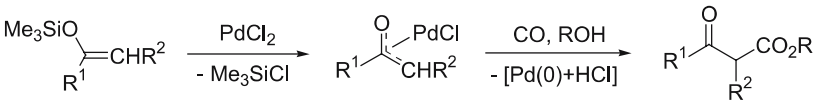

Scheme 23

Ketene can also be oxidatively carbonylated, using $PdCl_2$ as the catalyst and alkyl nitrites as the oxidant, to give dialkyl malonates (Eq. 26) [125]. Ketodiesters have been obtained from diketene (Eq. 27) [126].

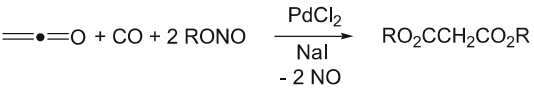

(26)

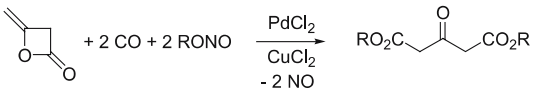

(27)

Oxidative carbonylation can also be achieved by metal-assisted C – H activation. The Pd(II)-promoted oxidative carbonylation of **arenes** to give aromatic acids has been reported to occur under stoichiometric [127, 128] as well as catalytic [129–138] conditions (Eqs. 28–30). In the case of alkylbenzenes, the Pd-catalyzed reaction shows only a moderate selectivity towards the *para* position. Better *p*-selectivities have however been attained by employing Rh(III) or Ir(III) catalysts [139–146].

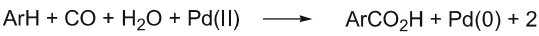

(28)

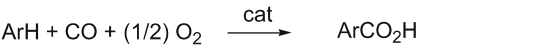

(29)

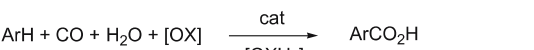

(30)

The reaction is believed to begin with the metalation of the substrate via aromatic electrophilic substitution (S_EAr) followed by CO insertion and nucleophilic displacement by water or another protic nucleophile such as trifluoroacetic acid (TFFA) to give, respectively, the aromatic carboxylic acid or its mixed anhydride derivative, from which the acid is freed by hydrolysis (Scheme 24).

In a similar way, carboxylic esters have been obtained stoichiometrically by ortho palladation of aromatic amides (Scheme 25) [147] and of phenyl-substituted isoxazoles or oxazoles [148] followed by alkoxycarbonylation.

Even **aliphatic hydrocarbons** are susceptible to oxidative carbonylation. From an industrial point of view, the most important process concerns the direct conversion of methane into acetic acid. This transformation has been achieved with Rh(III)-based catalysts using oxygen as the oxidizing agent [149–153], and it is still object of investigations aimed at developing more efficient catalytic systems working under mild conditions.

Oxidative carbonylation is not necessarily associated with C – C bond formation. Indeed, heteroatom carbonylation may occur exclusively, as in the oxidative carbonylation of **alcohols or phenols** to carbonates, of alcohols and amines to carbamates, of aminoalcohols to cyclic carbamates, and of **amines** to ureas. All these reactions are of particular significance, in view of the possibility to prepare these very important classes of carbonyl compounds through a phosgene-free approach. These carbonylations are usually carried out in the presence of an appropriate oxidant under catalytic conditions (Eqs. 31–33), and in some cases can be promoted not only by transition metals but also by

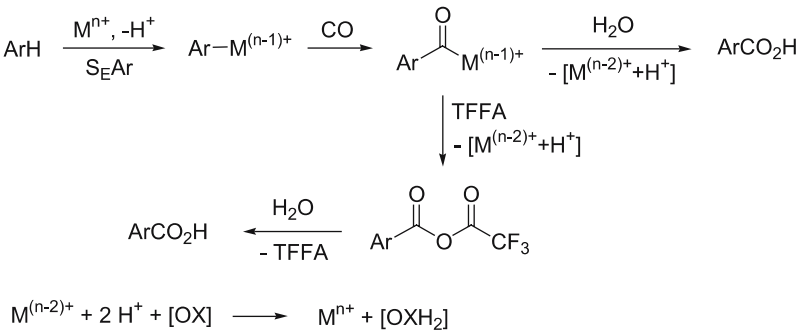

Scheme 24

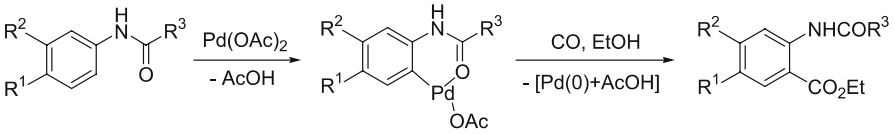

Scheme 25

main-group elements such as chalcogens.

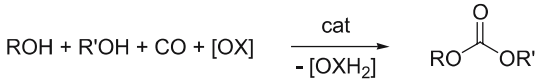

(31)

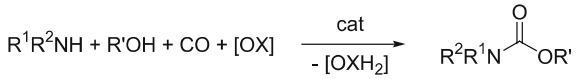

(32)

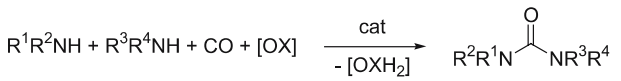

(33)

The metal-promoted processes follow a general mechanistic route, involving the intermediate formation of an alkoxycarbonyl- or a carbamoyl-metal species from the reaction between MX_2, CO and NuH (NuH = alcohol, phenol or amine), followed by nucleophilic attack by Nu′H (Nu′H = alcohol, phenol or amine) (Scheme 26).

In the case of carbonylation of primary amines, the carbamoylmetal complex may undergo β-H elimination from the M – C(O) – NHR unit, with intermediate formation of an isocyanate, from which the final product is originated by nucleophilic attack by Nu′H (Scheme 27).

An isocyanate intermediate may also be involved in the selenium-catalyzed process, which starts with the formation of carbonyl selenide from the reaction between selenium and CO, followed by nucleophilic attack by NuH (Scheme 28). When NuH = primary amine, the resulting RNH(CO)SeH intermediate may eliminate H_2Se to give the isocyanate, which then reacts with Nu′H to give the final product (Scheme 28, *path a*). Alternatively, oxidation of Nu(CO)SeH by O_2 may lead to a bis(carbamoyl)diselenide species, which is attacked by NuH (Scheme 28, *path b*).

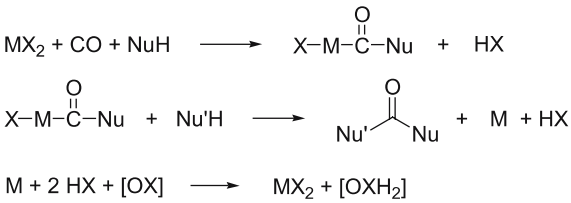

Scheme 26

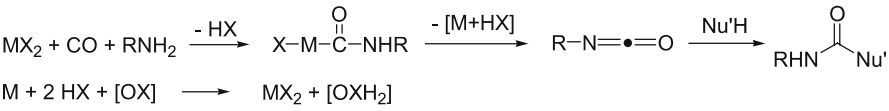

Scheme 27

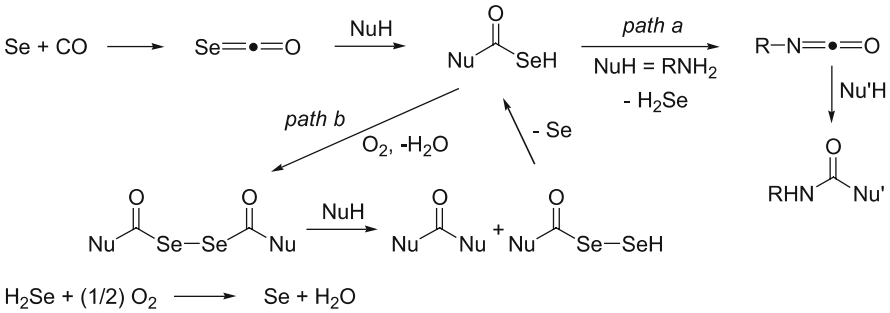

Scheme 28

The oxidative carbonylation of alcohols and phenols to carbonates can be catalyzed by palladium or copper species [154–213]. This reaction is of particular practical importance, since it can be developed into an industrial process for the phosgene-free synthesis of dimethyl carbonate (DMC) and diphenyl carbonate (DPC), which are important industrial intermediates for the production of polycarbonates. Moreover, DMC can be used as an eco-friendly methylation and carbonylation agent [214, 215]. The industrial production of DMC by oxidative carbonylation of methanol has been achieved by Enichem [216] and Ube [217].

The direct conversion of alcohols and amines into carbamate esters by oxidative carbonylation is also an attractive process from an industrial point of view, since carbamates are useful intermediates for the production of polyurethanes. Many efforts have, therefore, been devoted to the development of efficient catalysts able to operate under relatively mild conditions. The reaction, when applied to amino alcohols, allows a convenient synthesis of cyclic urethanes. Several transition metal complexes, based on Pd [218–239], Cu [240–242], Au [243, 244], Os [245], Rh [237, 238, 246, 247], Co [248], Mn [249], Ru [224, 250–252], Pt [238] are able to promote the process. The formation of ureas, oxamates, or oxamides as byproducts can in some cases lower the selectivity towards carbamates.

The oxidative carbonylation of amines to give ureas is at present one of the most attractive ways for synthesizing this very important class of carbonyl compounds via a phosgene-free approach. Ureas find extensive application as agrochemicals, dyes, antioxidants, resin precursors, synthetic intermediates (also for the production of carbamates and isocyanates), and HIV-inhibitors. Many transition metals (incuding Au [244], Co [248, 253–255], Cu [242], Mn [249, 256–258], Ni [259], Rh [246, 247, 260–262], Ru [224, 260, 263] and especially Pd [219, 225, 226, 264–276], and, more recently, W [277–283]) as well as main-group elements (such as sulfur [284–286] and selenium [287–292]) have been reported to promote the oxidative carbonylation of amines, usually under catalytic conditions. In some cases, carbamates and/or oxamides are formed as byproducts, thus lowering the selectivity of the process.

Optimal conditions for the synthesis of symmetrically disubstituted or tetrasubstituted ureas as well as of unsymmetrically disubstituted or trisubstituted ureas have, however, been developed (see also next Section).

Under appropriate conditions, alcohols and amines can undergo an oxidative double carbonylation process, with formation of oxalate esters (Eq. 34), oxamate esters (Eq. 35) or oxamides (Eq. 36). These reactions are usually catalyzed by Pd(II) species and take place trough the intermediate formation of bis(alkoxycarbonyl)palladium, (alkoxycarbonyl)(carbamoyl)palladium or bis(carbamoyl)palladium complexes, as shown in Scheme 29 (NuH, Nu′H = alcohol or amine) [227, 231, 267, 293–300].

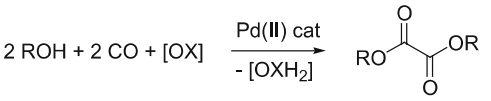

(34)

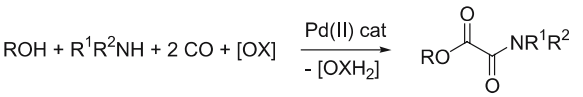

(35)

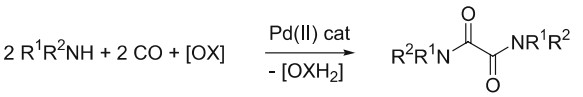

(36)

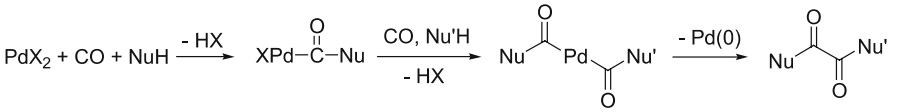

Scheme 29

2 PdI_2-catalyzed Oxidative Carbonylations

In our laboratories, we have found that PdI_2, in conjunction with an excess of iodide anions, constitutes an exceptionally efficient, selective and versatile catalyst for promoting a variety of oxidative carbonylation processes, leading to important acyclic as well as heterocylic carbonyl compounds.

Particularly significant results have been obtained in the oxidative carbonylation of simple and functionalized alkynes. Thus, the PdI_2/KI-catalyzed oxidative carbonylation of simple alkyl- or arylacetylenes, as well as of propynyl alcohol and propynyl acetate, carried out in alcoholic solvents under mild conditions (15–25 atm of CO, 4–9 atm of air, 25–80 °C), led to the formation of maleic derivatives (together with small amounts of fumaric derivatives) and 5,5-dialkoxyfuran-2(5*H*)-ones, in high yields and with unprecedented catalytic efficiencies for this kind of reaction (up to ca. 4000 mol of product

per mol of Pd) (Eq. 37) [76, 77]. The furanone derivatives were easily converted into maleic esters by acid-promoted alcoholysis. The process could also be applied to the synthesis of maleic acids or maleic anhydrides [86] working in DME-H_2O or water-containg dioxane, respectively, under appropriate conditions.

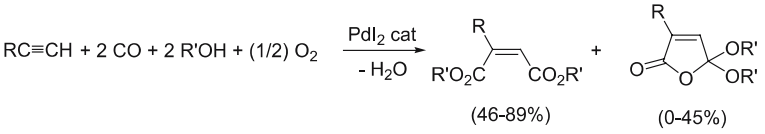

(37)

Scheme 30 shows the proposed reaction mechanism, which involves the formation of an acylpalladium species as the key intermediate, in tautomeric equilibrium with a cyclic π-allyl complex (in this and in the following Schemes, unreactive ligands are omitted for clarity). The main reason for the high activity of the PdI_4^{2-}-based catalyst in this process lies in the very efficient mechanism of reoxidation of Pd(0), which involves oxidation of HI by O_2 to I_2, followed by oxidative addition of the latter to Pd(0). It is worth nothing that under these conditions Pd(0) reoxidation occurs readily without need for Cu(II) or organic oxidants.

The application of this methodology to suitably functionalized alkynes has allowed a direct and easy synthesis of important heterocyclic compounds starting from readily available substrates. New β-lactone [100, 101] and β-lactam [102] derivatives were synthesized in good yields from α,α-disubstituted propynyl alcohols and amines, respectively (Eq. 38), through the mechanistic route shown in Scheme 18, *path a*. The substitution α to the triple bond was a necessary requisite for cyclization to occur, owing to the reactive rotamer effect [301].

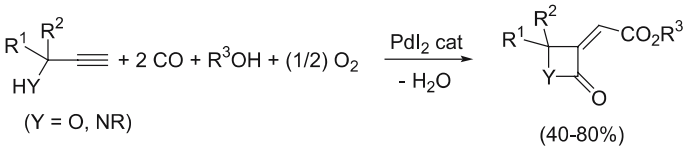

(38)

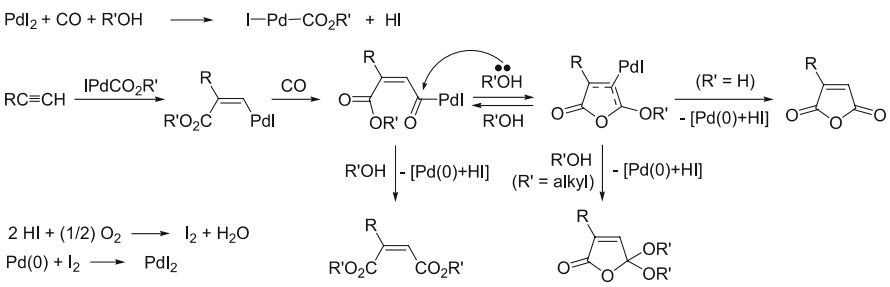

Scheme 30

On the other hand, γ-lactone [101] and dihydroindol-2-one [103] derivatives were obtained in fair to excellent yields from 3-yn-1-ols and 2-ethynylanilines, respectively (Eqs. 39–40), through the *path b* of Scheme 18 (double bond isomerization occurred in the latter case).

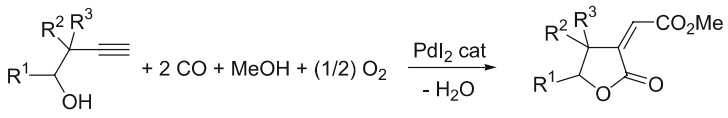

(39)

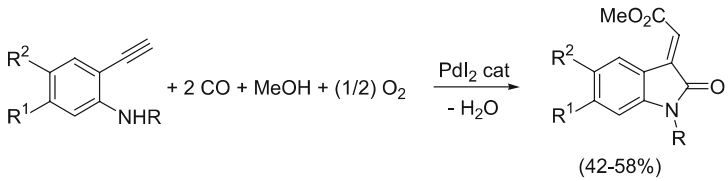

(40)

Although less efficient than PdI_2/KI, a catalytic system consisting of Pd/C – KI could also be used in these reactions. In this case, the catalytically active species PdI_4^{2-} was clearly formed in situ by Pd(0) oxidation under the reaction conditions.

All these reactions are examples of oxidative cyclocarbonylation–alkoxycarbonylation. However, the PdI_2/KI catalytic system turned out to be a very efficient catalyst also for promoting cyclization–alkoxycarbonylation processes. In fact, optimal conditions were found for selectively converting 4-yn-1-ols into tetrahydrofuran derivatives (Eq. 41) [107] through 5-*exo-dig* cyclization followed by alkoxycarbonylation (Scheme 19, *path a*). This kind of process was not possible for the propynyl, 3-yn-1-ol, and 2-ethynylaniline substrates, seen before, for stereoelectronic reasons [302]. With the latter substrates, the *endo* cyclization mode (Scheme 19, *path b*), although in principle stereoelectronically allowed, was not observed.

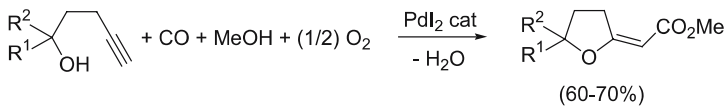

(41)

Of particular interest was the carbonylation of (*Z*)-2-en-4-yn-1-ols and (*Z*)-(2-en-4-ynyl)amines, which afforded furan-2-acetic [104, 105] and pyrrole-2-acetic [116] esters, respectively, in good yields, through spontaneous or acid-promoted aromatization of the initially formed (*E*)-2-(alkoxycarbonyl)-methylene-2,5-dihydro-furans or -pyrroles (Scheme 31).

In the case of carbonylation (*Z*)-(2-en-4-ynyl)amines, a peculiar promoting effect by CO_2 has been found. In fact, CO_2 "buffers" the basicity of the substrate, with formation of a carbamate anion, thus "freeing" the HI neces-

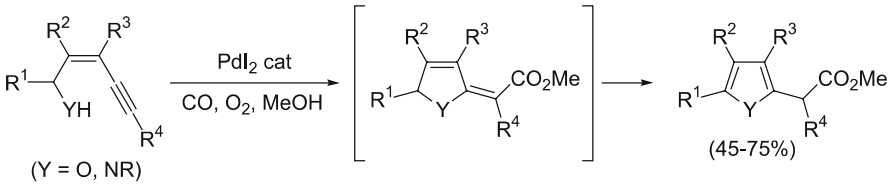

Scheme 31

sary for Pd(0) reoxidation. The nitrogen of the carbamate, while less basic than in the starting amine, may still act as nucleophile since CO_2 can be eliminated during the cyclization step leading to the five-membered product (Scheme 32).

On the other hand, when the oxidative carbonylation of α,α-disubstituted propynylamines was carried out in the presence of an excess of CO_2, the intermediate carbamate species could undergo cyclization with incorporation of CO_2 into the five-membered cycle, either by direct nucleophilic attack of the carbamate oxygen to the triple bond coordinated to Pd(II) (Scheme 33, *path a*) or through the intermediate formation of a palladium carbamate complex followed by triple bond insertion (Scheme 33, *path b*). Carbon monoxide insertion into the Pd – C bond of the resulting stereoisomeric vinylpalladium intermediates then led to the final oxazolidinone derivatives.

The overall sequence (Eq. 42) represents the first example reported in the literature of catalytic incorporation of both CO and CO_2 into an organic sub-

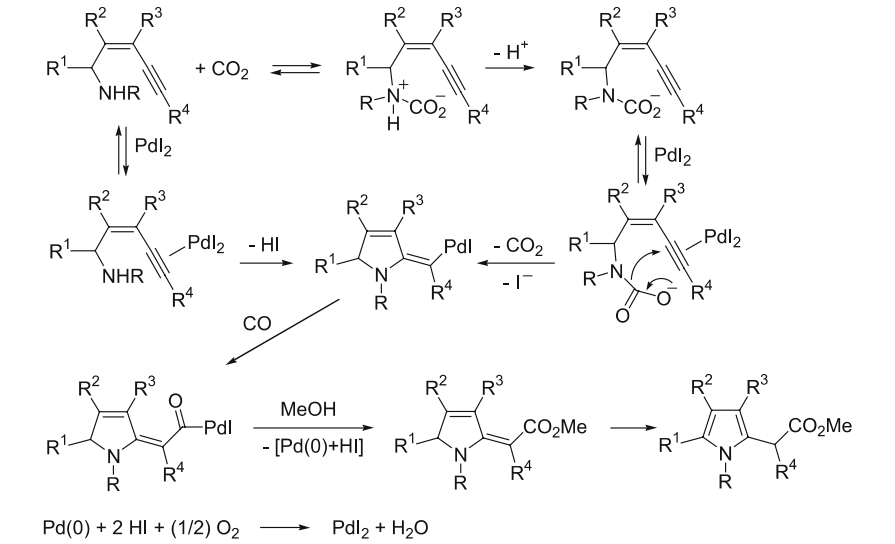

Scheme 32

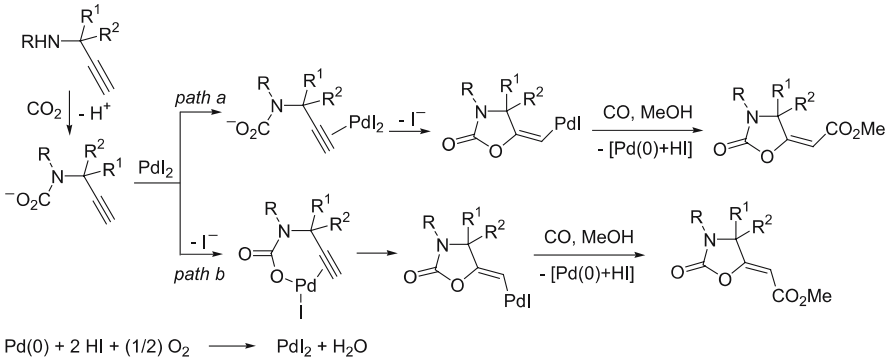

Scheme 33

strate [114, 115].

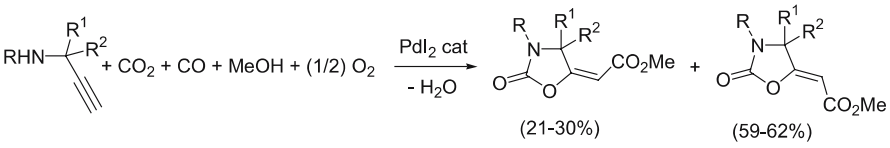

(42)

In contrast with the reaction of 4-yn-1-ols, both 6-*endo-dig* and 5-*exo-dig* cyclization modes were observed in the PdI_2/KI-catalyzed oxidative carbonylation of 2-(1-alkynylbenzyl)alcohols (Eq. 43) [120]. The preferential formation of the 1*H*-isochromene or the 1,3-dihydroisobenzofuran derivative turned out to be dependent on the substitution pattern of the substrate. In particular, 1*H*-isochromenes were obtained as the main reaction products when the triple bond was substituted with an alkyl group and with a primary alcoholic group, while the isobenzofurans were preferentially formed with a tertiary alcoholic group and when the triple bond was terminal or conjugated with a phenyl group.

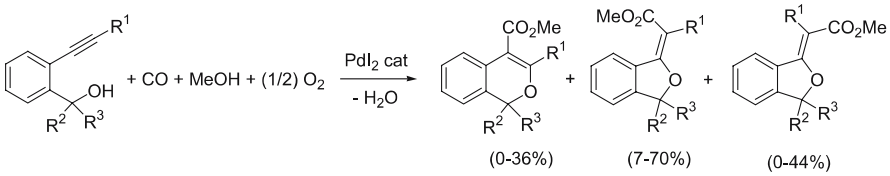

(43)

A suitably placed carbonyl oxygen can also act as intramolecular nucleophile in PdI_2/KI-catalyzed oxidative cyclization–alkoxycarbonylation re-

actions. The nucleophilicity of simple aldehydic or ketonic groups is not sufficient to give a direct attack to a coordinated triple bond; however, in the presence of an alcohol as external nucleophile, the formation of a tetrahedral intermediate takes place, in which the oxygen atom becomes nucleophilic. Therefore, a cyclization–alkoxycarbonylation sequence can be triggered by an initial external attack by an alcohol to an aldehydic or ketonic carbonyl group. This possibility has been verified by reacting 2-(1-alkynyl)benzaldehydes or 2-(1-alkynyl)phenylketones in ROH – CH_3CN mixtures under oxidative conditions (Scheme 34) [120]. As in the case of 2-(1-alkynylbenzyl)alcohols, formation of both six-membered and five-membered rings took place and, as expected, formation of isochromenes was favored starting from aldehydes, while ketones mainly afforded dihydroisobenzofurans.

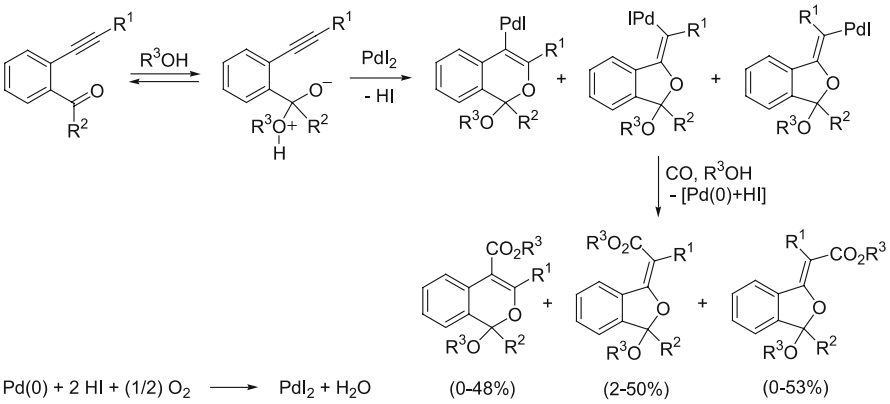

Scheme 34

In the case of acetylenic amides, the carbonyl oxygen atom turned out to be nucleoplilic enough to directly attack the coordinated triple bond, owing to the conjugation with the amide moiety. Thus, α,α-dialkyl substituted 2-ynylamides smoothly underwent oxidative cyclization–alkoxycarbonylation to afford new oxazoline derivatives in good yields (Eq. 44) [102, 113].

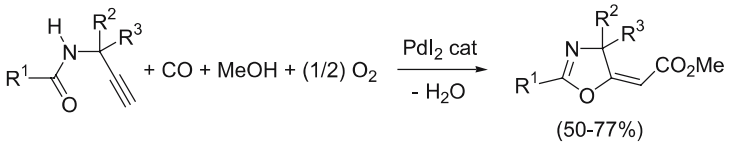

(44)

In a similar way, *N*-(2-ethynylphenyl)benzamides, formed in situ by deprotection of the triple bond of *N*-(2-trimethylsilylethynyl)benzamides, were

easily converted into benzoxazine derivatives according to Eq. 45 [121].

(45)

N-(1,1-Dialkylprop-2-ynyl)ureas, bearing a bidentate ureic function, afforded oxazoline and cyclic ureas derivatives simultaneously, depending on whether the cyclization was initiated by the oxygen or the nitrogen atom (Eq. 46) [106]. The nature of the nitrogen substituent strongly influenced the product distribution.

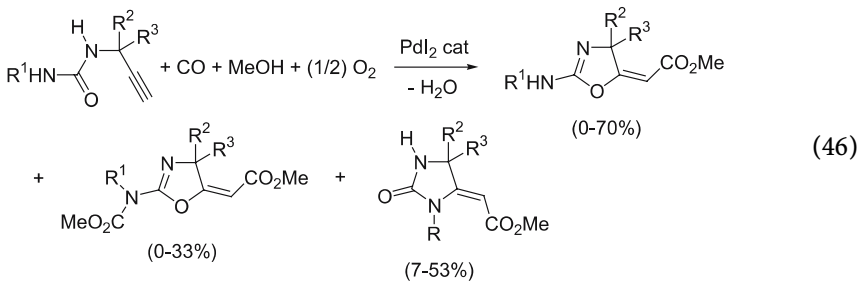

(46)

In a similar way, 3-(2-ethynylphenyl)ureas, formed in situ by deprotection of the triple bond of 3-(2-trimethylsilylethynylphenyl)ureas, afforded benzoxazine or quinazoline derivatives, as exemplified by Eqs. 47 and 48 [121].

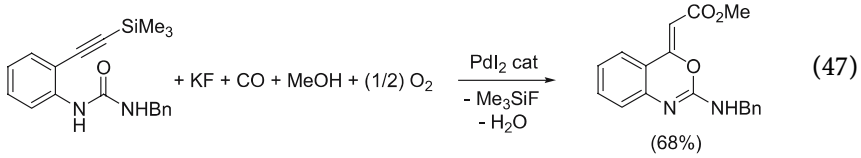

(47)

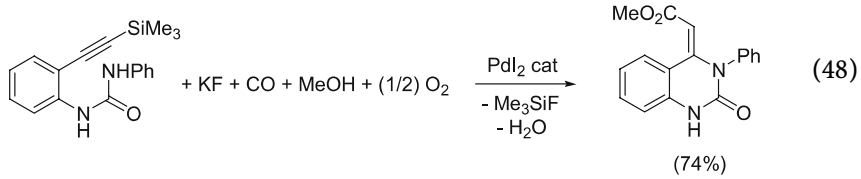

(48)

An interesting reaction course was followed in the case of dipropargyl amides and dipropargyl sulfide. With these diynes, in fact, triple bond insertion into the Pd – C bond of an alkoxycarbonylpalladium complex was followed by insertion of the second triple bond and alkoxycarbonylation (Scheme 35) [303,

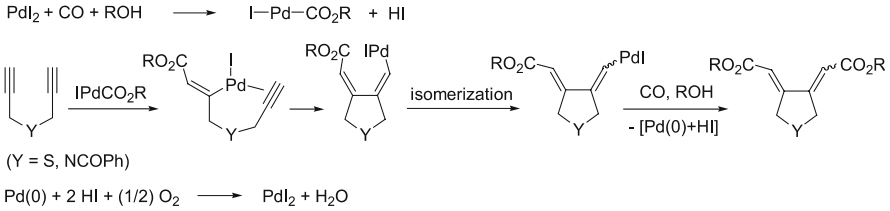

Scheme 35

304]. The resulting tetrahydropyrroles and tetrahydrothiophenes could be easily aromatized under basic conditions (Scheme 36), thus allowing a convenient access to a new class of pyrrole and thiophene derivatives, which have found application in the preparation of new organic materials [304–308].

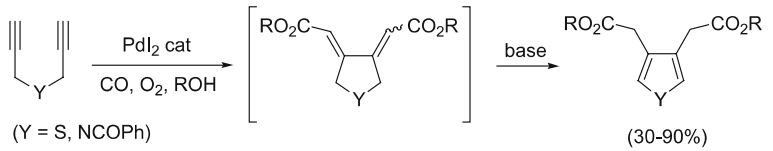

Scheme 36

The PdI_2 – KI system is an excellent catalyst also for promoting the oxidative monoaminocarbonylation of terminal alkynes, carried out in the presence of a nucleophilic secondary amine in 1,4-dioxane as the solvent (Eq. 49) [309].

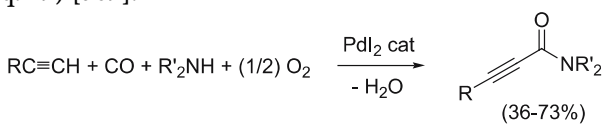

(49)

The shift towards the monoaminocarbonylation, obtained under these conditions, as compared with the dialkoxycarbonylation observed in alcoholic solvents, is due to the basicity of the amine, which favors the formation of an alkynylpalladium complex (Scheme 37). This species then inserts carbon monoxide with formation of an alkynoylpalladium intermediate, which undergoes nucleophilic displacement by R_2NH to give the final 2-ynamide.

This kind of reactivity turned out to be particularly attractive when applied to suitably functionalized terminal alkynes. Oxidative monoaminocarbonylation of 4-yn-1-ols led to the formation of tetrahydrofuran derivatives through intramolecular conjugate addition of –OH group to the triple bond of the initially formed 6-hydroxy-2-ynamide intermediates (Scheme 38) [310].

Even more interesting was the reaction of α-substituted propynyl alcohols and amines. In this case, in fact, the initially formed 4-hydroxy-2-ynamides

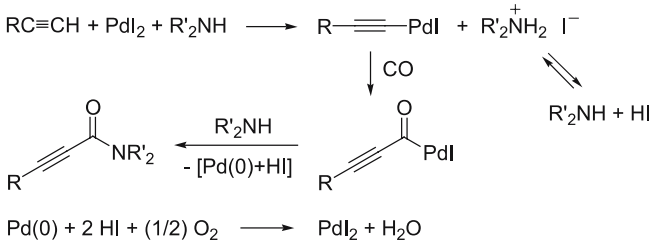

Scheme 37

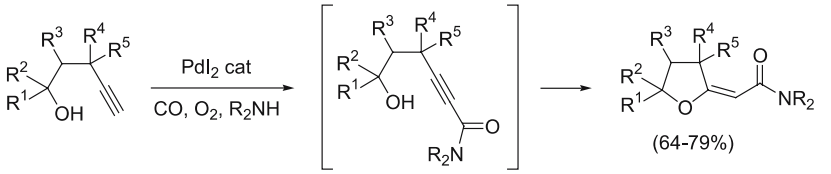

Scheme 38

or 4-amino-2-ynamides, respectively, could not undergo intramolecular conjugate addition for stereoelectronic reasons. These intermediates, however, underwent *external* conjugate addition of R_2NH, with formation of (*E*)-3-dialkylamino-4-hydroxy-2-enamides or (*E*)-3-dialkylamino-4-amino-2-enamides, which could easily eliminate R_2NH to afford 4-dialylamino-5*H*-furan-2-ones [311] or 4-dialkylamino-1,5-dihydropyrrol-2-ones [312], respectively (Scheme 39). These heterocyclic derivatives could be easily transformed into tetronic acids and tetramic acids, respectively, by acid-promoted hydrolysis (Eq. 50).

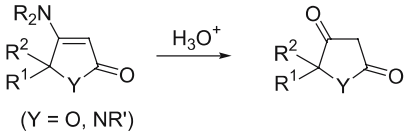

(50)

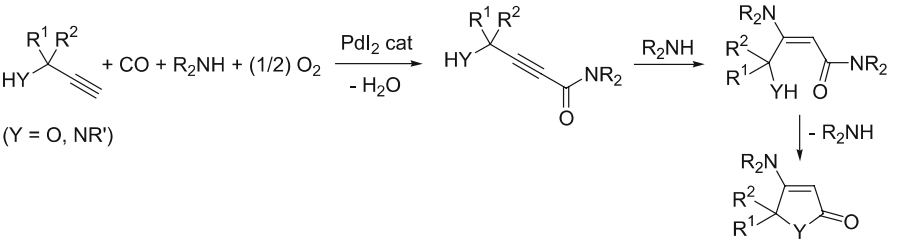

Scheme 39

The versatility of the PdI_2/KI catalytic system is further demonstrated by its ability to catalyze the oxidative carbonylation of primary amines to symmetrically substituted ureas (Eq. 51), still under mild conditions (100 °C, 16 atm of CO, 4 atm of air in DME as the solvent) and with unprecedented catalytic efficiencies for this kind of reaction (up to ca. 2500 mol of product per mol of Pd) [274, 275]. In some cases, working in the presence of an excess of CO_2 (40 atm) had a beneficial effect on the reaction rate and product selectivity.

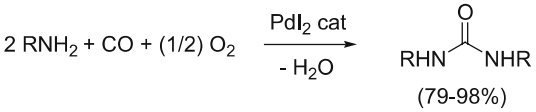

(51)

The methodology did not work for secondary amines, thus suggesting the formation of an isocyanate as intermediate (Scheme 27, $MX_2 = PdI_2$, [OX] = (1/2) O_2]. However, by reacting a primary amine in the presence of a secondary nucleophilic amine, a general and selective synthesis of trisubstituted ureas has been achieved, through trapping of the isocyanate intermediate by the secondary amine (Eq. 52) [274, 275].

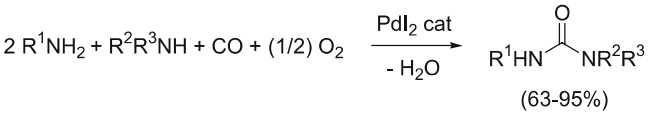

(52)

Intramolecular trapping was also possible, as exemplified by the synthesis of cyclic ureas (Eq. 53) [275] and oxazolidin-2-ones [232, 234] (Eqs. 54 and 55).

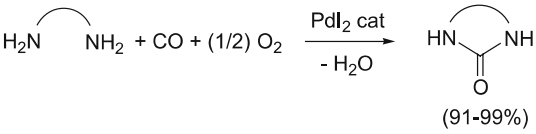

(53)

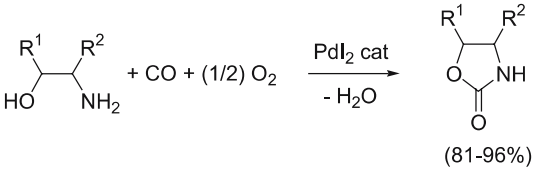

(54)

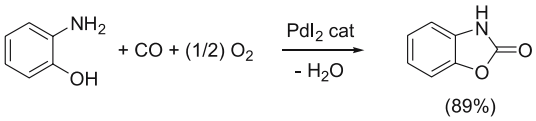

(55)

References

1. Tsuji J, Morokawa M, Kiji M (1964) J Am Chem Soc 86:4851
2. Tsuji J (1969) Acc Chem Res 2:144
3. Yukawa T, Tsutsumi S (1969) J Org Chem 34:738
4. Fenton DM (Union Oil Co of California) (1968) US Patent 3397226
5. Stille JK, Hines LF (1970) J Am Chem Soc 92:1798
6. Fenton DM, Steinwand PJ (1972) J Org Chem 37:2034
7. Fenton DM, Olivier KL (1972) Chemtech: 220
8. Heck RF (1972) J Am Chem Soc 94:2712
9. Stille JK, James DE (1975) J Am Chem Soc 97:674
10. James DE, Hines LF, Stille JK (1976) J Am Chem Soc 98:1806
11. James DE, Stille JK (1976) J Am Chem Soc 98:1810
12. Stille JK, Divakaruni RJ (1979) J Org Chem 44:3474
13. Toda S, Miyamoto M, Kinoshita H, Inomata K (1991) Bull Chem Soc Jpn 64:3600
14. Nefkens SCA, Sperrle M, Consiglio G (1993) Angew Chem, Int Ed Engl 32:1719
15. Sperrle M, Consiglio G (1996) J Organomet Chem 506:177
16. Hayashi M, Takezaki H, Hashimoto Y, Takaoki K, Saigo K (1998) Tetrahedron Lett 39:7529
17. Sperrle M, Consiglio G (1999) J Mol Catal A: Chem 143:263
18. Sperrle M, Consiglio G (2000) Inorg Chim Acta 300–302:264
19. Bianchini C, Lee HM, Mantovani G, Meli A, Oberhauser W (2002) New J Chem 26:387
20. Yokota T, Sakaguchi S, Ishii Y (2002) J Org Chem 67:5005
21. Cometti G, Chiusoli G (1979) J Organomet Chem 181:C14
22. Bianchini C, Mantovani G, Meli A, Oberhauser W, Brüggeller P, Stampfl T (2001) J Chem Soc, Dalton Trans, p 690
23. Henry PM (1980) Palladium-catalyzed oxidation of hydrocarbons. Reidel, Dordrecht, p 193–217
24. Carturan G, Graziani M, Belluco U (1972) J Chem Soc, Dalton Trans, p 262
25. Hemmer H, Rambaud J, Tkatchenko I (1975) J Organomet Chem 97:C57
26. Stille JK, Divakaruni R (1978) J Am Chem Soc 100:1303
27. Hegedus LS, Darlington WH (1980) J Am Chem Soc 102:4980
28. Wieber GM, Hegedus LS, Åkermark B, Michalson ET (1989) J Org Chem 54:4649
29. Urata H, Fujita A, Fuchikami T (1988) Tetrahedron Lett 29:4435
30. Hegedus LS, Allen GF, Olsen DJ (1980) J Am Chem Soc 102:358
31. Semmelhack MF, Bozell JJ, Sato T, Wulff W, Spiess E, Zark A (1982) J Am Chem Soc 104:5850
32. Semmelhack MF, Bodurow C (1984) J Am Chem Soc 106:1496
33. Semmelhack MF, Kim C, Zhang N, Bodurow C, Sanner M, Dobler W, Meier M (1990) Pure Appl Chem 62:2035
34. Hosokawa T, Murahashi T (1990) Acc Chem Res 23:49
35. McCormick M, Monuhan R III, Soria J, Goldsmith D, Liotta D (1989) J Org Chem 54:4485
36. Tamaru Y, Hojo M, Higashimura H, Yoshida Z (1988) J Am Chem Soc 110:3994
37. Yadav JS, Sreenivasa Rao E, Rao CS, Choudary BM (1989) J Mol Catal 49:L61
38. Yadav JS, Sreenivasa Rao E, Sreenivasa V, Choudary BM (1990) Tetrahedron Lett 31:2491
39. Tamaru Y, Hojo M, Yoshida Z (1991) J Org Chem 56:1099

40. Ukaji Y, Miyamoto M, Mikuni M, Takeuchi S, Inomata K (1996) Bull Chem Soc Jpn 69:735
41. White JD, Hong J, Robarge LA (1999) Tetrahedron Lett 40:1463
42. Kraus G, Li J, Gordon MS, Jensen JH (1993) J Am Chem Soc 115:5859
43. Harayama H, Abe A, Sakado T, Kimura M, Fugami K, Tanaka S, Tamaru Y (1997) J Org Chem 62:2113
44. Semmelhack MF, Bodurow C, Baum M (1984) Tetrahedron Lett 25:3171
45. Tamaru Y, Higashimura H, Naka K, Hoyo M, Yoshida Z (1985) Angew Chem Int Ed Engl 24:1045
46. Tamaru Y, Kobayashi T, Kawamura S, Ochiai H, Hojo M, Yoshida Z (1985) Tetrahedron Lett 26:3207
47. Tamaru Y, Hojo M, Yoshida Z (1988) J Org Chem 53:5731
48. Paddon-Jones GC, McErlean CSP, Hayes P, Moore CJ, Konig WA, Kitching W (2001) J Org Chem 66:7487
49. Milstein D (1982) Organometallics 1:888
50. Söderberg BC, Åkermark B, Hall SS (1988) J Org Chem 53:2925
51. Ozawa F, Nakano M, Aoyama I, Yamamoto T, Yamamoto A (1986) J Chem Soc, Chem Commun, p 382
52. Kesling HS Jr, Zehner LR (Atlantic Richfield Co) (1979) US Patent 4166913
53. Drent E (Shell Int Res Co) (1988) Eur Patent 275591
54. Lin JJ, Knifton JF (1985) US Patent 4552976
55. Fergusson SB, Alper H (1986) J Mol Catal 34:381
56. Riegel HJ, Hoberg H (1984) J Organomet Chem 260:121
57. Tsuji J, Susuki T (1965) Tetrahedron Lett, p 3027
58. Alper H, Hartstock FW, Despeyroux B (1984) J Chem Soc, Chem Commun, p 905
59. Alper H, Hartstock FW, Despeyroux B (1986) J Mol Catal 34:381
60. Fañanás FJ, Hoberg H (1984) J Organomet Chem 275:249
61. Walkup RD, Park G (1987) Tetrahedron Lett 28:1023
62. Walkup RD, Park G (1990) J Am Chem Soc 112:1597
63. Walkup RD, Mosher MD (1993) Tetrahedron Lett 49:9285
64. Lathbury D, Vernon P, Gallagher T (1986) Tetrahedron Lett 27:6009
65. Fox DNA, Gallagher T (1990) Tetrahedron 46:4697
66. Fox DNA, Lathbury D, Mahon MF, Molloy KC, Gallagher T (1991) J Am Chem Soc 113:2652
67. Gallagher T, Davies IW, Jones SW, Lathbury D, Mahon MF, Molloy KC, Shaw RW, Vernon P (1992) J Chem Soc Perkin Trans 1, p 433
68. Kimura M, Saeki N, Uchida S, Harayama H, Tanaka S, Fugami K, Tamaru Y (1993) Tetrahedron Lett 34:7611
69. Jacobsen G, Spaethe (1962) German Patent 1138760
70. Tsuji J, Morikawa M, Iwamoto N (1964) J Am Chem Soc 86:4350
71. Li J-H, Jiang H, Feng A, Jia L (1999) J Org Chem 64:5984
72. Li J-H Tang S, Xie Y-X (2005) J Org Chem 70:477
73. Chiusoli GP, Venturello C, Merzoni S (1968) Chem Ind (London), p 977
74. Cassar L, Chiusoli GP, Guerrieri F (1973) Synthesis, p 509
75. Alper H, Despeyroux B, Woell JB (1983) Tetrahedron Lett 24:5691
76. Gabriele B, Costa M, Salerno G, Chiusoli GP (1992) J Chem Soc, Chem Commun, p 1007
77. Gabriele B, Costa M, Salerno G, Chiusoli GP (1994) J Chem Soc Perkin Trans 1, p 83
78. Li J, Jiang H, Jia L (1999) Synth Commun, p 3733

79. Giannoccaro P, Aresta M, Doronzo S, Ferragina C (2000) Appl Organomet Chem 14:581
80. Hartstock FW, McMahon LB, Tell IP (1993) Tetrahedron Lett 34:8067
81. Zargarian D, Alper H (1991) Organometallics 10:2914
82. Gabriele B, Salerno G, Costa M, Chiusoli GP (1999) Chem Commun, p 1381
83. Sakurai Y, Sakaguchi S, Ishii Y (1999) Tetrahedron Lett 40:1701
84. Bruk LG, Kozlova AP, Marshakha OV, Oshanina IV, Temkin ON, Kaliya OL (1999) Russ Chem Bull 48:1875
85. Li J, Li G, Jiang H, Chen M (2001) Tetrahedron Lett 42:6923
86. Gabriele B, Veltri L, Salerno G, Costa M, Chiusoli GP (2003) Eur J Org Chem, p 1722
87. Hoberg H, Fañanás FJ (1984) J Organomet Chem 262:C24
88. Okumoto H, Nishihara S, Nakagawa H, Suzuki A (2000) Synlett, p 217
89. Tsuji J, Takahashi M, Takahashi T (1980) Tetrahedron Lett, p 849
90. Giannoccaro P, Aresta M, Doronzo S, Ferragina C (2000) Appl Organomet Chem 14:581
91. Zung TT, Bruk LG, Temkin ON (1994) Mendeleev Commun, p 2
92. Bruk LG, Gorodskii SN, Zeigarnik AV, Valdés-Péres RE, Temkin ON (1998) J Mol Catal A: Chem 130:29
93. Vasilevsky SF, Trofimov BA, Mal'kina AG, Bradsma L (1994) Synth Commun, p 85
94. Chiarotto I, Carelli I (2002) Synth Commun 32:881
95. Kulik AV, Bruk LG, Temkin ON, Khabibulin VR, Belsky VK, Zavodnik VE (2002) Mendeleev Commun, p 47
96. Izawa Y, Shimizu I, Yamamoto A (2004) Bull Chem Soc Jpn 77:2033
97. Hoberg H, Riegel HJ (1983) J Organomet Chem 241:245
98. Fañanás FJ, Hoberg H (1984) J Organomet Chem 277:135
99. Gabriele B, Salerno G, Veltri L, Costa M (2001) J Organomet Chem 622:84
100. Gabriele B, Costa M, Salerno G, Chiusoli GP (1994) J Chem Soc, Chem Commun, p 1429
101. Gabriele B, Salerno G, De Pascali F, Costa M, Chiusoli GP (1997) J Chem Soc Perkin Trans 1, p 147
102. Bonardi A, Costa M, Gabriele B, Salerno G, Chiusoli GP (1995) Tetrahedron Lett 36:7495
103. Gabriele B, Salerno G, Veltri L, Costa M, Massera C (2001) Eur J Org Chem, p 4607
104. Gabriele B, Salerno G, De Pascali F, Tomasi Scianò G, Costa M, Chiusoli GP (1997) Tetrahedron Lett 38:6877
105. Gabriele B, Salerno G, De Pascali F, Costa M, Chiusoli GP (1999) J Org Chem 64:7693
106. Bacchi A, Chiusoli GP, Costa M, Sani C, Gabriele B, Salerno G (1998) J Organomet Chem 562:35
107. Gabriele B, Salerno G, De Pascali F, Costa M, Chiusoli GP (2000) J Organomet Chem 594:409
108. Marshall JA, Yanik MM (2000) Tetrahedron Lett 41:4717
109. Kato K, Nishimura A, Yamamoto Y, Akita H (2001) Tetrahedron Lett 42:4203
110. Kato K, Tanaka M, Yamamoto Y, Akita H (2002) Tetrahedron Lett 43:1511
111. Kato K, Yamamoto Y, Akita H (2002) Tetrahedron Lett 43:4915
112. Kato K, Yamamoto Y, Akita H (2002) Tetrahedron Lett 43:6587
113. Bacchi A, Costa M, Gabriele B, Pelizzi G, Salerno G (2002) J Org Chem 67:4450
114. Bacchi A, Chiusoli GP, Costa M, Gabriele B, Righi C, Salerno G (1997) Chem Commun, p 1209

115. Chiusoli GP, Costa M, Gabriele B, Salerno G (1999) J Mol Catal A: Chem 143:297
116. Gabriele B, Salerno G, Fazio A, Campana FB (2002) Chem Commun, p 1408
117. Kondo Y, Sakamoto T, Yamanaka H (1989) Heterocycles, p 1013
118. Kondo Y, Shiga F, Murata N, Sakamoto T, Yamanaka H (1994) Tetrahedron 50:11803
119. Lütjens H, Scammels PJ (1999) Synlett, p 1079
120. Bacchi A, Costa M, Della Cà N, Fabbricatore M, Fazio A, Gabriele B, Nasi C, Salerno G (2004) Eur J Org Chem, p 574
121. Costa M, Della Cà N, Gabriele B, Massera C, Salerno G, Soliani M (2004) J Org Chem 69:2469
122. Hamed O, El-Qisairi A, Henry PM (2001) J Org Chem 66:180
123. Ito Y, Nakatsuka M, Kise N, Sageusa T (1980) Tetrahedron Lett 21:2873
124. Trost BM, Verhoeven TR (1982) In: Wilkinson G, Stone FGA, Abel EW (eds) Comprehensive Organometallic Chemistry. Pergamon Press, Oxford, p 838
125. Itatani H, Kashima M, Suehiro T (1983) (Ube Industries, Japan), Eur Patent 77542
126. Uchiumi S, Ataka K, Sakou K (1985) (Ube Industries, Japan) JP Patent 60120838
127. Fujiwara Y, Takaki K, Taniguchi H (1980) J Chem Soc, Chem Commun, p 220
128. Fujiwara Y, Kawata I, Kawauchi T, Taniguchi H (1982) J Chem Soc, Chem Commun, p 132
129. Ichikawa Y, Yamaji T (1975) US Patent 3920734
130. Waller FJ (Du Pont, USA) (1984) US Patent 4431839
131. Arzoumanidis GG, Rauch FC (1980) J Mol Catal 9:335
132. Zhizhinas EG, Matveev KI, Kuznetsova LI (1985) Kinet Katal 26:461
133. Fujiwara Y, Kawata I, Sugimoto H, Taniguchi H (1983) J Organomet Chem 256:C35
134. Jintoku T, Fujiwara Y, Kawata I, Kawauchi T, Taniguchi H (1990) J Organomet Chem 385:297
135. Ugo R, Chiesa A (1987) J Chem Soc, Perkin Trans 1, p 2625
136. Taniguchi H, Yamaoka Y, Nakata K, Takaki K, Fujiwara Y (1995) Chem Lett, p 345
137. Fujiwara Y, Takaki K, Taniguchi H (1996) Synlett, p 591
138. Jintoku K, Taniguchi H, Fujiwara Y (1987) Chem Lett, p 1159
139. Waller FJ (1986) Catal Rev Sci Eng 28:1
140. Kalinovskii IO, Lescheva AA, Kuteinikova MM, Gel'bshtein AI (1990) J Gen Chem USSR (Engl Transl) 60:108
141. Leshcheva AA, Kalinovskii IO, Pogorelov VV, Noskov YG, Gel'bshtein AI (1998) Kinet Katal 39:389
142. Kalinovskii IO, Gel'bshtein AI, Pogorelov VV (2001) Russ J Gen Chem (Engl Transl) 71:1457
143. Kalinovskii IO, Gel'bshtein AI, Pogorelov VV (2001) Russ J Gen Chem (Engl Transl) 71:1463
144. Grushin VV, Marshall WJ, Thorn DL (2001) Adv Synth Catal 343:161
145. Grushin VV, Thorn DL (2001) (E.I. DuPont de Nemours & Co.) World Patent 0107387
146. Grushin VV, Thorn DL (2003) (E.I. DuPont de Nemours & Co.) US Patent 6548698
147. Horino H, Inoue N (1981) J Org Chem 46:4416
148. Sakakibara T, Kuma T, Ohyabu T, Hase T (1989) Chem Pharm Bull 37:1694
149. Chepaikin EG, Bezruchenko AP, Boiko GN, Leshcheva AA (2003) Petroleum Chem 43:395
150. Chepaikin EG, Bezruchenko AP, Leshcheva AA (2002) Kinet Catal 43:507
151. Chepaikin EG, Bezruchenko AP, Leshcheva AA, Boiko GN, Kuzmenkov IV, Grigoryan EH, Shilov AE (2001) J Mol Catal A: Chem 169:89

152. Chepaikin EG, Boiko GN, Bezruchenko AP, Leshcheva AA, Grigoryan EH (1998) J Mol Catal A: Chem 129:15
153. Wang Y, Katagiri M, Otsuka K (1997) Chem Commun, p 1187
154. Hallgren JE, Lucas GM, Matthews RO (1981) J Organomet Chem 204:135
155. Cao Y, Yang P, Yao CZ, Yi N, Feng WL, Dai WL, Fan KN (2004) Appl Catal A: Gen 272:15
156. Feng WL, Cao Y, Yi N, Dai WL, Fan K (2004) Chem Lett 33:958
157. Anderson SA, Root TW (2004) J Mol Catal A: Chem 220:247
158. Kim WB, Joshi UA, Lee JS (2004) Ind Eng Chem Res 43:1897
159. Mo WL, Huang RS, Xiong H, Liu HT, Li GX (2004) Chinese J Catal 25:243
160. Jiang T, Han BX, Zhao GY, Chang YH, Gao L, Zhang JM, Yang GY (2003) J Chem Res (S):549
161. Cao W, Zhang HB, Yuan YZ (2003) Catal Lett 91:243
162. Skupinska J, Kuczynska L, Wielgosz Z (2003) React Kinetics Catal Lett 80:269
163. Spivack JL, Cawse JN, Whisenhunt DW, Johnson BF, Shalyaev KV, Male J, Pressman EJ, Ofori JY, Soloveichik GL, Patel BP, Chuck TL, Smith DJ, Jordan TM, Brennan MR, Kilmer RJ, Williams ED (2003) Appl Catal A: Gen 254:5
164. Itoh H, Watanabe Y, Mori K, Umino H (2003) Green Chem 5:558
165. Okuyama K, Sugiyama J, Nagahata R, Asai M, Ueda M, Takeuchi K (2003) Green Chem 5:563
166. Yasuda H, Maki N, Choi JC, Sakakura T (2003) J Organomet Chem 682:66
167. Okuyama K, Sugiyama J, Nagahata R, Asai M, Ueda M, Takeuchi K (2003) Macromolecules 36:6953
168. Okuyama K, Sugiyama J, Nagahata R, Asai M, Ueda M, Takeuchi K (2003) J Mol Catal 203:21
169. Han MS, Lee BG, Ahn BS, Kim HS, Moon DJ, Hong SI (2003) J Mol Catal 203:137
170. Kim WB, Park ED, Lee CW, Lee JS (2003) J Catal 218:334
171. Roh NS, Dunn BC, Eyring EM, Pugmire RJ, Meuzelaar HLC (2003) Fuel Process Technol 83:27
172. Anderson SA, Root TW (2003) J Catal 217:396
173. Hatanaka I, Mitsuyasu N, Yin G, Fujiwara Y, Kitamura T, Kusakabe K, Yamaji T (2003) J Organomet Chem 674:96
174. Yang P, Cao Y, Dai WL, Deng JF, Fan KN (2003) Appl Catal A: Gen 243:323
175. Cao Y, Hu JC, Yang P, Dai WL, Fan KN (2003) Chem Commun, p 908
176. Kim WB, Park ED, Lee JS (2003) Appl Catal A: Gen 242:335
177. Yang P, Cao Y, Hu JC, Dai WL, Fan KN (2003) Appl Catal A: Gen 241:363
178. Jiang RX, Wang SF, Zhao XQ, Wang YJ, Zhang CF (2003) Appl Catal A: Gen 238:131
179. Linsen KJL, Libens J, Jacobs PA (2002) Chem Commun, p 2728
180. Kim WB, Lee JS (2002) J Appl Polym Sci 86:937
181. Hu JC, Cao Y, Yang P, Deng JF, Fan KN (2002) J Mol Catal A: Chem 185:1
182. Jiang RX, Wang YJ, Zhao XQ, Wang SF, Jin CQ, Zhang CF (2002) J Mol Catal A: Chem 185:159
183. Kim WB, Park KH, Lee JS (2002) J Mol Catal 184:39
184. Ma XB, Li ZH, Wang BW, Xu GH (2002) React Kinet Catal Lett 76:179
185. Yasuda H, Choi JC, Lee SC, Sakakura T (2002) Organometallics 21:1216
186. Dunn BC, Guenneau C, Hilton SA, Pahnke J, Eyring EM (2002) Energy & Fuels 16:177
187. Kim WB, Lee JS (2001) Chem Lett, p 1044
188. Raab V, Merz M, Sundermeyer J (2001) J Mol Catal A: Chem 175:51

189. Ishii H, Takeuchi K, Asai M, Ueda M (2001) J Synth Org Chem Jpn 59:790
190. Yin GC, Jia CG, Kitamura T, Yamaji T, Fujiwara Y (2001) J Organomet Chem 630:11
191. Han MS, Lee BG, Suh I, Kim HS, Ahn BS, Hong SI (2001) J Mol Catal A: Chem 170:225
192. Ishii H, Goyal M, Ueda M, Takeuchi K, Asai M (2001) Macromol Rapid Commun 22:376
193. Li Z, Xie KC, Slade RCT (2001) Appl Catal A: Gen 205:85
194. Sato Y, Souma Y (2000) Catal Surveys Jpn 4:65
195. Chin CS, Shin D, Won G, Ryu J, Kim HS, Lee BG (2000) J Mol Catal A: Chem 160:315
196. Goyal M, Novosad J, Necas M, Ishii H, Nagahata R, Sugiyama J, Asai M, Ueda M, Takeuchi K (2000) Appl Organomet Chem 14:629
197. Yin GC, Jia CG, Kitamura T, Yamaji T, Fujiwara Y (2000) Catal Lett 69:89
198. Ishii H, Goyal M, Ueda M, Takeuchi K, Asai M (2000) Appl Catal A: Gen 201:105
199. Song HY, Park ED, Lee JS (2000) J Mol Catal A: Chem 154:243
200. Ishii H, Goyal M, Ueda M, Takeuchi K, Asai M (2000) Catal Lett 65:57
201. Sato Y, Yamamoto Y, Souma Y (2000) Catal Lett 65:123
202. Vavasori A, Toniolo L (2000) J Mol Catal A: Chem 151:37
203. Sato Y, Kagotani M, Souma Y (2000) J Mol Catal A: Chem 151:79
204. Ishii H, Goyal M, Ueda M, Takeuchi K, Asai M (1999) J Mol Catal A: Chem 148:289
205. Ishii H, Ueda M, Takeuchi K, Asai M (1999) J Mol Catal A: Chem 144:369
206. Ishii H, Ueda M, Takeuchi K, Asai M (1999) J Mol Catal A: Chem 144:477
207. Ishii H, Ueda M, Takeuchi K, Asai M (1999) J Mol Catal A: Chem 138:311
208. Goyal M, Nakahata R, Sugiyama J, Asai M, Ueda M, Takeuchi K (1999) J Mol Catal A: Chem 137:147
209. Goyal M, Nakahata R, Sugiyama J, Asai M, Ueda M, Takeuchi K (1999) Catal Lett 54:29
210. Takagi M, Miyagi H, Yoneyama T, Ohgomori Y (1998) J Mol Catal A: Chem 129:L1
211. Delledonne D, Rivetti F, Romano U (1995) J Organomet Chem 488:C15
212. Yuan YZ, Cao W, Weng WZ (2004) J Catal 228:311
213. Zhang Z, Ma XB, Zhang J, He F, Wang SP (2005) J Mol Catal A: Chem 227:141
214. Tundo S, Selva M (2002) Acc Chem Res 35:706
215. Delledonne D, Rivetti F, Romano U (2001) Appl Catal A: General 221:241
216. Romano U, Rivetti F, Di Muzio N (1982) US Patent 4318862
217. Nishihira K, Mizutare K, Tanaka S (1991) (Ube Industries, Japan) Eur Patent 425197
218. Toochinda P, Chuang SSC (2004) Ind Eng Chem Res 43:1192
219. Shi F, Peng JJ, Deng YQ (2003) J Catal 219:372
220. Shi F, Deng YQ, SiMa TL, Yang HZ (2001) J Catal 203:525
221. Wan BS, Liao SJ, Yu DR (1999) Appl Catal A: Gen 183:81
222. Valli VLK, Alper H (1995) Organometallics 14:80
223. Giannoccaro P (1994) J Organomet Chem 470:249
224. Kanagasabapathy S, Gupte SP, Chaudhari RV (1994) Ind Eng Chem Res 33:1
225. Kelkar AA, Kolhe DS, Kanagasabapathy S, Chaudhary RV (1992) Ind Eng Chem Res 31:172
226. Giannoccaro P, Nobile CS, Moro G, La Ginestra A, Ferragina C, Massucci MA, Patrono P (1989) J Mol Catal 53:349
227. Alper H, Vasapollo G, Hartstock FW, Mlekuz M, Smith DJH, Morris GE (1987) Organometallics 6:2391
228. Fukuoka S, Chono M, Khono M (1984) Chem Tech, p 670
229. Fukuoka S, Chono M, Khono M (1984) J Org Chem 49:1458

230. Tam W (1986) J Org Chem 51:2977
231. Imada Y, Mitsue Y, Ike K, Washizuka K, Murahashi S-I (1996) Bull Chem Soc Jpn 69:2079
232. Gabriele B, Salerno G, Brindisi D, Costa M, Chiusoli GP (2000) Org Lett 2:625
233. Chiarotto I, Feroci M (2001) Tetrahedron Lett 42:3451
234. Gabriele B, Mancuso R, Salerno G, Costa M (2003) J Org Chem 68:601
235. Li FW, Xia CG (2004) J Catal 227:542
236. Merger F, Platz R, Towae F (1980) German Patent 2910132
237. Becker R, Grolig J, Rasp C (1981) US Patent 4297501
238. Waller FJ (1986) (Du Pont, USA) US Patent 4806674
239. Alper H, Smith DJH (1987) US Patent 4694097
240. Chen B, Chuang SSC (2003) Green Chem 5:484
241. Chen B, Chuang SSC (2003) J Mol Catal A: Chem 195:37
242. Sheludyakov YL, Golodov VA (1982) React Kinet Catal Lett 20:39
243. Shi F, Deng YQ (2001) Chem Commun, p 443
244. Shi F, Deng YQ (2002) J Catal 211:548
245. Li Y, Pan WX, Wong WT (2002) J Cluster Sci 13:223
246. Giannoccaro P, De Giglio E, Gargano M, Aresta M, Ferragina C (2000) J Mol Catal A: Chem 157:131
247. Prasad KV, Chaudhari RV (1994) J Catal 145:204
248. Bolzacchini E, Meinardi S, Orlandi M, Rindone B (1996) J Mol Catal A: Chem 111:281
249. Li KT, Peng YJ (1993) J Catal 143:631
250. Leung TW, Dombek BD (1992) J Chem Soc, Chem Commun, p 205
251. Halligudi SB, Bhatt KN, Khan MMT (1991) J Mol Catal 68:261
252. Khan MMT, Halligudi SB, Rao NS (1990) J Mol Catal 59:303
253. Bossoli A, Rindone B, Tollari S, Chioccara F (1990) J Mol Catal 60:41
254. Benedini F, Nali M, Rindone B, Tollari S, Cenini S, La Monica G, Porta F (1986) J Mol Catal 34:155
255. Hong FE, Chang YC (2004) Organometallics 23:718
256. Srivastva SC, Shrimal AK, Srivastva A (1991) J Organomet Chem 414:65
257. Dombeck BD, Angelici RJ (1977) J Organomet Chem 134:203
258. Calderazzo F (1965) Inorg Chem 4:293
259. Giannoccaro P, Nobile CF, Mastrorilli P, Ravasio N (1991) J Organomet Chem 419:251
260. Mulla SAR, Rode CV, Kelkar AA, Gupte SP (1997) J Mol Catal 122:103
261. Mulla SAR, Gupte SP, Chaudhari RV (1991) J Mol Catal 67:L7
262. Yang P, Cao Y, Bao XH, Dai WL, Fan KN (2004) Chinese J Catal 25:995
263. Shi F, Deng Y, SiMa T, Yang H (2001) Tetrahedron Lett 42:2161
264. Sheludyakov YL, Golodov VA (1984) Bull Chem Soc Jpn 57:251
265. Giannoccaro P (1987) J Organomet Chem 336:271
266. Choudary BM, Koteswara Rao K, Pirozhkov SD, Lapidus AL (1991) Synth Commun, p 1923
267. Pri-Bar I, Alper H (1990) Can J Chem 68:1544
268. Dahlen GM, Sen A (1993) Macromolecules 26:1784
269. Gupte SP, Chaudhari RV (1988) J Catal 114:246
270. Gupte SP, Chaudhari RV (1992) Ind Eng Chem Res 31:2069
271. Yang H, Deng Y, Shi F (2001) J Mol Catal A: Chem 176:73
272. Shi F, Deng YQ, SiMa TL, Yang HZ (2001) Tetrahedron Lett 42:2161
273. Chiarotto I, Feroci M (2003) J Org Chem 68:7137

274. Gabriele B, Mancuso R, Salerno G, Costa M (2003) Chem Commun, p 486
275. Gabriele B, Salerno G, Mancuso R, Costa M (2004) J Org Chem 69:4741
276. Hiwatari K, Kayaki Y, Okita K, Ukai T, Shimizu I, Yamamoto A (2004) Bull Chem Soc Jpn 77:2237
277. McCusker JE, Abboud KA, McElwee-While L (1997) Organometallics 16:3863
278. McCusker JE, Logan J, McElwee-While L (1998) Organometallics 17:4037
279. McCusker JE, Grasso CA, Main AD, McElwee-White L (1999) Org Lett 1:961
280. McCusker JE, Main AD, Johnson KS, Grasso CA, McElwee-White L (2000) J Org Chem 65:5216
281. McCusker JE, Qian F, McElwee-White L (2000) J Mol Catal A: Chem 159:11
282. Hylton K-G, Main AD, McElwee-White L (2003) J Org Chem 68:1615
283. Qian F, McCusker JE, Zhang Y, Main AD, Chlebowski M, Kokka M, McElwee-White L (2002) J Org Chem 67:4086
284. Franz RA, Applegath F, Morriss FV, Baiocchi F (1961) J Org Chem 26:3306
285. Franz RA, Applegath F, Morris FV, Baiocchi F, Bolze C (1961) J Org Chem 26:3309
286. Franz RA, Applegath F, Morriss FV, Baiocchi F, Breed LW (1962) J Org Chem 27:4341
287. Sonoda N (1993) Pure Appl Chem 65:699
288. Yoshida T, Kambe N, Murai S, Sonoda N (1987) Bull Chem Soc Jpn 60:1793
289. Kim HS, Kim YJ, Bae JY, Kim SJ, Lah MS, Chin CS (2003) Organometallics 22:2498
290. Kihlberg T, Karimi F, Långström B (2002) J Org Chem 67:3687
291. Kim HS, Kim YJ, Lee H, Park KY, Lee C, Chin CS (2002) Angew Chem Int Ed 41:4300
292. Kim HS, Kim YJ, Lee H, Lee SD, Chin CS (1999) J Catal 184:526
293. Fenton DM, Steinwand PJ (1974) J Org Chem 39:701
294. Rivetti F, Romano U (1978) J Organomet Chem 154:323
295. Rivetti F, Romano U (1979) J Organomet Chem 174:221
296. Rivetti F, Romano U (1980) Chem Ind (Milan) 62:7
297. Murahashi SI, Mitsue Y, Ike K (1987) J Chem Soc, Chem Commun, p 125
298. Tam W (1986) J Org Chem 51:2977
299. Burk PL, Van Engen D, Campo KS (1984) Organometallics 3:493
300. Tahara S, Fuji K, Nishihira K, Matsuda M, Mizutare K (1984) (Ube Industries, Japan) US Patent 4467109
301. Sammes PG, Weller DJ (1995) Synthesis, p 1205
302. Baldwin JE (1976) J Chem Soc, Chem Commun, p 734
303. Fazio A, Gabriele B, Salerno G, Destri S (1999) Tetrahedron 55:485
304. Paganuzzi V, Guattieri P, Riccardi P, Sacchelli I, Barnerá J, Costa M, Dalcanale E (1999) Eur J Org Chem, p 1527
305. Destri S, Giovanella U, Fazio A, Porzio W, Gabriele B, Zotti G (2002) Org Electron 3:149
306. Destri S, Porzio W, Meinardi F, Tubino R, Salerno G (2003) Macromolecules 36:273
307. Cupelli D, Nicoletta FP, De Filpo G, Chidichimo G, Fazio A, Gabriele B, Salerno G (2004) Appl Phys Lett 85:3292
308. Nicoletta FP, Chidichimo G, Cupelli D, De Filpo G, De Benedittis M, Gabriele B, Salerno G, Fazio A (2005) Adv Funct Mater 15:995
309. Gabriele B, Salerno G, Veltri L, Costa M (2001) J Organomet Chem 622:84
310. Gabriele B, Salerno G, Plastina P (2004) Lett Org Chem 1:136
311. Gabriele B, Salerno G, Plastina P, Costa M, Crispini A (2004) Adv Synth Catal 346:351
312. Gabriele B, Plastina P, Salerno G, Costa M (2005) Synlett, p 935

Author Index Volumes 1–18

The volume numbers are printed in italics

Abdel-Magid AF, see Mehrmann SJ (2004) *6*: 153–180
Akiyama K, see Mikami M (2005) *14*: 279–322
Allardyce CS, Dyson PJ (2006) Medicinal Properties of Organometallic Compounds. *17*: 177–210
Alper H, see Grushin VV (1999) *3*: 193–225
Anwander R (1999) Principles in Organolanthanide Chemistry. *2*: 1–62
Arends IWCE, Kodama T, Sheldon RA (2004) Oxidations Using Ruthenium Catalysts. *11*: 277–320
Armentrout PB (1999) Gas-Phase Organometallic Chemistry. *4*: 1–45

Barluenga J, Rodríguez F, Fañanás FJ, Flórez J (2004) Cycloaddition Reaction of Group 6 Fischer Carbene Complexes. *13*: 59–121
Basset J-M, see Candy J-P (2005) *16*: 151–210
Beak P, Johnson TA, Kim DD, Lim SH (2003) Enantioselective Synthesis by Lithiation Adjacent to Nitrogen and Electrophile Incorporation. *5*: 139–176
Beller M, see Jacobi von Wangelin A (2006) *18*: 207–221
Beller M, see Strübing D (2006) *18*: 165–178
Bertus P, see Szymoniak J (2005) *10*: 107–132
Bien J, Lane GC, Oberholzer MR (2004) Removal of Metals from Process Streams: Methodologies and Applications. *6*: 263–284
Blechert S, Connon SJ (2004) Recent Advances in Alkene Metathesis. *11*: 93–124
Bonino F, see Bordiga S (2005) *16*: 37–68
Bordiga S, Damin A, Bonino F, Lamberti C (2005) Single Site Catalyst for Partial Oxidation Reaction: TS-1 Case Study. *16*: 37–68
Böttcher A, see Schmalz HG (2004) *7*: 157–180
Braga D (1999) Static and Dynamic Structures of Organometallic Molecules and Crystals. *4*: 47–68
Breuzard JAJ, Christ-Tommasino ML, Lemaire M (2005) Chiral Ureas and Thioureas in Asymmetric Catalysis. *15*: 231–270
Brüggemann M, see Hoppe D (2003) *5*: 61–138
Bruneau C (2004) Ruthenium Vinylidenes and Allenylidenes in Catalysis. *11*: 125–153
Brutchey RL, see Fujdala KL (2005) *16*: 69–115
Butler PA, Kräutler B (2006) Biological Organometallic Chemistry of B_{12}. *17*: 1–55

Candy J-P, Copéret C, Basset J-M (2005) Analogy between Surface and Molecular Organometallic Chemistry. *16*: 151–210
Castillón S, see Claver C (2006) *18*: 35–64
Catellani M (2005) Novel Methods of Aromatic Functionalization Using Palladium and Norbornene as a Unique Catalytic System. *14*: 21–54

Cavinato G, Toniolo L, Vavasori A (2006) Carbonylation of Ethene in Methanol Catalysed by Cationic Phosphine Complexes of Pd(II): from Polyketones to Monocarbonylated Products. *18*: 125–164
Chatani N (2004) Selective Carbonylations with Ruthenium Catalysts. *11*: 173–195
Chatani N, see Kakiuchi F (2004) *11*: 45–79
Chaudret B (2005) Synthesis and Surface Reactivity of Organometallic Nanoparticles. *16*: 233–259
Chlenov A, see Semmelhack MF (2004) *7*: 21–42
Chlenov A, see Semmelhack MF (2004) *7*: 43–70
Chinkov M, Marek I (2005) Stereoselective Synthesis of Dienyl Zirconocene Complexes. *10*: 133–166
Christ-Tommasino ML, see Breuzard JAJ (2005) *15*: 231–270
Chuzel O, Riant O (2005) Sparteine as a Chiral Ligand for Asymmetric Catalysis. *15*: 59–92
Claver C, Diéguez M, Pàmies O, Castillón S (2006) Asymmetric Hydroformylation. *18*: 35–64
Clayden J (2003) Enantioselective Synthesis by Lithiation to Generate Planar or Axial Chirality. *5*: 251–286
Connon SJ, see Blechert S (2004) *11*: 93–124
Copéret C, see Candy J-P (2005) *16*: 151–210
Costa M, see Gabriele B (2006) *18*: 239–272
Cummings SA, Tunge JA, Norton JR (2005) Synthesis and Reactivity of Zirconaaziridines. *10*: 1–39

Damin A, see Bordiga S (2005) *16*: 37–68
Damin A, see Zecchina A (2005) *16*: 1–35
Dechy-Cabaret O, see Kalck P (2006) *18*: 97–123
Delaude L, see Noels A (2004) *11*: 155–171
Dedieu A (1999) Theoretical Treatment of Organometallic Reaction Mechanisms and Catalysis. *4*: 69–107
Delmonte AJ, Dowdy ED, Watson DJ (2004) Development of Transition Metal-Mediated Cyclopropanation Reaction. *6*: 97–122
Demonceau A, see Noels A (2004) *11*: 155–171
Derien S, see Dixneuf PH (2004) *11*: 1–44
Deubel D, Loschen C, Frenking G (2005) Organometallacycles as Intermediates in Oxygen-Transfer Reactions. Reality or Fiction? *12*: 109–144
Diéguez M, see Claver C (2006) *18*: 35–64
Dixneuf PH, Derien S, Monnier F (2004) Ruthenium-Catalyzed C–C Bond Formation. *11*: 1–44
Dötz KH, Minatti A (2004) Chromium-Templated Benzannulation Reactions. *13*: 123–156
Dowdy EC, see Molander G (1999) *2*: 119–154
Dowdy ED, see Delmonte AJ (2004) *6*: 97–122
Doyle MP (2004) Metal Carbene Reactions from Dirhodium(II) Catalysts. *13*: 203–222
Drudis-Solé G, Ujaque G, Maseras F, Lledós A (2005) Enantioselectivity in the Dihydroxylation of Alkenes by Osmium Complexes. *12*: 79–107
Dyson PJ, see Allardyce CS (2006) *17*: 177–210

Eilbracht P, Schmidt AM (2006) Synthetic Applications of Tandem Reaction Sequences Involving Hydroformylation. *18*: 65–95
Eisen MS, see Lisovskii A (2005) *10*: 63–105

Fañanás FJ, see Barluenga (2004) *13*: 59–121
Flórez J, see Barluenga (2004) *13*: 59–121
Fontecave M, Hamelin O, Ménage S (2005) Chiral-at-Metal Complexes as Asymmetric Catalysts. *15*: 271–288
Fontecilla-Camps JC, see Volbeda A (2006) *17*: 57–82
Fraile JM, García JI, Mayoral JA (2005) Non-covalent Immobilization of Catalysts Based on Chiral Diazaligands. *15*: 149–190
Frenking G, see Deubel D (2005) *12*: 109–144
Freund H-J, see Risse T (2005) *16*: 117–149
Fu GC, see Netherton M (2005) *14*: 85–108
Fujdala KL, Brutchey RL, Tilley TD (2005) Tailored Oxide Materials via Thermolytic Molecular Precursor (TMP) Methods. *16*: 69–115
Fürstner A (1998) Ruthenium-Catalyzed Metathesis Reactions in Organic Synthesis. *1*: 37–72

Gabriele B, Salerno G, Costa M (2006) Oxidative Carbonylations. *18*: 239–272
García JI, see Fraile JM (2005) *15*: 149–190
Gates BC (2005) Oxide- and Zeolite-supported "Molecular" Metal Clusters: Synthesis, Structure, Bonding, and Catalytic Properties. *16*: 211–231
Gibson SE (née Thomas), Keen SP (1998) Cross-Metathesis. *1*: 155–181
Gisdakis P, see Rösch N (1999) *4*: 109–163
Görling A, see Rösch N (1999) *4*: 109–163
Goldfuss B (2003) Enantioselective Addition of Organolithiums to C=O Groups and Ethers. *5*: 12–36
Gossage RA, van Koten G (1999) A General Survey and Recent Advances in the Activation of Unreactive Bonds by Metal Complexes. *3*: 1–8
Gotov B, see Schmalz HG (2004) *7*: 157–180
Gras E, see Hodgson DM (2003) *5*: 217–250
Grepioni F, see Braga D (1999) *4*: 47–68
Gröger H, see Shibasaki M (1999) *2*: 199–232
Groppo E, see Zecchina A (2005) *16*: 1–35
Grushin VV, Alper H (1999) Activation of Otherwise Unreactive C–Cl Bonds. *3*: 193–225
Guitian E, Perez D, Pena D (2005) Palladium-Catalyzed Cycloaddition Reactions of Arynes. *14*: 109–146

Hamelin O, see Fontecave M (2005) *15*: 271–288
Harman D (2004) Dearomatization of Arenes by Dihapto-Coordination. *7*: 95–128
Hatano M, see Mikami M (2005) *14*: 279–322
Haynes A (2006) Acetic Acid Synthesis by Catalytic Carbonylation of Methanol. *18*: 179–205
He Y, see Nicolaou KC (1998) *1*: 73–104
Hegedus LS (2004) Photo-Induced Reactions of Metal Carbenes in organic Synthesis. *13*: 157–201
Hermanns J, see Schmidt B (2004) *13*: 223–267
Hidai M, Mizobe Y (1999) Activation of the N–N Triple Bond in Molecular Nitrogen: Toward its Chemical Transformation into Organo-Nitrogen Compounds. *3*: 227–241
Hirao T, see Moriuchi T (2006) *17*: 143–175
Hodgson DM, Stent MAH (2003) Overview of Organolithium-Ligand Combinations and Lithium Amides for Enantioselective Processes. *5*: 1–20
Hodgson DM, Tomooka K, Gras E (2003) Enantioselective Synthesis by Lithiation Adjacent to Oxygen and Subsequent Rearrangement. *5*: 217–250

Hoppe D, Marr F, Brüggemann M (2003) Enantioselective Synthesis by Lithiation Adjacent to Oxygen and Electrophile Incorporation. *5*: 61–138
Hou Z, Wakatsuki Y (1999) Reactions of Ketones with Low-Valent Lanthanides: Isolation and Reactivity of Lanthanide Ketyl and Ketone Dianion Complexes. *2*: 233–253
Hoveyda AH (1998) Catalytic Ring-Closing Metathesis and the Development of Enantioselective Processes. *1*: 105–132
Huang M, see Wu GG (2004) *6*: 1–36
Hughes DL (2004) Applications of Organotitanium Reagents. *6*: 37–62

Iguchi M, Yamada K, Tomioka K (2003) Enantioselective Conjugate Addition and 1,2-Addition to C=N of Organolithium Reagents. *5*: 37–60
Ito Y, see Murakami M (1999) *3*: 97–130
Ito Y, see Suginome M (1999) *3*: 131–159
Itoh K, Yamamoto Y (2004) Ruthenium Catalyzed Synthesis of Heterocyclic Compounds. *11*: 249–276

Jacobi von Wangelin A, Neumann H, Beller M (2006) Carbonylations of Aldehydes. *18*: 207–221
Jacobsen EN, see Larrow JF (2004) *6*: 123–152
Johnson TA, see Break P (2003) *5*: 139–176
Jones WD (1999) Activation of C–H Bonds: Stoichiometric Reactions. *3*: 9–46

Kagan H, Namy JL (1999) Influence of Solvents or Additives on the Organic Chemistry Mediated by Diiodosamarium. *2*: 155–198
Kakiuchi F, Murai S (1999) Activation of C–H Bonds: Catalytic Reactions. *3*: 47–79
Kakiuchi F, Chatani N (2004) Activation of C–H Inert Bonds. *11*: 45–79
Kalck P, Urrutigoïty M, Dechy-Cabaret O (2006) Hydroxy- and Alkoxycarbonylations of Alkenes and Alkynes. *18*: 97–123
Kanno K, see Takahashi T (2005) *8*: 217–236
Keen SP, see Gibson SE (née Thomas) (1998) *1*: 155–181
Kendall C, see Wipf P (2005) *8*: 1–25
Kiessling LL, Strong LE (1998) Bioactive Polymers. *1*: 199–231
Kim DD, see Beak P (2003) *5*: 139–176
King AO, Yasuda N (2004) Palladium-Catalyzed Cross-Coupling Reactions in the Synthesis of Pharmaceuticals. *6*: 205–246
King NP, see Nicolaou KC, He Y (1998) *1*: 73–104
Kobayashi S (1999) Lanthanide Triflate-Catalyzed Carbon–Carbon Bond-Forming Reactions in Organic Synthesis. *2*: 63–118
Kobayashi S (1999) Polymer-Supported Rare Earth Catalysts Used in Organic Synthesis. *2*: 285–305
Kodama T, see Arends IWCE (2004) *11*: 277–320
Kondratenkov M, see Rigby J (2004) *7*: 181–204
Koten G van, see Gossage RA (1999) *3*: 1–8
Kotora M (2005) Metallocene-Catalyzed Selective Reactions. *8*: 57–137
Kräutler B, see Butler PA (2006) *17*: 1–55
Kumobayashi H, see Sumi K (2004) *6*: 63–96
Kündig EP (2004) Introduction. *7*: 1–2
Kündig EP (2004) Synthesis of Transition Metal η^6-Arene Complexes. *7*: 3–20
Kündig EP, Pape A (2004) Dearomatization via η^6 Complexes. *7*: 71–94

Lamberti C, see Bordiga S (2005) *16*: 37–68
Lane GC, see Bien J (2004) *6*: 263–284
Larock R (2005) Palladium-Catalyzed Annulation of Alkynes. *14*: 147–182
Larrow JF, Jacobsen EN (2004) Asymmetric Processes Catalyzed by Chiral (Salen)Metal Complexes *6*: 123–152
Lemaire M, see Breuzard JAJ (2005) *15*: 231–270
Li CJ,Wang M (2004) Ruthenium Catalyzed Organic Synthesis in Aqueous Media. *11*: 321–336
Li Z, see Xi Z (2005) *8*: 27–56
Lim SH, see Beak P (2003) *5*: 139–176
Lin Y-S, Yamamoto A (1999) Activation of C–O Bonds: Stoichiometric and Catalytic Reactions. *3*: 161–192
Lisovskii A, Eisen MS (2005) Octahedral Zirconium Complexes as Polymerization Catalysts. *10*: 63–105
Lledós A, see Drudis-Solé G (2005) *12*: 79–107
Loschen C, see Deubel D (2005) *12*: 109–144

Ma S (2005) Pd-catalyzed Two or Three-component Cyclization of Functionalized Allenes. *14*: 183–210
Mangeney P, see Roland S (2005) *15*: 191–229
Marciniec B, Pretraszuk C (2004) Synthesis of Silicon Derivatives with Ruthenium Catalysts. *11*: 197–248
Marek I, see Chinkov M (2005) *10*: 133–166
Marr F, see Hoppe D (2003) *5*: 61–138
Maryanoff CA, see Mehrmann SJ (2004) *6*: 153–180
Maseras F (1999) Hybrid Quantum Mechanics/Molecular Mechanics Methods in Transition Metal Chemistry. *4*: 165–191
Maseras F, see Drudis-Solé G (2005) *12*: 79–107
Le Maux P, see Simonneaux G (2006) *17*: 83–122
Mayoral JA, see Fraile JM (2005) *15*: 149–190
Medaer BP, see Mehrmann SJ (2004) *6*: 153–180
Mehrmann SJ, Abdel-Magid AF, Maryanoff CA, Medaer BP (2004) Non-Salen Metal-Catalyzed Asymmetric Dihydroxylation and Asymmetric Aminohydroxylation of Alkenes. Practical Applications and Recent Advances. *6*: 153–180
De Meijere, see Wu YT (2004) *13*: 21–58
Ménage S, see Fontecave M (2005) *15*: 271–288
Michalak A, Ziegler T (2005) Late Transition Metal as Homo- and Co-Polymerization Catalysts. *12*: 145–186
Mikami M, Hatano M, Akiyama K (2005) Active Pd(II) Complexes as Either Lewis Acid Catalysts or Transition Metal Catalysts. *14*: 279–322
Minatti A, Dötz KH (2004) Chromium-Templated Benzannulation Reactions. *13*: 123–156
Miura M, Satoh T (2005) Catalytic Processes Involving b-Carbon Elimination. *14*: 1–20
Miura M, Satoh T (2005) Arylation Reactions via C–H Bond Cleavage. *14*: 55–84
Mizobe Y, see Hidai M (1999) *3*: 227–241
Molander G, Dowdy EC (1999) Lanthanide- and Group 3 Metallocene Catalysis in Small Molecule Synthesis. *2*: 119–154
Monnier F, see Dixneuf (2004) *11*: 1–44
Mori M (1998) Enyne Metathesis. *1*: 133–154
Mori M (2005) Synthesis and Reactivity of Zirconium-Silene Complexes. *10*: 41–62
Moriuchi T, Hirao T (2006) Ferrocene–Peptide Bioconjugates. *17*: 143–175
Morokuma K, see Musaev G (2005) *12*: 1–30

Mulzer J, Öhler E (2004) Olefin Metathesis in Natural Product Syntheses. *13*: 269–366
Muñiz K (2004) Planar Chiral Arene Chromium (0) Complexes as Ligands for Asymetric Catalysis. *7*: 205–223
Murai S, see Kakiuchi F (1999) *3*: 47–79
Murakami M, Ito Y (1999) Cleavage of Carbon–Carbon Single Bonds by Transition Metals. *3*: 97–130
Musaev G, Morokuma K (2005) Transition Metal Catalyzed s-Bond Activation and Formation Reactions. *12*: 1–30

Nakamura I, see Yamamoto Y (2005) *14*: 211–240
Nakamura S, see Toru T (2003) *5*: 177–216
Nakano K, Nozaki K (2006) Carbonylation of Epoxides. *18*: 223–238
Namy JL, see Kagan H (1999) *2*: 155–198
Negishi E, Tan Z (2005) Diastereoselective, Enantioselective, and Regioselective Carboalumination Reactions Catalyzed by Zirconocene Derivatives. *8*: 139–176
Netherton M, Fu GC (2005) Palladium-catalyzed Cross-Coupling Reactions of Unactivated Alkyl Electrophiles with Organometallic Compounds. *14*: 85–108
Neumann H, see Jacobi von Wangelin A (2006) *18*: 207–221
Nicolaou KC, King NP, He Y (1998) Ring-Closing Metathesis in the Synthesis of Epothilones and Polyether Natural Products. *1*: 73–104
Nishiyama H (2004) Cyclopropanation with Ruthenium Catalysts. *11*: 81–92
Noels A, Demonceau A, Delaude L (2004) Ruthenium Promoted Catalysed Radical Processes toward Fine Chemistry. *11*: 155–171
Nolan SP, Viciu MS (2005) The Use of N-Heterocyclic Carbenes as Ligands in Palladium Mediated Catalysis. *14*: 241–278
Normant JF (2003) Enantioselective Carbolithiations. *5*: 287–310
Norton JR, see Cummings SA (2005) *10*: 1–39
Nozaki K, see Nakano K (2006) *18*: 223–238

Oberholzer MR, see Bien J (2004) *6*: 263–284
Obst D, see Wiese K-D (2006) *18*: 1–33
Öhler E, see Mulzer J (2004) *13*: 269–366

Pàmies O, see Claver C (2006) *18*: 35–64
Pape A, see Kündig EP (2004) *7*: 71–94
Pawlow JH, see Tindall D, Wagener KB (1998) *1*: 183–198
Pena D, see Guitian E (2005) *14*: 109–146
Perez D, see Guitian E (2005) *14*: 109–146
Prashad M (2004) Palladium-Catalyzed Heck Arylations in the Synthesis of Active Pharmaceutical Ingredients. *6*: 181–204
Prestipino C, see Zecchina A (2005) *16*: 1–35
Pretraszuk C, see Marciniec B (2004) *11*: 197–248

Riant O, see Chuzel O (2005) *15*: 59–92
Richmond TG (1999) Metal Reagents for Activation and Functionalization of Carbon–Fluorine Bonds. *3*: 243–269
Rigby J, Kondratenkov M (2004) Arene Complexes as Catalysts. *7*: 181–204
Risse T, Freund H-J (2005) Spectroscopic Characterization of Organometallic Centers on Insulator Single Crystal Surfaces: From Metal Carbonyls to Ziegler–Natta Catalysts. *16*: 117–149

Rodríguez F, see Barluenga (2004) *13*: 59–121
Roland S, Mangeney P (2005) Chiral Diaminocarbene Complexes, Synthesis and Application in Asymmetric Catalysis. *15*: 191–229
Rösch N (1999) A Critical Assessment of Density Functional Theory with Regard to Applications in Organometallic Chemistry. *4*: 109–163
Roucoux A (2005) Stabilized Noble Metal Nanoparticles: An Unavoidable Family of Catalysts for Arene Derivative Hydrogenation. *16*: 261–279

Sakaki S (2005) Theoretical Studies of C–H s-Bond Activation and Related by Transition-Metal Complexes. *12*: 31–78
Salerno G, see Gabriele B (2006) *18*: 239–272
Satoh T, see Miura M (2005) *14*: 1–20
Satoh T, see Miura M (2005) *14*: 55–84
Savoia D (2005) Progress in the Asymmetric Synthesis of 1,2-Diamines from Azomethine Compounds. *15*: 1–58
Schmalz HG, Gotov B, Böttcher A (2004) Natural Product Synthesis. *7*: 157–180
Schmidt AM, see Eilbracht P (2006) *18*: 65–95
Schmidt B, Hermanns J (2004) Olefin Metathesis Directed to Organic Synthesis: Principles and Applications. *13*: 223–267
Schrock RR (1998) Olefin Metathesis by Well-Defined Complexes of Molybdenum and Tungsten. *1*: 1–36
Schulz E (2005) Use of *N*,*N*-Coordinating Ligands in Catalytic Asymmetric C–C Bond Formations: Example of Cyclopropanation, Diels–Alder Reaction, Nucleophilic Allylic Substitution. *15*: 93–148
Semmelhack MF, Chlenov A (2004) (Arene)$Cr(Co)_3$ Complexes: Arene Lithiation/Reaction with Electrophiles. *7*: 21–42
Semmelhack MF, Chlenov A (2004) (Arene)$Cr(Co)_3$ Complexes: Aromatic Nucleophilic Substitution. *7*: 43–70
Sen A (1999) Catalytic Activation of Methane and Ethane by Metal Compounds. *3*: 81–95
Severin K (2006) Organometallic Receptors for Biologically Interesting Molecules. *17*: 123–142
Sheldon RA, see Arends IWCE (2004) *11*: 277–320
Shibasaki M, Gröger H (1999) Chiral Heterobimetallic Lanthanoid Complexes: Highly Efficient Multifunctional Catalysts for the Asymmetric Formation of C–C, C–O and C–P Bonds. *2*: 199–232
Simonneaux G, Le Maux P (2006) Carbene Complexes of Heme Proteins and Iron Porphyrin Models. *17*: 83–122
Staemmler V (2005) The Cluster Approach for the Adsorption of Small Molecules on Oxide Surfaces. *12*: 219–256
Stent MAH, see Hodgson DM (2003) *5*: 1–20
Strassner T (2004) Electronic Structure and Reactivity of Metal Carbenes. *13*: 1–20
Strong LE, see Kiessling LL (1998) *1*: 199–231
Strübing D, Beller M (2006) The Pauson–Khand Reaction. *18*: 165–178
Suginome M, Ito Y (1999) Activation of Si–Si Bonds by Transition-Metal Complexes. *3*: 131–159
Sumi K, Kumobayashi H (2004) Rhodium/Ruthenium Applications. *6*: 63–96
Suzuki N (2005) Stereospecific Olefin Polymerization Catalyzed by Metallocene Complexes. *8*: 177–215
Szymoniak J, Bertus P (2005) Zirconocene Complexes as New Reagents for the Synthesis of Cyclopropanes. *10*: 107–132

Takahashi T, Kanno K (2005) Carbon–Carbon Bond Cleavage Reaction Using Metallocenes. *8*: 217–236
Tan Z, see Negishi E (2005) *8*: 139–176
Tilley TD, see Fujdala KL (2005) *16*: 69–115
Tindall D, Pawlow JH, Wagener KB (1998) Recent Advances in ADMET Chemistry. *1*: 183–198
Tobisch S (2005) Co-Oligomerization of 1,3-Butadiene and Ethylene Promoted by Zerovalent 'Bare' Nickel Complexes. *12*: 187–218
Tomioka K, see Iguchi M (2003) *5*: 37–60
Tomooka K, see Hodgson DM (2003) *5*: 217–250
Toniolo L, see Cavinato G (2006) *18*: 125–164
Toru T, Nakamura S (2003) Enantioselective Synthesis by Lithiation Adjacent to Sulfur, Selenium or Phosphorus, or without an Adjacent Activating Heteroatom. *5*: 177–216
Tunge JA, see Cummings SA (2005) *10*: 1–39

Uemura M (2004) (Arene)$Cr(Co)_3$ Complexes: Cyclization, Cycloaddition and Cross Coupling Reactions. *7*: 129–156
Ujaque G, see Drudis-Solé G (2005) *12*: 79–107
Urrutigoïty M, see Kalck P (2006) *18*: 97–123

Vavasori A, see Cavinato G (2006) *18*: 125–164
Viciu MS, see Nolan SP (2005) *14*: 241–278
Volbeda A, Fontecilla-Camps JC (2006) Catalytic Nickel–Iron–Sulfur Clusters: From Minerals to Enzymes. *17*: 57–82

Wagener KB, see Tindall D, Pawlow JH (1998) *1*: 183–198
Wakatsuki Y, see Hou Z (1999) *2*: 233–253
Wang M, see Li CJ (2004) *11*: 321–336
Watson DJ, see Delmonte AJ (2004) *6*: 97–122
Wiese K-D, Obst D (2006) Hydroformylation. *18*: 1–33
Wipf P, Kendall C (2005) Hydrozirconation and Its Applications. *8*: 1–25
Wu GG, Huang M (2004) Organolithium in Asymmetric Process. *6*: 1–36
Wu YT, de Meijere A (2004) Versatile Chemistry Arising from Unsaturated Metal Carbenes. *13*: 21–58

Xi Z, Li Z (2005) Construction of Carbocycles via Zirconacycles and Titanacycles. *8*: 27–56

Yamada K, see Iguchi M (2003) *5*: 37–60
Yamamoto A, see Lin Y-S (1999) *3*: 161–192
Yamamoto Y, see Itoh K (2004) *11*: 249–276
Yamamoto Y, Nakamura I (2005) Nucleophilic Attack by Palladium Species. *14*: 211–240
Yasuda H (1999) Organo Rare Earth Metal Catalysis for the Living Polymerizations of Polar and Nonpolar Monomers. *2*: 255–283
Yasuda N, see King AO (2004) *6*: 205–246

Zecchina A, Groppo E, Damin A, Prestipino C (2005) Anatomy of Catalytic Centers in Phillips Ethylene Polymerization Catalyst. *16*: 1–35
Ziegler T, see Michalak A (2005) *12*: 145–186

Subject Index

N,N-Acetal (aminal-) formation 72
N,O-Acetal formation 69
O,O-Acetal formation 68
Acetic acid synthesis, carbonylation of methanol 179
N-Acetyl-α-arylglycines 212
Acetylene, dichlorocarbonylation 245
Acid optimisation (AO) technology 185
Acrylonitrile 208
N-Acylamino acids, enzymatic hydrolysis 214
Acylanions 217
Alcohols 239, 252
Aldehydes 35
–, acyllithium addition 217
–, acylzirconocene addition 218
–, *C,C*-bond formation via hydroformylation 79
–, hydroformylation 3
–, –, heterofunctionalization 67
–, rhodium-catalyzed silylformylation 215
Aldol reactions 65
Aldolization, hydroformylation 2
Aliphatic hydrocarbons 239, 252
Alkenes 2, 97, 239, 241
–, alkoxycarbonylation 104
–, hydroxycarbonylation 98
β-Alkoxyalkanoic esters 241
Alkoxycarbonylations 103, 235
–, asymmetric 111
Alkylacetylenes, oxidative carbonylation 255
Alkyllithium 217
Alkynes 97, 239, 245
–, alkoxycarbonylation 112
–, hydroxycarbonylation 101
Allenes 239
Allylcyanide, rhodium-catalyzed asymmetric hydroformylation 58
Amides, acetylenic 260
Amidocarbonylations 208
Amines 239
Amino acids 208
4-Amino-2-ynamides 263
β-Aminoamides, unsaturated 245
Aminocarbonylation 235
Arenes, Pd(II)-promoted oxidative carbonylation 251
Aromatic hydrocarbons 239
Arylacetylenes, oxidative carbonylation 255
Aspartame 211

BDPP 51
Benzaldehydes, palladium-catalyzed amidocarbonylation 213
Benzofuranones 218
Bicyclopentenones 170
BINAPHOS 47
BINOL 47
Bis(diazaphospholidine) ligands 54
2,5-Bis(trichloromethyl)-1,3-dioxolan-4-ones 219
Bisphosphites 10
Bite-angle 8
Bromoacrylates 246
Butanal, hydroformylation 2
Butene, pivalic acid 219

Carbon monoxide 239
Carbonium ions 219
Carbonyl compounds 239
Carbonyl reactivity 79
Carbonylation 125
–, iridium-catalysed 196
–, rhodium-catalysed 183

Catalysts, formylation 8
Cellulose acetate, acetic anhydride 181
Chloral, carbonylation 219
β-Chloroalkanoyl chlorides 241
Chlorohydrin 219
Chloropeptin I ((*S*)-3,5-dichloro-4-hydroxyphenylglycine) 214
p-Chlorophenyl alanine 214
3-Chloropropionyl chloride 241
CO building block 97
CO–C_2H_4 copolymerisation 128
Cobalt, hydroformylation 1
Cobalt/tungsten, heterobimetallic 167
Cobalt catalysis 208
Conjugated dienes, Pd-catalyzed oxidative carbonylations 243
β-Cupraenone 171
Cycloaddition 165
Cyclopentenones 165

N-(1,1-Dialkylprop-2-ynyl)ureas 261
Diamidocarbonylation 208
Dienes 239
Diethyl ketone, selective synthesis 156
Dihydrofurans, rhodium-catalyzed asymmetric hydroformylation 55
2-Diphenyl-phosphinobenzoic acid 191
Diphosphine catalysts 151
Diphosphine ligands 54
Diphosphite ligands 42, 52, 57
Dodecenes, branched 28
Domino isomerization-amidocarbonylation, allylic alcohols 211

Enantioselectivity 35
Epoxides, alkoxycarbonylation/aminocarbonylation 235
–, alternating copolymerization 229
–, hydroformylation/silylformylation 232
–, ring-expansion carbonylation 224
Epoxydictymene 171
Ethene 125
2-Ethylhexanol 28
3-(2-Ethynylphenyl)ureas 261

Ferrocenylethyldiphosphine 39
Fischer indole synthesis 65
Formaldehyde, hydroformylation 214
Furanones, cyclocarbonylation 218
Furanoside diphosphite ligands 45

Glufosinate (phosphinotricine) 211

Heterocycles 239
Hexacarbonyldicobalt 166
Hirsuten 173
Hirsutene 171
Homogeneous catalysis 165, 239
Hydrido–cobalt–tetracarbonyl 5
Hydroaminomethylation 65
Hydroformylation 1, 35, 214
–, asymmetric 36
Hydroformylation/acetal formation 68
Hydroformylation/aldol reaction 84
Hydroformylation/allylation 79
Hydroformylation/aromatic substitution 83
Hydroformylation/carbonyl ene reaction 89
Hydroformylation/Fischer indole synthesis 90
Hydroformylation/imine/enamine formation 72
Hydroformylation/reductive amination 75
6-Hydroxy-2-ynamide 262
Hydroxycarbonylation reactions 98
Hydroxystreptazolone 171

Iodide salts 185
Iridium 196
Iron pentacarbonyl 167
Isocarbacyclin 172
Isovaleraldehyde, palladium-catalyzed amidocarbonylation 212

Ketenes 239, 251
Ketones 239, 249

Lactonization 97
Ligands, hydroformylation 1
Lithium enolates, 1,2-silicon shift 217
Loganin 171

Methanol 125
–, carbonylation 179
Methanolysis 135

Methionine 214
N-Methyl fatty acid amides 211
Methyl propanoate 147
2-Methylpropanal 2
Methylvinylphosphinate, domino hydroformylation-amidocarbonylation 211
Molybdenum hexacarbonyl 167
Monocarbonylation 125
Monochloroacetic acid 181
Monophosphine catalysts 148
Monsanto process 180

Naphthofuran-2(3*H*)-ones 218
Nitriles, unsaturated, rhodium-catalyzed asymmetric hydroformylation 57
Norbornene, phenylacetylene–hexacarbonyldicobalt 166
Norpentalene 173

OXO process 21

Palladium 125
Palladium catalysis 212
Palladium iodide 97, 239
Pauson–Khand reaction 165
– – –, alkynes/allenes 216
– – –, catalytic 168
– – –, hetero 216
– – –, mechanistic proposal 167
– – –, stereoselective 173
– – –, transfer carbonylation 174
Penta-2,4-dienamides 244
Phenols 239, 252
Phenylacetic acid derivatives 219
Phenylacetylene–hexacarbonyldicobalt complex 166
Phenylmalonate 220
Phosphabarrelenes 12
Phosphabenzenes 12
Phosphanes 8
Phosphine ligands 186
Phosphine-phosphite ligands 47, 52, 56
Phosphines 125
Phosphinites 8
Phosphites 8
Phosphonates 8
Pivalic acid 219
Poly(3-hydroxyalkanoate) 223
Poly(4-vinylpyridine-*co*-styrene-*co*-divinylbenzene) 195
Polyketones 125
Polymer-supported catalysts 194
Polyvinylpyridines 194
Propene, hydroformylation 2, 23
Propynyl acetate, oxidative carbonylation 255
Propynyl alcohol, oxidative carbonylation 255
Propynylamines, α,α-disubstituted, oxidative carbonylation 258
Prostaglandins 172
Protonolysis 134

Rhodium, hydroformylation 1

Sarcosinates, Hoechst process 211
Silylformylations 214
Succinic diesters 241

Tetrahydropyrroles 262
Tetrahydrothiophenes 262
Tetrapropene 28
TPPTS 11
Transfer carbonylation 165
Triphenylphosphane 8
Tungsten pentacarbonyl 167

Umpolung, carbon-monoxide-free 217
Ureidocarbonylation, palladium-catalyzed 213

Valeraldehyde, raffinate II 26
Vinyl acetate 180
–, hydroformylation 52
–, rhodium-catalyzed asymmetric hydroformylation 52
Vinyl arenes 42
–, rhodium-catalyzed asymmetric hydroformylation 41

Water gas shift (WGS) reaction 182

XANTPHOS, sulfonated 11
Xylene, terephthalic acid 181

2-Ynonate esters 247
2-Ynylamides, α,α-dialkyl substituted 260

Zirconium 167